Signal Separation Methods based on Singular Value Decomposition and their Application to the Real-Time Extraction of the Fetal Electrocardiogram from Cutaneous Recordings

Ir. Dirk Callaerts

Signal Separation Methods based on Singular Value Decomposition and their Application to the Real-Time Extraction of the Fetal Electrocardiogram from Cutaneous Recordings

Ir. Dirk Callaerts

KATHOLIEKE UNIVERSITEIT LEUVEN
FACULTEIT TOEGEPASTE WETENSCHAPPEN
Afdeling ESAT
Kard. Mercierlaan 94 - 3030 Leuven (Heverlee), Belgium

Signal Separation Methods based on Singular Value Decomposition and their Application to the Real-Time Extraction of the Fetal Electrocardiogram from Cutaneous Recordings

Jury :
Voorzitter Prof. J. Berlamont, vice-dekaan
Prof. J. Vandewalle, promotor
Prof. W. Sansen, promotor
Prof. J. Janssens
Prof. G. Vantrappen
Prof. A. Oosterlinck
Prof. A. van Oosterom (K.U. Nijmegen, NL)
Dr. D. Van Compernolle

U.D.C. 615.84

Proefschrift voorgedragen tot
het behalen van het doctoraat
in de toegepaste wetenschappen
door

Dirk CALLAERTS

December 1989

Preface

Dit werk is tot stand gekomen met de enthousiaste steun en medewerking van vele mensen.

Eerst en vooral zou ik mijn beide promotoren, *Joos Vandewalle* en *Willy Sansen*, willen bedanken. Gedurende meer dan vijf jaar kon ik hun enorme belangstelling voor mijn werk ervaren. Ik dank hen zeer hartelijk voor de tijd die ze regelmatig uittrokken om opgedoken problemen te bespreken en om suggesties te geven. In het bijzonder zou ik Joos willen bedanken voor de moed die hij mij gaf om door te bijten, op ogenblikken dat het me wat moeilijker werd. Joos en Willy, jullie brede interdisciplinaire wetenschappelijke kennis, jullie internationale ervaring, jullie inspanningen om de persoonlijke contacten binnen de groep te bevorderen, werken buitengewoon stimulerend.

Ook de leden van het leescomité *Prof. J. Janssens* en *Dirk Van Compernolle*, zou ik willen bedanken voor het nalezen van dit proefschrift, alsook de juryleden, de professoren *Jean Berlamont*, *André Oosterlinck*, *G. Vantrappen* en *Adriaan van Oosterom* (K.U. Nijmegen, NL). Ook veel dank aan *Prof. Kamiel Vandenberghe* (Verloskunde-Echografie, U.Z. Gasthuisberg) en *Dr. Marc Gewillig* (Kindercardiologie, U.Z. Gasthuisberg) voor het nalezen van de tekst en voor de suggesties in verband met de clinische relevantie van de ontwikkelde technieken.

Verder wil ik de professoren *G. Vantrappen* en *J. Janssens* van de afdeling Gastro-intestinale Fysiopathologie (Dept. Medische Navorsing, U.Z. Gasthuisberg) bedanken voor de opvolging van mijn werk langs medische zijde. Hun afdeling en hun mensen hielpen mij aan de nodige meetgegevens. Daarom gaat mijn dank ook uit naar *Toon De Greef*, *Rita Vos*, *Eric Van Cutsem* en *Jan Servaes* (nu werkzaam bij Scheikunde).

A special place in this work has been taken by the European project "New Methods in Perinatal Surveillance". The workshops in Heidelberg, Nottingham and Ischia, as well as the many contacts with Nijmegen and Amsterdam were extremely interesting. Thanks to my friends in Holland, *Adriaan van Oosterom, Henk Jongsma, Thom Oostendorp, Jan Menssen, Henk Goovaerts, Otto Rompelman, Herman Van Geyn* and *Frans Copray* and thanks to the close cooperation in the project, I started to think more "European".

Mijn collega's en ex-collega's binnen ESAT hebben steeds voor de gepaste, stimulerende atmosfeer gezorgd. In het bijzonder wil ik de vrienden en collega's in de onderzoeksgroepen ESAT/SISTA en ESAT/MICAS danken voor de toffe vergaderingen, koffiepauzes, volleybalmatchen (soms), samenkomsten bij Joos en Willy thuis, enz. Hartelijk dank aan *Bart De Moor, Marc Moonen, Sabine Van Huffel, Dirk Van Compernolle, Jan Vanderschoot, André Barbé, Guido Tijskens, Frank De Bondt, Philippe Meulemans, Jan Swevers, Shaohua Tan en Jiande Chen* voor hun directe of indirecte inbreng in dit werk. Bart en Marc lazen de tekst ook méér dan kritisch na en gaven de nodige suggesties voor verbetering. Speciale dank ook aan de system managers *Marc Elsen* en *Johan De Boer*. Hierbij wil ik ook het I.W.O.N.L. bedanken, dat mijn werk gedurende vier jaren, met onderbreking voor mijn legerdienst, met een specialisatiebeurs heeft ondersteund.

De professoren van de afdeling ESAT, *André Oosterlinck, René Govaerts, Piet Luypaert, Jan Peperstraete, Willy Sansen, Paul Suetens, Antoon Van de Capelle, Joos Vandewalle, Luc Van Eycken en Patrick Wambacq* zorgden voor de ideale omstandigheden waarin ik mijn onderzoek kon voltooien. Samen met hen startten we het Industrieel Contact Programma op, waarvan ik nu reeds twee jaar de contactpersoon ben. Dit programma geeft mij de uitstekende mogelijkheid om de band tussen de universiteit en de bedrijfswereld op een georganiseerde, gestruktureerde en verantwoorde wijze aan te halen. Het is vooral dank zijn de ongelofelijke steun en het vertrouwen dat ik hiervoor krijg van *André Oosterlinck*, dat ik in staat ben mij hiervoor ten volle in te zetten. Hij heeft ESAT gedurende de laatste jaren uitgebouwd tot een onderzoekslab ($\pm$ 130 mensen), met een zeer uitgebreide know-how op het gebied van elektronika.

Dank ook aan Leuven Research & Development en in het bijzonder aan *Prof. Jacques Van der Eecken, Hans Claes, Betty Hoste* en het secretariaat. Zij zorgen voor een juridische en contractuele ondersteuning van onze projecten met de industrie.

Verder wil ik alle medewerkers van ESAT en het departement Elektrotechniek bedanken, en in het bijzonder de secretariaten. Dat heb ik inderdaad gedurende al die jaren geleerd : bij de secretaresses moet je goed proberen te staan ! Dank aan *Ingrid Tokka, Lou Schol, Patricia Waege, Danielle Vermetten, Elvira Wouters, Annitta De Messemaeker, Nora Peeters, Jackie Jaspers* en ook aan *Marine Van Opstal, Luc Boone, Camille Evers, Jacques Delin, Guy Hermans*, enz.

Mijn dank gaat tevens uit naar *Prof. Hugo De Man, Franky Catthoor en Ingrid Verbauwhede* (divisie VSDM, IMEC v.z.w.) omdat zij mijn werk verder aanvullen door mijn algoritme in een levensechte chip te implementeren.

Een grote steun in werk en vrije tijd ondervind ik ook vanwege vele vrienden. Zonder namen te noemen, uit vrees toch altijd wel iemand over het hoofd te zien, wil ik hen in het bijzonder danken, omdat ze toch veel voor mij betekenen.

Tenslotte zou ik al mijn familieleden willen bedanken. *Pa en Ma Callaerts, Wim en Isabelle, Bart en Lieve en de kleine Julie, Gert, Bobonneke, Papa en Mama van Zoest*, mijn schoon-zusje *Ellen*, mijn tantes en nonkels, nichten en kozijns. Jullie zijn een fantastische steun voor mij. Ik hou van jullie. Veel ...
Pa, mijn bewondering voor jouw werk heeft mij in de richting van dit onderzoek gebracht.

En dan, mijn allerliefste *Renée*, ben jij er. Jij was er bij van het eerste moment dat ik met dit werk begon : in de zomer van 1984. Jij hielp mij er bovenop als het minder ging, jij hebt eenzame avonden moeten doorbrengen op ons appartementje, terwijl ik werkte. Jij staat volledig achter mij. Dat voel ik ! We hebben er ons samen doorgeslagen ! Het is gelukt !!

Ik hou van jou, mijn liefste, liefste vrouw.

Dirk Callaerts
Leuven, december 1989.

Voor Renée

Contents

1 Introduction and Outline of the thesis 1

2 Cutaneous Detection of the Fetal Electrocardiogram 9
- 2.1 Introduction 10
- 2.2 Detection of the Fetal Electrocardiogram 10
  - 2.2.1 Defining the problem 10
  - 2.2.2 Clinical relevance of the cutaneously recorded FECG . 13
  - 2.2.3 Existing methods for MECG-elimination 17
- 2.3 Modelling the FECG-problem 20
  - 2.3.1 The signal model 20
  - 2.3.2 Model uncertainty 22
  - 2.3.3 Noise considerations 24
- 2.4 Solving the FECG-problem 25
- 2.5 Conclusion 28

3 Formulation of Mathematical Concepts using Singular Value Decomposition 29
- 3.1 Introduction 30
- 3.2 Basic theorems for OSVD and QSVD 30
  - 3.2.1 The Ordinary Singular Value Decomposition (OSVD) 30
  - 3.2.2 The Quotient Singular Value Decomposition (QSVD) 32
- 3.3 The measurement space and the signal space 33
- 3.4 The oriented energy of a vector sequence 35
- 3.5 The oriented signal-to-signal ratio of two vector sequences. . . 38
- 3.6 Conclusion 43

4 A new on-line algorithm for SVD-based signal separation 44
- 4.1 Introduction 45
- 4.2 SVD : a valuable tool for the DSP-engineer 46

4.3 Development of the algorithmic scheme 48
4.4 Comparison with the normal equations 54
4.5 Adaptivity of the algorithm 56
4.6 Diagonalization of a symmetric matrix 59
4.6.1 Introduction 59
4.6.2 The classical Jacobi method 60
4.6.3 Generalization of the rotation 61
4.6.4 Simpler determination of the rotation angle 65
4.7 Minimal computation approach for the on-line SVD-based algorithm 68
4.8 Conclusion 72

5 Signal separation by OSVD of the extended data matrix 73
5.1 Introduction 74
5.2 Signal separation principle based on the concept of oriented energy 75
5.2.1 Solution under ideal conditions 75
5.2.2 Non-orthogonality of the transfer vectors 79
5.2.3 Positioning of measurement points 83
5.3 FECG-extraction by computing the OSVD of the data matrix 85
5.3.1 Clinical Experiments 85
5.3.2 Extraction of a MECG-free fetal ECG 86
5.3.3 Fetal contributions in the recorded signals 92
5.3.4 Detection of the P-wave in the FECG 94
5.3.5 The importance of the thoracic signals 95
5.3.6 The on-line adaptive algorithm for FECG-extraction . 98
5.4 Elimination of 50 Hz net interference 102
5.4.1 Introduction 102
5.4.2 Sources of net interference 102
5.4.3 Removal of net interference by filtering 103
5.4.4 Removal of net interference by linear combinations . . 103
5.5 Conclusion 108

6 Signal separation by QSVD of two matrices 109
6.1 Introduction 110
6.2 Signal separation principle based on the concept of oriented signal-to-signal ratio 111
6.2.1 Outline of the method 111
6.2.2 A two-dimensional example 113

6.2.3 Computation of the Quotient SVD 117
6.3 MECG-elimination and FECG-detection by the QSVD of two matrices 120
6.3.1 Off-line extraction of the MECG-free fetal ECG 120
6.3.2 FECG-extraction with the on-line QSVD-method . . . 128
6.4 Conclusion 130

7 Comparison of the SVD-based signal separation methods 131
7.1 Introduction 132
7.2 Comparison of the methods with general criteria. 133
7.3 Pro's and contra's of the methods for FECG-extraction . . . 135
7.4 Comparison with other methods for FECG-extraction 142
7.4.1 A two-step spatial filter for FECG-extraction 142
7.4.2 Adaptive Noise Cancelling for MECG-elimination . . . 147
7.5 Conclusion 150

8 Summary of the main results and future work 151
8.1 Summary of the main results 152
8.2 Future research 156
8.2.1 Beamforming and antenna array applications 156
8.2.2 Speech Enhancement 158
8.2.3 The Electro-Encephalogram (EEG) 160

A Feasibility study of a real-time implementation of the on-line algorithm 163
A.1 Introduction 164
A.2 PC-based unit for real-time signal separation 164
A.2.1 Feasibility study 164
A.2.2 A PC-based system 168
A.3 A digital chip implementation of the on-line adaptive algorithm 172

B Pascal routines on VAX / VMS 173

List of Figures

1.1 *General configuration of signal sources, spatially distributed in a medium and observed by p measurement points.* 3

2.1 *Two potential signals, recorded on the maternal abdomen and containing both MECG and FECG.* 12
2.2 *The cardiac cycle with the three important waves : the P-wave, the QRS-complex and the T-wave.* 14
2.3 *Tocodynamometry : the relation between the instantaneous FHR (upper tracing) and the contractions of the uterus (lower tracing).* 15
2.4 *The basic scheme of the FECG-problem.* 21

3.1 *The cloud of points in a 2-dimensional measurement space, corresponding with a* 2×500 *data matrix.* 34
3.2 *Polar plot of the oriented energy of a vector sequence in two dimensions.* 36
3.3 *(a) Polar plot of the oriented energy of two vector sequences in two dimensions. (b) Polar plot of the corresponding oriented signal-to-signal ratio in two dimensions.* 38
3.4 *Polar plot of the oriented signal-to-signal ratio for several configurations of the oriented energies of two vector sequences.* 41

4.1 *General scheme of the on-line adaptive algorithm.* 51
4.2 *Detailed scheme of the on-line adaptive algorithm.* 52
4.3 *The function* α^i *for (1)* $\alpha = 0.999$, *(2)* $\alpha = 0.997$, *(3)* $\alpha = 0.995$, *(4)* $\alpha = 0.99$, *(5)* $\alpha = 0.98$ *and (6)* $\alpha = 0.95$ 58
4.4 *Variation of* γ *as a function of* ϕ *for* $K = 1$ 63
4.5 *Variation of* γ *as a function of* ϕ *for* $K = 4$ 64
4.6 *The variation of* γ *as a function of* K *for each of the three methods.* 66

4.7 *The variation of Δ as a function of K for each of the three methods.* 67
4.8 *The ratio ρ for different values of α and p.* 70

5.1 *The normalized transfer vectors $\mathbf{t}_1$ and $\mathbf{t}_2$* 79
5.2 *The angle ε between $\mathbf{t}_1$ and $\mathbf{u}_1$ as a function of α for some values of σ.* 80
5.3 *The ratio between weak and strong signal contribution in the projection onto $\mathbf{u}_2$ as a function of α for some values of σ.* . . 81
5.4 *Positioning of two observation points for two signal sources : a) Two observation points close to the source of interest. b) Spatial separation of the observation points.* 83
5.5 *A signal recorded on the abdomen of patient A and containing both MECG and FECG.* 86
5.6 *Three signals (patient A), picking up the MECG independently.* 87
5.7 *The four resultant orthogonal signals : signal 4 is completely free of MECG and contains a clean FECG.* 88
5.8 *Three simultaneously recorded abdominal signals (patient A), containing both MECG and FECG.* 89
5.9 *The six orthogonal signals, obtained as a linear combination of the recorded signals : signals 4 and 5 are free of MECG and contain the FECG.* 91
5.10 *The contribution of fetal ECG in each of the six recorded signals of Figures 5.6 and 5.8.* 93
5.11 *Mean FECG waveforms for each of the electrode pairs. The arrows indicate the clearly visible P-wave.* 94
5.12 *(a) Signal recorded on the abdomen of patient B, containing both MECG and FECG.* 95
5.12 *(b) Three thoracic signals (patient B), picking up the maternal ECG independently. (c) The resultant MECG-free fetal signal after application of the OSVD-method.* 96
5.13 *(a) A second signal, recorded on the abdomen of patient B and containing both MECG and FECG. (b) The resultant signal after application of the OSVD-method still contains both MECG and FECG.* 97
5.14 *The six resultant orthogonal signals, after application of the on-line algorithm with $\alpha = 0.9986$.* 100

5.15 *The first signal is a simulation of a sudden change in an abdominal signal, while the second signal results after applying the on-line algorithm.* 101
5.16 *The angle ε between $\mathbf{u}_3$ and the normal $\mathbf{n}$ onto the subspace span $\{\tau_2, \tau_3\}$.* 105
5.17 *The ratio ρ between signal-to-interference in the obtained signal and original signal as a function of θ for different values of C/A* 106
5.18 *Removal of net interference applied to real ECG-data. (a) Spectrum of recorded ECG-signal with net interference. (b) Spectrum of the signal after removal of the net interference. (c) Difference of the two spectra.* 107

6.1 *Angle ε_1 as a function of α for different values of s_{m1}* . . . 115
6.2 *Different configurations of transfer vectors.* 116
6.3 *Signals 1 to 8 of the 32-channel data set.* 121
6.3 *Signals 9 to 16 of the 32-channel data set.* 122
6.3 *Signals 17 to 24 of the 32-channel data set.* 123
6.3 *Signals 25 to 32 of the 32-channel data set.* 124
6.4 *Three MECG-free fetal signals obtained with the second signal separation method, applied to a set of 32 recorded signals.* . . 125
6.5 *Two MECG-free fetal signals, obtained with the second signal separation method, applied to a set of 8 recorded signals.* . . . 126
6.6 *Eight channel data set recorded on patient B.* 127
6.7 *On-line QSVD-based extraction of the fetal ECG, applied to an eight-channel data set. Four intervals, each of 4 seconds, are shown.* 129

7.1 *The 8 resultant signals after application of the first SVD-based signal separation method to the 8-channel data set.* 140
7.2 *The 8 resultant signals after application of the QSVD-based signal separation method to the 8-channel data set.* 141
7.3 *Some of the obtained fetal signals for different values of r_u.* . 146
7.4 *The Adaptive Noise Canceller for MECG-elimination.* 147
7.5 *Results obtained with the Adaptive Noise Canceller. The first signal is the filter output, while the second signal should be the MECG-free fetal signal.* 148

7.6 *Resultant signals obtained with the Adaptive Noise Canceller for an experiment with four signals (1 primary and 3 reference) over a period of 10 seconds. The first signal is the filter output, while the second signal should be the MECG-free fetal signal.* 149

8.1 *A beamformer for narrowband signals (a) forms a linear combination of the recorded signals, while a beamformer for broadband signals (b) combines delayed versions of the sensor outputs.* 156
8.2 *The Griffiths-Jim beamformer.* 159
8.3 *Electrode positioning on the scalp according to the international 10-20 system.* 161

A.1 *The general layout of the prototype board with TMS-32010.* . 165
A.2 *Diagram with relative timing of the tasks that the TMS-processor has to perform each 4 ms.* 167
A.3 *General layout of the PC-based system for real-time extraction of the fetal ECG.* 168

List of Tables

4.1 *Percentual contribution of diagonal and off-diagonal to the Frobenius-norm of B_i for different values of ρ.* 69
4.2 *Thresholds for ρ after convergence of the algorithm.* 69

5.1 The forgetting factor α^k for different values of α. 99

List of publications

1. CALLAERTS, D., DE BONDT, F., "Real-time scheiding van het elektrocardiogram van moeder en foetus", Master's thesis, Dept. of Elec. Eng., K.U. Leuven (B), July 1984.

2. CALLAERTS, D., "Het ontwerp van on-line technieken voor signaalverwerking die gebruik maken van Singuliere Waarden Ontbinding (deel 1)", Jaarverslag 1e mandaat specialisatiebeurs I.W.O.N.L., Sept. 1985.

3. VANDERSCHOOT, J., VANTRAPPEN, G., JANSSENS, J., SANSEN, W., VANDEWALLE, J., CALLAERTS, D., "The use of Singular Value Decomposition in Multilead Abdominal FECG", *Europ. J. Obst. Gynec.*, reprod., Biol. 20, 1985.

4. CALLAERTS, D., VANDERSCHOOT, J., VANDEWALLE, J., SANSEN, W., VANTRAPPEN, G., JANSSENS, J., "An adaptive on-line method for the extraction of the complete fetal electrocardiogram from cutaneous multilead recordings", *Journal of Perinatal Medicine*, vol. 14, no. 6, pp. 421-433, 1986.

5. CALLAERTS, D., "Het ontwerp van on-line technieken voor signaalverwerking die gebruik maken van Singuliere Waarden Ontbinding (deel 2)", Jaarverslag 2e mandaat specialisatiebeurs I.W.O.N.L., Sept. 1986.

6. CALLAERTS, D., VANDERSCHOOT, J., VANDEWALLE, J., SANSEN, W., "An on-line adaptive algorithm for signal processing using SVD", in *Signal Processing III*, Amsterdam, NL (Elsevier Science Publ., North Holland), EURASIP 86, The Hague, pp. 953-956, Sept. 1986.

7. CALLAERTS, D., VANDEWALLE, J., SANSEN, W., " On-line separation of vector signals using a new adaptive SVD-algorithm ", *Proc. of Benelux Meeting on Systems and Control*, Houthalen (B), p. 187, Jan 1987.

8. CALLAERTS, D., VANDERSCHOOT, J., VANDEWALLE, J., SANSEN, W., VANTRAPPEN, G., JANSSENS, J., " Fetal Electrocardiogram Measuring Method and Equipment (FEMME)", *Journal of Perinatal Medicine*, vol. 15, Suppl. 1, World Symp. on Computers in the Care of Mother, Fetus and Newborn, Vienna, pp. 33, March 1987.

9. VANDERSCHOOT, J., CALLAERTS, D., SANSEN, W., VANDEWALLE, J., VANTRAPPEN, G., JANSSENS, J., "Two Methods for Optimal MECG Elimination and FECG Detection from Skin Electrode Signals ", *IEEE Trans. Biomed. Eng.*, vol. BME-34, No. 3, pp. 233-243, March 1987.

10. CALLAERTS, D., VANDEWALLE, J., SANSEN, W., MOONEN, M., " On-line Algorithm for Signal Separation based on SVD", in *SVD and Signal Processing : Algorithms, Applications and Architectures*, Deprettere, E., Editor, North-Holland, pp. 269-276, Sept. 1987.

11. CALLAERTS, D., SANSEN, W., VANDEWALLE, J., "Description of a real-time system to extract the Fetal Electrocardiogram", To appear in *Clinical Physics and Physiological Measurements*, Workshop on Current Status and Future of Fetal Electro- and Phonocardiography, Ischia (I), Sept. 1988.

12. VANDEWALLE, J., CALLAERTS, D., "Singular Value Decomposition : a powerful concept and tool in signal processing", *Proc. of Conf. on Mathematics in Signal Processing*, Warwick (UK), Dec. 1988.

13. CALLAERTS, D., DE MOOR, B., VANDEWALLE, J., SANSEN, W., "Comparison of SVD-methods to extract the Fetal Electrocardiogram from cutaneous electrode recordings", Submitted to Medical & Biological Eng. & Comp., Jan. 1989.

14. CALLAERTS, D., VANDEWALLE, J., "The use of SVD-based techniques for signal separation", *Proc. of the Tenth Symp. on Inform. Theory in the Benelux*, Houthalen (B), pp. 109-115, May 1989.

15. CALLAERTS, D., VANDEWALLE, J., SANSEN, W., "Comparison of signal separation methods based on SVD and GSVD", *Proc. of 12ieme Coll. sur le Traitement du Signal et des Images (GRETSI-89)*, Juan-les-Pins (Fr), pp. 177-180, June 1989.

16. CALLAERTS, D., VANDEWALLE, J., "Adaptive Singular Value Decomposition and its use for Adaptive Signal Separation", *Proc. of the Int. Symp. on Math. Theory of Networks and Systems, MTNS-89*, Amsterdam, June 1989.

List of lectures

- **January 8, 1986 :** "Adaptive on-line method for real-time Singular Value Decomposition", lecture at the division Network Theory of the Departement Elektrotechniek, **T.U. Delft (NL)** upon invitation of P. De Wilde and E. Deprettere.

- **April 4, 1986 :** "Chip design for on-line Singular Value Decomposition", lecture at the division VSDM of IMEC, **Leuven (B)** upon invitation of J. Rabaey.

- **May 1, 1989 :** "SVD-methods for MECG-FECG separation", lecture at the division Medical Physics and Biophysics, **K.U. Nijmegen (NL)** upon invitation of A. van Oosterom and T. Oostendorp.

- **Juli 13, 1989 :** "An on-line adaptive algorithm for Singular Value Decomposition based techniques in signal separation", lecture during the *Summer Course on Parallel Processing and Matrix Problems, Applications on Signals, Control and Systems*, Session on Applications to Signal Processing, **Valencia (SP)** upon invitation of V. Hernandez.

Presentations on international conferences or workshops

- **November 19, 1984 :** *Third Workshop of the Working Group on Description and Evaluation of CTG's in the European Community Project "Perinatal Monitoring"*, **Heidelberg - Neckargemünd (D).**
  Title : The use of SVD in multilead abdominal FECG [85].
  Session : Processing of non-invasive signals from the fetal heart.

- **November 26, 1985 :** *Int. Workshop on Fetal Electrocardiography in the European Community Project "Perinatal Monitoring"*, **Nottingham (UK).**
  Title : An adaptive on-line method for the extraction of the complete fetal electrocardiogram from cutaneous multilead recordings [12].
  Session : Detecting the FECG-Complex and Monitoring FHR Variations.

- **September 3, 1986 :** *3rd European Signal Processing Conference (EUSIPCO-86)*, **The Hague (NL).**
  Title : An on-line adaptive algorithm for signal processing applications using SVD [14].
  Session : Detection and Estimation 1.

- **January 22, 1987 :** *Benelux Meeting on Systems and Control*, **Houthalen (B).**
  Title : On-line separation of vector signals using a new adaptive SVD-algorithm [15].
  Postersession : Systems and Control.

- **March 9, 1987 :** *First World Symp. on "Computers in the care of mother, fetus and newborn"*, **Vienna (A).**
  Title : Fetal Electrocardiogram Measuring Method & Equipment [16].
  Session : FECG / Doppler Cardiography.

- **September 22, 1987 :** *Int. Workshop on SVD and Signal Processing*, **Les Houches (F).**
  Title : On-line algorithm for signal separation based on SVD [17].
  Postersession : SVD in Signal Processing Applications.

- **September 16, 1988 :** *Int. Workshop on Current Status and Future of Fetal Electro- and Phono Cardiography*, **Ischia (I)**.
  Title : Description of a real-time system to extract the FECG [18].
  Session : Prospects for abdominal FECG.

- **December 14, 1988 :** *2nd IMA Conf. on Mathematics in Signal Processing*,
  Warwick (UK).
  Presented by J. Vandewalle.
  Title : Singular Value Decomposition : a powerful concept and tool in Signal Processing [90].

- **May 26, 1989 :** *10th Symp. on Information Theory in the Benelux*, **Houthalen (B)**.
  Title : The use of SVD-based techniques for signal separation [20].
  Session : Signal Processing I.

- **June 13, 1989 :** *12ième Colloque sur le Traitement du Signal et des Images, (GRETSI-89)*, **Juan-les-Pins (F)**.
  Title : Comparison of signal separation methods based on SVD and GSVD [21].
  Session : Detection and Estimation.

- **June 22, 1989 :** *Int. Symp. on the Mathematical Theory of Networks and Systems (MTNS-89)*, **Amsterdam (NL)**.
  Title : Adaptive Singular Value Decomposition and its use for adaptive signal separation [22]. (Presented by J. Vandewalle)
  Session : Adaptive Filtering.

Glossary of medical terms

abdomen (abdominal) : belly

amniotic fluid : fluid between the fetus and the membranes.

antepartum : time before labour.

arrhythmia : deviations from a regular sinus rhythm.

bradycardia : a very low heart rate, for a fetus below 100 beats per minute.

intrapartum : time during labour.

supraventricular : the upper part of the heart, above the ventricles.

tachycardia : a very high heart rate, for a fetus more than 200 beats per minute.

thorax (thoracic) : chest (from the chest)

ventricular : concerning the ventricles.

vernix caseosa : electrically isolating, greasy, cheese-like fluid on the skin of the fetus.

Chapter 1

Introduction and Outline of the thesis

In real life, many problems, processes or systems can be described by one or more signals, that reflect some information about the system under observation :

- In control and surveillance applications e.g. a change in the characteristics of some monitoring signals will indicate whether or not some action has to be taken.
- In radar applications, signals coming from different directions are captured with antennas or arrays of antennas.
- In telecommunications, signals are the carrier of information, sent from one place to another.
- In analysis and testing applications signals will tell us something about the condition or situation of the system under consideration.

Detection and **estimation** is an engineering discipline that deals with measuring, recording or capturing signals and deriving or estimating from these some parameters or other information. However, where it is the aim to observe some specific phenomenon by detecting signals, the observations are often disturbed by unwanted influences and by signals coming from undesired phenomena.

The general situation can then be outlined as in Figure 1.1. Consider a number of phenomena X_l $(l = 1, \ldots, x)$ (furtheron called signal sources), spatially distributed in a medium. Some of these phenomena are **desired**, as they contain useful information, while others are **unwanted**, since they disturb the observation of of the interesting phenomena in one way or another. Observations made at a point somewhere in the medium will always contain contributions from both wanted and unwanted phenomena. Suppose that each phenomenon X_l can be described by a number of independent signals, called source signals $s_j(t)$. If the medium is linear, static and time-invariant, each observation is a signal $m_i(t)$, which is the superposition of a limited number of desired and undesired source signals $s_j(t)$, disturbed by additive noise $n_i(t)$:

$$m_i(t) = \sum_{j=1}^{r} t_{ij}\, s_j(t) + n_i(t) \qquad (i = 1, \ldots, p) \tag{1.1}$$

In this equation, the coefficients t_{ij} are a measure for the transfer of signals from source to observation point.

Since it is our aim to observe one specific phenomenon individually, **signal separation** methods have to be applied. The best known signal separation method is classical filtering (analog and/or digital), an operation in the frequency domain. However, this technique is only successful if the different phenomena have a bandlimited non-overlapping frequency content. Indeed, if the spectra of the observed phenomena overlap, some frequency components of the wanted phenomenon will disappear, together with the elimination of the undesired influences. This might have an important influence on the waveform of the signals. E.g. removal of 50 Hz net interference by filtering in electrocardiography will also remove frequency components of the electrocardiogram, changing its waveform in the time-domain. In such cases, other solutions have to be looked for.

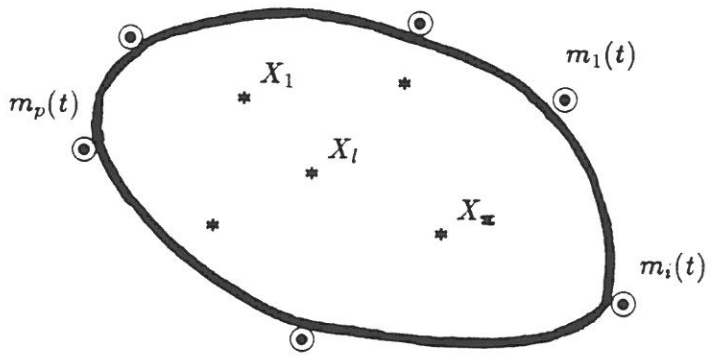

Figure 1.1: *General configuration of signal sources, spatially distributed in a medium and observed by p measurement points.*

This dissertation presents two signal separation methods based on Singular Value Decomposition (SVD) of a data matrix, constructed by digitizing a set of recorded analog signals. Both techniques are applied with success to the real-time extraction of the fetal electrocardiogram (FECG) from potential signals, recorded on the skin of the mother and therefore basically disturbed by the maternal electrocardiogram (MECG). It is also described how the first signal separation method can be used to remove 50-60 Hz net interference from biomedical recordings. In the last Chapter of this work, some indications, hints and expectations are given for the use of the presented SVD-based methods in other signal processing applications such as adaptive antenna array processing, speech enhancement using multiple microphone arrays and principal component analysis in electro-encephalography (EEG).

We will now shortly describe the content of and the main results obtained in each Chapter of this dissertation.

Chapter 2 : Cutaneous Detection of the Fetal Electrocardiogram.

The detection of the Fetal Electrocardiogram (FECG) from potential signals, obtained from electrodes on the skin of the mother, is the main application for the presented signal separation techniques. In this Chapter we will therefore introduce this biomedical inverse problem. After a summary of the specific practical difficulties encountered in this case, the clinical relevance of the cutaneously recorded FECG during pregnancy is indicated. Furthermore, an overview of several existing methods for eliminating the strong Maternal Electrocardiogram (MECG) and detecting the weak FECG from abdominal recordings is given. In order to describe the problem in mathematical terms, a signal model is defined. Some considerations are made concerning uncertainty of this model and noise. Then a general solution is outlined. It is proved in Section 2.4 that the signal separation can be obtained by finding the right coefficients in linear combinations of the recorded signals. The methods, presented in Chapters 5 and 6, give two possible ways to obtain such coefficients based on the computation of a Singular Value Decomposition.

Chapter 3 : Formulation of Mathematical Concepts using Singular Value Decomposition.

This Chapter describes the mathematical foundations of this dissertation. The Singular Value Decomposition, a technique known from linear algebra, provides an excellent framework to define, describe and compute some mathematical concepts. We define in this Chapter some concepts that are important in multichannel signal processing applications : the measurement space, the signal space, the oriented energy of a signal set and the oriented signal-to-signal ratio of two signal sets. The SVD can indeed be used to "explain" these concepts, but offers also a way to compute some extremal values for each of the defined concepts. We also make the difference between the Ordinary SVD of a matrix and the Quotient SVD of two matrices. We will refer to OSVD and QSVD when it is particularly needed, but indicate SVD when both methods are referred to in general.

Chapter 4 : A new on-line algorithm for SVD-based signal separation.

The Ordinary Singular Value Decomposition (OSVD) is a technique, that, similar to the Eigenvalue Decomposition, decomposes a matrix as the product of three other matrices with special properties. Most of the existing routines for the computation of the OSVD, implement an off-line strategy : all data have to be present before the computation of the OSVD can start. But in real-time signal processing, where the data become available sequentially in time, such an off-line technique gives some problems with respect to the amount of computational work and to the adaptivity of the method. In many applications only the left singular matrix has to be known such that it is not necessary to compute the complete decomposition (the three matrices). Therefore, an algorithmic scheme is designed for the on-line adaptive computation of the left singular matrix of a given matrix, whose columns become sequentially available. Each time a new column is appended to the matrix, the current left singular matrix is updated.

Since the basis of the algorithm is the update of the covariance structure of the data matrix, the Jacobi plane rotation for diagonalizing a symmetric matrix is used in one of the algorithmic steps. Although this Jacobi method is ideal with respect to the determination of the rotation angle, a new method is presented that determines this angle without computing any square root. The Jacobi method annihilates an off-diagonal element of a symmetric matrix, while the new method reduces this element substantially, corresponding with a so called over- or underrelaxation. This has more advantages in microcomputing environments, since rounding errors in the Jacobi technique might prevent the element for being annihilated completely. In the final stages of a diagonalization process (for small rotation angles), the new method has the same quadratic convergence as the original Jacobi method.

Since it is very difficult to prove the convergence of the on-line adaptive algorithm analytically, an empirical approach is given. This approach shows that the algorithm converges very fast to a near-diagonal matrix, even if only one plane rotation (with the approximating new method for the determination of the rotation angle) is applied in each cycle. This reduces the computational work for each cycle in the algorithm substantially. It will be shown in Chapters 5 and 6 that this algorithmic scheme can be used in both of the presented signal separation methods, after appropriate initialization.

Chapter 5 : Signal separation by OSVD of the extended data matrix.

This Chapter presents the first signal separation method, based on the concept of oriented energy of a signal set. The coefficients in the linear combination of the recorded signals, required to separate the signal contributions (see general solution in Chapter 2), are found by computing the left singular matrix in the OSVD of an "extended" data matrix. This means that the data matrix is not only constructed from signals, containing both wanted and undesired signals, but is extended with some extra independent signals, that pick up the disturbing source individually. In a first section the solution is presented and proved under ideal conditions (orthogonal transfer of the signals from source to observation point). Then the influence of non-orthogonality of the transfer is studied and this results in some conclusions about locations of the measurement sensors.

In a next section this signal separation technique is applied to the elimination of the MECG and the extraction of the FECG. This requires the recording of abdominal signals, containing both MECG and FECG, as well as thoracic signals, that pick up the MECG individually. By this spatial distribution of the electrodes, near-orthogonality of the transfer is obtained. The importance of these thoracic signals is shown with an example. It is also indicated how the fetal contributions in each of the recorded signals can be obtained separately. Averaging successive fetal complexes of the obtained MECG-free fetal signals, such that the statistical noise is removed, provides furthermore some information about the fetal ECG waveform (QRS-duration, P-wave, etc.). The possible detection of the P-wave in the fetal complex, is a spectacular result for cardiologists. Furthermore, the on-line algorithm is used to separate the fetal and maternal ECG's adaptively. In a last section we prove the removal of 50 Hz net interference from biomedical recordings, by extending the data matrix with a signal, picked up directly from the power network, and the same signal in quadrature or phase-shifted.

Chapter 6 : Signal separation by QSVD of two matrices.

This Chapter presents a second signal separation method, in this case based on the concept of oriented signal-to-signal ratio of a two signal sets. The coefficients in the linear combination of the recorded signals, required to separate the signal contributions (see general solution in Chapter 2), are now found by computing the QSVD of a matrix pair. This matrix pair consists of the data matrix, containing the original signals, and a matrix, constructed by selecting one or more intervals in which the undesired signal

dominates. With a two-dimensional example it is shown that this method is successful and that the orthogonality of the signal transfer from source to measurement point has some influence on this success.

An important point is the observation that a QSVD of two matrices can be computed as two consecutive OSVD's. This is used to define an "adaptive" computation strategy for the QSVD. If the transfer of the disturbing phenomenon is time-invariant, the computation of the first OSVD is used as an initialization for the second step, that is applied to the whole data matrix and that tries to detect the wanted signal. The method is designed só, that this second step can be performed adaptively, by applying the on-line algorithmic scheme. This implies that the transfer of the wanted phenomenon can be time-variant.

In a following section this signal separation technique and its on-line version are again applied to the elimination of the MECG and the extraction of the FECG. Although this method is successful, since it obtains in most cases a very useful MECG-free fetal signal, it is not elegant to apply in a clinical environment, due to the visual selection of the intervals and the difficult initialization step.

Chapter 7 : Comparison of the SVD-based signal separation methods.

In this Chapter the two presented SVD-based signal separation methods are compared with each other. Both of these try to find the coefficients in the linear combination of the recorded signals, in order to separate different signal contributions. First, the methods are compared in general with respect to some criteria : restrictions for applicability, suitability for automation, requirement for orthogonality of the transfer and the number of recorded signals. Then some pro's and contra's of the methods are mentioned, if they are applied for FECG-extraction. The most important conclusion is that both methods give good results, however, the first method is the most elegant and suitable for use in a clinical environment.

In a second part of this Chapter, we will compare the two methods with two existing methods for MECG-elimination and FECG-detection. First, an SVD based technique for FECG-extraction ([60], [61]) is presented and modified, such that our on-line algorithm can be used for it. Despite the fact that in most cases a useful MECG-free fetal signal is obtained, the method suffers from important drawbacks. Secondly, the famous adaptive filtering technique by Widrow ([95]) is presented and applied to one of our data sets. The results were however not very satisfying.

Chapter 8 : Summary of the main results and future work.

This last Chapter gives a brief overview of the developed techniques, their usefulness and the main results obtained in this work. Furthermore, some indications are given for future research with the signal separation methods in the field of beamforming and adaptive antenna array processing, speech enhancement using multiple microphones (cockpit conversation, mobile telephone, cocktail party ...) and principle component analysis of the electro-encephalogram (EEG).

Appendix A : Feasibility study of a real-time implementation of the on-line algorithm.

In Chapter 4 an on-line adaptive algorithm for the computation of the left singular basis of a matrix is outlined. It was shown in Chapters 5 and 6 that this algorithm can be used for adaptive signal separation. But also in other signal processing applications, based on principle component reduction or rank determination, the on-line algorithm can reduce the computational effort and allow real-time implementations. In this Appendix we discuss two possible implementations of this algorithm. The first one is a software implementation into a system consisting of a Personal Computer, extended with a DSP-board, and the second one is the implementation of the algorithm into hardware by the design of an Application Specific Integrated Circuit (ASIC).

Chapter 2

Cutaneous Detection of the Fetal Electrocardiogram

This means that each $\mathbf{x}_j$ contains the coefficients of a linear combination of the rows of A and the rows of B, such that the ratio of the squared norms of these linear combinations

$$\frac{\|\mathbf{x}_j^t\, A\, A^t\, \mathbf{x}_j\|}{\|\mathbf{x}_j^t\, B\, B^t\, \mathbf{x}_j\|} = \frac{\|\mathbf{x}_j^t\, A\|^2}{\|\mathbf{x}_j^t\, B\|^2}$$

reaches an extremal value, which equals γ_j^2. From this property we establish the link between the oriented signal-to-signal ratio of two vector sequences and the QSVD of the corresponding matrices in the following theorem :

Theorem 4 : Relation between oriented S-S ratio and QSVD ([27], [28])

Consider a $p \times q$ matrix A and a $p \times k$ matrix B with QSVD as defined in Eq. (3.12). Then $(i = 1, \ldots, r \text{ with } r = \text{rank}(B))$

$$R_{\mathbf{e}}\,[A, B] = \gamma^2 \quad \text{for} \quad \mathbf{e} = \frac{\mathbf{x}_i}{\|\mathbf{x}_i\|} \tag{3.14}$$

where $\mathbf{x}_i$ is the i-th column of matrix X in the QSVD of (A, B).

Proof : Define the linear transformation $T = D_B^{-1}\, X^t$, then, due to the invariance property of the S-S ratio

$$\begin{aligned} R_{\mathbf{e}}\,[A, B] &= R_{\mathbf{e}'}\,[TA,\, TB] \\ &= R_{\mathbf{e}'}\,[D_B^{-1}\, D_A\, Q_A^t,\, U_B^t] \\ &= E_{\mathbf{e}'}\,[D_B^{-1}\, D_A\, Q_A^t] \end{aligned} \tag{3.15}$$

for

$$\mathbf{e}' = \frac{T^{-t}\, \mathbf{e}}{\|T^{-t}\, \mathbf{e}\|} = \frac{D_B\, X^{-1}\, \mathbf{e}}{\|D_B\, X^{-1}\, \mathbf{e}\|}$$

Due to the relation between oriented energy and OSVD of $C = D_B^{-1}\, D_A\, Q_A^t$ (see Theorem 3)

$$E_{\mathbf{u}_{ci}}\,[C] = \sigma_{ci}^2 = \gamma^2 \tag{3.16}$$

In other words, $E_{\mathbf{e}'}\,[C]$ is extremal for $\mathbf{e}' = \mathbf{u}_{ci}$, such that $R_{\mathbf{e}}\,[A, B]$ is extremal for

$$\mathbf{e} = \frac{\mathbf{t}_i}{\|\mathbf{t}_i\|} = \frac{\mathbf{x}_i}{\|\mathbf{x}_i\|}$$

□

The QSVD thus provides the extrema of the oriented S-S ratio (the squared quotient singular values) and also the directions in which those extrema occur (the columns of the matrix X, which are not orthonormal). In signal processing applications this means that the QSVD of two data matrices A and B detects directions for which the ratio of oriented energy of A to oriented energy of B reaches an extremal value.

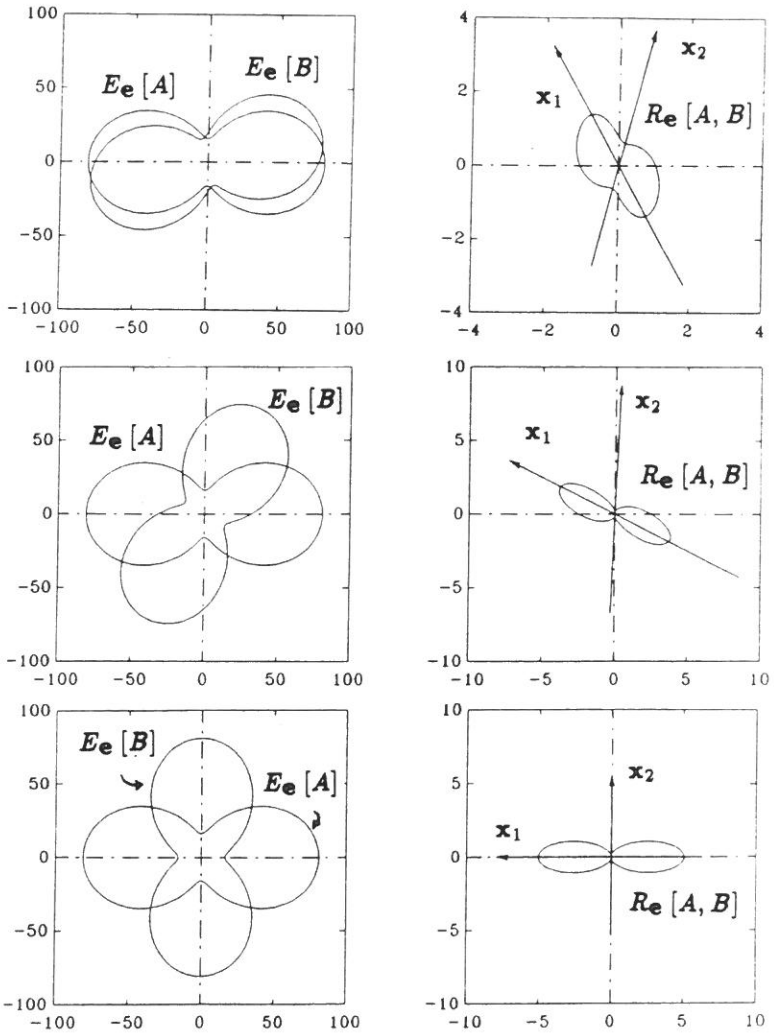

Figure 3.4: *Polar plot of the oriented signal-to-signal ratio for several configurations of the oriented energies of two vector sequences.*

Figure 3.4 shows the S-S ratio polar plots of two matrices A and B that have the same singular values, but where the left singular basis of B is rotated over some angle with respect to the left singular basis of A. This corresponds to the following case

$$\begin{aligned} A &= U_A \Sigma_A V_A^t = \Sigma V_A^t \\ B &= U_B \Sigma_B V_B^t = \begin{pmatrix} \cos\theta & -\sin\theta \\ \sin\theta & \cos\theta \end{pmatrix} \Sigma V_B^t \end{aligned}$$

The left pictures show the plots of oriented energy of A and B in the same p-dimensional space, while in the right pictures the oriented S-S ratio and extremal directions are plotted. It can be seen from this figure that the directions $\mathbf{x}_1$ and $\mathbf{x}_2$ of extremal oriented S-S ratio are orthogonal in the case $\theta = \pi/2$. This can be generalized in the following theorem.

Theorem 5 :

Suppose A $(p \times q)$ and B $(p \times k)$ are two real matrices with OSVD given by

$$A = U_A \Sigma_A V_A^t \quad \text{and} \quad B = U_B \Sigma_B V_B^t \tag{3.17}$$

and with QSVD of (A, B) given by

$$\begin{cases} A = X^{-t} D_A Q_A^t \\ B = X^{-t} D_B Q_B^t \end{cases} \tag{3.18}$$

The columns of X in Eq. (3.18) are orthogonal, only if $U_B = U_A \tilde{I} S$, where $\tilde{I}$ is a matrix consisting of a permutation of the columns of the identity matrix I and $S = \text{diag}(\pm 1)$.

Proof :

Suppose that X is an orthogonal matrix, then $X^t X = D_x$ and $X^{-t} = X D_x^{-1}$. Therefore, Eq. (3.18) changes into

$$\begin{cases} A = X D_x^{-1} D_A Q_A^t \\ B = X D_x^{-1} D_B Q_B^t \end{cases} \tag{3.19}$$

Due to the uniqueness of the OSVD of A and B, it follows that

$$X = U_A \tilde{I}_a S_a = U_B \tilde{I}_b S_b$$

where $\tilde{I}_a$ and $\tilde{I}_b$ are permutation matrices, that change the order of the columns of U_A and U_B, and where S_a and S_b are diagonal matrices with ± 1 on the diagonal.

□

3.6 Conclusion

In this Chapter we defined and presented the mathematical foundation of this dissertation. First, the basic theorems of the Ordinary and the Quotient Singular Value Decomposition are given. These matrix decomposition techniques, known from linear algebra, form the basis for this work. Then some mathematical concepts are defined : the measurement space, the signal space, the oriented energy of a vector sequence and the oriented signal-to-signal ratio of two vector sequences. With these concepts we will develop two signal separation principles in Chapters 5 and 6. At the same time they provide some means to determine in which sense the signal separation methods are optimal.

Chapter 4

A new on-line algorithm for SVD-based signal separation

4.1 Introduction

This Chapter describes the development of an on-line algorithm for updating the left singular matrix in the OSVD of a data matrix, each time a new column is appended. In the first section of this Chapter it is stated that the SVD is used with growing interest in DSP applications. In the near future SVD is expected to be a tool in signal processing, just as FFT is since the mid seventies. Moreover, the need for an on-line computational strategy in multichannel signal processing applications is stated. In the next section an algorithmic scheme will be developed, which is essentially based on a rank-one update of the covariance matrix of the problem. Section 4.4 furthermore shows that the classical numerical difficulties that accompany the problem of the normal equations (rank deficiency due to round-off errors) are avoided in this scheme.

The algorithm is basically a rank-one updating of the covariance matrix. New elements in this on-line algorithm are :

1. the application of only one single plane rotation, instead of complete diagonalization of the covariance matrix, per new column appended (see section 4.7)
2. its adaptivity by applying exponential weighting (see section 4.5)
3. a new approach to compute the rotation angle, such that no square root has to be computed, nor rounding errors are made (see section 4.6)

An analytical convergence proof for the algorithm has not been found : the worst case conditions for each step in the algorithm resulted in unrealistic values. Therefore a more empirical approach for convergence of the algorithm is given in section 4.7. The main result is that for each appended p-column, the algorithm requires $O(4p^2+13p)$ additions and multiplications for obtaining the updated left singular matrix.

4.2 SVD : a valuable tool for the DSP-engineer

It will be demonstrated in the following Chapters that the Ordinary Singular Value Decomposition (OSVD) of a matrix (see Eq. (3.1)), constitutes a main tool in signal separation problems. But also in linear least squares problems (adaptive filtering, linear prediction), in methods using principal component reduction (image and speech processing, modal analysis), in rank-determination problems (identification, model reduction) etc. SVD is used with growing interest.

Designers of digital signal processing systems for medical, automotive or consumer applications or in telecommunications, automation or fabrication, usually are given a variety of signals measured with a certain precision (say 10%) and are requested to extract in real-time useful information from these data. Because of the limited accuracy of the measurements, the data should be handled with care, while on the other hand the speed is rather crucial because of the real-time nature of the application. In the design process a number of tools, like FFT, are offered from applied mathematics, with which the designer can experiment in order to find a signal processing algorithm which meets the specifications. These tools can be used and evaluated at a high (software) level in the top-down design. Moreover, depending on the needs, these tools can be tuned or adapted to the specific constraints of the application, in order to obtain a cost-effective and reliable signal processing system. FFT has been such a tool in signal processing since the mid seventies and SVD is expected to become an additional one in the near future.

In recent years one can witness an enormous expansion of computational power at all levels : supercomputers, workstations, minicomputers and microcomputers, VLSI, etc. In addition the measurement power is increasing by cheap sensors, transducers and data acquisition equipment. However in practice it is much more difficult to increase the accuracy of the measurements than to increase the volume of the measurements. Hence the need for methods and software which can extract more accurate information from the measured data is more acute even at the expense of Kflops of computations. In this situation we believe that SVD is a very important tool which allows to take profit of the expansion of the computational power in order to improve the accuracy. However, its widespread use is still hampered by the computational burden. Hence for SVD, like for FFT, special efficient algorithms (software), coprocessors and application specific integrated circuits (ASIC's) (hardware) are needed.

2.1 Introduction

The detection of the antepartum fetal electrocardiogram (FECG) from signals recorded with electrodes on the mother's skin, is a typical signal processing application, where the weak signal of interest (the FECG) is disturbed by the presence of much stronger, unwanted signals (the maternal ECG).

In this Chapter, we will therefore introduce the reader into this biomedical signal separation application and its specific problems. Then the clinical relevance of the cutaneously recorded FECG is discussed. We will furthermore give a brief overview of the existing methods for the elimination of the maternal ECG (MECG) from abdominal recordings. These methods can be divided into two classes : the subtraction methods and those that use linear combinations of the recorded signals to eliminate the MECG. In Section 2.3 we will formulate the FECG-problem in mathematical terms, which leads to a general signal model. Furthermore, considerations are made about the uncertainty of this model and about noise. Finally, the last section of this Chapter gives a general solution for the elimination of the MECG by finding the coefficients in the linear combinations of the recorded signals. In Chapters 5 and 6 two SVD-based techniques are presented for determining these coefficients appropriately.

2.2 Detection of the Fetal Electrocardiogram

2.2.1 Defining the problem

The heart is the engine of our body. It maintains the circulation of blood through the blood vessels to transport oxygen and nutrients to the various organs and tissues all over the body. After "desoxigenation", the blood is recollected by the heart and pumped to the lungs, where fresh oxygen is added. This mechanical action of the heart is preceded by an electrical depolarization wave through the heart muscle, followed by a repolarization wave. This electrical activity generates an electrical current that propagates through the body and results in potential differences, measurable between electrodes on the skin. The registration and graphical representation of these potential differences, recorded as a function of time, is called the **electrocardiogram** (ECG).

As for the adult ECG it should be possible to obtain a set of potential tracings, describing the electrical activity of the fetal heart. Most accurate methods in this field are invasive as they use an electrode, placed on the fetal scalp ([41], [44]). This technique has become common practice in obstetrics, but is only feasible during labour, after rupture of the membranes. Therefore it is important to look for non-invasive techniques to permit the registration of a fetal electrocardiogram (FECG) during pregnancy, making an earlier diagnosis possible. The task of obtaining a fetal electrocardiogram from electrodes on the mother's skin, is fundamentally equivalent to the adult ECG problem, but some **specific practical difficulties** arise in this case :

- The omnipresent maternal ECG (MECG) forms the main interference: even in abdominal signals it is still 3 to 15 times larger than any fetal contribution.

- Since the FECG is of low voltage, other noise levels become relatively high : electromyographic activity of the maternal abdomen and uterus, 50 Hz net-interference and even noise from electrodes and amplifiers are not negligible anymore.

- Another problem is the large variability of the way cutaneous potentials are generated by the internal bioelectric sources. This is in the first place due to differences between subjects. But for one subject, changes in the configuration of the volume conductor, depending on the stage of pregnancy, can also play an important role. Some examples of these changes are fetal growth, creation of new conducting paths, changes in the characteristics of the amniotic fluid and placenta, the changing geometry of the abdomen during pregnancy, etc.

- The position of the electrodes is also of capital importance. Due to fetal movements, it appears that rather well chosen electrode locations can become completely useless in the course of an experiment.

- The respiration of the mother, at last, can also have a critical influence on the signals, since it is a kind of amplitude modulation.

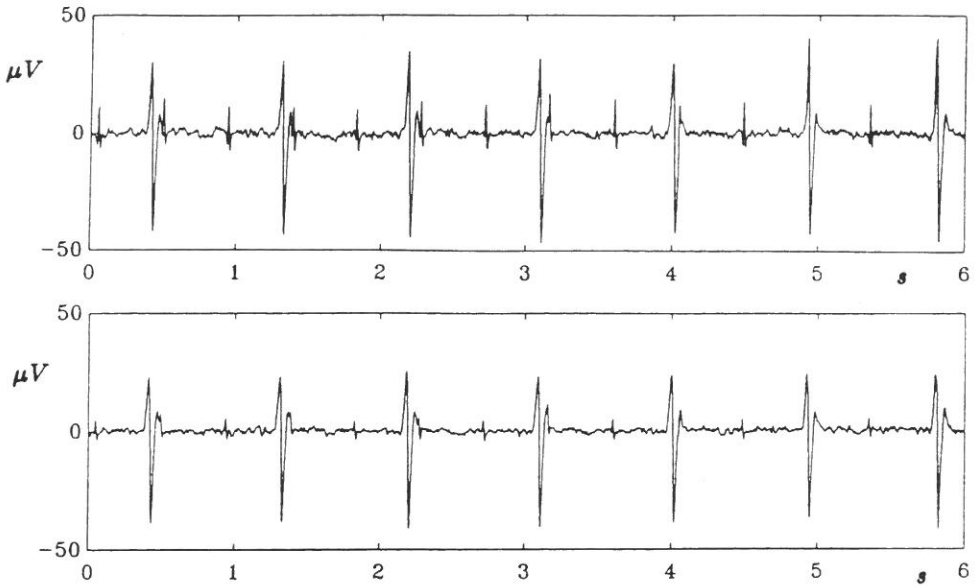

Figure 2.1: *Two potential signals, recorded on the maternal abdomen and containing both MECG and FECG.*

In Figure 2.1 two signals, recorded with electrodes on the maternal abdomen, are shown. This illustrates the small size of the FECG compared to the much stronger MECG. It can be observed from the figure that the fetal heart rate is almost twice the rate of the maternal heart. Sometimes fetal heart complexes coincide with maternal complexes, which hampers an easy analysis of the fetal electrocardiogram, e.g. for monitoring the fetal heart rate (FHR).

2.2.2 Clinical relevance of the cutaneously recorded FECG

The antepartum fetal electrocardiogram has not been analysed extensively up till now, mainly because of two reasons : first it was very difficult to obtain clear, abdominally recorded, fetal heart signals from which diagnostic parameters could be derived, and secondly not much is known about the distribution and propagation of the fetal cardiac currents in the maternal body. The usefulness and relevance of the antepartum FECG is in two main areas : *fetal monitoring* and *diagnosis* of the fetal physical condition. In this section we will discuss some applications where the antepartum fetal ECG can be very useful.

1. **Monitoring the fetal heart rate (FHR)**
   The primary goal of **fetal monitoring** is to observe the "well-being" of the fetus ([32], [66], [71]). This is usually accomplished by observing the fetal heart rate (FHR) and its beat-to-beat variability. The variations of the instantaneous fetal heart rate (FHR) are a result of a continuous interaction of the nervous system. A loss of beat-to-beat variability may be an indication of a potential danger for the fetus. On the other hand, a healthy and happy fetus moves and kicks from time to time, resulting in variations of the FHR. Existing methods are based on the Doppler-shifted ultrasonic heart echo (ultrasonocardiography) and on audio techniques (phonocardiography) ([56]). However, those techniques have some important drawbacks and technical limitations :

   - The Doppler ultrasound method requires that the beam is pointed to the fetal heart, which is very difficult to meet, due to fetal and maternal movements during the course of the experiment.
   - Classical monitoring techniques don't record the real beat-to-beat variability, but a mean over three beats, which hampers the detection of extrasystoles (i.e. one extra beat in between the regular beat-to-beat pattern).
   - Monitoring units are often only able to monitor a fetal heart rate up to 220 bpm (beats per minute). In case of higher rates (e.g. 240 bpm), this number is divided by 2, resulting in a quite normal, but erroneous rate (120 bpm). In reality the baby is in tachycardia (a heart rate higher than 200 bpm).

An electrocardiogram (ECG) however can provide much more information about the fetal condition. Furthermore, it provides more accurate information about the fetal heart rate. Since the mechanical pumping action of the heart is initiated by an electrical signal, techniques monitoring the electrical action of the heart, are more reliable.

2. **FECG for differential diagnosis of tachycardia**
   The fetal electrocardiogram has also a **diagnostic** value. By observing the FHR, arrhythmia, such as tachycardia (FHR higher than 200 bpm) and bradycardia (FHR lower than 100 bpm), as well as decelerations and accelerations of the heart rate can be detected. However, the waveform (see Figure 2.2) of the fetal ECG contains extra information to discriminate between various pathological situations. The duration of the QRS-complex e.g. is a measure to determine whether the tachycardia is *supraventricular* (a normal narrow QRS-complex) or *ventricular* (a wide QRS-complex) [23]. Supraventricular means that the cause of the tachycardia is in the upper part of the heart, above the ventricles. This is where the normal electrical action of the heart is initiated (in the sinus node) and propagated to the AV (Atrio-Ventricular) node. Ventricular tachycardia originate in the ventricular muscle; they are known to be more dangerous and require a totally different therapeutic approach.

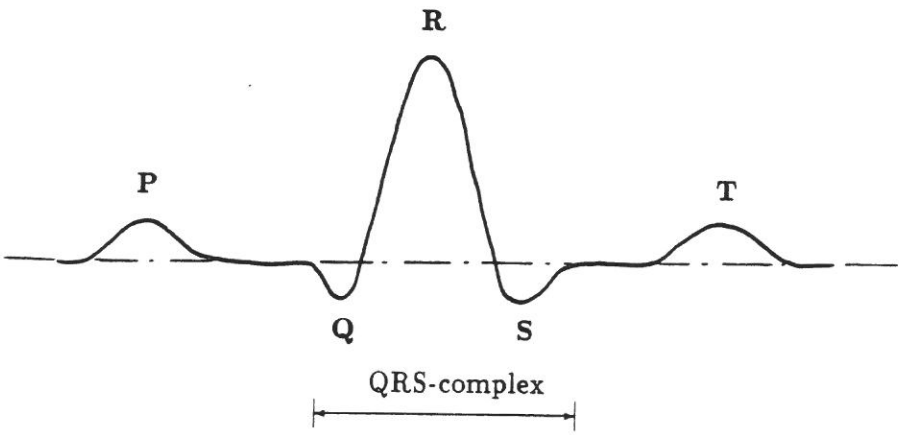

Figure 2.2: *The cardiac cycle with the three important waves : the P-wave, the QRS-complex and the T-wave.*

Not only the QRS-complex in the FECG waveform has a diagnostic value, also the P-wave plays a key role. In order to discriminate between the different forms of supraventricular tachycardia (e.g. Atrio Ventricular Nodal Reentry Tachycardia, Wolff Parkinson White Syndrome, etc.) [23], the position and the sign of the P-wave in the ECG is very important, which requires a technique to detect this P-wave (see Chapter 5).

3. **The FECG for monitoring of therapy**
   Another important application of the antepartum fetal ECG is the monitoring of therapy for intermittant fetal tachycardia. It is possible to reduce the periods of some fetal tachycardia by medication. However, since this therapy is transplacentar, it is very difficult to determine the right dosis and to evaluate the effect of the therapy on the fetal heart rate. Indeed, in order obtain therapeutic levels in the fetus, the mother has to be brought into a subtoxic state. Here, a fetal ECG would again be very helpful, such that the effect of the drugs can be monitored constantly, preventing that the mother would unnecessarily be exposed to toxic levels.

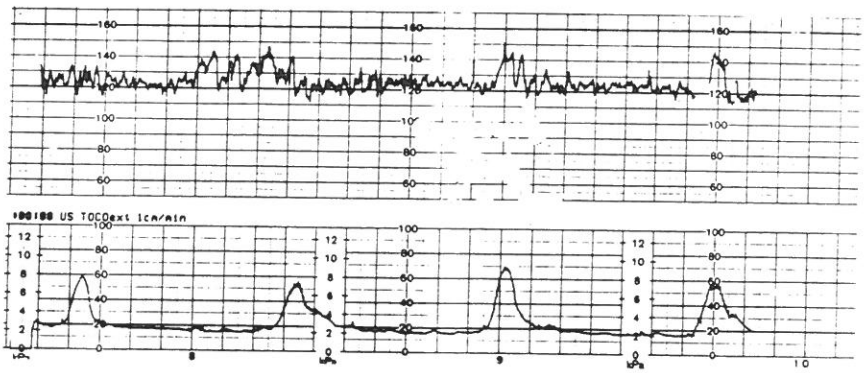

Figure 2.3: *Tocodynamometry : the relation between the instantaneous FHR (upper tracing) and the contractions of the uterus (lower tracing).*

4. **The FECG in tocodynamometry**
   Not only fetal tachycardia (a very high FHR) but also fetal bradycardia (a very low FHR) have to be diagnosed. Tocodynamometric recordings (see Figure 2.3) e.g. monitor the relation between the contractions of the uterus during labour, and the instantaneous fetal heart rate. Due to an increase of pressure in the uterus or due to an insufficient supply of oxygen, the fetus comes into a bradycardial situation. It

is important for the obstetrician to diagnose whether this situation is critical or not.

5. **Quantification of fetal movements**
   Another interesting topic for obstetricians is the possibility to quantify fetal movements, if information about the orientation of the electrical axis of the fetal heart can be combined with information about the fetal position and orientation. This is only possible if more than one fetal signal can be derived, such that the equivalent fetal heart vector can be construced. Changes of the position and orientation of this vector would then be an indication of fetal movements. Up till now the only way to observe fetal movements is by echographic recordings or simply by the feeling of the mother. With our signal separation method it would be possible to provide the obstetrician with information such as : "during the last hour, the baby changed his position seven times".

6. **Quantification of fetal respiratory sinus arrhythmia (FRSA)**
   In [39] *Goovaerts* did an extensive study with respect to the quantification of fetal respiratory sinus arrhythmia (FRSA), a mechanism, by which respiration modulates the heart rate. Therefore, data about the fetal heart rate (obtained after FECG-detection from abdominal potential signals) and fetal breathing movements, obtained with a special transducer, are combined in this study.

7. **FECG for determination of the systolic time intervals**
   Finally, an antepartum fetal ECG might also be important in studies that try to determine the systolic time intervals ([55]) and more specifically the pre-ejection period (PEP) and the ventricular ejection time (VET). The measurement of the systolic time intervals shows a relationship with myocardial contractility, and the knowledge of changes in this myocardial contractility may supplement the interpretation of FHR patterns as an indicator of the presence or absence of fetal distress.

Summarizing, the measurement of a clear antepartum fetal electrocardiogram could yield a large amount of information for monitoring the fetal condition. In this dissertation some SVD-based methods are developed and applied to eliminate the much stronger maternal ECG and to extract the fetal ECG from the cutaneously recorded potential signals.

2.2.3 Existing methods for MECG-elimination

The first one to measure the fetal electrocardiogram in recordings on the maternal abdomen was *Cremer* [24] in 1906, using silver electrodes and a string galvanometer. From that moment on a lot of methods have been developed to eliminate the much stronger disturbing maternal ECG from the recordings. The earliest attempts and the most straightforward approaches to solve the FECG-problem have involved a **direct scaled subtraction** of a thoracic or near-thoracic MECG from an abdominally measured composite of maternal and fetal heart signals.

Sureau and Trocellier [77] tried to detect a pure MECG signal, e.g. from the maternal thorax, similar in amplitude and waveform to the MECG that appears in the abdominal signal. This pure MECG signal was, after appropriate amplification, subtracted from the abdominal signal. It has been proved, however, that the relationship between thoracic and abdominal ECG is not, in general, a simple scalar multiplication.

Schuler [72] and *Van Eyk* [31] created a virtual depth electrode by electrically adding the signals coming from the surface electrodes. To this end, they used respectively a resistor network and a two-dimensional thick film potentiometer. The reduction of the MECG in the surface electrode signal was accomplished by subtraction of the virtual depth electrode signal from it.

Wheeler [94] combined a blanking and subtraction method to obtain a completely pure FECG. Two threshold levels discriminated between FECG and MECG or MECG + FECG complexes. If a coincident MECG + FECG complex was detected, a pure MECG complex, residing in memory, was subtracted from it. Other non-coincident MECG complexes were blanked. A major drawback of this method is its dependency on the size of the fetal R-wave. The system did not detect the FECG complex if for some reason its amplitude decreases, e.g. between 27 and 34 weeks of gestation.

Reichert and Longini [69] proposed an orthogonalization method (using the Gram-Schmidt procedure) for three measured signals. The MECG contribution in an abdominal signal was then obtained as a linear combination of these three orthogonal signals. Again subtraction of this combination from the abdominal FECG + MECG signal gave the desired FECG. But due to a certain degree of correlation between the constructed combination

signal and the FECG, not only the MECG was cancelled, but the FECG was also be diminished.

To reduce this error, *Longini* [49] proposed to orthogonalize three thoracic MECG signals and to use these three near-orthogonal functions to cancel the MECG of an abdominal signal. He also used a Gram-Schmidt orthogonalization process.

The main difficulty with these presented **"subtraction methods"** is the fact that the shapes of sequential MECG complexes not always are identical due to breathing and changing configurations. Furthermore, the maternal signal is usually 3 to 15 times larger than the fetal signal, so that the errors in such direct attempts for cancellation are generally too large to permit the resolution of individual fetal ECG complexes.

More complex methods to reduce the MECG used signal processing techniques such as averaging, matched filters, auto- and crosscorrelation and estimation. *Van Bemmel* [4] used two averagers, one of which was synchronized with the maternal ECG, while the other was synchronized with the fetal ECG. The problem here is that this method is only applicable for the special case of pulse-like signals that are almost periodical.

Ferrara [33] developed a two-stage method. In the first step the MECG was eliminated using the adaptive noise canceller of *Widrow* [95]. The signal resulting from this step is a linear combination of one abdominal recording containing both MECG and FECG and a set of filtered signals containing only MECG (thoracic recordings). In the second step the FECG-to-noise ratio was improved by using time-sequenced adaptive filtering in order to track the rapidly time varying statistical character of recurring pulses in noise. The computational and data storage requirements for this technique seem to be extensive.

Typical for all these mentioned methods is the fact that the FECG contribution in the output is never larger than the portion that was already present in the input abdominal recording. This is due to the fact that they try to eliminate all MECG contribution in one signal only, in some way or another (usually by simple subtraction). The only method that tries to improve the FECG-to-noise ratio, accomplishes it by reducing the noise.

On the other hand one can consider a second big group of methods that try to obtain a "clean" FECG by a **linear combination** or weighted sum of a number of electrode signals. This is a kind of "spatial filtering". The methods differ in the way they determine the (weighting) coefficients in this linear combination.

Bergveld and Meyer [6], [7] used the optimization procedure of Hildreth and d' Esopo with the boundary conditions that the coefficients should all be positive and that their summation should exceed some positive value. The method only used abdominal leads and a back-electrode, because it was stated that the use of thoracic leads would have a negative effect on the FECG-to-noise ratio. With respect to electrode placement, some standard positions are proposed but the problem is then that, if no FECG contribution appears in the recordings, no FECG will be detected in the resulting signal. This technique only found some signal as a linear combination of electrode signals, that was not even optimal in some FECG-to-noise sense.

Van Oosterom ([60], [61]) obtained an MECG-free FECG-signal by using a two step Singular Value Decomposition based method. The method combined only abdominal recordings to perform the "spatial filtering". But it depends on a manual identification of one segment containing only one maternal QRS-complex and another segment containing only one fetal QRS-complex. The fact that only these intervals were considered to contain useful information, together with the numerical difficulties that resulted from it, are two important drawbacks of the method.

All of the mentioned methods result in only one FECG signal that should be free of MECG contributions. However, for the adult ECG at least three signals are required to describe the electrical heart activity adequately. It is expected therefore that the FECG should also consist of more than one signal. Another drawback of most published methods is that the application in a clinical environment is too sensitive to actual electrode location, human interaction, stage of pregnancy, position of the fetus, etc.

The methods that will be presented in this dissertation belong to the second class of methods, as they try to eliminate the MECG by linear combinations of the recorded potential signals. The coefficients are determined using Singular Value Decomposition based techniques.

2.3 Modelling the FECG-problem

2.3.1 The signal model

The formulation of the FECG-problem in mathematical and geometrical terms consists of a two step procedure. First, the electrical activity of the heart — as well as of other organs — has to be modelled as a bioelectric current source. The second part in the analysis concerns the question how the potential distribution on the skin is obtained due to the current generation by all present bioelectric sources. The solution to the first problem is based on the observation that, at a considerable distance from the heart, its electrical activity can be represented in first order approximation by an equivalent current source dipole vector with fixed position ([67], [78]). The magnitude and direction of this dipole vector may change with time. This variation can be described by a set of time-orthogonal signals.

In general, one can associate with each bioelectric current source X_l a set of time-independent signals, that describe the electrical activity of the source. It is always possible to orthogonalize these signals (by applying an orthonormal rotation, by the Gram-Schmidt method, etc.), to form a set of time-orthogonal signals, the so called **source signals**. E.g. the maternal heart and the fetal heart are two bioelectric sources, that each can be described by a number of time-orthogonal signals. Assume that there are in general x bioelectric sources in a medium and that r source signals suffice to represent the electrical activity of all these internal sources. Then a source signal vector $\mathbf{s}(t)$ can be defined as

$$\mathbf{s}(t) = \begin{pmatrix} s_1(t) \\ \vdots \\ s_r(t) \end{pmatrix} \tag{2.1}$$

However, the main problem is that one cannot measure these internal source signals directly. Instead, the time variance of the potential differences between electrode pairs placed on the body surface, are measurable and are called the **measurement signals** $m_i(t)$.

Suppose that p measurement signals from cutaneous electrode pairs are measured and arranged in a measurement signal vector

$$\mathbf{m}(t) = \begin{pmatrix} m_1(t) \\ \vdots \\ m_p(t) \end{pmatrix} \tag{2.2}$$

Due to the resistive and quasi-static behaviour of the body as a conducting medium in the frequency range of interest (between about 0.5 Hz and 100 Hz) [67], there exists a linear relationship between the measurement signal vector $\mathbf{m}(t)$ and the source signal vector $\mathbf{s}(t)$. Indeed, each measurement signal $m_i(t)$ can be written as a linear combination of r source signals $s_j(t)$, plus additive measurement noise, represented by a signal $n_i(t)$. This leads to the following relations

$$\begin{cases} m_1(t) = t_{11}s_1(t) + \ldots + t_{1r}s_r(t) + n_1(t) \\ \vdots \\ m_p(t) = t_{p1}s_1(t) + \ldots + t_{pr}s_r(t) + n_p(t) \end{cases} \tag{2.3}$$

or in signal vector notation

$$\mathbf{m}(t) = T\,\mathbf{s}(t) + \mathbf{n}(t) \tag{2.4}$$

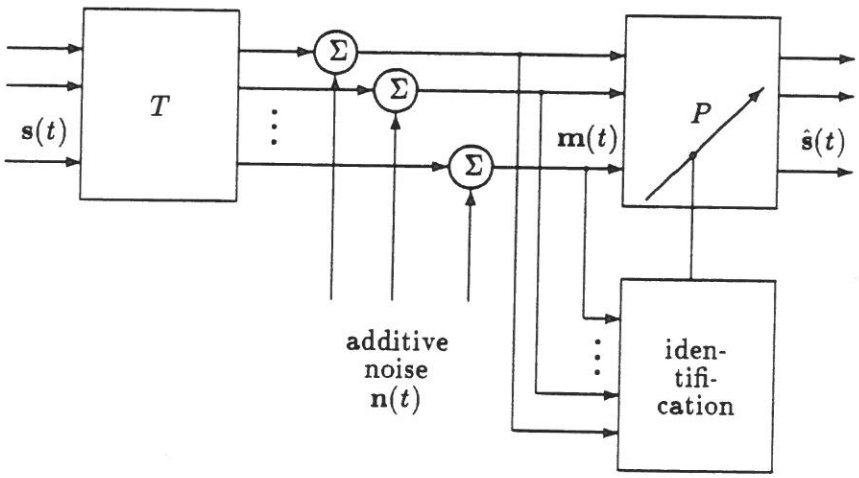

Figure 2.4: *The basic scheme of the FECG-problem.*

In this equation, only $\mathbf{m}(t)$ is known. The matrix T, that contains all coefficients in the linear combinations, is called the **transfer matrix** and is completely determined by the geometry of the body, the electrode and source positions, and the conductivities of the body tissues.

The separation of the MECG and FECG can now be accomplished by finding estimates for the source signals $s_j(t)$. Indeed, some of these source signals describe the electrical activity of the fetal heart, others describe the activity of the maternal heart, etc. Actually, characterizing the electrical activity of the fetal and adult heart is a so called **inverse problem** : it consists in estimating the internal source signals that have generated a given set of external measurement signals. The methods that will be presented here try to find an inverse for the transfer matrix T (Figure 2.4). Application of this "inverse transfer" to the measurement signal vector $\mathbf{m}(t)$ should then result in an estimation $\hat{\mathbf{s}}(t)$ of the source signal vector $\mathbf{s}(t)$.

2.3.2 Model uncertainty

In the previous section a mathematical model for the signal transfer from bioelectric current sources to body surface electrodes has been defined. This transfer is assumed to be linear, resistive, quasi-static, isotropic and uniform [67], as expressed by Eq. (2.3) and Eq. (2.4). However, the transfer coefficients in these relations are subject to some uncertainty, since they depend on the geometry of the body, on the conductivities of the different organs, tissues, bones, muscles, lungs, etc. on the positions of the electrodes on the skin and of the sources within the body.

- A first cause of uncertainty is the large interpatient variability. It is obvious that data concerning length, weight, contour, volume, etc. differ on a patient to patient basis. But besides this geometrical diversity many studies and publications furthermore disagree with respect to conductivity and resistivity values of the body tissues [59].
- Furthermore, the geometrical and conductivity data of one patient vary with time. In fetal electrocardiography, changes in the transfer occur due to fetal growth, due to the creation of new conducting paths, due to another position of the fetus in the uterus, due to changes in the characteristics of the amniotic fluid and placenta, due to the changing geometry of the abdomen during pregnancy, etc.

- But also respiration influences the recordings, as it changes the resistivity as well as the geometry of the lungs. This can be observed as an amplitude modulation in most ECG-recordings. The influence of gastro-intestinal activity and of the contents of the stomach becomes important in abdominal recordings, while in fetal ECG recording the fetal movements as well as the possible contractions of the uterus can affect the measurements considerably.

- In clinical practice, finally, the positioning of the electrodes on the skin is subject to some errors and deviations from previously specified locations.

Due to this large variability and uncertainty in the transfer, no fixed "body-model" for signal transfer from bioelectric current sources to the electrodes, placed on the skin, can be developed. As a consequence, it is very difficult to define a standard pattern for electrode positioning in order to obtain an optimal signal. An extensive study on the conduction of the fetal heart signal to the body surface of the mother has been carried out by Oostendorp [59].

A very important phenomenon that has been observed already by many researchers, who try to record the fetal electrocardiogram from the maternal abdomen, is the decrease in amplitude of this FECG around the 30th week, while this is generally accepted to be the most important period for monitoring the fetal condition. This is mainly due to the isolating effect of the vernix caseosa, which surrounds the fetus at that time [57], [59], [70]. Up till now no suitable solution to solve this problem has been proposed. For this reason, some doctors still prefer phonocardiography or ultrasound techniques above the abdominally recorded FECG.

2.3.3 Noise considerations

During the transfer from source to measurement device, a signal may undergo changes, some desirable and some undesirable. An example of a desirable change is the Doppler shift of a radar echo caused by relative motion between source and object which caused the echo. However, most changes are undesirable. This leads to the following possible definition of noise :

> *Noise are the undesired changes a signal undergoes in its transfer from one place to another.*

In biomedical measurements three classes of noise can be distinguished : additive noise, quantization noise and multiplicative or modulation noise.

We will now discuss in more detail each of these three classes of noise :

1. Most noise is an addition to the signal of various forms of disturbance, and therefore called **additive noise**. The disturbance occurring as additive noise in bioelectric measurements is mainly caused by two phenomena. First, the use of electronic recording equipment implies the existence of **thermal noise**. The power of this noise is proportional to the absolute temperature and since its spectrum is flat, it is also called white noise. It can be shown that the mean power of such a random process after filtering is proportional to the bandwidth of the filter. Therefore lowpass filters must be designed such that the bandwidth of the measured signal is reduced to that of the useful signal.

   A second noise phenomenon is caused at the contact between electrode and human body. In theory, the junction potential that exists over this connection is the same for all electrodes. This means that, if a potential difference is measured between two electrodes, the junction potentials of both electrodes compensate each other and add up to zero. In practice however, some instabilities exist in the junction potential due to pressure, movements, bad contact, sweat, etc. These instabilities differ for each electrode such that a resulting fluctuating potential difference will be recorded. The spectrum of this disturbance is typically that of $1/f$-noise. Therefore a high pass filter must be designed in order to suppress as much as possible this kind of noise.

2. Another kind of undesirable changes that a signal can undergo are the fluctuations which result from certain transformations of a non-linear

nature. An example is the so called **quantization noise**, which results from sampling a signal and converting it into a series of quantized values. Although this process is not strictly additive, it is usually modelled as additive noise.

3. The third class of noise that appears in biomedical recordings is an unwanted modulation introduced by a time varying transmission medium. This is often called **multiplicative** or **modulation noise**. An example of this is the influence of respiration in ECG recordings.

Summarizing, we can refer to the mathematical model of Eq. (2.4), where the noise signal vector $\mathbf{n}(t)$ contains the additive noise and quantization noise, while the influence of the multiplicative noise can be expressed by the time-dependence of the transfer coefficients in matrix T.

> *"Nous concluerons en disant que ce qui distingue le signal du bruit c'est que l'un transporte une information qui nous interesse, l'autre une information qui ne nous interesse pas, pour le moment tout au moins "* [51]

2.4 Solving the FECG-problem

Suppose p signals $m_i(t)$ are recorded from electrodes on the maternal skin and a $p \times q$ data matrix M is constructed, where the rows of M contain q samples of the p measured signals. According to the model described by Eq. (2.3), each of these signals is a linear combination of r signals $s_j(t)$, generated by a number of electrical sources and therefore called source signals. Essential to this signal separation problem is that we are very interested in some of these source signals (the fetal heart signals), while we would like to eliminate as much as possible some others (the maternal heart signals, 50 Hz interference, EMG from maternal muscles, etc.) from the measured signals. Furthermore some very weak signals of minor importance may occur in the observations.

The source signal vector $\mathbf{s}(t)$ can then be partitioned as follows

$$\mathbf{s}(t) = \begin{pmatrix} \mathbf{s}_u(t) \\ \mathbf{s}_w(t) \\ \mathbf{s}_o(t) \end{pmatrix} \begin{matrix} r_u \\ r_w \\ r_o \end{matrix} \qquad \text{with} \quad r_u + r_w + r_o = r \tag{2.5}$$

where $\mathbf{s}_u(t)$ is the signal vector that contains r_u source signals to be eliminated from the observations (e.g. the MECG), $\mathbf{s}_w(t)$ is the signal vector that contains r_w source signals to be extracted from the observations (e.g. the FECG) and $\mathbf{s}_o(t)$ is a signal vector containing r_o source signals of minor importance (e.g. the electrical activity of the stomach and the muscles).

Suppose that the p observations $m_i(t)$, called the measurement signals, are arranged in a measurement signal vector $\mathbf{m}(t)$ as in Eq. (2.2). These observations contain contributions from all source signals, as expressed by Eq. (2.4).

The columns of the $p \times r$ transfer matrix T are vectors in the p-dimensional column space of data matrix M. In analogy with the partitioning of the source signal vector $\mathbf{s}(t)$, the columns of T are grouped, such that

$$T = \begin{matrix} r_u & r_w & r_o \\ \multicolumn{3}{c}{\begin{pmatrix} T_u & T_w & T_o \end{pmatrix}} \end{matrix} \begin{matrix} \\ p \end{matrix} \tag{2.6}$$

and such that Eq. (2.4) can be written as

$$\begin{aligned} \mathbf{m}(t) &= \begin{pmatrix} T_u & T_w & T_o \end{pmatrix} \begin{pmatrix} \mathbf{s}_u(t) \\ \mathbf{s}_w(t) \\ \mathbf{s}_o(t) \end{pmatrix} + \mathbf{n}(t) \\ &= T_u\, \mathbf{s}_u(t) + T_w\, \mathbf{s}_w(t) + T_o\, \mathbf{s}_o(t) + \mathbf{n}(t) \end{aligned} \tag{2.7}$$

It is our goal to find the weight coefficients in the linear combinations of the p measured signals, such that in the resultant signals all undesired contributions are eliminated and an optimal detection of the wanted source signals is obtained. This can be described mathematically as follows : find a $p \times r_w$ weight matrix W such that

$$\begin{aligned} \hat{\mathbf{s}}_w(t) &= W^t\, \mathbf{m}(t) = W^t\, T\, \mathbf{s}(t) + W^t\, \mathbf{n}(t) \\ &= W^t T_u\, \mathbf{s}_u(t) + W^t T_w\, \mathbf{s}_w(t) + W^t T_o\, \mathbf{s}_o(t) + W^t \mathbf{n}(t) \end{aligned} \tag{2.8}$$

where $\hat{\mathbf{s}}_w(t)$ is an estimation of the signal vector $\mathbf{s}_w(t)$, containing the source signals of interest.

It is clear from Eq. (2.8) that these linear combinations contain no contributions from the undesired signals anymore and that they approach the original wanted source signals in an optimal way if

$$W^t T_u = 0 \quad \text{and} \quad W^t T_w = I \tag{2.9}$$

Geometrically, this can be interpreted as follows : an r_w-dimensional subspace W of the p-dimensional column space of the data matrix has to be found, which is orthogonal to the subspace spanned by the columns of T_u and which is equal to the subspace spanned by the columns of T_w. These conditions are only fulfilled if the subspaces T_u and T_w are orthogonal to each other. However, this is the big problem, since the transfer coefficients (the elements of the matrix T) are unknown and depend on the configuration of sources and observation points as well as on the signal transfer characteristics of the medium.

In Chapters 5 and 6 two signal separation methods will be outlined. The two methods find a subspace W such that the condition $W^t T_u = 0$ is approximately satisfied. Projection onto that subspace will then eliminate all contributions from the disturbing source.

1. signal separation by orthonormal linear combinations of the measured signals ($W^tW = I$) : this method is based on the concept of oriented energy and can be computed by the OSVD of the data matrix.

2. signal separation by non-orthogonal linear combinations of the measured signals ($W^tW \neq I$) : this method is based on the concept of oriented signal-to-signal ratio and can be computed by the Quotient SVD of the data matrix and a matrix constructed by selecting some special intervals from the data matrix.

Both methods will be applied to the problem of extracting the cutaneous FECG and in Chapter 7 a comparison of the signal separation methods is made.

2.5 Conclusion

In this Chapter we stated the problem of detecting the fetal electrocardiogram from a set of cutaneous potential signals. The SVD-based signal separation methods, that are described in this dissertation, will be applied to this biomedical signal processing application. In the first section, the FECG-problem is defined and an overview is given of all existing methods in this field. Then the problem is modelled in mathematical terms and equations, and finally a general solution is derived. It is not the aim of this dissertation to study the abdominal fetal electrocardiogram from a clinical point of view. Instead we will present methods, based on the Singular Value Decomposition, to obtain a fetal ECG, recorded from the maternal abdomen and free from any contribution of the maternal ECG. We will therefore study the Singular Value Decomposition and some useful mathematical concepts in the next Chapter.

Chapter 3

Formulation of Mathematical Concepts using Singular Value Decomposition

3.1 Introduction

At the conceptual level the Ordinary Singular Value Decomposition (OSVD) and the Quotient Singular Value Decomposition (QSVD) provide a unifying framework and a numerically robust approach for the formulation and computation of new mathematical concepts.

In this chapter we focus on some concepts that have already proven to be very instrumental in order to design new algorithms for a wide variety of problems in signal processing and identification. For each presented concept (the measurement space, the signal space, the oriented energy of a set of signals and the oriented signal-to-signal ratio's of two signal sets) we indicate the link or the relation with the Ordinary and Quotient Singular Value Decomposition. These numerically reliable techniques, known from linear algebra, not only provide a means to formulate a concept, but also make the computation of some special values and parameters for each concept possible. Furtheron in this dissertation, the defined concepts are used to develop some signal separation principles.

3.2 Basic theorems for OSVD and QSVD

3.2.1 The Ordinary Singular Value Decomposition (OSVD)

We will restrict the following theorem to real matrices, since this will be sufficient for the mathematical concepts and signal separation methods, described later in this dissertation.

Theorem 1 : Autonne-Eckhart-Young theorem ([3], [30], [36], [38], [46])

For any real $p \times q$ matrix A, there exists a real factorization

$$A_{p,q} = U_{p,p}\, \Sigma_{p,q}\, V^t_{q,q} \tag{3.1}$$

in which the matrices U and V are real orthogonal

$$U\,U^t = U^t\,U = I_p \quad \text{and} \quad V\,V^t = V^t\,V = I_q$$

and $\Sigma_{p,q}$ is a real pseudo-diagonal matrix with nonnegative diagonal elements. The factorization of Eq. (3.1) is called the Ordinary Singular Value Decomposition of matrix A.

Some definitions and nomenclature :

- economical factorization : since we only consider the case $p < q$ in the rest of this work, the decomposition of A can be written in a more economical way, with smaller dimensions of the matrices, as follows

$$A_{p,q} = U_{p,p}\, \Sigma_{p,p}\, V^t_{p,q}$$

- singular values σ_i : the diagonal elements of the pseudo-diagonal matrix Σ , ordered in a nonincreasing way, are called the singular values of A

$$\sigma_1 \geq \ldots \geq \sigma_p \geq 0, \qquad (p < q)$$

- singular vectors : the columns $\mathbf{u}_i$ $(\mathbf{v}_i)$ of U (V) are called the left (right) singular vectors of A.

- singular triplet : the triplet $(\mathbf{u}_i, \sigma_i, \mathbf{v}_i)$ is called the i-th singular triplet of A.

- rank of A : the number of singular values, different from zero, equals the algebraic rank of A

$$\text{if } \sigma_1 \geq \ldots \geq \sigma_r > \sigma_{r+1} = \ldots = \sigma_p = 0 \quad \text{then} \quad r = \text{rank}\,(A)$$

- dyadic decomposition : if the OSVD of a matrix A is known, then A can be written as the sum of $r = \text{rank}\,(A)$ rank one matrices

$$A = \sum_{i=1}^{r} \mathbf{u}_i\, \sigma_i\, \mathbf{v}_i^t$$

3.2.2 The Quotient Singular Value Decomposition (QSVD)

Also for this case we will restrict the basic theorem to real matrices. We will furthermore only use the "economical" notation, in which the pseudo-diagonal matrices are replaced by diagonal ones.

Theorem 2 : The Quotient SVD ([29], [38], [48], [63], [64], [76])

Let A be a real $p \times q$ and B a $p \times k$ matrix (with $p < q$ and $p < k$), then there exist matrices Q_A $(q \times p)$ and Q_B $(k \times p)$, both with p orthonormal columns, and a non-singular $p \times p$ matrix X such that

$$\begin{cases} A = X^{-t} D_A Q_A^t \\ B = X^{-t} D_B Q_B^t \end{cases} \tag{3.2}$$

where D_A and D_B are square diagonal $p \times p$ matrices, with $D_A = \mathrm{diag}(\alpha_1, \ldots, \alpha_p)$ and $D_B = \mathrm{diag}(\beta_1, \ldots, \beta_p)$, $\alpha_i, \beta_i \geq 0$ and with $\beta_1 \geq \ldots \geq \beta_r > \beta_{r+1} = \ldots = \beta_p = 0$, $r = \mathrm{rank}(B)$.

Some definitions and nomenclature :

- quotient singular values : the elements of the set $\left\{ \frac{\alpha_1}{\beta_1}, \frac{\alpha_2}{\beta_2}, \ldots, \frac{\alpha_r}{\beta_r} \right\}$ with $r = \mathrm{rank}(B)$ are called the quotient singular values of the matrix pair (A, B). By convention, these quotient singular values are ordered in a nonincreasing way, such that

$$\gamma(A, B) = \{\gamma_1, \gamma_2, \ldots, \gamma_r\} = \mathrm{orden} \left\{ \frac{\alpha_1}{\beta_1}, \ldots, \frac{\alpha_r}{\beta_r} \right\}$$

  with $\gamma_1 \geq \ldots \geq \gamma_r$.

- generalized eigenvectors : since the matrix X diagonalizes both $A A^t$ and $B B^t$, its columns are the solution for the generalized symmetric eigenvalue problem

$$A A^t \mathbf{x}_i = B B^t \mathbf{x}_i \gamma_i^2$$

  The columns $\mathbf{x}_i$ of X are therefore called the generalized eigenvectors of (A, B). By convention, they will be ordered such that the corresponding quotient singular values are in nonincreasing order.

3.3 The measurement space and the signal space

In multichannel signal processing applications the starting point is usually a set of recorded, measured, captured or acquired signals. These signals are often continuous-time or analog signals. Digital processing of these measured analog signals therefore requires sampling and quantization, a process by which a signal is converted into a series of discrete values.

In view of a mathematical and geometrical formulation of the problem, suppose that p is the number of recorded signals over some time-interval of τ seconds. If a sampling frequency f_s is applied, the given interval contains $q = f_s \tau$ samples per signal. This enables the arrangement of the digitized signals into a matrix structure, the **data matrix** M. This matrix has p rows, that contain the q samples of each signal.

$$\begin{array}{c} \begin{array}{ccccccc} t_1 & t_2 & t_3 & \dots & t_k & \dots & t_q \end{array} \\ \begin{pmatrix} * & * & * & \dots & * & \dots & * \\ * & * & * & \dots & * & \dots & * \\ \vdots & \vdots & \vdots & & \vdots & & \vdots \\ * & * & * & \dots & * & \dots & * \end{pmatrix} \end{array} \quad p \text{ signals} \tag{3.3}$$

In applications where the time relation between the recorded signals is essential (e.g. the registration of an electrocardiogram), simultaneous sampling of all data acquisition channels is required, in order not to introduce a time delay between two successive channels. For the case of simultaneous sampling of the p signals, one can easily give another interpretation to the construction of the data matrix M : at each sampling instant t_k, p values are obtained from the data channels. These p values constitute precisely the k-th column of the data matrix M.

Geometrically, the p values can be regarded as the components of a vector in a p-dimensional space, the **measurement space**, which is a virtual space, whose reference axes are associated with each measured signal. If each vector is represented as a point in the measurement space, the data matrix M gives rise to a cloud of points. Figure 3.1 shows the cloud of points that arises from sampling two random analog signals.

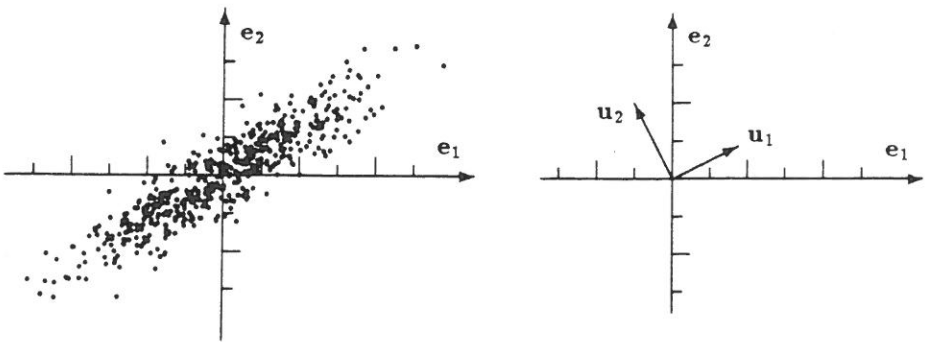

Figure 3.1: *The cloud of points in a 2-dimensional measurement space, corresponding with a* 2×500 *data matrix.*

If the Ordinary SVD of the data matrix M is given by

$$M = U_M \, \Sigma_M \, V_M^t$$

then the columns of the matrix U_M constitute a set of p orthonormal basis vectors for the p-dimensional measurement space. Moreover, if only r of the p singular values of M differ from zero ($r < p$), then the first r columns of U_M constitute an orthonormal basis for an r-dimensional subspace of the measurement space, called the **signal space.** If $r = p$ then both signal and measurement space are spanned by the columns of U_M. In Figure 3.1 the basis vectors $\mathbf{u}_1$ and $\mathbf{u}_2$, found as the columns of U_M for this two-dimensional example, are drawn.

3.4 The oriented energy of a vector sequence

In the previous section we mentioned that it is possible to transform a set of p signals into a sequence of p-vectors, when the p data channels are simultaneously sampled. In this section we will introduce the concept of oriented energy of a vector sequence and show that the Ordinary SVD of the corresponding matrix constitutes the main tool to compute extremal values for this concept.

Definition 1 : Oriented energy : ([27], [28], [75])

Consider a sequence of p-vectors $\{\mathbf{a}_i\}$, $i = 1, \ldots, q$ *and arrange them as the columns of a* $p \times q$ *matrix* A. *Then* $E_{\mathbf{e}}[A]$ *is called the energy of the vector set in the direction of unit vector* $\mathbf{e} \in \Re^p$ *and is defined as :*

$$E_{\mathbf{e}}[A] = \sum_{i=1}^{q} (\mathbf{e}^t \mathbf{a}_i)^2 = \|\mathbf{e}^t A\|^2 \tag{3.4}$$

with $\|\cdot\|$ *the Euclidean norm.*

In words, the oriented energy of a vector sequence $\{\mathbf{a}_i\}$ in some direction $\mathbf{e}$ of the p-dimensional measurement space is a sum of squared projections of the vectors $\mathbf{a}_i$ onto direction $\mathbf{e}$. More generally, one can define the oriented energy of a vector set in a subspace $Q \subset \Re^p$ as

$$E_Q[A] = \sum_{i=1}^{q} \|P_Q(\mathbf{a}_i)\|^2 \tag{3.5}$$

with $P_Q(\mathbf{a}_i)$ the orthogonal projection of the vector set onto subspace Q.

Figure 3.2 shows the polar plot of the oriented energy of the set of vectors for the two-dimensional example of Figure 3.1. Such a polar plot is found by drawing a vector with length $E_{\mathbf{e}}[A]$ in the direction of a variable unit vector $\mathbf{e}$, and this for all possible directions $\mathbf{e}$ in the measurement space $\Re^2$. If $r_A = \text{rank}(A)$, then the figure shows in general a r_A-dimensional surface with r_A directions of extremal energy : one direction of maximal oriented energy, one of minimal energy and $r_A - 2$ directions with an intermediate extremal energy (saddle points).

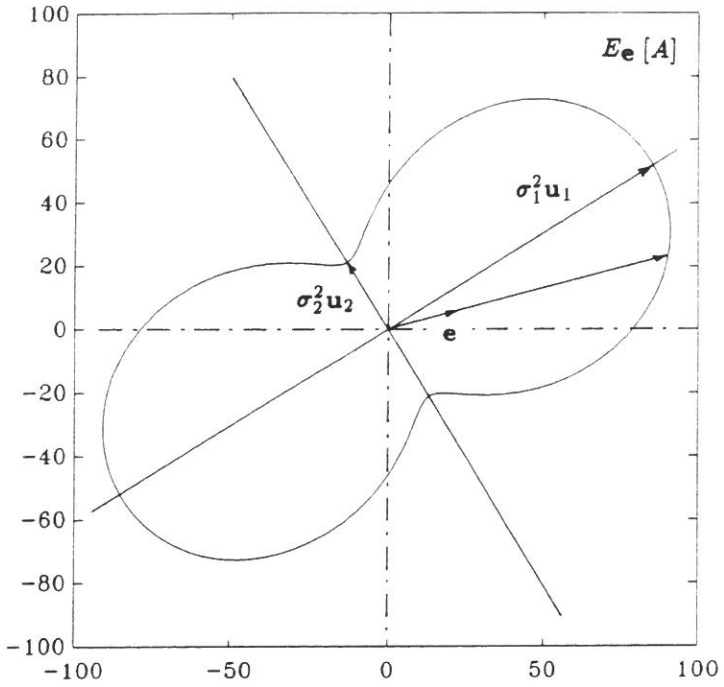

Figure 3.2: *Polar plot of the oriented energy of a vector sequence in two dimensions.*

Consider now the $p \times q$ matrix A that corresponds to the sequence of q p-vectors $\{\mathbf{a}_i\}$ and its OSVD, given by (see Theorem 1)

$$A_{p,q} = U_{p,p}\,\Sigma_{p,p}\,V_{p,q}^t \qquad (\text{for } p < q) \tag{3.6}$$

Each column $\mathbf{u}_j$ of the matrix U in the OSVD of A has the following interesting property $(j = 1, \ldots, p)$:

$$\begin{aligned} \forall\, \mathbf{x} \in \Re^p, \quad \text{with} \quad \mathbf{x}^t\mathbf{u}_i &= 0, \qquad (i = 1, \ldots, j-1) \\ \frac{\|\mathbf{x}^t\, A\|^2}{\|\mathbf{x}\|^2} &\leq \|\mathbf{u}_j^t\, A\|^2 = \sigma_j^2 \end{aligned} \tag{3.7}$$

with σ_j the j-th singular value of A. This means that each $\mathbf{u}_j$ contains the coefficients of a linear combination of the rows of A, such that the squared norm of this linear combination

$$\|\mathbf{u}_j^t\, A\, A^t\, \mathbf{u}_j\| = \|\mathbf{u}_j^t\, A\|^2$$

reaches an extremal value, which equals σ_j^2.

From this property we establish the link between the oriented energy of a vector sequence and the OSVD of the corresponding matrix in the following theorem :

Theorem 3 : Relation between oriented energy and OSVD :

Consider a $p \times q$ matrix A with OSVD as defined in Eq. (3.6). Then

$$E_{\mathbf{u}_i}[A] = \|\mathbf{u}_i^t A\|^2 = \sigma_i^2 \tag{3.8}$$

Furthermore

$$\forall\ \mathbf{e} = \sum_{i=1}^{p} \gamma_i\, \mathbf{u}_i, \qquad E_{\mathbf{e}}[A] = \sum_{i=1}^{p} \gamma_i^2\, \sigma_i^2 \tag{3.9}$$

Proof : see [27]

In words, the OSVD of a $p \times q$ matrix A looks for directions in the column space $\Re^p$ of A, for which the oriented energy of A is extremal. In signal processing applications with a given $p \times q$ data matrix M, this means that the OSVD of M provides an elegant way to determine an orthonormal basis in the measurement space $\Re^p$, according to the energy distribution in this space. Indeed, the vectors of this orthonormal basis correspond to directions of extremal oriented energy in the measurement space. For a more detailed analysis and more properties of the concept of oriented energy, we refer to [27], [28], [75], [83], [84], [87].

3.5 The oriented signal-to-signal ratio of two vector sequences.

Based on the concept of oriented energy of a vector sequence, as defined in the previous section, a similar definition can be formulated for the case of two vector sequences. The oriented signal-to-signal ratio (S-S ratio) of two vector sequences is defined as the ratio of their oriented energies, as follows

Definition 2 : Oriented signal-to-signal ratio : ([27], [28], [87])

The oriented signal-to-signal ratio $R_{\mathbf{e}}[A, B]$ *of two sets of p-vectors* $\{\mathbf{a}_i\}$ *and* $\{\mathbf{b}_j\}$, $(i = 1, \ldots, q$ *and* $j = 1, \ldots, k)$, *in the direction of unit vector* $\mathbf{e} \in \Re^p$, *is defined as :*

$$R_{\mathbf{e}}[A, B] = \frac{E_{\mathbf{e}}[A]}{E_{\mathbf{e}}[B]} = \frac{\|\mathbf{e}^t A\|^2}{\|\mathbf{e}^t B\|^2} \tag{3.10}$$

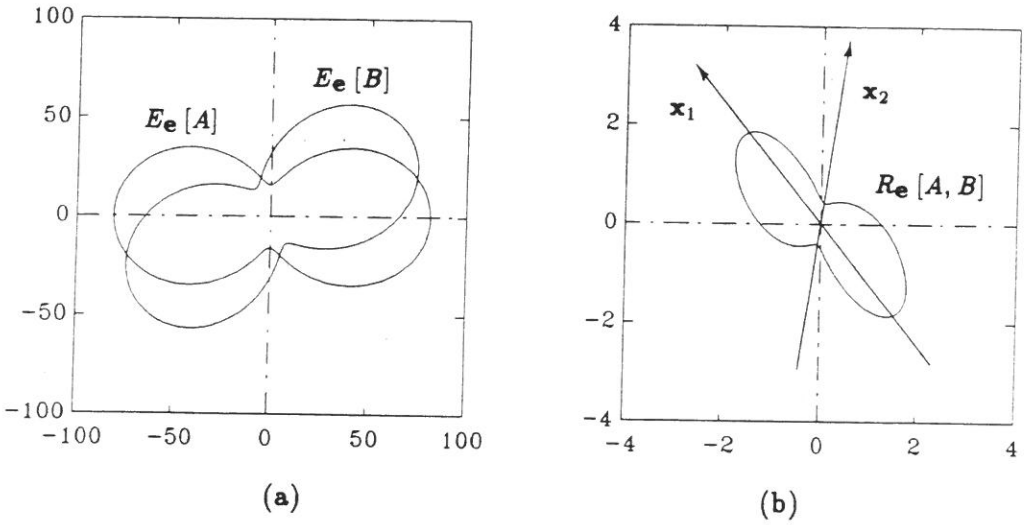

Figure 3.3: *(a) Polar plot of the oriented energy of two vector sequences in two dimensions. (b) Polar plot of the corresponding oriented signal-to-signal ratio in two dimensions.*

A similar plot as Figure 3.2 can now be constructed by drawing a vector with length $R_{\mathbf{e}}[A,B]$ in the direction of a variable unit vector $\mathbf{e}$, and this for all possible directions $\mathbf{e}$ in the column space $\Re^p$ of A and B. In Figure 3.3 this is done in two dimensions ($p = 2$). Figure 3.3.a shows the oriented energy polar plot of two vector sets $\{\mathbf{a}_i\}$ and $\{\mathbf{b}_j\}$, while Figure 3.3.b is the polar plot for the oriented S-S ratio in all directions. Note that there are again 2 directions (in general $r_B = \text{rang}(B)$) of extremal S-S ratio, which are not orthogonal in this case.

It is very important to mention that both vector sequences must have the same dimension p, but their lengths may differ. In signal processing terms this means that the vector sequences $\{\mathbf{a}_i\}$ and $\{\mathbf{b}_j\}$ must both result from sampling the same data channels, but e.g. over some other time interval. In that case both intervals define a cloud of points in the same measurement space. With each cloud a set of orthonormal directions of extremal oriented energy corresponds. But with both clouds only one set of non-orthogonal directions of extremal oriented signal-to-signal ratio corresponds.

A very important property of the S-S ratio is its invariance through a basis transformation in $\Re^p$, characterized by the non-singular $p \times p$ matrix T ([27], [28]). Indeed, one can verify that

$$R_{\mathbf{e}}[A,B] = R_{\mathbf{e}'}[TA,TB] \qquad \text{for} \quad \mathbf{e}' = \frac{T^{-t}\,\mathbf{e}}{\|T^{-t}\,\mathbf{e}\|} \tag{3.11}$$

Consider now the $p \times q$ matrix A and the $p \times k$ matrix B that correspond to the sequences of p-vectors $\{\mathbf{a}_i\}$ and $\{\mathbf{b}_j\}$ ($i = 1,\ldots,q$ and $j = 1,\ldots,k$). Then the QSVD of the matrix pair (A,B) is defined by (see Theorem 2)

$$\begin{cases} A = X^{-t}\,D_A\,Q_A^t \\ B = X^{-t}\,D_B\,Q_B^t \end{cases} \tag{3.12}$$

Each column $\mathbf{x}_j$ of the matrix X in the QSVD of (A,B) has the following interesting property ($j = 1,\ldots,r$) :

$$\forall\,\mathbf{y} \in \Re^p, \quad \text{with} \quad \mathbf{y} \text{ not in span}\{\mathbf{x}_1,\ldots\mathbf{x}_{j-1}\}$$
$$\frac{\|\mathbf{y}^t\,A\|^2}{\|\mathbf{y}^t\,B\|^2} \leq \frac{\|\mathbf{x}_j^t\,A\|^2}{\|\mathbf{x}_j^t\,B\|^2} = \gamma_j^2 \tag{3.13}$$

with γ_j the j-th quotient singular value of (A,B).

The wide acceptance of the OSVD as a reliable method in numerical algebra is due to the existence of a stable and accurate algorithm for its computation : the Golub-Reinsch algorithm [37]. There are many subroutines from well established libraries available, using this basic Golub-Reinsch algorithm. These subroutines compute the three matrices U, Σ and V^t of the **complete** decomposition. In most cases, however, only the U-matrix is required at any time, (e.g. for adaptive AR modelling). It is easy to show that, given data matrix A and knowing U, the other matrices Σ and V in the OSVD can be derived from

$$(U^t A)(A^t U) = \Sigma^2 \tag{4.1}$$

$$U^t A = \Sigma V^t \tag{4.2}$$

To avoid problems with squaring the singular values, it can be preferable to know also the matrix Σ.

The Golub-Reinsch algorithm furthermore implements a typical **off-line** strategy of data analysis : all data should be available at once before the computational work can start. In signal processing applications, this off-line technique has a number of important drawbacks. First, the dimensions $(p \times q)$ of the data matrix A can be very large. Here p is the number of signals and q the number of time instants at which these signals are sampled. In real-time applications q is growing all the time and this often results in an inadmissible computation time $O(qp^2)$. Big efforts have been made to reduce this objection e.g. by introducing strategies for parallel computing, by applying fast Givens rotations, by computing the partial OSVD, by inserting acceleration steps in the iterative part of the algorithm, by using very powerful computers, ...

Furthermore, even if these approaches could accelerate the computational work, an off-line strategy is still not optimal with regard to time variations within the time interval q under consideration. This requires an **adaptive** technique, such that the method is able to "follow" the most recent events, occurring in the data, and to "forget" events, that happened in the far past.

It is therefore also important that **a priori** knowledge can be incorporated, for instance the OSVD of a previous step. This is elementary in signal processing applications, where usually the dimensions of the data matrix are growing with time, such that updating of the computed parameters is required, each time a new column or row is added.

This clearly stresses the importance of and the need for an **adaptive on-line computation strategy** for SVD-based signal processing applications. This new technique should provide U (and Σ) at any instant, by processing data and using these for updating, as soon as they become available.

4.3 Development of the algorithmic scheme

The algorithm that will be developed and outlined in this section is based on some features of the OSVD of a matrix A and its relation with the eigenvalue decomposition of $A\,A^t$. The algorithmic scheme is founded on the following very important theorem :

Theorem 6 : Updating the OSVD after adding a column :

Given a $p \times k$ matrix $A_k = [\mathbf{a}_1\ \mathbf{a}_2\ \ldots\ \mathbf{a}_k]$ with known OSVD

$$A_k = U_k\,\Sigma_k\,V_k^t \tag{4.3}$$

Add one column $\mathbf{a}_{k+1}$ to A_k such that

$$A_{k+1} = [A_k\ \mathbf{a}_{k+1}] = [\mathbf{a}_1\ \mathbf{a}_2\ \ldots\ \mathbf{a}_{k+1}] \tag{4.4}$$

The matrices U_{k+1} and Σ_{k+1} in the OSVD of A_{k+1} can be computed from U_k, Σ_k and $\mathbf{a}_{k+1}$ as follows

$$\Sigma_{k+1}^2 = Q^t\,(\Sigma_k^2 + U_k^t\,\mathbf{a}_{k+1}\,\mathbf{a}_{k+1}^t\,U_k)\,Q \tag{4.5}$$

$$U_{k+1} = U_k\,Q \tag{4.6}$$

where Q is an orthogonal $p \times p$ matrix.

Proof

Since the matrix V_k in the OSVD of A_k has the property that $V_k^t\,V_k = I$, it is clear that

$$A_k\,A_k^t = (U_k\,\Sigma_k\,V_k^t)\,(V_k\,\Sigma_k\,U_k^t) = U_k\,\Sigma_k^2\,U_k^t \tag{4.7}$$

Due to the fact that U_k is an orthogonal matrix ($U_k^t\,U_k = U_k\,U_k^t = I$), and because of the associativity of matrix multiplications, one can prove from Eq. (4.7) that $U_k^t\,(A_k\,A_k^t)\,U_k = (U_k^t\,A_k)\,(A_k^t\,U_k) = \Sigma_k^2$ where Σ_k^2 is a square diagonal matrix with nonnegative elements on the diagonal.

After adding a column $\mathbf{a}_{k+1}$ to A_k, a symmetric matrix C_{k+1} can be defined as the product

$$\begin{aligned} C_{k+1} &= (U_k^t\, A_{k+1})\,(A_{k+1}^t\, U_k) \\ &= \begin{bmatrix} U_k^t\, A_k & U_k^t\, \mathbf{a}_{k+1} \end{bmatrix} \begin{bmatrix} A_k^t\, U_k \\ \mathbf{a}_{k+1}^t\, U_k \end{bmatrix} \\ &= (U_k^t\, A_k)\,(A_k^t\, U_k) + (U_k^t\, \mathbf{a}_{k+1})\,(\mathbf{a}_{k+1}^t\, U_k) \\ &= \Sigma_k^2 + (U_k^t\, \mathbf{a}_{k+1})\,(\mathbf{a}_{k+1}^t\, U_k) \end{aligned} \tag{4.8}$$

The extra term in Eq. (4.8) is a rank-one perturbation of the diagonal matrix Σ_k^2, such that C_{k+1} is not diagonal anymore. It can be proven that there exists an orthogonal matrix Q, such that

$$B_{k+1} = Q^t\, C_{k+1}\, Q \tag{4.9}$$

is diagonal. This matrix Q can easily be computed due to the existence of stable algorithms to reduce the symmetric matrix C_{k+1} to diagonal form (symmetric QR-iteration, Jacobi methods, Lanczos diagonalization, etc.). Substitute Eq. (4.8) into Eq. (4.9), such that

$$B_{k+1} = (Q^t\, U_k^t)\,(A_{k+1}\, A_{k+1}^t)\,(U_k\, Q) \tag{4.10}$$

Since $U_k\, Q$ is orthogonal, since B_{k+1} is diagonal and since the OSVD of A_{k+1} is unique, it follows from Eq. (4.10) that

$$\Sigma_{k+1}^2 = Q^t\,(\Sigma_k^2 + U_k^t\, \mathbf{a}_{k+1}\, \mathbf{a}_{k+1}^t\, U_k)\, Q \tag{4.11}$$

$$U_{k+1} = U_k\, Q \tag{4.12}$$

□

Based on the previously defined theorem, an on-line algorithm can be outlined. This algorithm assumes that the matrix A is built up column by column. Each time a column $\mathbf{a}_i$ is added to $A_{i-1} = [\mathbf{a}_1 \ldots \mathbf{a}_{i-1}]$, it computes the U_i- and Σ_i-matrices in the OSVD of A_i by updating the matrices U_{i-1} and B_{i-1} from the previous step.

The algorithmic scheme can then be presented as follows :

Initialization

$$U_0 = I_{p,p} \quad \text{and} \quad B_0 = O_{p,p} \tag{4.13}$$

Loop for $i = 1$ to q

generate output

$$\mathbf{y}_i = U_{i-1}^t \, \mathbf{a}_i \tag{4.14}$$

compute C_i

$$C_i = B_{i-1} + \mathbf{y}_i \, \mathbf{y}_i^t \tag{4.15}$$

update B_i by diagonalizing C_i

$$B_i = Q_i^t \, C_i \, Q_i \tag{4.16}$$

update U_i

$$U_i = U_{i-1} \, Q_i \tag{4.17}$$

end loop

At the end of each loop, the matrices U_i and $\Sigma_i^2 = B_i$ in the OSVD of matrix $A_i = [\mathbf{a}_1 \, \mathbf{a}_2 \, \ldots \, \mathbf{a}_i]$ are exactly known. The memory requirements for this on-line method are restricted to p^2 locations for the elements of U_i and $p(p+1)/2$ locations for the upper triangle of C_i. For the p elements of B_i, one can use p locations on the diagonal of C_i.

Among the existing methods for computing the rank-one modification of the symmetric eigenproblem in literature, the studies of Bunch, Nielsen and Sorensen ([8], [9]) are the best known. Their algorithm proceeds in three stages : (1) initial deflation in the case of multiple eigenvalues, (2) computation of the explicit eigenvalues of the rank-one modified symmetric matrix, and (3) updating of the eigenvectors of this modified matrix. The computation of eigenvalues and eigenvectors is done through analytical formulas. The major drawback is however that the updating of the eigenvectors requires about $O(p^3)$ multiplications. No reduction in computational cost has thus been achieved, when compared to a completely new eigenvalue decomposition of the rank-one updated matrix.

Another adaptive algorithm for estimation of the covariance eigenstructure of a data matrix is described by Sharman [73]. He outlines an adaptive implementation of the QR-algorithm, employing two simultaneous recursions. Moonen et al [54] also describe a QR-based updating scheme for a rank-one perturbation of the Ordinary Singular Value Decomposition. A disadvantage here is that the complexity of the computational work is extended, since two rotation angles per rotation have to be computed. The QR-updating techniques require a sweep of rotations, while the Jacobi technique (that will be used in our on-line updating scheme) is iterative in nature : each single rotation brings the symmetric matrix closer to diagonality. The schemes of Sharman [73] and Moonen et al. [54] are however very suitable for an efficient hardware implementation using parallel and systolic processing techniques.

In many multichannel signal processing applications (e.g. the FECG-MECG separation problem) the output is a set of linear combinations or weighted sums of the input signals. The coefficients in these linear combinations are found as the columns of the U-matrix. Since the input is assumed to be gradually available (column per column), the algorithm can generate immediately an output column for each available input column and knowing the U-matrix at that instant. This is exactly the first step in the algorithm.

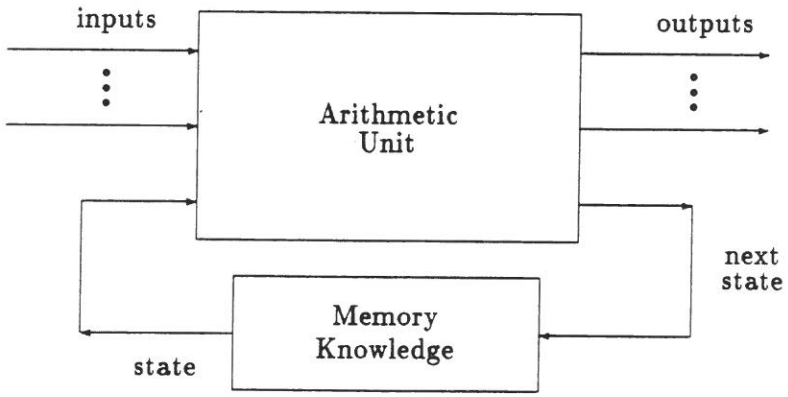

Figure 4.1: *General scheme of the on-line adaptive algorithm.*

Let us try to model the algorithm with a **system description.** The reader may notice that in this case a priori knowledge about the past is incorporated in the data processing. Therefore, the matrix B_i is a summary or condensed information of the past. In systems theory this is usually called **a state.** This state is updated according to the new incoming data, to form the next state C_i . The arithmetic part of the system must perform the following actions :

1. generate an output column by linearly combining the elements of the input column.

2. update the singular values and the singular basis vectors residing in memory, in order to contain the information of the last input column.

This model can be illustrated by the scheme of Figure 4.1 or more detailed in Figure 4.2

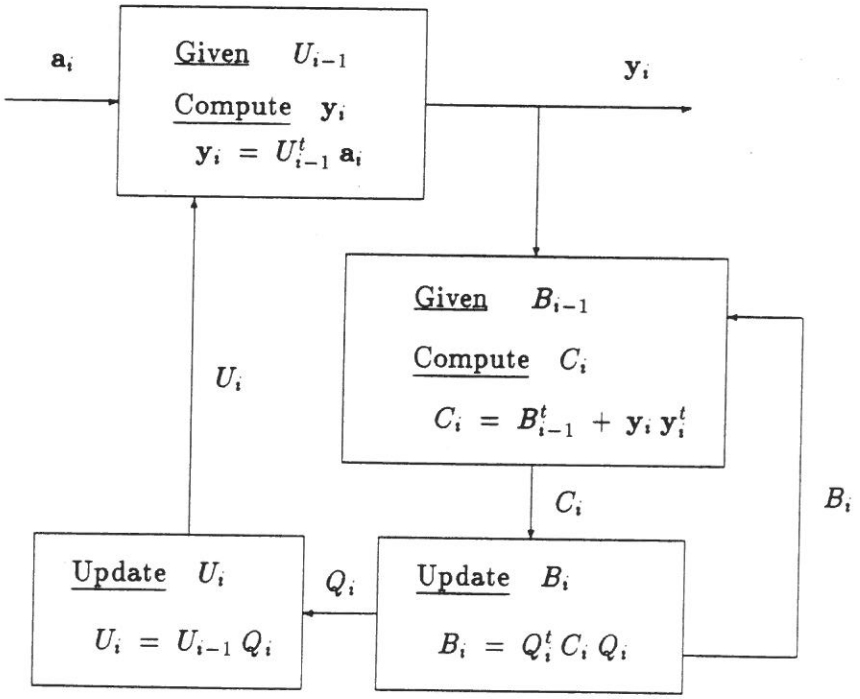

Figure 4.2: *Detailed scheme of the on-line adaptive algorithm.*

The main constraints of the method are the required memory and the pace set by the incoming data. It is important that the arithmetic unit is able to obey this pace, such that, each time an input appears to the system, an output can be generated using the updated information from the previous step. The part that takes most of the time $O(p^3)$ in each loop is the diagonalization of the symmetric matrix C_i. Convergence tests will show further that complete diagonalization is not required, only some reduction of the norm of the off-diagonal elements in each cycle (see Section 4.7). This diminishes the computational work of this step in the algorithm substantially, such that the arithmetic unit can much easier obey the pace of the incoming data.

4.4 Comparison with the normal equations

The attentive reader may have noticed that the matrix product AA^t appears in the outline of the new algorithm. It is a well-known problem in numerical algebra that the "normal" matrix AA^t is frequently ill-conditioned and influenced greatly by round-off errors [37]. Especially the small singular values are sensitive to the implicit squaring [46]. Consider the set of q linear equations $A^t x = b$ where A is a $p \times q$ matrix $(q > p)$ and b is a given q-vector. A least squares solution is obtained by multiplying both sides of the equation by A, such that

$$A A^t x = A b \tag{4.18}$$

and then solving these p normal equations. The formation of AA^t usually introduces a loss of information due to rounding errors. This is illustrated by the following example

$$A = \begin{pmatrix} 1 & \epsilon & 0 \\ 1 & 0 & \epsilon \end{pmatrix} \quad \text{then} \quad A A^t = \begin{pmatrix} 1+\epsilon^2 & 1 \\ 1 & 1+\epsilon^2 \end{pmatrix} \tag{4.19}$$

The rank of AA^t is 2 and the eigenvalues are $2+\epsilon^2$ and ϵ^2. Let us assume that the elements of AA^t are computed using double precision arithmetic, and then rounded to single precision accuracy. Suppose η is the machine precision i.e. the largest number on the computer such that $\mathrm{fl}(1.0+\eta) \equiv 1.0$, where $\mathrm{fl}(\ldots)$ indicates the floating point computation. If $|\epsilon| < \sqrt{\eta}$ then rank $(AA^t) = 1$. No matter how accurate the method for computing the eigenvalues and eigenvectors of AA^t, it is impossible to solve the p normal equations. Attempts to improve the condition of AA^t are useless, once this normal matrix has been formed.

Osborne [62], however, proves that the loss of information, resulting from forming AA^t, is minimal in case the normal matrix is diagonal. Therefore the matrix A is first premultiplied by a $p \times p$ matrix Q to form a new matrix $B = QA$, such that $B B^t$ is diagonal. This is almost exactly what is done in the presented algorithm. The matrix Q in question is in this case the orthogonal matrix U_{i-1} from the previous update. The formation of C_i is implicitly not performed as

$$C_i = U_{i-1}^t \, (A_i \, A_i^t) \, U_{i-1} \quad \text{but as} \quad C_i = (U_{i-1}^t \, A_i) \, (U_{i-1}^t \, A_i)^t$$

making C_i almost diagonal, since U_{i-1} is an estimate of U_i. Using double precision arithmetic on the diagonal of C_i only, further reduces ill-conditioning of the problem.

To illustrate this, let's take up the same example and perform the algorithmic steps, one by one

Initialization

$$A = \begin{pmatrix} 1 & \epsilon & 0 \\ 1 & 0 & \epsilon \end{pmatrix}$$

$$U_0 = \begin{pmatrix} 1 & 0 \\ 0 & 1 \end{pmatrix} \qquad B_0 = \begin{pmatrix} 0 & 0 \\ 0 & 0 \end{pmatrix}$$

Pass 1 of the loop

$$\mathbf{a}_1 = \begin{pmatrix} 1 \\ 1 \end{pmatrix} \qquad \mathbf{y}_1 = U_0^t \, \mathbf{a}_1 = \begin{pmatrix} 1 \\ 1 \end{pmatrix}$$

$$C_1 = B_0 + \mathbf{y}_1 \, \mathbf{y}_1^t = \begin{pmatrix} 1 & 1 \\ 1 & 1 \end{pmatrix}$$

$$B_1 = Q_1^t \, C_1 \, Q_1 = \begin{pmatrix} 2 & 0 \\ 0 & 0 \end{pmatrix}$$

$$U_1 = U_0 \, Q_1 = Q_1 = \begin{pmatrix} \frac{\sqrt{2}}{2} & -\frac{\sqrt{2}}{2} \\ \frac{\sqrt{2}}{2} & \frac{\sqrt{2}}{2} \end{pmatrix}$$

Pass 2 of the loop

$$\mathbf{a}_2 = \begin{pmatrix} \epsilon \\ 0 \end{pmatrix} \qquad \mathbf{y}_2 = U_1^t \, \mathbf{a}_2 = \begin{pmatrix} \frac{\sqrt{2}}{2}\epsilon \\ -\frac{\sqrt{2}}{2}\epsilon \end{pmatrix}$$

$$C_2 = B_1 + \mathbf{y}_2 \, \mathbf{y}_2^t \simeq \begin{pmatrix} 2 & -\frac{\epsilon^2}{2} \\ -\frac{\epsilon^2}{2} & \frac{\epsilon^2}{2} \end{pmatrix}$$

Since the off-diagonal elements are very small compared to the difference between the diagonal elements, the Jacobi rotation angle will be very small such that the orthogonal matrix Q_2 is close to the unity matrix. After diagonalization of C_2 we have that

$$B_2 = Q_2^t \, C_2 \, Q_2 \simeq \begin{pmatrix} 2 & 0 \\ 0 & \frac{\epsilon^2}{2} \end{pmatrix}$$

and $U_2 = U_1 \, Q_2 \simeq U_1$.

Pass 3 of the loop

$$\mathbf{a}_3 = \begin{pmatrix} 0 \\ \epsilon \end{pmatrix} \qquad \mathbf{y}_3 = U_2^t \mathbf{a}_3 = \begin{pmatrix} \frac{\sqrt{2}}{2}\epsilon \\ \frac{\sqrt{2}}{2}\epsilon \end{pmatrix}$$

$$C_3 = B_2 + \mathbf{y}_3 \mathbf{y}_3^t \simeq \begin{pmatrix} 2 & \frac{\epsilon^2}{2} \\ \frac{\epsilon^2}{2} & \epsilon^2 \end{pmatrix}$$

After diagonalization of C_3 we have that

$$B_3 \simeq \begin{pmatrix} 2 & 0 \\ 0 & \epsilon^2 \end{pmatrix}$$

which reflects the real rank of A, namely 2. For this example it is clear that the method avoids the classical problems that accompany the formation of AA^t by diagonalizing in each step and using double precision on the diagonal. For a theoretical proof we refer to the paper by Osborne [62].

4.5 Adaptivity of the algorithm

It should be stressed at this point that the algorithm, outlined in this section, is **on-line**, because data are processed as soon as they are available, but not **adaptive**.

> *Adaptivity is the possibility of the method to follow time variations, to recover from sudden changes and to track new events.*

In signal processing applications, the number of columns of the data matrix is proportional to time. The matrices B_i and U_i at the end of each loop in the presented algorithm contain the information from all previous matrix columns. They constitute the knowledge that the system has built up from the past. This knowledge determines the way of processing (see Figure 4.2) and it is quite evident that it should be as actual as possible. Therefore, it is desirable that events from the remote past don't have any influence on the present processing anymore, while on the other hand, the very recent events will have to correct the processing severely.

Another problem that occurs, while the on-line process proceeds, is the fact that the norm of the diagonal elements of the matrix B_i increases. A result of this is that the contribution of $\mathbf{y}_i\,\mathbf{y}_i^t$ to the matrix C_i will be of less importance for the deviation of diagonality of B_{i-1}. This means that the orthogonal transformation Q_i that reduces C_i to diagonal form, will be almost equal to the identity matrix. New information will not have any influence on the present processing anymore. These problems can be solved by **windowing** or **exponentially weighting** the data signals.

1. **Windowing** : The most straightforward way to restrict the "knowledge", that the system builds up, to the recent past is accomplished by windowing : while a new contribution updates the present knowledge, a contribution from the past is removed simultaneously. If w is the width of the window, then the second step in the algorithm would change into

$$C_i = B_{i-1} + \mathbf{y}_i\,\mathbf{y}_i^t - U_{i-1}^t\,\mathbf{a}_{i-w}\,\mathbf{a}_{i-w}^t\,U_{i-1} \tag{4.20}$$

   This equation implements the ideal moving window-function. In practice, however, this is not the most elegant solution. It requires the storage of w input columns, in order to eliminate the "oldest" contribution. Moreover, the width of the window has to be considerably big, because the a priori knowledge must be based on enough information. For example, if the data are periodical, the width of the window must be at least one period.

2. **Exponential weighting :** Another solution is found by incorporating a "forgetting function" in an extremely simple way. In each pass of the loop in the presented algorithm, the elements of B_{i-1} are reduced slightly by multiplying them by some factor α lying between 0 and 1, such that step two of the algorithm changes into

$$C_i = \alpha\,B_{i-1} + \mathbf{y}_i\,\mathbf{y}_i^t \tag{4.21}$$

   This is equivalent to an exponential weighting of the input data with a factor $\sqrt{\alpha}$. The closer α lies to 1, the slower the system forgets data from the past and the more influence data from the remote past can still have. The smaller α, the faster some changes can be recovered by the method. However α should be large enough in order to limit sensitivity of the method to detailed short interval signal characteristics.

A criterion to determine a value for α is the following :

> *choose α such that α^k is equal to a percentage of 1. This amounts to reducing the influence of data from k time instants ago to some percentage*
>
> $$\alpha^k = \frac{PERC}{100}$$

Example : Suppose a process has a data acquisition rate of 1000 Hz. In systems theory a time constant τ is defined as the time that the impulse response requires to return to $1 - e^{-1} = 63.2\%$ of its maximal deviation. In analogy with this, assume that after 1 second ($k = 1000$), α^k is only 63.2%

$$\alpha^{1000} = \frac{63.2}{100}$$

$$\log \alpha = [log(63.2) - 2]/1000 = -0.0002$$

$$\alpha = 0.99954$$

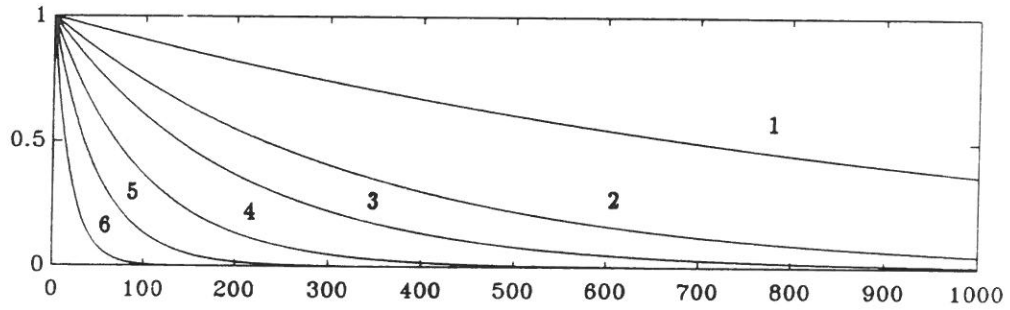

Figure 4.3: *The function α^i for (1) $\alpha = 0.999$, (2) $\alpha = 0.997$, (3) $\alpha = 0.995$, (4) $\alpha = 0.99$, (5) $\alpha = 0.98$ and (6) $\alpha = 0.95$.*

In Figure 4.3 the function α^i $(i = 1, \ldots, 1000)$ is plotted for different values of α. This Figure shows that a slight modification of α already results in a completely different exponential curve. There is some relation between sampling frequency, signal periodicity and stationary behaviour of the signals on one hand and the choice of an appropriate α on the other hand. For the MECG-FECG application, the choice of α is explained in Section 5.3.6.

4.6 Diagonalization of a symmetric matrix

4.6.1 Introduction

Many signal processing applications (image processing, speech recognition, source location and direction finding from sensor arrays, modal analysis, etc.) require the computation of the complete covariance eigenstructure of the incoming data. This often implies the solution of a real symmetric eigenvalue problem. Many methods exist for solving this real symmetric eigenvalue problem [38], [65], [96]. In order to reduce the matrix to diagonal form, most of those methods apply a series of orthonormal transformations for stability reasons, since orthonormal transformations preserve the matrix norms.

In Givens' method and Householder's method [47], [96] the symmetric matrix is transformed into tridiagonal form first, followed by a symmetric QR-iteration for the computation of the eigenvalues and eigenvectors. These methods receive a lot of attention concerning computational speed and accuracy. Inverse iteration gives a very satisfactory solution to the problem as far as reasonably well-separated eigenvalues are concerned. The problem of determining reliably full digital information in the subspace spanned by eigenvectors corresponding to coincident or pathologically close eigenvalues has never been satisfactorily solved [96].

However, there are three main reasons for preferring **Jacobi's eigenreduction**, that uses a sequence of orthonormal plane rotations to transform a real symmetric matrix A to diagonal form. First, the method of Jacobi is essentially iterative in character. This means that the process consists of a number of identical steps that each bring us closer to the desired solution. In an on-line method, this has some advantages since the iterative process can be stopped after any number of steps according to some stopcriterion. The tridiagonalization that appears in Givens' and Householder's methods, on the other hand, is not iterative and requires a fixed number of computations.

Secondly, in cases where good estimates of the eigenvectors and -values of the symmetric matrix are known, a Jacobi technique is preferable with regard to computational speed. This is because the a priori information can be incorporated while in other methods one starts each time from "scratch". Finally, the compactness and the extreme simplicity of Jacobi's method from the programming point of view makes it also attractive in minicomputing environments.

These three reasons advocate the use of Jacobi's method for diagonalization of the symmetric matrix C_i in the on-line algorithm. In the following subsections we try to give a general analysis of the Jacobi rotation and more specifically we try to look for an alternative method to determine the angles of the subsequent rotations, so that the off-diagonal elements of maximum modulus are not annihilated (as in the classical Jacobi method) but reduced substantially. This concept was already introduced by Pope & Tompkins [68] in 1957 and by Forsythe and Henrici [35] in 1960 and is called under- or overrotation.

4.6.2 The classical Jacobi method

A symmetric $n \times n$ matrix A can be diagonalized by the following iterative process :

$$A_{k+1} = Q_k \, A_k \, Q_k^t \quad (k = 0, 1, 2, \ldots) \qquad (A_0 = A) \tag{4.22}$$

where the orthonormal rotation matrix Q_k is the $n \times n$ identity matrix, except for

$$\begin{aligned} Q_k(p,p) &= Q_k(q,q) &&= \cos\phi \\ Q_k(p,q) &= -Q_k(q,p) &&= -\sin\phi \qquad \textit{with } p < q \end{aligned} \tag{4.23}$$

The indices p and q are found as the position of the off-diagonal element a_{pq} in A_k with maximum modulus. The angle θ is computed so that, after application of the rotation, the element $A_{k+1}(p,q) = A_{k+1}(q,p) = 0$. This means that θ can be found from [65]

$$\tan 2\theta = \frac{2\,a_{pq}}{a_{qq} - a_{pp}} = \frac{1}{\xi} \quad (\textit{with } a_{ij} = A_k(i,j)) \tag{4.24}$$

$$\tan\theta = \frac{sign(\xi)}{|\xi| \pm \sqrt{\xi^2 + 1}} \tag{4.25}$$

$$\cos\theta = \frac{1}{\sqrt{1 + \tan^2\theta}} \qquad \sin\theta = \cos\theta . \tan\theta \tag{4.26}$$

In Eq. (4.25) the positive sign is preferred because then the rotation angle is always in the range $J = [-45^o, +45^o]$.

Since 1848, when Jacobi [45] introduced this method to compute the eigenvalue decomposition of a real symmetric matrix A by transforming it to diagonal form using a sequence of plane rotations, a number of variants on this "classical theme" has been composed. They all differ from each other mainly because they use a different strategy to choose the pivot element with position (p, q) in A_k. Where the classical method simply takes the off-diagonal element with maximum modulus, some row or column cyclic strategies have been developed to reduce the search time. A refinement of this cyclic strategy is the introduction of a threshold to ascertain the usefulness of some rotation. Also parallel strategies that perform more than one rotation simultaneously, have been designed and implemented.

Once a pivot element a_{pq} is indicated (by a cyclic method, maximum modulus, parallel strategy, etc.), the rotation angle, that annihilates this element, has to be computed from Eq. (4.25) and (4.26).

4.6.3 Generalization of the rotation

One step in the diagonalization process (Eq. (4.22)) is in fact a rotation in two dimensions over some angle. Suppose we start from matrix A_k , with elements $a_{ij} = A_k(i, j)$ and a rotation is performed through some arbitrary angle ϕ in the range $J = [-45^o, +45^o]$, then the modified values in A_{k+1} are $(a^*_{ij} = A_{k+1}(i, j))$

$$\begin{cases} a^*_{ip} = a^*_{pi} = a_{ip}\cos\phi - a_{iq}\sin\phi \\ a^*_{iq} = a^*_{qi} = a_{ip}\sin\phi + a_{iq}\cos\phi \qquad \text{for } i \neq p, q \end{cases} \tag{4.27}$$

$$\begin{cases} a^*_{pp} = a_{pp}\cos^2\phi + a_{qq}\sin^2\phi - 2\,a_{pq}\cos\phi\sin\phi \\ a^*_{qq} = a_{pp}\sin^2\phi + a_{qq}\cos^2\phi + 2\,a_{pq}\cos\phi\sin\phi \\ a^*_{pq} = (a_{pp} - a_{qq})\cos\phi\sin\phi + a_{pq}(\cos^2\phi - \sin^2\phi) \end{cases} \tag{4.28}$$

This means that only the elements in rows p and q and columns p and q are changed. All other values remain unchanged. In the further analysis, three elements play a key role : a_{pq}, a_{pp} and a_{qq}. A new parameter is defined as

$$K \equiv \frac{a_{pp} - a_{qq}}{a_{pq}} \tag{4.29}$$

and all formulas can be written as a function of K :

$$a^*_{pp} = a_{pp} - a_{pq}\sin\phi\ [K\sin\phi + 2\cos\phi] \tag{4.30}$$
$$a^*_{qq} = a_{qq} + a_{pq}\sin\phi\ [K\sin\phi + 2\cos\phi] \tag{4.31}$$
$$a^*_{pq} = -a_{pq} + a_{pq}\cos\phi\ [K\sin\phi + 2\cos\phi] \tag{4.32}$$

Suppose that a_{pq} is changed after this rotation, such that

$$a^*_{pq} = \gamma a_{pq} \tag{4.33}$$

then from Eq. (4.32) it follows that

$$\gamma\,(K,\phi) = \frac{K}{2}\sin 2\phi + \cos 2\phi \tag{4.34}$$

Then Eq. (4.30) and (4.31) can also be written as :

$$\begin{cases} a^*_{pp} = a_{pp} - a_{pq}\tan\phi\,(1+\gamma) \\ a^*_{qq} = a_{qq} + a_{pq}\tan\phi\,(1+\gamma) \end{cases} \tag{4.35}$$

The first objective of a rotation is to make A_{k+1} more diagonal than A_k, which results in the condition that $|\gamma| < 1$. We can also define a measure of diagonalization as the decrease Δ of the squared norm of the off-diagonal elements

$$\Delta \equiv \sum_{i\neq j} a^2_{ij} - \sum_{i\neq j} a^{*2}_{ij} = 2\,(a^2_{pq} - a^{*2}_{pq}) = 2\,a^2_{pq}\,(1-\gamma^2) \tag{4.36}$$

If $\Delta > 0$, then A_{k+1} is more diagonal than A_k. The parameter γ is a measure of the "relaxation" of the process.
For $\gamma = 0$, we have Jacobi's original method, with $a^*_{pq} = 0$ and $\Delta = 2a^2_{pq}$, the maximal value of Δ for that particular choice of the pivot element.
For $0 < \gamma < 1$, we have the so called **underrelaxation**, decreasing $|a_{pq}|$ without changing its sign.
For $-1 < \gamma < 0$, we have the so called **overrelaxation**, also decreasing $|a_{pq}|$ but changing the sign of a_{pq}.

We will now study the variation of γ as a function of ϕ for a given value of K, such that can be determined for which angles ϕ the matrix is more diagonal ($|\gamma| < 1$).

- $K = 0 \iff \gamma = \cos 2\phi$
  In this case $\forall\, \phi \neq 0 : |\gamma| < 1$, such that any angle $\phi \neq 0$ will make A_{k+1} more diagonal than A_k.

- $K = \pm 2 \iff \gamma = \cos 2\phi \pm \sin 2\phi$
  All angles ϕ ($\phi \neq 0$ and $\phi \neq \pm\frac{\pi}{4}$) with opposite sign of K will make A_{k+1} more diagonal than A_k, since then $|\gamma| < 1$.

- $|K| < 2$
  For small values of K (e.g. $K = 1$ in Figure 4.4), almost any angle $\phi \in J$ will make A_{k+1} more diagonal than A_k.

- $|K| > 2$
  For large values of K (e.g. $K = 4$ in Figure 4.5), only angles from a small interval of J will satisfy the condition $|\gamma| < 1$.

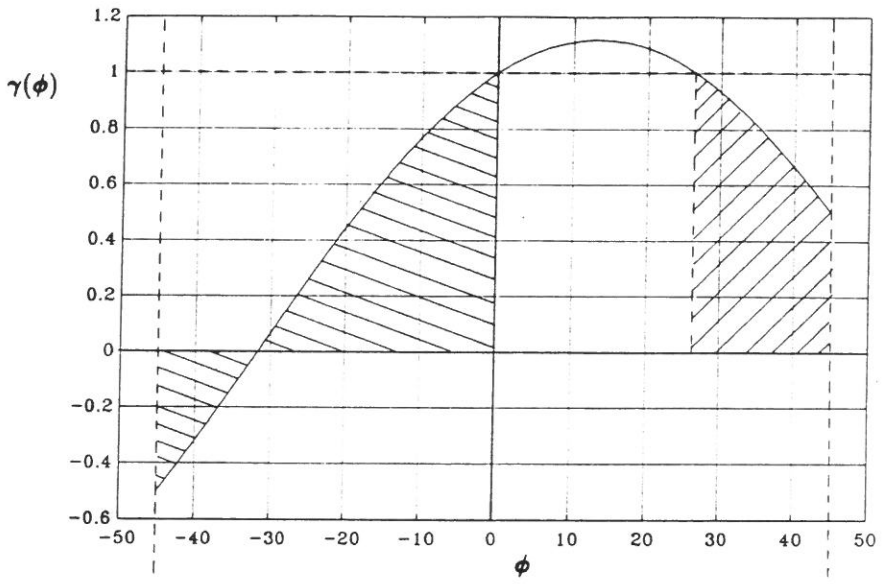

Figure 4.4: *Variation of γ as a function of ϕ for $K = 1$.*

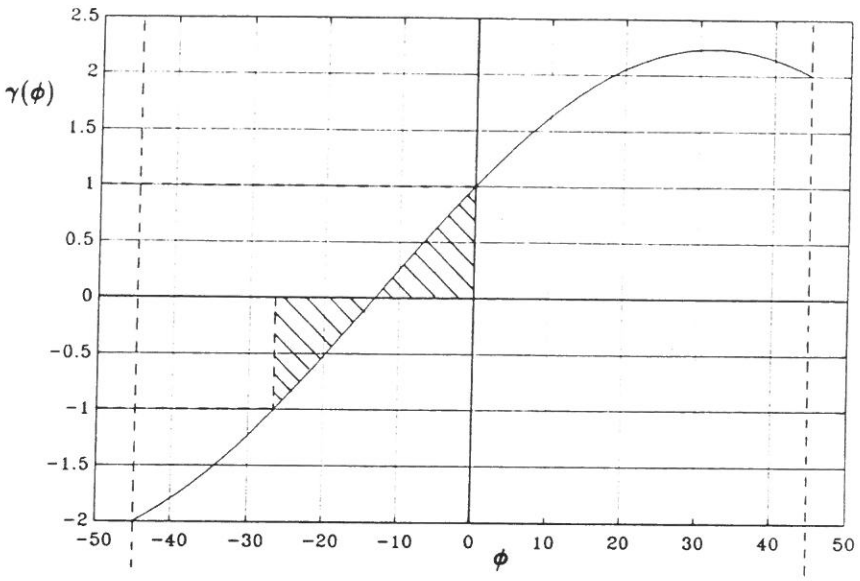

Figure 4.5: *Variation of* γ *as a function of* ϕ *for* $K = 4$.

4.6.4 Simpler determination of the rotation angle

The figures in the previous subsection suggest that it may be possible to find some angle ϕ, different from the optimal angle θ computed in Jacobi's method, such that the off-diagonal pivot element is not annihilated, but reduced substantially. The computation of $\tan\theta$, $\cos\theta$ and $\sin\theta$ from Eq. (4.25) and Eq. (4.26) gives on some computers or microprocessor systems problems with regard to finite precision arithmetic. The occurrence of two square roots in the equations, as well as the necessary rounding-off of numbers in a digital computer, means that a_{pq}^{*} can never exactly be replaced by zero. For this reason Pope & Tompkins [68] and Forsythe & Henrici [35] already mentioned the concept of **under- or overrotation.**

A possible approximation for small angles ϕ_{PT} is the following overrelaxation [68] :

$$T = \tan\left(\frac{\phi_{PT}}{2}\right) \simeq \frac{\tan 2\theta}{4} = \frac{-1}{2K} \tag{4.37}$$

$$\cos\phi_{PT} = \frac{4K^2-1}{4K^2+1} \qquad \sin\phi_{PT} = \frac{-4K}{4K^2+1} \tag{4.38}$$

provided that $\phi_{PT} \in (-\pi/4, +\pi/4)$ or $|K| > \dfrac{\sqrt{2}+1}{2}$.

For $|K| \leq \dfrac{\sqrt{2}+1}{2}$ the method simply takes $\phi_{PT} = -sign(K)\,\dfrac{\pi}{4}$.

For large values of the parameter K, this overrelaxation approaches the classical Jacobi method very well. But on the other hand, for small values of K the overrelaxation is rather rude.

We will now introduce a new approach for small K-values. Suppose

$$\tan 2\beta \equiv \tan(90 - 2\phi_C) = \frac{1}{\tan 2\phi_C} = \frac{-K}{2} \tag{4.39}$$

For $K \to 0$, one can see that $\beta \to 0$ and $\phi \to \pm\frac{\pi}{4}$. Then equivalently to Eq. (4.37), we have

$$T_C = \tan\left(\frac{\beta}{2}\right) \simeq \frac{\tan 2\beta}{4} = -\frac{K}{8} \tag{4.40}$$

One can prove further that

$$\cos\beta = \frac{64 - K^2}{64 + K^2} \quad \text{and} \quad |\sin\beta| = \frac{16\,|K|}{64 + K^2} \tag{4.41}$$

and the values for $\cos\phi_C$ and $\sin\phi_C$ are obtained from

$$\begin{cases} \cos\phi_C = \dfrac{\cos\beta + |\sin\beta|}{\sqrt{2}} \\ \sin\phi_C = sign(K).\dfrac{|\sin\beta| - \cos\beta}{\sqrt{2}} \end{cases} \tag{4.42}$$

This results in an underrelaxation for small K-values.

Let us now compare the following three methods :

- Method 1 : the original Jacobi method, where θ is calculated from Eq. (4.25) and Eq. (4.26)
- Method 2 : the overrelaxation proposed by Pope and Tompkins, where ϕ_{PT} is calculated from Eq. (4.38).
- Method 3 : a combination of the overrelaxation proposed by Pope and Tompkins for large K-values, and a new underrelaxed approach for small K-values, where ϕ_C is calculated from Eq. (4.41) and Eq. (4.42).

We will therefore observe the variation of γ and Δ as a function of K for each of the three approaches (see Figure 4.6 and Figure 4.7).

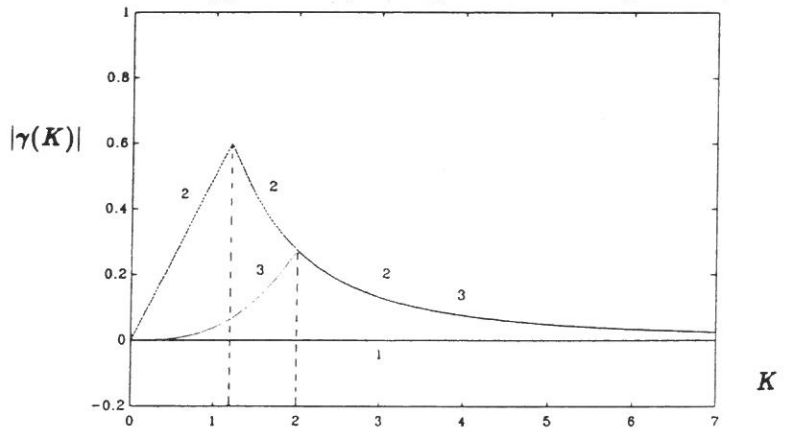

Figure 4.6: *The variation of γ as a function of K for each of the three methods.*

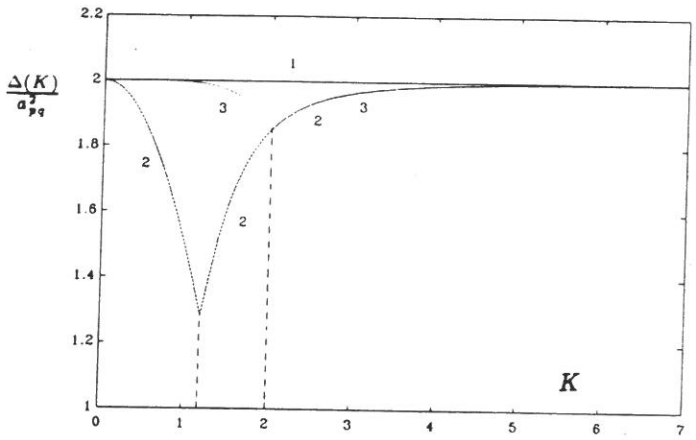

Figure 4.7: *The variation of Δ as a function of K for each of the three methods.*

One can notice from Figure 4.6 and Figure 4.7 that at $|K| = 2$

$$\Delta_{PT}(K) = \Delta_C(K) \text{ and } |\gamma_{PT}(K)| = |\gamma_C(K)|$$

This leads to the following strategy for Method 3 :

- find the off-diagonal element a_{pq} with maximum modulus
- compute K
- **if** $|K| \leq 2$ **then** use Eq. (4.41) and Eq. (4.42)
  else use Eq. (4.38)

With this mixed strategy it is always true that

$$1.85\, a_{pq}^2 \leq |\Delta(K)| \leq 2\, a_{pq}^2 \tag{4.43}$$

$$0 \leq |\gamma(K)| \leq 0.2734 \tag{4.44}$$

which means that A_{k+1} is always more diagonal than A_k and that the pivot element is reduced to about one fourth of its previous value. For this reason, if the method is used for diagonalization of a symmetric matrix, convergence is obvious. The most important advantage with respect to the computational work is that the computation of any square root is avoided. Since the method is the same as the overrelaxation of Pope and Tompkins for large K-values, but gives better results for small values of K by a new underrelaxation approach, it is expected and it can easily be verified that the convergence speed is somewhat better than the Pope-Tompkins method. In the limit, both methods have the same quadratic convergence as the original Jacobi method.

4.7 Minimal computation approach for the on-line SVD-based algorithm

As already mentioned, the part that takes most of the computational work $O(p^3)$ in each loop of the on-line algorithm is the diagonalization step of the symmetric matrix C_i. We will show here that complete diagonalization is not required in each step, only some reduction of the norm of the off-diagonal elements. It will be shown that **only one plane rotation per cycle** suffices for the algorithm to converge. It is even possible to compute the rotation angle with the new over- and underrelaxation approach, described in the previous section, such that the computation of any square root is avoided. This makes the algorithm extremely suitable in microcomputing environments.

Since it is very difficult to prove the convergence of the presented algorithm analytically, we will use a more empirical approach to show that the symmetric matrix B_i in the algorithm converges to diagonal form. Indeed, in that case the matrix U_i approaches the left singular matrix of the exponentially weighted data matrix. Therefore we consider the following test : the input p-vectors are random and contain elements that are in absolute value smaller than some real value M

$$\exists\, M \in \Re \;:\; \forall\, \mathbf{a}_i \in \Re^p \;:\; |\mathbf{a}_i(j)| \leq M \quad \text{for } j = 1, \ldots, p$$

such that their norm is limited to $\|\mathbf{a}_i\| \leq \sqrt{p}\, M$.

If off (B_i) is the matrix that only contains the off-diagonal elements of B_i and diag (B_i) is the matrix that only contains the diagonal elements of B_i, then

$$\begin{aligned} B_i &= \text{diag}\,(B_i) + \text{off}\,(B_i) \\ \|B_i\|_F^2 &= \|\text{diag}\,(B_i)\|_F^2 + \|\text{off}\,(B_i)\|_F^2 \end{aligned} \tag{4.45}$$

A measure for diagonality of the symmetric matrix B_i is the ratio

$$\rho = \frac{\|\text{diag}\,(B_i)\|_F}{\|\text{off}\,(B_i)\|_F} \tag{4.46}$$

Indeed, Table 4.7 gives for some values of ρ the percentages of the contribution of the diagonal and the off-diagonal to the squared Frobenius-norm of B_i

ρ	$\|B_i\|_F^2$	$\|\text{diag}\,(B_i)\|_F^2$	$\|\text{off}\,(B_i)\|_F^2$
5	100 %	96.15 %	3.85 %
10	100 %	99.01 %	0.99 %
25	100 %	99.84 %	0.16 %
50	100 %	99.96 %	0.04 %
100	100 %	99.99 %	0.01 %

Table 4.1: *Percentual contribution of diagonal and off-diagonal to the Frobenius-norm of B_i for different values of ρ.*

We plotted this ratio ρ for different values of p and α and some results are shown in Figure 4.8 for $(p = 3, 8, 16)$ and for $\alpha = 0.999, 0.99$. The input vectors of the algorithm were randomly generated (uniform distribution) and contain values between -1 and $+1$ $(M = 1)$. The following conclusions can be made from these experiments :

- No matter which value for p or α, in the limit the ratio ρ stays above some threshold. In Table 4.7 some thresholds for different values of α and p, as obtained in the experiments, are shown.

p	$\alpha = 0.999$	$\alpha = 0.99$	$\alpha = 0.9$
3	± 250	± 30	± 4
6	± 120	± 20	± 3
8	± 100	± 15	± 2
16	± 60	± 10	± 1.5

Table 4.2: *Thresholds for ρ after convergence of the algorithm.*

- For small values of p (e.g. $p = 3$) the ratio ρ varies substantially each time a new input vector is added, but this variation disappears for larger values of p (e.g. $p = 16$).
- Experiments with other values for M resulted in the same conclusions.

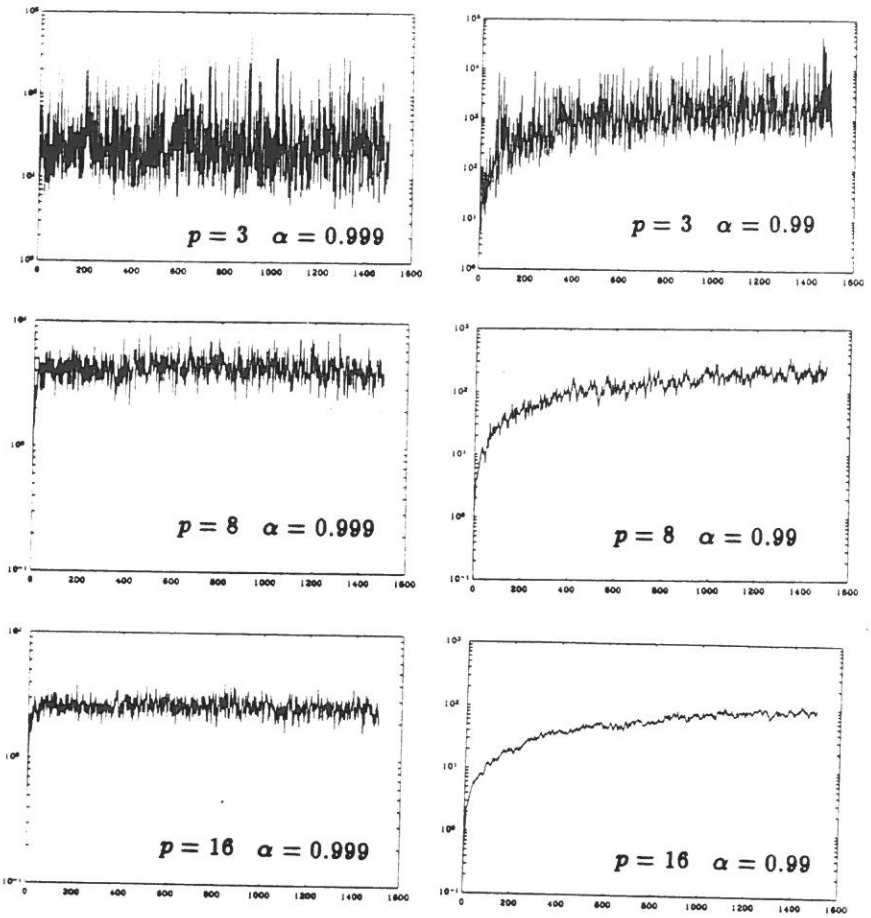

Figure 4.8: *The ratio ρ for different values of α and p.*

We may therefore claim that, with an appropriately chosen value of α, the matrix B_i is close enough to diagonal form in order to conclude the convergence of the algorithm.

We will now determine the amount of computational work that the algorithm has to perform in each cycle, supposing that only one plane rotation is performed in the diagonalization step and that the rotation angle is computed with the new method of over- and underrelaxation.

Step 1 : the generation of an output vector requires the product of a $p \times p$ matrix and a p-vector. The required computational work is then

p^2	additions
p^2	multiplications

Step 2 : the rank-one perturbation of the symmetric covariance matrix and multiplication with the forgetting factor α requires

$p(p+1)/2$	additions
$p(p+1)$	multiplications

Step 3 : the reduction of the off-diagonal norm of the covariance matrix by executing only one Jacobi rotation, requires

$2p+5$	additions
$4p+1$	multiplications
2	divisions

Step 4 : the updating of the U-matrix requires

$2p$	additions
$4p$	multiplications

Therefore the total computational work per cycle of the algorithm is

$(3p^2+9p+10)/2$	additions
$2p^2+9p+1$	multiplications
2	divisions

4.8 Conclusion

In this Chapter we presented an adaptive on-line algorithm for updating the left singular matrix in the OSVD of a matrix, each time a new column is added to the matrix. The algorithm is essentially a rank-one updating of the covariance structure of the problem, but it differs from other similar methods in the following ways :

- for each new column, appended to the data matrix, **only one plane rotation** is performed, instead of diagonalizing the covariance matrix completely.
- the algorithm is **adaptive** in the way that it forgets exponentially events from the past.
- a new approach has been developed to compute the **angle** of the plane rotation, which corresponds to a so called over- or underrelaxation.

All these approximations reduce the amount of the computational work substantially, such that real-time implementations of the algorithm for multichannel signal processing applications become feasible (see Appendix A).

Chapter 5

Signal separation by OSVD of the extended data matrix

5.1 Introduction

In Chapter 2 it was shown that the solution to the problem of eliminating the disturbing signals from a set of recorded signals consists in finding a subspace W of the p-dimensional measurement space, which is orthogonal to the subspace spanned by the transfer vectors of the undesired source signals. In the first section of this Chapter we will present a method, based on the concept of oriented energy, that finds an **orthonormal basis** for that subspace W by simply computing the Ordinary Singular Value Decomposition (OSVD) of the data matrix. Some basic assumptions about the source signals, the noise signals and the signal transfer from source to measurement points have to be made. It will be shown further that these assumptions are quite realistic.

In section 5.2.2 the influence of non-orthogonality of the transfer is described as a summary of results obtained from studies by *Vanderschoot* ([83], [84], [86]). This leads to some very important remarks on the positioning of measurement sensors (see section 5.2.3). Indeed, the success of the method strongly depends upon the appropriate location of the measurement points, since this is related to the orthogonality of the signal transfer.

In section 5.3 this first signal separation method is applied to the problem of eliminating the maternal electrocardiogram (MECG) and extracting the fetal ECG (FECG) from a set of potential signals, recorded on the skin of the mother. Off-line as well as on-line computations are performed with success. An important parameter in the on-line algorithm is the exponential forgetting factor α. We will therefore discuss the choice of a value for α. In the last section it is shown that this signal separation method can also be used very successfully for the removal of 50 Hz net interference from biomedical recordings.

5.2 Signal separation principle based on the concept of oriented energy

5.2.1 Solution under ideal conditions

Suppose x sources X_l $(l = 1, \ldots, x)$ are observed from p observation points, and each source can be described by one or more source signals, such that the p recorded signals are found as a linear combination of the r source signals $s_1(t), \ldots, s_r(t)$ with $r \geq x$ (see Eq. (2.3)). If the recorded signals are sampled simultaneously, we can assume that the columns $\mathbf{m}_k$ of the corresponding $p \times q$ data matrix M are found as :

$$\mathbf{m}_k = \mathbf{t}_1 \, s_1[k] + \ldots + \mathbf{t}_r \, s_r[k] + \mathbf{n}_k \tag{5.1}$$

with $\mathbf{n}_k = (\, n_1[k] \ldots n_p[k] \,)^t$ and where $s_j[k]$ and $n_i[k]$ are the values of the signals $s_j(t)$ and $n_i(t)$ at each sampling instant $t = k$ (with $j = 1, \ldots, r$ and $i = 1, \ldots, p$ and $k = 1, \ldots, q$). With each source signal $s_j(t)$, a transfer vector $\mathbf{t}_j$ in the p-dimensional measurement space corresponds. Therefore, each data point $\mathbf{m}_k$ in the measurement space is found as a combination of r transfer vectors and a noise vector $\mathbf{n}_k$, with as coefficients the values of the source signals at $t = k$.

At this point we refer to the definition of oriented energy of a vector sequence in the direction of a unit vector $\mathbf{e} \in \Re^p$ (see Chapter 3) :

$$\begin{aligned}
E_{\mathbf{e}}[M] &= \sum_{k=1}^{q} (\, \mathbf{e}^t \, \mathbf{m}_k \,)^2 \\
&= \sum_{k=1}^{q} (\mathbf{e}^t \, \mathbf{t}_1 \, s_1[k] + \ldots + \mathbf{e}^t \, \mathbf{t}_r \, s_r[k] + \mathbf{e}^t \, \mathbf{n}_k)^2 \\
&= \sum_{k=1}^{q} (\mathbf{e}^t \, \mathbf{t}_1 \, s_1[k])^2 + \ldots + \sum_{k=1}^{q} (\mathbf{e}^t \, \mathbf{t}_r \, s_r[k])^2 + \sum_{k=1}^{q} (\mathbf{e}^t \, \mathbf{n}_k)^2 \\
&+ 2 \sum_{k=1}^{q} (\mathbf{e}^t \, \mathbf{t}_1)(\mathbf{e}^t \, \mathbf{n}_k) \, s_1[k] + \ldots + 2 \sum_{k=1}^{q} (\mathbf{e}^t \, \mathbf{t}_r)(\mathbf{e}^t \, \mathbf{n}_k) \, s_r[k] \\
&+ 2 \sum_{i=1}^{r-1} \sum_{j=i+1}^{r} \left(\sum_{k=1}^{q} (\mathbf{e}^t \, \mathbf{t}_i) \, (\mathbf{e}^t \, \mathbf{t}_j) \, s_i[k] \, s_j[k] \right)
\end{aligned} \tag{5.2}$$

We will now prove the following theorem :

Theorem 7 : *Solution under ideal conditions.*

Given a set of p recorded signals $m_i(t)$ *as a linear combination of r original source signals* $s_j(t)$ *, such that*

$$m_i(t) = \sum_{j=1}^{r} \mathbf{t}_j \, s_j(t) + n_i(t) \quad (i = 1, \ldots, p) \tag{5.3}$$

Construct the corresponding data matrix M with given OSVD

$$M_{p,q} = U_{p,p} \, \Sigma_{p,p} \, V^t_{p,q} \tag{5.4}$$

If

1. *the signal sources* X_l *are uncorrelated with each other and the source signals of each source are time-orthogonal*

$$\sum_{k=1}^{q} s_i[k] \, s_j[k] = \delta_{ij} \, \sigma^2_{sj} \quad (i, j = 1, \ldots, r) \tag{5.5}$$

with σ^2_{sj} *the energy of the j-th source signal over a fixed interval of time.*

2. *the source signals have different non zero energies :*

$$\sigma^2_{s1} > \sigma^2_{s2} > \ldots > \sigma^2_{sr} > 0 \tag{5.6}$$

3. *the noise is uncorrelated with the signal sources* X_l *:*

$$\sum_{k=1}^{q} n_i[k] \, s_j[k] = 0 \quad \begin{matrix} i = 1, \ldots, p \\ j = 1, \ldots, r \end{matrix} \tag{5.7}$$

4. *the noise in the measured signals is uncorrelated and all noise signals have the same energy :*

$$\sum_{k=1}^{q} n_i[k] \, n_j[k] = \delta_{ij} \, \sigma^2_N \quad (i, j = 1, \ldots, p) \tag{5.8}$$

5. *the transfer vectors* $\mathbf{t}_j$ *are orthogonal*

Then

1. *with* $\mathbf{u}_i$ *the i-th column of* U *in the OSVD of* M,

$$\mathbf{u}_i = \pm \mathbf{t}_i / \|\mathbf{t}_i\| \qquad (i = 1, \ldots, r) \tag{5.9}$$

2. *with* σ_i *the i-th singular value of* M,

$$\begin{aligned} \sigma_i^2 &= \sigma_{si}^2 + \sigma_N^2 \qquad (i = 1, \ldots, r) \\ \sigma_i &= \sigma_N \qquad\quad (i = r+1, \ldots, p) \end{aligned} \tag{5.10}$$

3. *with* $\hat{s}_j(t)$ *an estimation of the j-th source signal* $s_j(t)$

$$\hat{s}_j(t) = \mathbf{u}_j^t \, \mathbf{m}(t) \tag{5.11}$$

Proof : Trivial.

□

The conditions from Eq. (5.5) to Eq. (5.8) are quite realistic. Indeed, the more the problem is overdetermined, which is the case for larger values of q, corresponding to larger observation intervals in signal processing applications, the better the conditions of Eq. (5.7) and Eq. (5.8) are met. If the recording equipment, environmental disturbances and external interferences are the same for all of the recording channels, it is also quite realistic to assume that the contribution of noise is equally strong in each of the recorded signals (see Eq. (5.8)).

Furthermore, the assumption that source signals of a more-dimensional source are time-orthogonal (see Eq. (5.5)) is also realistic, since each more-dimensional phenomenon can be described by its principal components, each with another energy. These conditions change Eq. (5.2) into

$$E_{\mathbf{e}}[M] = \sum_{k=1}^{q} (\mathbf{e}^t \, \mathbf{t}_1 \, s_1[k])^2 + \ldots + \sum_{k=1}^{q} (\mathbf{e}^t \, \mathbf{t}_r \, s_r[k])^2 + \sigma_N^2 \tag{5.12}$$

Eq. (5.12) shows that the oriented energy of data matrix M in the direction of a unit vector $\mathbf{e}$ is the superposition of several oriented energies, each in the direction of the transfer vector $\mathbf{t}_j$ and equal to

$$\|\mathbf{t}_j\| \, \sigma_{sj}^2 \qquad (j = 1, \ldots, r)$$

while the noise is assumed to have the same oriented energy in all directions.

If the transfer vectors $\mathbf{t}_j$ are orthogonal, then the directions $\mathbf{e}$ for which the oriented energy of M reaches an extremal value (the first r left singular vectors $\mathbf{u}_j$) coincide with those transfer vectors. This statement is based on the uniqueness of the OSVD. Therefore

$$\begin{aligned} \mathbf{u}_j^t\,\mathbf{m}(t) &= \frac{\mathbf{t}_j^t}{\|\mathbf{t}_j\|}\sum_{i=1}^{r}\mathbf{t}_i\,s_i(t) + \frac{\mathbf{t}_j^t}{\|\mathbf{t}_j\|}\,\mathbf{n}(t) \qquad (j=1,\ldots,r) \\ &= \|\mathbf{t}_j\|\,s_j(t) + \frac{\mathbf{t}_j^t}{\|\mathbf{t}_j\|}\,\mathbf{n}(t) = \hat{s}_j(t) \end{aligned} \tag{5.13}$$

If the ideal conditions apply (see Theorem 7), the solution of the problem can be outlined as follows :

1. Record p signals from appropriately (see section 5.2.3) located observation points
2. Construct the corresponding data matrix M
3. Compute the Ordinary SVD of $M = U_M\,\Sigma_M\,V_M^t$
4. Use the columns of the matrix U_M for the linear combinations of the p recorded signals to obtain an estimate of the original source signals.

5.2.2 Non-orthogonality of the transfer vectors

In the previous section it was shown that the orthogonality of the transfer vectors is an important condition to find a solution for the signal separation problem, based on the concept of oriented energy. However, in practice this ideal situation is not always realizable. Since the transfer coefficients in Eq. (2.3) are unknown, the orthogonality of the transfer is a rather difficult requirement to meet. Therefore, we will illustrate in this section with a two-dimensional example the effect of non-orthogonality of the transfer vectors on the solution, as presented in the previous subsection.

Suppose that two sources X_1 and X_2, that each can be described by only one signal, $s_1(t)$ and $s_2(t)$ respectivily, are observed from two observation points, such that the recorded signals $m_1(t)$ and $m_2(t)$ are found as a linear combination of the two source signals, disturbed by noise signals $n_1(t)$ and $n_2(t)$, then

$$\begin{pmatrix} m_1(t) \\ m_2(t) \end{pmatrix} = \begin{pmatrix} \mathbf{t}_1 & \mathbf{t}_2 \end{pmatrix} \begin{pmatrix} s_1(t) \\ s_2(t) \end{pmatrix} + \begin{pmatrix} n_1(t) \\ n_2(t) \end{pmatrix} \tag{5.14}$$

Suppose furthermore that signal $s_1(t)$ is unwanted and uncorrelated with the weaker signal of interest $s_2(t)$, then data matrix M can be written as

$$M = T \begin{pmatrix} \sigma_{s1} & 0 \\ 0 & \sigma_{s2} \end{pmatrix} \begin{pmatrix} s_1^*[1] & s_1^*[2] & \dots & s_1^*[q] \\ s_2^*[1] & s_2^*[2] & \dots & s_2^*[q] \end{pmatrix} + N \tag{5.15}$$

with σ_{sj} the square root of the energy of source signal $s_j(t)$ during the interval under consideration and with $s_j^*[k]$ the normalized values of the signals $s_j(t)$ at sampling instant $t = k$.

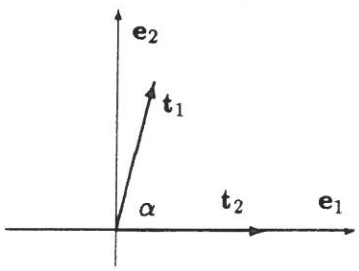

Figure 5.1: *The normalized transfer vectors* $\mathbf{t}_1$ *and* $\mathbf{t}_2$.

In order to take into account the non-orthogonality of the transfer vectors $\mathbf{t}_1$ and $\mathbf{t}_2$ in T, the transfer will be modelled as follows (see Figure 5.1)

$$T = (\mathbf{t}_1 \quad \mathbf{t}_2) = \begin{pmatrix} \cos\alpha & 1 \\ \sin\alpha & 0 \end{pmatrix} \begin{pmatrix} \|\mathbf{t}_1\| & 0 \\ 0 & \|\mathbf{t}_2\| \end{pmatrix} \tag{5.16}$$

Define the ratio σ as

$$\sigma = \frac{\|\mathbf{t}_1\| \ \sigma_{s1}}{\|\mathbf{t}_2\| \ \sigma_{s2}} \tag{5.17}$$

then $E_{\mathbf{e}}[M]$, the oriented energy of matrix M in the direction of unit vector $\mathbf{e} = (\cos\theta \quad \sin\theta)^t$, is equal to

$$E_{\mathbf{e}}[M] = \|\mathbf{t}_1\|^2 \sigma_{s1}^2 \cos^2(\alpha - \theta) + \|\mathbf{t}_2\|^2 \sigma_{s2}^2 \cos^2\theta + \sigma_N^2 \tag{5.18}$$

The term σ_N^2 is constant for all directions $\mathbf{e}$. In order to find those values of θ for which $E_{\mathbf{e}}[M]$ is extremal, the first derivative has to be set zero. This results in the following relation between α, σ and $\varepsilon = \alpha - \theta$.

$$\tan 2\varepsilon = \frac{\sin 2\alpha}{\sigma^2 + \cos 2\alpha} \tag{5.19}$$

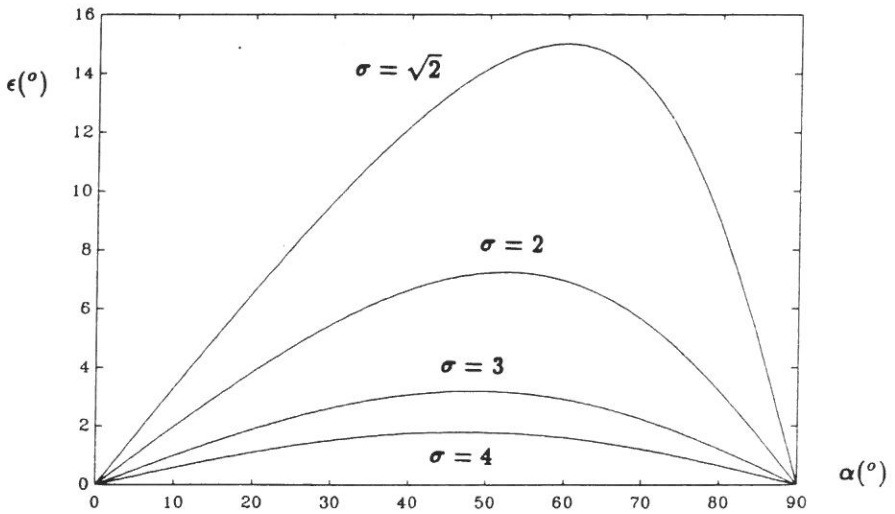

Figure 5.2: *The angle ε between $\mathbf{t}_1$ and $\mathbf{u}_1$ as a function of α for some values of σ.*

The OSVD of the data matrix M finds two orthonormal directions $\mathbf{u}_1$ and $\mathbf{u}_2$ in the two-dimensional measurement space for which the oriented energy is extremal. An important conclusion from the curves, shown in Figure 5.2, is that even for moderate values of σ, the deviation angle ε between $\mathbf{u}_1$ and $\mathbf{t}_1$ remains very small (e.g. for $\sigma = 4$, $\varepsilon < 2^o$ for $0^o \leq \alpha \leq 90^o$).
The following reasoning can then be applied :

1. the transfer vector $\mathbf{t}_1$ corresponds to the strongest source signal $s_1(t)$
2. the stronger $s_1(t)$ is observed in the p recorded signals with respect to $s_2(t)$ (bigger values for σ), the closer the direction $\mathbf{u}_1$ of maximal oriented energy is to $\mathbf{t}_1$
3. since $\mathbf{u}_2$ is orthogonal to $\mathbf{u}_1$, the orthogonal projection of all columns of M onto $\mathbf{u}_2$ will contain only a very small portion of the strongest source signal.

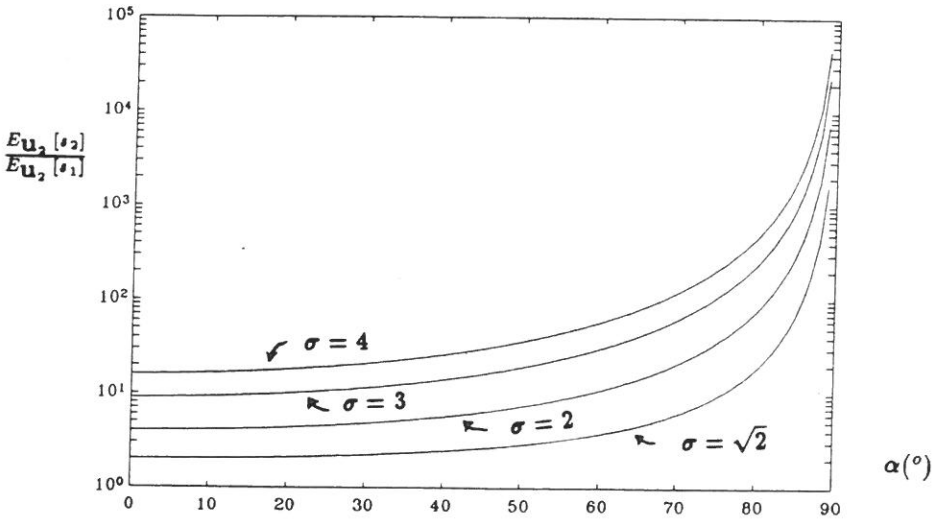

Figure 5.3: *The ratio between weak and strong signal contribution in the projection onto* $\mathbf{u}_2$ *as a function of* α *for some values of* σ.

In [84] an expression is derived for the ratio between the energy contribution of weak signal $s_2(t)$ and the portion of strong signal $s_1(t)$, that appears in the projection of the columns of M onto $\mathbf{u}_2$:

$$\left(\frac{E_{\mathbf{u}_2}[s_2]}{E_{\mathbf{u}_2}[s_1]}\right) = \frac{\sin^2(\varepsilon - \alpha)}{\sigma^2 \sin^2 \varepsilon} \tag{5.20}$$

In Figure 5.3 this ratio is plotted as a function of α for some values of σ. For near-orthogonal transfer vectors $\alpha \rightarrow \pi/2$, this ratio is very high and tends to infinity. The remarkable thing now is that for every $\mid \alpha \mid > 0$, this ratio will never decrease below a certain limit, that is proven to be

$$\lim_{\alpha \rightarrow 0} \left(\frac{E_{\mathbf{u}_2}[s_2]}{E_{\mathbf{u}_2}[s_1]}\right) = \sigma^2 \tag{5.21}$$

These results are now summarized as follows :

1. Even for moderate ratios (σ) of the two source signals, the first singular vector $\mathbf{u}_1$ in the OSVD of data matrix M is very close to the first transfer vector $\mathbf{t}_1$.

2. The ratio between the wanted signal $s_2(t)$ and the disturbing signal $s_1(t)$ in the orthonormal projection onto $\mathbf{u}_2$ is always better than the inverse ratio of the sources themselves. In other words, the stronger the disturbing signal with respect to the wanted signal, the higher the ratio of wanted signal to unwanted signal in the projection.

The findings of [82], [84] and [86] can be extended to more-dimensional sources only on a qualitative basis, because the analysis in a formal, general way is too complicated. In general, for any number of sources, a linear combination of the recorded signals with a certain left singular basis vector of the data matrix, may contain a large portion of a weak source signal, while the strong disturbing sources are almost completely eliminated or at least reduced substantially.

5.2.3 Positioning of measurement points

Although the difference in strength between the source signals is already an important parameter for the success of the signal separation method, it is still required to obtain transfer vectors which are as orthogonal as possible. An important observation here involves the **spatial separation** of signal sources. Let us again consider the example with only two sources X_1 and X_2, that can each be described by one source signal, $s_1(t)$ and $s_2(t)$, respectively. The two sources are at distinct positions in some medium. Suppose one can only pick up signals from both sources with observation points at the surface of the medium. Assume furthermore that $s_2(t)$ is the signal of interest, while $s_1(t)$ is the disturbing source signal. If only two observations are made and if the medium is linear, the signals $m_1(t)$ and $m_2(t)$ are expressed as

$$\begin{cases} m_1(t) = t_{11}\, s_1(t) + t_{12}\, s_2(t) \\ m_2(t) = t_{21}\, s_1(t) + t_{22}\, s_2(t) \end{cases} \tag{5.22}$$

$$\text{with} \quad \begin{pmatrix} t_{11} \\ t_{21} \end{pmatrix} = \mathbf{t}_1 \quad \text{and} \quad \begin{pmatrix} t_{12} \\ t_{22} \end{pmatrix} = \mathbf{t}_2$$

The transfer coefficients t_{ij} become relatively small, if the observations are made far from a source, whatever the strength of that source is.

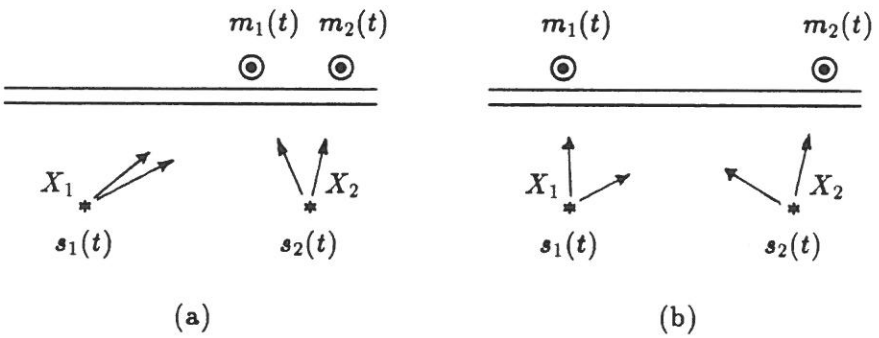

Figure 5.4: *Positioning of two observation points for two signal sources : a) Two observation points close to the source of interest. b) Spatial separation of the observation points.*

Consider now the following two alternative choices for the position of the measurement points.

1. Put the two observation points close to the source of interest in order to pick up as much of the useful signal as possible (see Figure 5.4.a). Both components of $\mathbf{t}_1$ are then very small, while the components of $\mathbf{t}_2$ are both very big. It is almost impossible to guarantee orthogonality of $\mathbf{t}_1$ and $\mathbf{t}_2$ in that case.

2. Put an observation point close to each source (see Figure 5.4.b). In this case one component of $\mathbf{t}_1$ is bigger than the other ($t_{11} \gg t_{21}$), while for $\mathbf{t}_2$ it is inverse ($t_{12} \ll t_{22}$). In this case near-orthogonality of the transfer vectors is guaranteed by spatial separation of the observation points.

If more-dimensional signal sources have to be observed, more than one observation point must be placed in the neighbourhood of each source, in order to force the transfer vector subspaces, corresponding with each source, to be near-orthogonal to each other. This principle will be used e.g. in the application for separating maternal and fetal ECG by putting electrodes on the maternal abdomen (close to the fetal heart), but also electrodes on the maternal thorax (see section 5.3).

Summarizing this analysis, it is very important for the outlined SVD-based signal separation method that :

1. the disturbing source is picked up as strongly as possible in order to eliminate it successfully.

2. some of the observation points are put close to the disturbing source, such that near-orthogonality of the transfer is obtained.

5.3 FECG-extraction by computing the OSVD of the data matrix

5.3.1 Clinical Experiments

In this section we will apply the first SVD-based signal separation method, as described in the previous section of this Chapter, to the problem of eliminating the maternal ECG and extracting the fetal ECG from a set of potential signals. The experiments were carried out in cooperation with the Laboratory of Gastrointestinal Motility of the Department of Medical Research of the U.Z. Gasthuisberg, K.U. Leuven (B).

The signals are recorded with disposable Ag/AgCl electrodes on the mother's skin and are **bipolar**. This means that they are taken from pairs of electrodes, spaced apart over about $\pm$ 15 – 20 cm, and that no central reference electrode is used, since the choice of the position for the reference electrode is critical for the required spatial separation of the electrodes. A disadvantage of bipolar recordings is the large number of degrees of freedom for the positioning strategy, while unipolar recordings permit to define an easy standard electrode placement protocol. It is then also possible to obtain bipolar signals from subtracting unipolar recordings in. This results however in a higher noise level in the resultant signal, than the noise that would be present in a directly recorded bipolar signal.

The recordings are filtered using a second order lowpass filter with cut-off frequency $f_0 = 70$ Hz and a first order highpass filter with time constant $\tau_0 = 50$ ms ($\simeq 3$ Hz). The sampling frequency is usually 250 Hz, unless stated otherwise, which satisfies the Nyquist theorem because the frequency range of interest is between 0.5 Hz and 100 Hz. In the following paragraphs some experiments and results are described. In the last section of this Chapter, the main conclusions about these experiments in clinical practice are repeated.

5.3.2 Extraction of a MECG-free fetal ECG

Experiment 1 : *How to eliminate the contribution of the maternal ECG from one recording ?*

Figure 5.5 shows a signal of 6 seconds, recorded on the abdomen of patient A. It contains a mixture of clearly visible fetal ECG and a much stronger signal from the maternal heart. We will now eliminate the contribution of maternal ECG from this signal by adding three independent signals, that pick up only contributions from the maternal heart. The reason for adding **three** signals is the following : the electrical activity of the adult heart can be modelled as a rotating dipole vector.

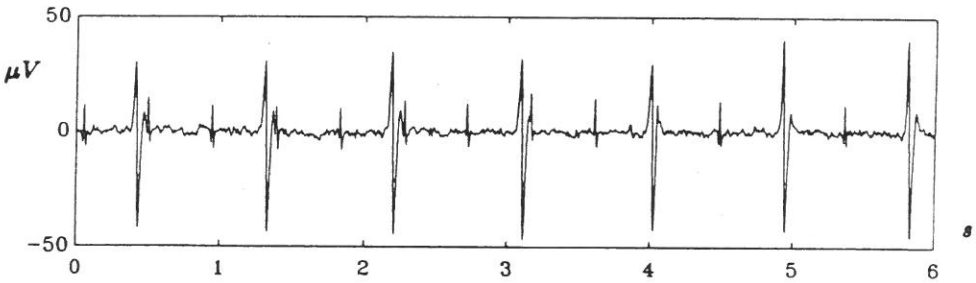

Figure 5.5: *A signal recorded on the abdomen of patient A and containing both MECG and FECG.*

Therefore, in theory at least three orthogonal signals are sufficient to describe the rotation of that vector. Adding more than three thoracic signals increases the possibility for obtaining a fetal signal, free from any maternal ECG contributions. On the other hand, less than three signals is not sufficient to describe the electrical activity of the maternal heart. Since these signals are measured from electrodes in the neighbourhood the maternal thorax, we will call them thoracic signals (see Figure 5.6). Care should however be taken that one does not record signals from electrodes, too close to the maternal heart, because then the approximating dipole hypothesis no longer holds.

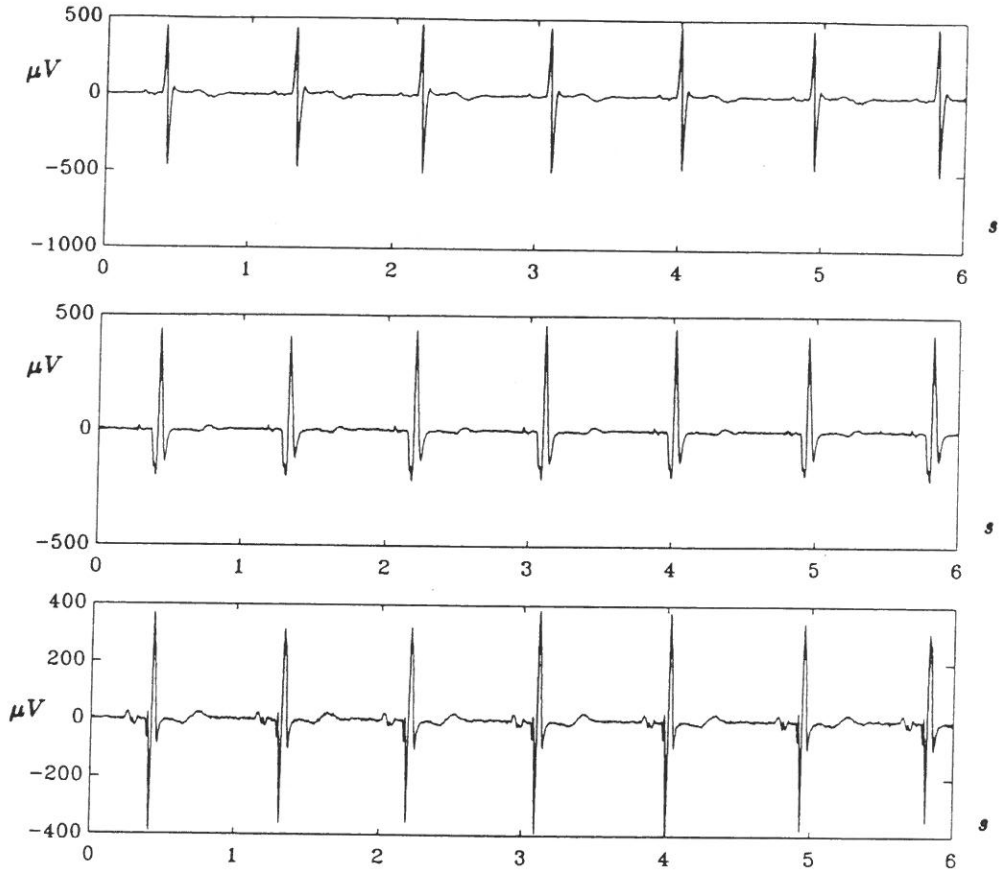

Figure 5.6: *Three signals (patient A), picking up the MECG independently.*

A data matrix with dimension 4×1500 is constructed by digitizing the four recorded signals with a sampling frequency of 250 Hz and its OSVD is computed. Combining the four recorded signals by using the columns of the U-matrix, results in the four orthogonal signals, shown in Figure 5.7. The first three signals in this figure are orthogonal signals that describe the electrical activity of the maternal heart, while the fourth signal is a "clean" fetal heart signal, free from any maternal ECG. All contributions from the strongest source (the maternal heart) are eliminated.

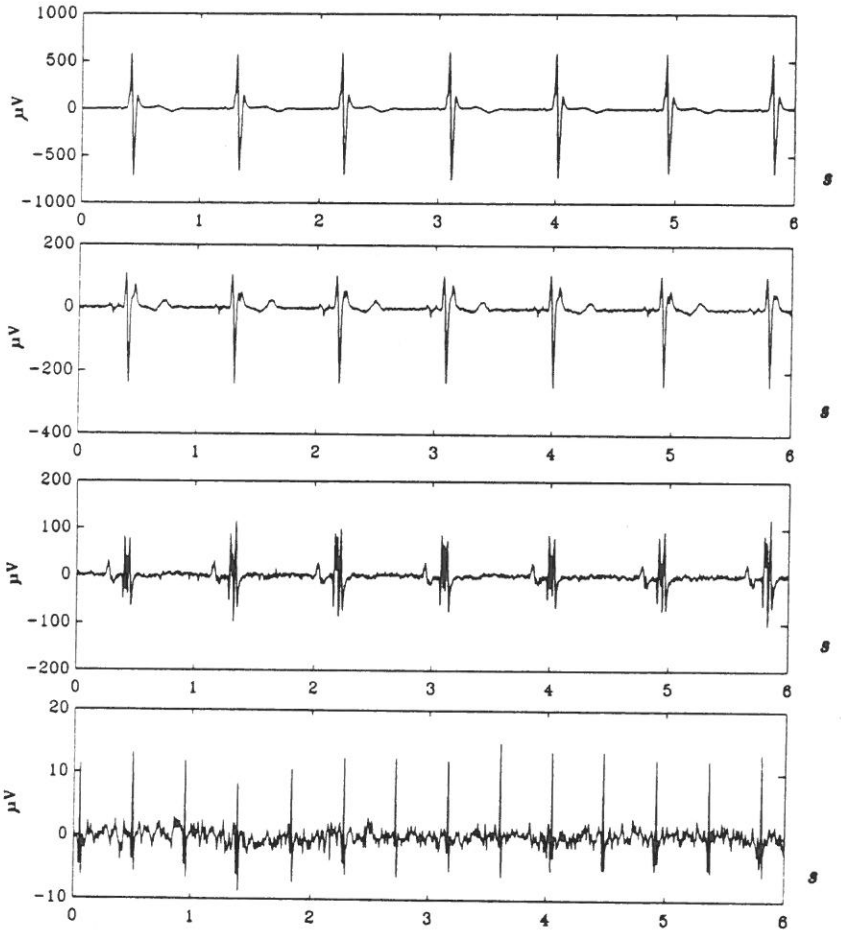

Figure 5.7: *The four resultant orthogonal signals : signal 4 is completely free of MECG and contains a clean FECG.*

Experiment 2 : *How to obtain the optimal fetal signal, after elimination of the maternal ECG ?*

In the previous experiment it was demonstrated how to remove the maternal ECG from a recording that contains both MECG and FECG. The resultant fetal signal is then free of MECG, but its signal-to-noise ratio is not better than that of the original recorded signal. We will therefore record more than one abdominal signal, hoping that all fetal contributions in those signals add up to result in a fetal signal with higher signal-to-noise ratio than in any of the recorded signals. Figure 5.8 shows three abdominal signals, recorded over a period of 6 seconds.

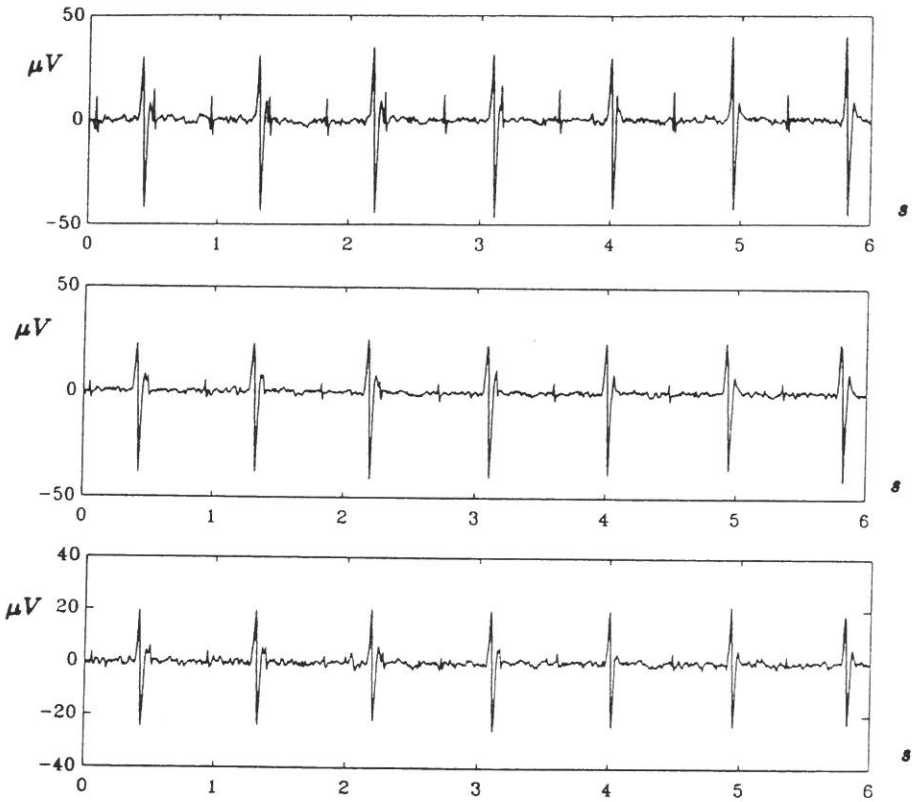

Figure 5.8: *Three simultaneously recorded abdominal signals (patient A), containing both MECG and FECG.*

For the elimination of the MECG three thoracic signals are added, that pick up the MECG separately (see Figure 5.6). Application of the OSVD-based method to the corresponding 6×1500 data matrix results in the six orthogonal signals shown in Figure 5.9. The first three signals describe the electrical activity of the maternal heart, while signals four and five are signals from the fetal heart. The last signal only contains some noise.

The interpretation of the results is as follows. Due to the properties of the OSVD, the resultant signals are ordered according to their oriented energy. Since the maternal heart is the strongest source, present in the recordings, and since this source has dimension three (a rotating dipole vector), the first three resulting signals correspond to the maternal ECG. Furthermore, since the fetal heart is the second strongest source present in the recordings, the fourth signal is the MECG-free linear combination of the six recorded signals, with the highest signal-to-noise ratio. In this sense, the fourth signal is the "optimal" MECG-free fetal signal present in these six recorded signals.

Moreover, a second MECG-free fetal signal is found. This means that the electrical activity of the fetal heart, as observed by cutaneous electrodes, cannot always be represented by one signal only. As for the adult heart, the electrical activity of the fetal heart corresponds to a rotating dipole, such that more orthogonal signals are needed to describe the "complete" fetal ECG. Due to changes in the conductive medium during pregnancy, it is even possible that the electrical activity of the fetal heart is observed as a rotating dipole in earlier pregnancies, while in later pregnancies this activity is observed as a fixed dipole ([57], [59]). This is one of the topics for further research, once a real-time signal separation unit is ready for practical use.

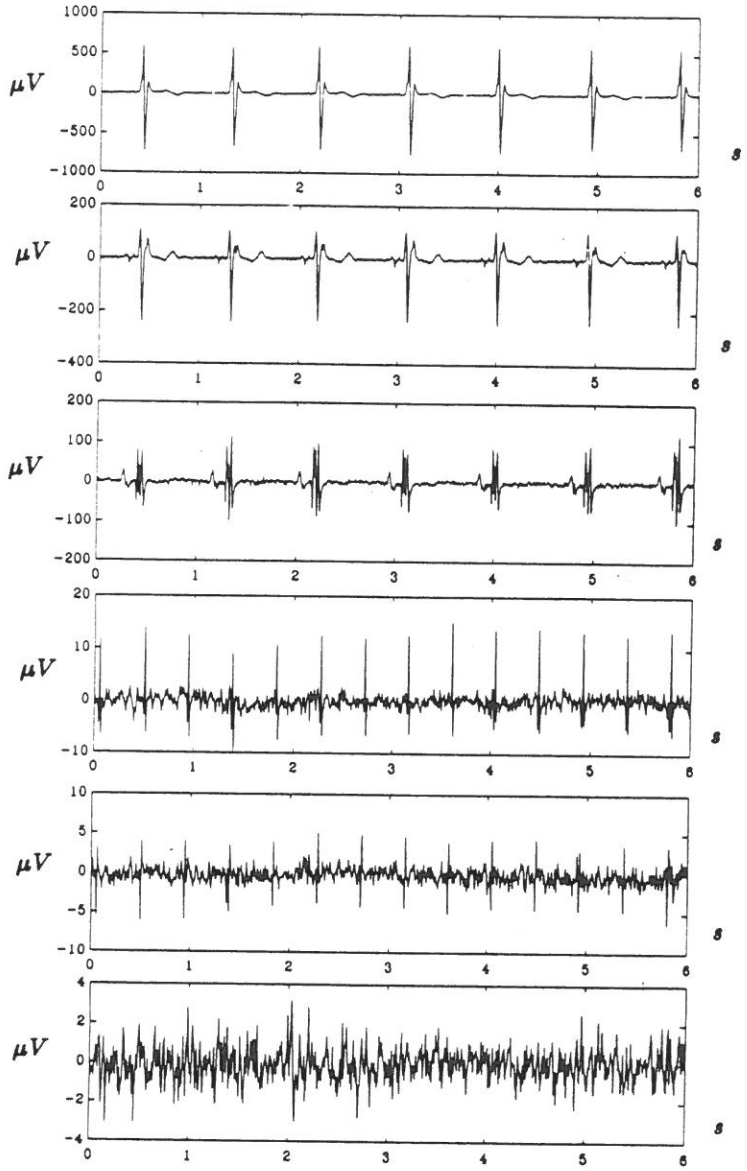

Figure 5.9: *The six orthogonal signals, obtained as a linear combination of the recorded signals : signals 4 and 5 are free of MECG and contain the FECG.*

5.3.3 Fetal contributions in the recorded signals

Experiment 3 : *Is it possible to obtain the contributions of the FECG in each of the recorded signals ?*

The two MECG-free fetal signals, obtained in Figure 5.9, are for an obstetrician or cardiologist very difficult to interpret, since they are not "real" signals measured between two electrodes. They are more "virtual" signals, that are not physically measurable. In fact, those two fetal signals are so called **principal** signals, since they form an orthogonal signal basis in the measurement space. This means that every fetal contribution in the recorded signals of Figure 5.6 and Figure 5.8 can be reconstructed as an appropriate linear combination of those two principal fetal signals.

Indeed, suppose that U_F is the matrix, constructed from thóse left singular vectors of the data matrix, that lie in the fetal subspace, then $\hat{S}_F = U_F^t M$ is the matrix that contains the two obtained fetal signals. A matrix F, with the same dimension as the data matrix M, can then be obtained, containing all FECG contributions in each of the p recorded signals, as follows

$$F = U_F U_F^t M \tag{5.23}$$

The six signals obtained in F are shown in Figure 5.10. This figure clearly shows that even in the thoracic signals (the first three signals) a fetal ECG component exists, although much weaker than the fetal ECG contribution in the abdominally recorded signals. Now a physician can interpret these signals much better, since they refer to exactly known electrode positions.

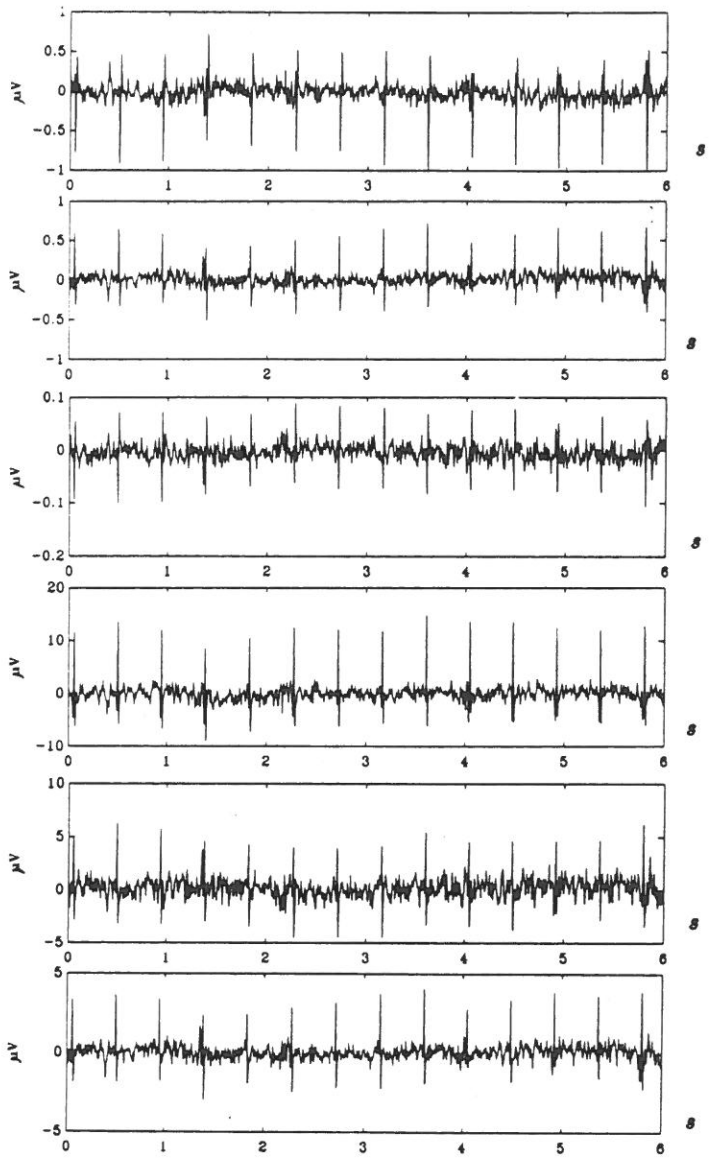

Figure 5.10: *The contribution of fetal ECG in each of the six recorded signals of Figures 5.6 and 5.8.*

5.3.4 Detection of the P-wave in the FECG

Experiment 4 : *Is it possible to detect the P-wave in the obtained MECG-free fetal signals ?*

Each fetal PQRST-waveform slightly differs due to noise, baseline drift, maternal breathing, etc. It is therefore very difficult to extract some parameters, such as the duration of the QRS-complex, the position of the P-wave, etc., from the raw signals. However, if for each of the signals in Figure 5.10 a mean FECG cardiac cycle is constructed by averaging 10 consecutive PQRST-waveforms, then much smoother FECG waveforms are obtained (see Figure 5.11).

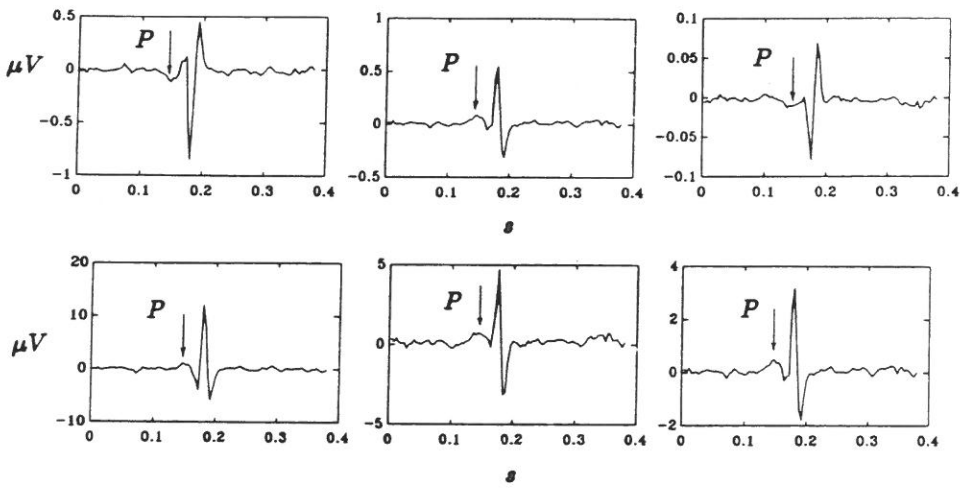

Figure 5.11: *Mean FECG waveforms for each of the electrode pairs. The arrows indicate the clearly visible P-wave.*

While it was nearly impossible to detect the P-wave in the signals of Figure 5.10, a clearly visible P-wave is found in the mean fetal cardiac cycles of Figure 5.11. The detection of the P-wave makes the differential diagnosis of eventually occurring supraventricular tachycardia possible. From the same plots of Figure 5.11, the duration of the QRS-comples can be derived, providing diagnostic information to discriminate between ventricular or supraventricular tachycardia, if needed.

5.3.5 The importance of the thoracic signals

Experiment 5 : *Is the elimination of the MECG sensitive to the choice of the thoracic signals ?*

It is shown with an example that the OSVD-based signal separation principle is sensitive to the positioning of the electrodes. Figure 5.12.a shows a signal of 8 seconds, recorded on the abdomen of patient B. Again three thoracic signals are added (see Figure 5.12.b to the data set. Application of the OSVD-method results in the MECG-free fetal signal shown in Figure 5.12.c. For this particular case, one can therefore conclude that the positioning of the electrodes was good, resulting in a near-orthogonal transfer, such that the OSVD-method was successful.

Simultaneously, a second abdominal signal (see Figure 5.13.a) was recorded. If for this signal the same thoracic signals of Figure 5.12.b are added, the OSVD-method results in the signal, shown in Figure 5.13.b. In this case no separation of the MECG and FECG occurs. The fact that there is no separation of MECG and FECG this time can be explained in two ways : **either** the positioning of the thoracic electrodes was not ideal, such that the transfer vectors associated to the maternal heart signals are not orthogonal to those associated to the fetal heart signals, **or** the fetal ECG is so strongly present in the recordings that the gap between the smallest singular value associated to the maternal subspace and the largest singular value associated to the fetal subspace is not high enough. This means that the maternal ECG is not strongly enough present in the recordings, relative to the presence of the fetal heart signals.

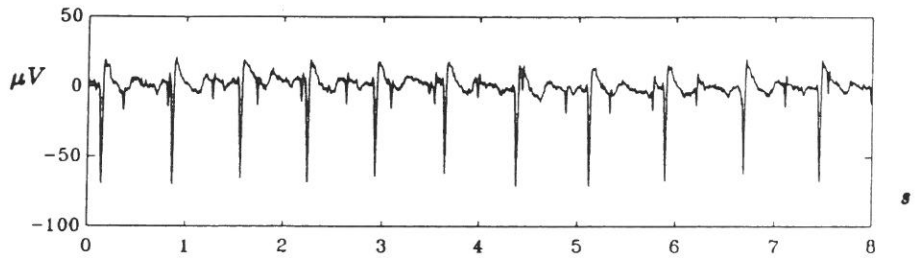

Figure 5.12: *(a) Signal recorded on the abdomen of patient B, containing both MECG and FECG.*

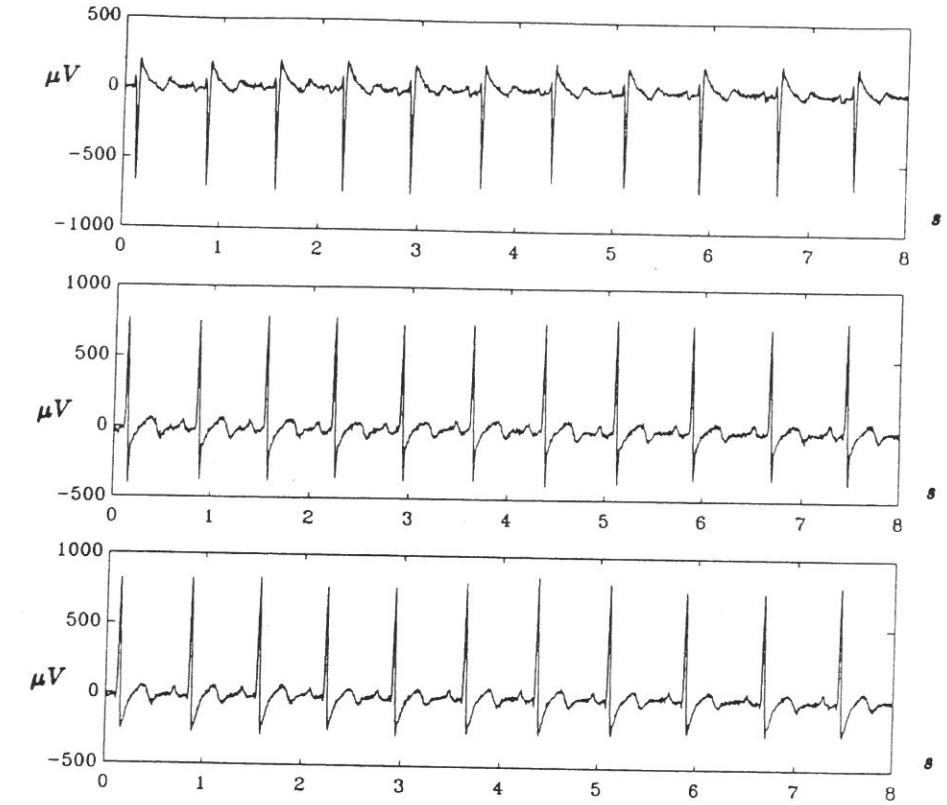

(b)

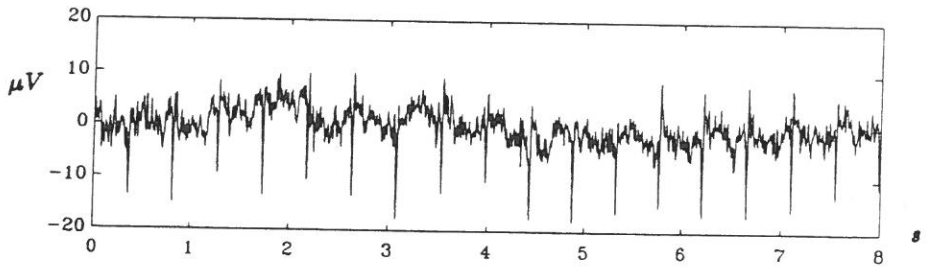

(c)

Figure 5.12: *(b) Three thoracic signals (patient B), picking up the maternal ECG independently. (c) The resultant MECG-free fetal signal after application of the OSVD-method.*

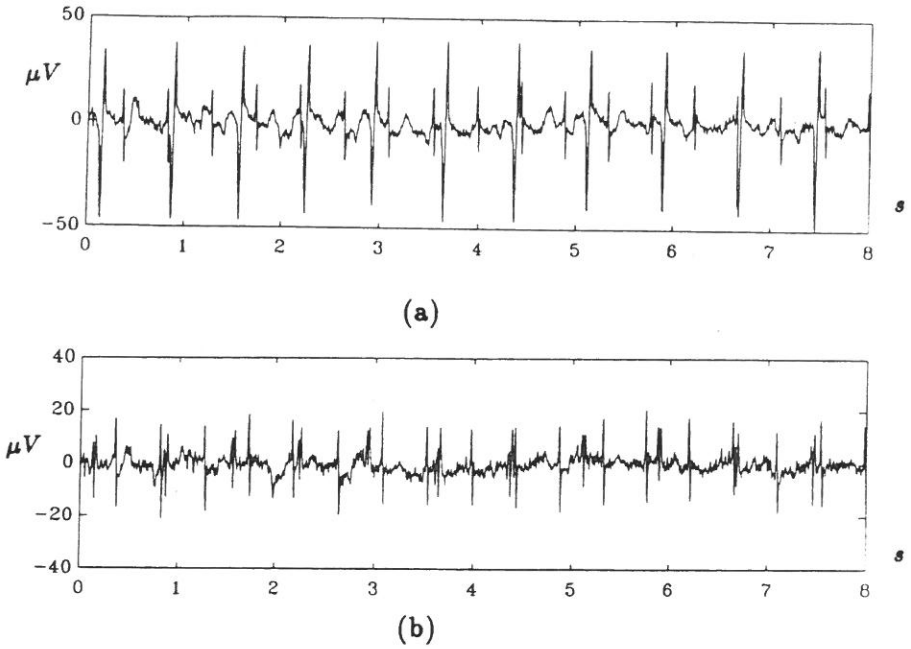

Figure 5.13: *(a) A second signal, recorded on the abdomen of patient B and containing both MECG and FECG. (b) The resultant signal after application of the OSVD-method still contains both MECG and FECG.*

These two problems can be overcome if more than three thoracic recordings are added. However, since all experiments were not carried out in real-time, the computations and processing techniques were applied after the experiments had been recorded on tape and digitized later. It was therefore impossible to evaluate the chosen electrode positions during the course of an experiment. Inappropriately chosen positions with respect to the orthogonality of the (unknown) transfer could therefore not be corrected. This advocates the need for a real-time system for OSVD-based signal separation, such that the chosen electrode positions can be evaluated immediately.

In practice, this means that the choice of the electrode positions has to be done iteratively : first, find an abdominal signal with clearly visible fetal ECG; then extend the signal set with some (at least three) thoracic signals that pick up the maternal ECG independently and such that a processing unit for real-time signal separation (see Appendix A) finds an MECG-free fetal signal by combining the signals, recorded up till now; finally, extend the signal set with some more abdominal signals with clear contributions of FECG, in order to obtain an optimal fetal ECG.

5.3.6 The on-line adaptive algorithm for FECG-extraction

There are several reasons that advocate the application of an on-line technique for MECG-elimination and FECG-extraction.

- Since the positioning of the electrodes is very critical for the success of the method, and since the use of bipolar recordings implies a large number of degrees of freedom in electrode placement, a real-time evaluation of the chosen electrode location is required.
- Fetal movements may change the transfer from signal sources to measurement points, such that an adaptive technique, able to follow those variations is needed. The variations are however not of that type that they result in a completely different transfer from one sampling instant to another. Changes will indeed occur more smoothly.
- Since an electrocardiogram results in a near-periodical data matrix, the left singular matrix does not change that much over the subsequent periods (± 1 s). Therefore, a method that only updates this left singular matrix each time a new column is appended to the data matrix, is desirable.

Instead of computing the OSVD of a data matrix off-line, we will apply the adaptive on-line algorithm, developed in Chapter 4 to this problem of MECG-elimination and FECG-extraction. A very important parameter in this on-line algorithm is the exponential forgetting factor α, lying between 0 and 1. The closer α is to 1, the larger the exponential window and the greater the influence of inputs from the remote past. The smaller α, the quicker the method forgets about the past. In section 4.5 we already mentioned that an appropriate choice for α depends upon the sampling frequency and the stationary behaviour or periodicity of the signals.

The MECG-FECG application has very stationary signals, that are almost periodical. Indeed, the U-matrix in the OSVD of the data matrix varies only slightly from one maternal heartbeat to another. The MECG has a periodicity of 60-80 per minute, such that the time between two successive maternal heartbeats is at the most about 1 second. If the sampling rate is 250 Hz, then input values of 1 second before are multiplied with a factor α^{250}. In order to be sure that the method will not forget too quickly, we will design an exponential window, such that contributions to the covariance matrix C_i in the algorithm are multiplied by $1/4$ after 4 seconds (

$\simeq$ 1000 samples). Therefore $\alpha^{1000} = 1/4$ or $\alpha = 0.9986$. This corresponds to an exponential weighting of the input data with a factor $\sqrt{\alpha} = 0.9993$. Table 5.3.6 gives the value α^k with which the contributions to the covariance matrix are multiplied after k samples, for different values of α. This shows that, for our application with 250 Hz sampling rate, the method will forget almost anything after only 2 seconds for values of α below 0.995 (for $\alpha = 0.995$ and $k = 500$, $\alpha^k = 0.0816$).

α	$k = 250$	$k = 500$	$k = 750$	$k = 1000$
0.999	0.7787	0.6064	0.4722	0.3677
0.998	0.6062	0.3675	0.2228	0.1351
0.997	0.4718	0.2226	0.1050	0.0496
0.996	0.3671	0.1348	0.0495	0.0182
0.995	0.2856	0.0816	0.0233	0.0067
0.993	0.1727	0.0298	0.0052	0.0009
0.99	0.0811	0.0066	0.0005	0.0
0.98	0.0064	0.0	0.0	0.0
0.97	0.0005	0.0	0.0	0.0

Table 5.1: The forgetting factor α^k for different values of α.

Experiment 6 : *The use of the on-line algorithm for MECG-elimination and FECG-extraction.*

We applied the on-line algorithm to a set of six signals : 3 signals recorded on the abdomen of patient A (see Figure 5.8) and 3 signals recorded from the thorax (see Figure 5.6). Each sampling instant an input vector of 6 values is obtained as a column of the data matrix. The corresponding output vector also contains 6 values and is generated as soon as a new input vector is available. This results in the six signals shown in Figure 5.14. One can notice that the signals are initially still quite erroneous. But after about 1 s, the signals four and five will be virtually free of MECG, and will approximate the same results as obtained in Figure 5.9. Indeed, after one maternal QRS-complex already enough information has been acquired in order to determine the maternal and fetal subspaces, such that the maternal ECG can be removed. The algorithm was applied with only one plane rotation per cycle and with the forgetting factor $\alpha = 0.9986$.

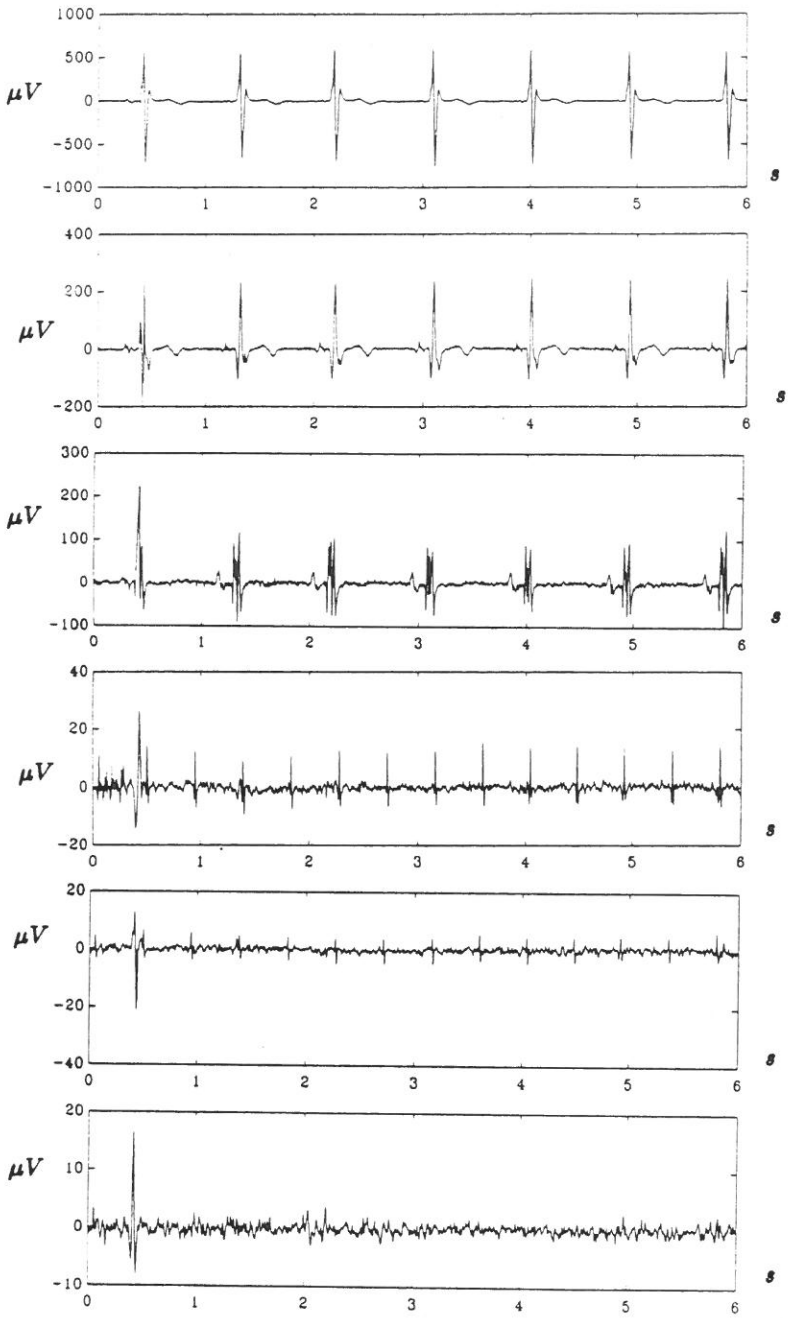

Figure 5.14: *The six resultant orthogonal signals, after application of the on-line algorithm with* $\alpha = 0.9986$.

Experiment 7 : *How quickly does the adaptive method recover from a sudden change in the data ?*

In order to demonstrate the adaptive ability of the on-line algorithm, we will simulate a sudden change in the transfer, and observe the recovery of the algorithm. We therefore start with the 3 thoracic signals of Figure 5.6 and the abdominal signal of Figure 5.5, observed over 6 s. After about 2.5 s, the abdominal signal was replaced by another signal, that was recorded simultaneously from another electrode pair on the abdomen of patient A. Figure 5.15 shows this "simulated" abdominal signal, where the arrow points the moment of the sudden change.

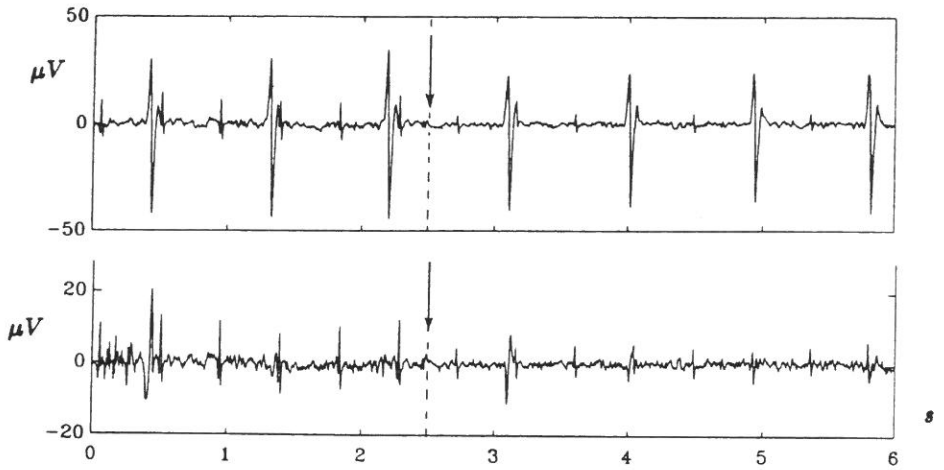

Figure 5.15: *The first signal is a simulation of a sudden change in an abdominal signal, while the second signal results after applying the on-line algorithm.*

In practice, this sudden change never occurs, but due to fetal movements, the fetal position relative to the electrodes may change during an experiment. In this sense the simulation is a worst case situation of a fetal movement. The algorithm is executed with $\alpha = 0.9986$ and one of the resultant signals is shown in Figure 5.15. As can be seen, only one maternal QRS-complex is required after the change to restore the separation. The amplitude of the resulting FECG is smaller than before the change, since the input signal contained a weaker FECG. This experiment illustrates that the method is able to recover from even very abrupt changes. A change in the location of the abdominal electrodes only influences the fetal-signal-to-noise ratio in the resultant signal, not the quality of the MECG-elimination.

5.4 Elimination of 50 Hz net interference

5.4.1 Introduction

One of the major problems encountered in recording ECG's is the appearance of unwanted 50 Hz (USA : 60 Hz) net interference in the recorded signals. In this section we will describe very shortly how this kind of interference enters in the recordings and afterwards we will present a possible solution for removing this interference from the recorded signals. In the further outline of this section we assume the net frequency to be 50 Hz, as in the European situation.

5.4.2 Sources of net interference

In any biopotential recording situation, interference from 50 Hz AC, often called AC pickup or hum, can be a serious problem. Since at least the room has to be lighted and the recording equipment has to be powered, the AC line potential from the net is unavoidably present in any clinical situation. The net interference is caused by the presence of AC fields that can be classified into two independent categories [43] : magnetic and electric fields.

A changing magnetic field B produced by AC can induce in any nearby conductive loop (e.g. the loops between the electrode leads) an electromotive force, which results in an AC-potential. On the other hand, a changing electric field E, produced by an AC potential, can also produce interference by causing AC displacement currents that flow through tissue and electrode impedances, thus producing AC potentials. Huhta and Webster [43] define and describe many possible ways by which interference can enter ECG recordings. They develop simple tests and provide remedies in order to minimize the effects of net interference. Since this is beyond the scope of this work, we will not proceed on this topic here.

5.4.3 Removal of net interference by filtering

The most straightforward way to remove this kind of interference is the use of a very sharp notch filter with as center frequency the net frequency [2]. This notch filtering has however an important drawback. In practical situations it occurs that the net frequency is not always exactly 50 Hz : it can even vary from 45 to 55 Hz. This makes the definition of a notch filter extremely difficult. In that case the "sharp notch" should be replaced by a "small bandstop" around 50 Hz. It is however possible that the wanted signal contains frequency components of interest in the region of 50 Hz. These components are also filtered out such that important information may be lost. This can result in distortion of the signal. We may therefore conclude that simple filtering provides no adequate solution for the 50-60 Hz problem.

5.4.4 Removal of net interference by linear combinations

Some important observations point to a more elegant solution to the problem :

1. One can assume that the interferences, present in the measured bioelectric signals, contain only the first harmonic (with frequency ω) of the interfering source. Since the interference is mainly additive, the disturbance of a signal $s(t)$ by an interference with known frequency ω can be expressed as

$$s(t) + B \sin(\omega t + \varphi) \tag{5.24}$$

   with B and φ unknown.

2. Any harmonic function with given frequency can be written as a sum of two harmonic functions with the same frequency but in quadrature. In other words, whatever the value of B or φ, there always exist a $B_1 = B \cos\varphi$ and $B_2 = B \sin\varphi$ such that

$$B \sin(\omega t + \varphi) = B_1 \sin\omega t + B_2 \cos\omega t \tag{5.25}$$

3. Since the power network signal is available, it can be measured as a separate signal.

According to the signal separation method presented in this chapter, the following strategy can be applied in order to reduce the harmonic disturbance in a signal $m_1(t) = A\,s(t) + B\,\sin(\omega t + \varphi)$

- Add two extra signals that pick up the interference independently : one signal $m_2(t)$ is taken directly from the power network, while the other signal $m_3(t)$ is a phase-shifted version of $m_2(t)$. In theory, the optimal phase shift is 90°, but in practice it can be realized by shifting the digitized signal $m_2(t)$ over one or more sampling instants. The extended measurement set is then

$$\begin{pmatrix} m_1(t) \\ m_2(t) \\ m_3(t) \end{pmatrix} = \begin{pmatrix} A & B\cos\varphi & B\sin\varphi \\ 0 & C & 0 \\ 0 & C\cos\theta & C\sin\theta \end{pmatrix} \begin{pmatrix} s(t) \\ \sin\omega t \\ \cos\omega t \end{pmatrix} \tag{5.26}$$

$$= (\tau_1 \quad \tau_2 \quad \tau_3) \begin{pmatrix} s(t) \\ \sin\omega t \\ \cos\omega t \end{pmatrix} \tag{5.27}$$

- Compute the OSVD of the data matrix $M = U_M\,\Sigma_M\,V_M^t$ and take $U_M = (\mathbf{u}_1 \quad \mathbf{u}_2 \quad \mathbf{u}_3)$
- Project the data matrix onto $\mathbf{u}_3$ to obtain a signal

$$\hat{s}(t) = \mathbf{u}_3^t \begin{pmatrix} m_1(t) \\ m_2(t) \\ m_3(t) \end{pmatrix} \tag{5.28}$$

The stronger the extra signals $m_2(t)$ and $m_3(t)$ and the more orthogonal the transfer matrix (this is true for $\theta \to \pi/2$ and for large values of C/B and C/A), the better span $\{\mathbf{u}_1, \mathbf{u}_2\}$ will approach the subspace formed by $\tau_2 = [B\cos\varphi \quad C \quad C\cos\theta]^t$ and $\tau_3 = [B\sin\varphi \quad 0 \quad C\sin\theta]^t$. This means that $\mathbf{u}_3$ is almost orthogonal to span $\{\tau_2, \tau_3\}$, such that $\hat{s}(t)$ will be almost free of the disturbing interference. Suppose $\mathbf{n}$ is the vector, orthogonal to span $\{\tau_2, \tau_3\}$ and given by

$$\mathbf{n} = [C\sin\theta \quad B\sin(\varphi - \theta) \quad -B\sin\varphi]^t \tag{5.29}$$

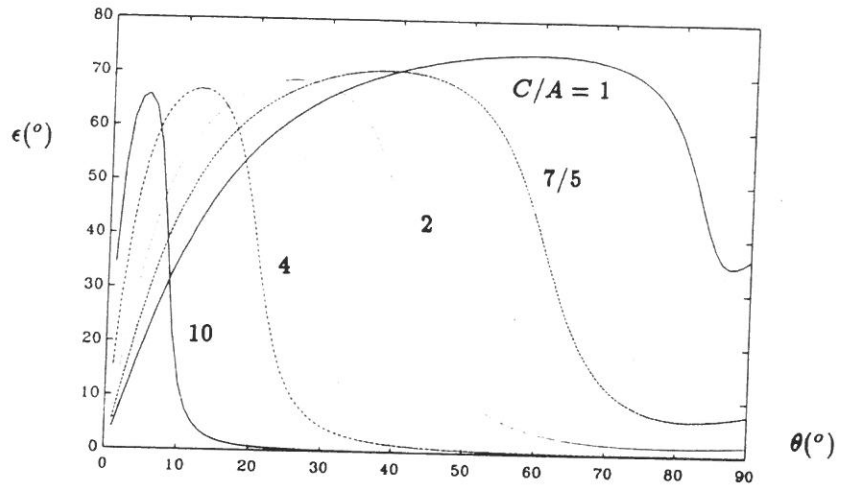

Figure 5.16: *The angle* ε *between* $\mathbf{u}_3$ *and the normal* $\mathbf{n}$ *onto the subspace span* $\{\tau_2, \tau_3\}$.

In Figure 5.16 the angle ε between $\mathbf{u}_3$ and $\mathbf{n}$ is plotted as a function of θ for $A/B = 5$, $\varphi = \pi/3$ and for different values of C/A. This Figure shows indeed that for large values of C/A (with given A/B) the angle ε is almost zero for most of the delays θ.

Another way to illustrate the success of the method is by comparing the ratio of signal-to-interference in the original signal $m_1(t)$, which is equal to

$$\mathrm{SN}_{in} = \frac{A^2}{B^2 \cos^2 \varphi + B^2 \sin^2 \varphi} = \frac{A^2}{B^2} \tag{5.30}$$

with the signal-to-interference ratio in the obtained signal $\hat{s}(t)$, equal to

$$\mathrm{SN}_{out} = \frac{(\mathbf{u}_3^t \tau_1)^2}{(\mathbf{u}_3^t \tau_2)^2 + (\mathbf{u}_3^t \tau_3)^2} \tag{5.31}$$

The ratio $\rho = \mathrm{SN}_{out}/\mathrm{SN}_{in}$ is a measure for the success of the technique, since it indicates whether the signal-to-interference ratio is improved after application of the method (> 1) or not (< 1). In Figure 5.17 this ratio ρ is plotted as a function of θ for $A/B = 5$, $\varphi = \pi/3$ and for different values of C/A. Experiments with other values for A/B and φ resulted in nearly similar plots as Figure 5.16 and Figure 5.17. The most important parameter in this context is always the parameter C/A.

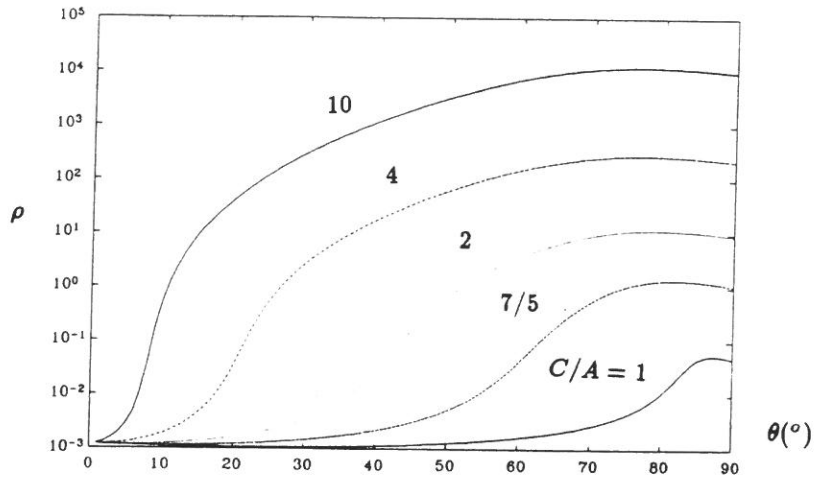

Figure 5.17: *The ratio ρ between signal-to-interference in the obtained signal and original signal as a function of θ for different values of C/A .*

Example 1 : Suppose an ECG-signal, disturbed by net interference, is recorded, while simultaneously a signal from the power network is picked up. If the sampling frequency is 250 Hz and the signal from the power net is delayed over one sampling instant to obtain the second extra signal, then $\theta = 72^o$. For this value of θ , the method is perfect whenever $C/A > 5$. The technique was applied to real data. Figure 5.18.a shows the spectrum of an ECG-signal, disturbed by net interference, while Figure 5.18.b shows the spectrum of the signal after removal of the net interference. The spectrum is in both cases quite similar and one can notice that the technique does not remove all 50 Hz contributions in the signal, as a notch filter would do. Figure 5.18.c shows the difference of the two spectra and this clearly illustrates that all interference with frequency $\simeq$ 45 Hz is eliminated. The disturbance is for this case so weak (0.8 dB) that it was not visible in the recorded ECG-signals.

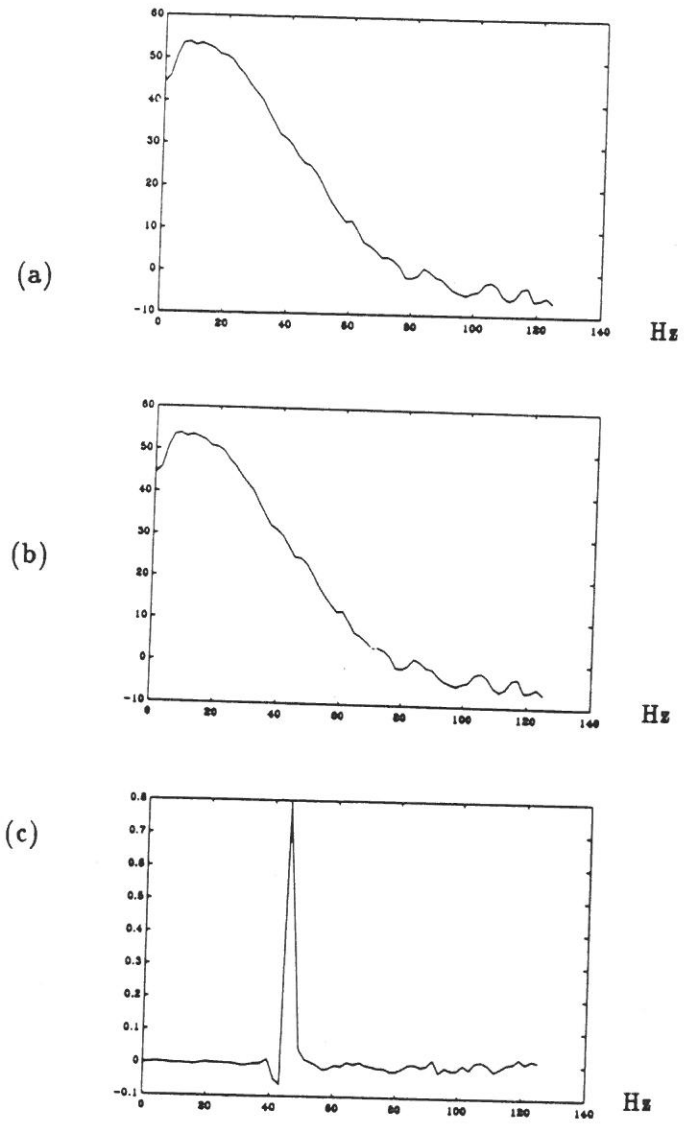

Figure 5.18: *Removal of net interference applied to real ECG-data. (a) Spectrum of recorded ECG-signal with net interference. (b) Spectrum of the signal after removal of the net interference. (c) Difference of the two spectra.*

5.5 Conclusion

In this Chapter we presented the first SVD-based signal separation method. The solution is based on the concept of oriented energy of a signal set and is first described under ideal conditions. Most of those conditions are realistic. but the most important one is However, in many applications the requirement for orthogonality of the transfer vectors is very difficult to meet, since this transfer is completely unknown. Therefore, we studied the influence of non-orthogonality of the transfer vectors. This leads to a very important result about the positioning of the measurement points : in order to eliminate a signal source from a set of recorded signals, add some signals to the set that pick up the disturbing source separately, such that the strongest contribution to the oriented energy of the complete signal set comes from that disturbing source.

This theoretical solution is then applied to the problem of eliminating the maternal ECG from recordings made on the abdomen of a pregnant women, in order to detect the fetal ECG. We described some of the experiments we did on real data, and the most successful results are the following :

- By adding at least three independent signals, that pick up the MECG separately, we are able to eliminate the contributions of the MECG from abdominal recordings.
- We showed that it is possible to extract an optimal fetal signal, with better signal-to-noise ratio than any of the recorded signals.
- It is possible to obtain more than one MECG-free fetal signal.
- We are able to eliminate the MECG and to extract the optimal FECG on-line, by applying the on-line adaptive algorithm of Chapter 4.
- We demonstrated that this algorithm is indeed adaptive, since it recovers very quickly from a sudden change.
- This method is also very suitable for the removal of 50 Hz net interference from biomedical recordings. For this application it acts as an "adaptive and selective notch filter".

In the next Chapter another signal separation principle is explained. In Chapter 7 these two methods will then be compared.

Chapter 6

Signal separation by QSVD of two matrices

6.1 Introduction

In this Chapter a second method for SVD-based signal separation is presented. This method differs from the first one (see Chapter 5) in the sense that the detection of signals of interest is now performed with non-orthonormal linear combinations of the recorded signals. The coefficients of these linear combinations are found from the Quotient Singular Value Decomposition of a matrix pair.

The first section will present a signal separation principle, based on the concept of oriented signal-to-signal ratio (see Chapter 3). Therefore it is required to consider two signal sets in the same measurement space : the data matrix M (with dimension $p \times q$), constructed from digitizing the p recorded signals and containing contributions from both wanted and unwanted phenomena, and a matrix Z (with dimension $p \times q_u$), derived from M by concatenating a number of intervals, selected from the data matrix, in which the undesired phenomenon contributes more than the source of interest.

In Section 6.2.2 the influence of non-orthogonality of the signal transfer is studied for a two-dimensional example. The main conclusion is that, the stronger the disturbing source is observed with respect to noise, the less will be the influence of non-orthogonality of the transfer. In Section 6.2.3 we present a way to compute the Quotient SVD as two successive OSVD's. This leads to an on-line version for the signal separation principle, where the adaptive on-line algorithm of Chapter 4 can be used for the second OSVD-computation.

In Section 6.3 the second signal separation method is applied to eliminate the maternal electrocardiogram from a set of potential signals, recorded with electrodes on the skin of the mother, in order to detect the fetal ECG. In a first paragraph we compute the Quotient SVD of the matrix pair off-line. Then also the importance of thoracic signals is studied and finally the adaptive on-line algorithm is used for on-line FECG-extraction from a set of p recorded potential signals.

6.2 Signal separation principle based on the concept of oriented signal-to-signal ratio

6.2.1 Outline of the method

Suppose p signals are recorded as a linear combination of r original source signals, some of which are of interest, while others are unwanted as they disturbe the p observations (see the general inverse problem of Eq. (2.3)). If these signals are sampled simultaneously and the corresponding data matrix M is constructed, then the columns of M form a cloud of points as a subspace in the p-dimensional measurement space (see Chapter 3). Suppose that, over a specific time interval, the undesired phenomenon contributes more in the recorded signals than the source of interest and that these intervals can selected from the data matrix M. Construct a matrix Z as a concatenation of the selected submatrices. This matrix Z defines another cloud of points in the same p-dimensional measurement space. Since the undesired source is dominantly present in this matrix Z , the cloud of points will be very close to or lie in the subspace, associated with the undesired phenomenon.

We now have two different clouds of points in the same measurement space :

- A cloud of points that corresponds to the data matrix M and contains contributions from all active signal sources some of which are undesired, while others are wanted.
- A cloud of points that corresponds to the constructed matrix Z and that mainly contains contributions from the undesired signal source.

In Chapter 3 we proved that the QSVD of the matrix pair (M, Z) finds some non-orthogonal directions in the measurement space for which the ratio of the oriented energy of M to the oriented energy of Z is extremal. Some of these directions must therefore be in the subspace, spanned by the transfer vectors of the wanted source signals.

The second SVD-based signal separation method can then be outlined as follows :

1. Record p signals that contain contributions from both the source of interest and the disturbing phenomenon.
2. Construct the corresponding data matrix M.
3. Select a number of intervals in which only the undesired phenomenon appears and construct a matrix Z by concatenating these intervals.
4. Compute the Quotient Singular Value Decomposition of (M, Z).
5. Use the columns of the matrix X in this QSVD for the linear combinations of the p recorded signals to obtain a matrix $S^* = X^t M$. Some rows of S^* contain the wanted source signals and are free from the undesired disturbance.

6.2.2 A two-dimensional example

Suppose two sources X_1 and X_2, that each can be described by only one signal, $s_1(t)$ and $s_2(t)$ respectively, are observed from two observation points and disturbed by additive noise $n_1(t)$ and $n_2(t)$, such that

$$\begin{pmatrix} m_1(t) \\ m_2(t) \end{pmatrix} = \begin{pmatrix} t_1 & t_2 \end{pmatrix} \begin{pmatrix} s_1(t) \\ s_2(t) \end{pmatrix} + \begin{pmatrix} n_1(t) \\ n_2(t) \end{pmatrix} \tag{6.1}$$

Suppose furthermore that signal $s_1(t)$ is unwanted and uncorrelated with the weaker wanted signal $s_2(t)$. The corresponding data matrix M is then constructed and a matrix Z, that contains only the undesired phenomenon, is derived from M. Since M and Z are both derived from the same measured signals, the respective signal models have the same normalized transfer vectors and involve the same original source signals : the only difference between M and Z in this model is the norm of each transfer vector and the energy of the noise. Therefore

$$M = T \begin{pmatrix} \sigma_{m1} & 0 \\ 0 & \sigma_{m2} \end{pmatrix} V_S^t + \begin{pmatrix} \sigma_{mN} & 0 \\ 0 & \sigma_{mN} \end{pmatrix} V_N^t \tag{6.2}$$

$$Z = T \begin{pmatrix} \sigma_{z1} & 0 \\ 0 & \sigma_{z2} \end{pmatrix} V_S^t + \begin{pmatrix} \sigma_{zN} & 0 \\ 0 & \sigma_{zN} \end{pmatrix} V_N^t \tag{6.3}$$

with $T = \begin{pmatrix} \cos\alpha & 1 \\ \sin\alpha & 0 \end{pmatrix}$ the normalized transfer matrix, and where V_S^t (V_N^t) contains the normalized source (noise) signals. The diagonal values σ_{m1}, σ_{m2}, σ_{z1} and σ_{z2} take into account the energies of the two source signals and the norms of the transfer vectors.

The oriented energy of M and Z in the direction of a random unit vector $\mathbf{e} = (\cos\theta \quad \sin\theta)^t$ is then equal to

$$E_{\mathbf{e}}[M] = \sigma_{m1}^2 \cos^2(\alpha - \theta) + \sigma_{m2}^2 \cos^2\theta + \sigma_{mN}^2 \tag{6.4}$$

$$E_{\mathbf{e}}[Z] = \sigma_{z1}^2 \cos^2(\alpha - \theta) + \sigma_{z2}^2 \cos^2\theta + \sigma_{zN}^2 \tag{6.5}$$

According to the definition of oriented signal-to-signal ratio,

$$R_{\mathbf{e}}[M, Z] = \frac{E_{\mathbf{e}}[M]}{E_{\mathbf{e}}[Z]} \tag{6.6}$$

This ratio reaches an extremal value, if its first derivative is set to zero.

This results in the following equation

$$2\,A\,\cos\,\theta\,\cos\,(\alpha-\theta)\,\sin\,\alpha\,+\,B\,\sin\,2(\alpha-\theta)\,-\,C\,\sin\,2\theta\,=\,0 \quad (6.7)$$

with

$$\begin{cases} A = s_{m1}^2\,s_{z2}^2 - s_{m2}^2\,s_{z1}^2 \\ B = s_{m1}^2 - s_{z1}^2 \\ C = s_{m2}^2 - s_{z2}^2 \end{cases} \quad (6.8)$$

and where $s_{m1} = \dfrac{\sigma_{m1}}{\sigma_{mN}}$, $s_{m2} = \dfrac{\sigma_{m2}}{\sigma_{mN}}$, $s_{z1} = \dfrac{\sigma_{z1}}{\sigma_{zN}}$ and $s_{z2} = \dfrac{\sigma_{z2}}{\sigma_{zN}}$.

From Eq. (6.7) a general expression can be derived for $\tan\,\theta$

$$\tan\,\theta\,=\,\frac{X\,-\,Y\,\cos\,\alpha\,\pm\,\sqrt{X^2\,+\,(C/B)\,Y^2}}{Y\,\sin\,\alpha} \quad (6.9)$$

with $X\,=\,A\,\sin^2\alpha\,+B-C$ and $Y\,=\,2B\cos\,\alpha$.

In fact, the ratio's s_{m1}, s_{m2}, s_{z1} and s_{z2} are signal-to-noise ratio's. Since matrix Z is constructed from parts of matrix M, that only contain the first (stronger) disturbing source signal, it is quite realistic to assume that the signal-to-noise ratio of the first source signal is the same in M as in Z, such that $s_{z1}\,=\,s_{m1}$ or that $B\,=\,0$ and $A\,=\,-s_{m1}^2\,C$ in Eq. (6.7). This equation can then be simplified into

$$\cos\,\theta\,\left(\,s_{m1}^2\,\cos\,(\alpha-\theta)\,\sin\,\alpha\,+\,\sin\,\theta\,\right)\,=\,0 \quad (6.10)$$

This results in two solutions for θ for which the oriented signal-to-signal ratio is extremal

$$\begin{cases} \tan\,\theta_1\,=\,\dfrac{-s_{m1}^2\,\tan\,\alpha}{1\,+\,(s_{m1}^2+1)\,\tan^2\alpha} \\ \\ \cos\,\theta_2\,=\,0 \quad \text{or} \quad \theta_2\,=\,\pi/2 \end{cases} \quad (6.11)$$

The second solution finds a direction $\mathbf{x}_2\,=\,(\cos\,\theta_2\;\sin\,\theta_2)^t$, perpendicular to the transfer vector $\mathbf{t}_2$, corresponding with the second source signal. This means that projection of the data matrix M onto $\mathbf{x}_2$ will not contain any contribution from the wanted source signal. Since it is our aim to eliminate the undesired source signal $s_1(t)$ and to detect the wanted source signal $s_2(t)$, we will omit this second solution.

The first solution corresponds with a direction $\mathbf{x}_1 = (\cos\theta_1 \ \sin\theta_1)^t$. We can also derive an expression for $\tan\varepsilon_1 = \tan(\alpha - \theta_1)$ as follows :

$$\tan\varepsilon_1 = (s_{m1}^2 + 1)\tan\alpha \tag{6.12}$$

In Figure 6.1 this angle ε_1 is plotted as a function of α for different values of $s_{m1} = s_{z1}$. This figure shows that angle ε_1 is close to 90° for large values of α. The larger s_{m1}, the more perpendicular direction $\mathbf{x}_1$ is onto $\mathbf{t}_1$, for more values of α. For a small angle α between the transfer vectors $\mathbf{t}_1$ and $\mathbf{t}_2$, $\mathbf{x}_1$ will lie very close to $\mathbf{t}_1$. In this case, projection onto $\mathbf{x}_1$ will not eliminate the disturbing source signal.

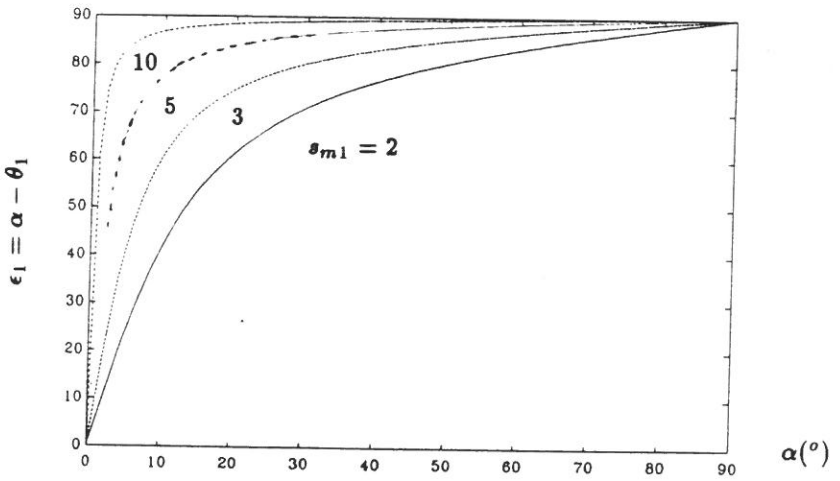

Figure 6.1: *Angle ε_1 as a function of α for different values of s_{m1}.*

These results are now summarized as follows :

1. The more orthogonal the transfer vectors $\mathbf{t}_1$ and $\mathbf{t}_2$ are $(\alpha \rightarrow 90^o)$, the more perpendicular $\mathbf{x}_1$ will be to $\mathbf{t}_1$, such that projection of the data matrix M onto $\mathbf{x}_1$ will contain only a very small portion of the undesired source signal.

2. The stronger the disturbing signal $s_1(t)$ is observed (the higher s_{m1}), the less will be the influence of non-orthogonality of the transfer on finding a direction $\mathbf{x}_1 \perp \mathbf{t}_1$.

We just showed that the orthogonality of the signal transfer is not a "conditio sine qua non" for signal separation with the QSVD-based method. On the other hand, the more orthogonal the transfer vectors, associated with the undesired source(s), are to the transfer vectors of the source(s) of interest, the higher the signal-to-noise ratio of the obtained signal(s), free from undesired contributions. This is illustrated in Figure 6.2 : it was shown that a vector $\mathbf{x}_1$ can be found, which is almost perpendicular to the transfer vector $\mathbf{t}_1$, that corresponds with the unwanted signal source. Projection of the data on this direction $\mathbf{x}_1$ will eliminate the unwanted disturbance, but the more orthogonal $\mathbf{t}_1$ and $\mathbf{t}_2$ are $(\alpha \rightarrow 90^o)$, the bigger the portion of wanted signal will be in the projection onto $\mathbf{x}_1$.

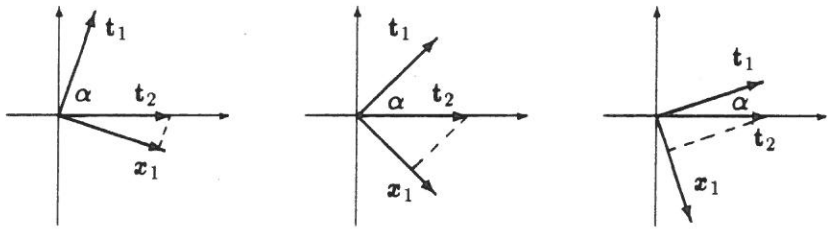

Figure 6.2: *Different configurations of transfer vectors.*

The ratio between the energy contribution of weak signal $s_2(t)$ and the portion of strong signal $s_1(t)$, that appears in the projection of the columns of M onto $\mathbf{x}_1$ is :

$$\left(\frac{E_{\mathbf{x}_1}[s_2]}{E_{\mathbf{x}_1}[s_1]}\right) = \frac{\sigma_{m2}^2}{\sigma_{m1}^2} \frac{\cos^2(\theta_1)}{\cos^2(\alpha - \theta_1} \tag{6.13}$$

This is a function of α that goes very quickly to infinity if $\alpha \rightarrow \pi/2$, and for every $|\alpha| > 0$, this ratio will never decrease below a certain limit, that is proven to be

$$\lim_{\alpha \rightarrow 0} \left(\frac{E_{\mathbf{x}_1}[s_2]}{E_{\mathbf{x}_1}[s_1]}\right) = \frac{\sigma_{m2}^2}{\sigma_{m1}^2} \tag{6.14}$$

If the signal of interest is much weaker in the recordings than the disturbing signal, then the ratio of Eq. (6.13) is very small for small angles between the transfer vectors. It is therefore recommended to make the transfer as orthogonal as possible.

6.2.3 Computation of the Quotient SVD

Many methods exist in order to compute the complete Quotient Singular Value Decomposition of two given matrices A and B (see C.F. van Loan [48], C.C. Paige [63], [64] and G.W. Stewart [76]). However, since we are only interested in finding the X-matrix in the QSVD of a matrix pair (it contains the directions of extremal oriented signal-to-signal ratio), we will now prove a theorem that enables us to obtain X by computing two consecutive Ordinary Singular Value Decompositions.

Theorem 8 : Computation of the X-matrix in the QSVD of (A, B)

Let A be a $p \times q$ and B a $p \times k$ matrix ($p < q$ and $p < k$) and suppose that the QSVD of the matrix pair (A, B) is given by

$$\begin{aligned} A &= X^{-t} D_A U_A^t \\ B &= X^{-t} D_B U_B^t \end{aligned} \tag{6.15}$$

with $U_A^t U_A = I_p$ and $U_B^t U_B = I_p$, with X a $p \times p$ non-singular matrix, and where $D_A = \mathrm{diag}(\alpha_1, \ldots, \alpha_p)$ and $D_B = \mathrm{diag}(\beta_1, \ldots, \beta_p)$, $(\alpha_i, \beta_i \geq 0)$, are square diagonal $p \times p$ matrices. The computation of the matrix X can be performed by the following four-step method [65], [75]

- *Step 1 :* *compute the OSVD of B*

$$B = U_B \Sigma_B V_B^t$$

- *Step 2 :* *define a transformation $Q = \Sigma_B^{-1} U_B^t$ on the matrix A such that*

$$Q A = A^* = \Sigma_B^{-1} U_B^t A$$

- *Step 3 :* *compute the OSVD of A^**

$$A^* = (U_A^*)(\Sigma_A^*)(V_A^*)^t$$

- *Step 4 :* *compute the X-matrix in the QSVD of (A, B) as*

$$X = Q^t U_A^* = U_B \Sigma_B^{-1} U_A^*$$

Proof :
If the QSVD of (A, B) is given as in Eq. (6.15), then

$$\begin{aligned} A\,A^t &= X^{-t}\,D_A^2\,X^{-1} \\ B\,B^t &= X^{-t}\,D_B^2\,X^{-1} \end{aligned} \tag{6.16}$$

In other words, matrix X diagonalizes both $A\,A^t$ and $B\,B^t$. The corresponding generalized symmetric eigenvalue problem has then the following formulation

$$A\,A^t\,\mathbf{x}_i = B\,B^t\,\mathbf{x}_i\,\lambda_i \tag{6.17}$$

with λ_i the i-th generalized eigenvalue. In the first step of the procedure the OSVD of B is computed, such that

$$B\,B^t = U_B\,\Sigma_B^2\,U_B^t = Q^{-1}\,Q^{-t} \tag{6.18}$$

Substitution into Eq. (6.17) then gives

$$A\,A^t\,\mathbf{x}_i = Q^{-1}\,Q^{-t}\,\mathbf{x}_i\,\lambda_i \tag{6.19}$$

This can also be written as

$$(Q\,A\,A^t\,Q^t)\,(Q^{-t}\,\mathbf{x}_i) = (Q^{-t}\,\mathbf{x}_i)\,\lambda_i \tag{6.20}$$

which is a normal symmetric eigenvalue problem. Diagonalization with an orthonormal matrix U_A^* of the symmetric matrix $Q\,A\,A^t\,Q^t$ and comparison with the first line of Eq. (6.16) results in

$$X = Q^t\,U_A^* = U_B\,\Sigma_B^{-1}\,U_A^* \tag{6.21}$$

□

Notice that the matrix X can be computed, without explicitly forming the numerically unstable products AA^t and BB^t, by just following the four step method as outlined in the theorem. If the undesired phenomenon is time-invariant, in the sense that its subspace does not change during the experiments, the first OSVD-step must only be computed once, as an initialization. The second step can then be performed by applying the on-line adaptive algorithm of Chapter 4, this time with $X_0 = U_B\,\Sigma_B^{-1}$ as initial linear combinations.

This leads to the following outline of an on-line version of the second SVD-based signal separation method :

1. Record p signals that contain contributions from both the source of interest and the disturbing phenomenon.
2. Select a number of intervals in which the periodic undesired phenomenon appears solely and construct a matrix Z by concatenating these intervals.
3. Compute the Ordinary SVD of $Z = U_z \Sigma_z V_z^t$ and initialize $X_0 = U_z \Sigma_z^{-1}$ and $B_0 = 0$
4. Apply the on-line adaptive algorithm from now on

Loop for $i = 1$ to q

$$\mathbf{y}_i = X_{i-1}^t \mathbf{m}_i \tag{6.22}$$
$$C_i = \alpha B_{i-1} + \mathbf{y}_i \mathbf{y}_i^t \tag{6.23}$$
$$B_i = Q_i^t C_i Q_i \tag{6.24}$$
$$X_i = X_{i-1} Q_i \tag{6.25}$$

end loop

6.3 MECG-elimination and FECG-detection by the QSVD of two matrices

6.3.1 Off-line extraction of the MECG-free fetal ECG

In this section we will apply the second signal separation method, based on the QSVD of two matrices, to the problem of extracting a fetal electrocardiogram (free from any contribution of the maternal ECG) from a set of cutaneously recorded potential signals.

We will illustrate the success of the method with a data set of 32 simultaneously recorded signals (see Figure 6.3). The set was recorded at the St. Radboud-Ziekenhuis in Nijmegen (NL) and was sampled at a rate of 500 Hz. The experiment has a length of 10 seconds, such that the dimension of the datamatrix is 32×5000. In Figure 6.3 the first 4 seconds of all recorded signals are shown. We selected six intervals from the data set in which a maternal QRS-complex appeared isolated in between two fetal complexes (three of these six intervals are indicated in Figure 6.3) and constructed a matrix Z (dimension 32×874) by concatenating these selected intervals. The fact that the time relation is lost between the signals in Z and the originally recorded signals has no influence. The most important thing is that Z defines a subspace in the measurement space, that approximates as good as possible the subspace, corresponding to the undesired phenomenon.

As explained in Chapter 3, the X-matrix in the QSVD of the matrix pair (M, Z) provides us directions in the measurement space for which the oriented signal-to-signal ratio is extremal. Orthogonal projection of the data matrix onto these directions leads to three MECG-free fetal ECG signals, shown in Figure 6.4. These three signals are non-orthogonal linear combinations of the 32 recorded signals, from which all MECG contributions are eliminated.

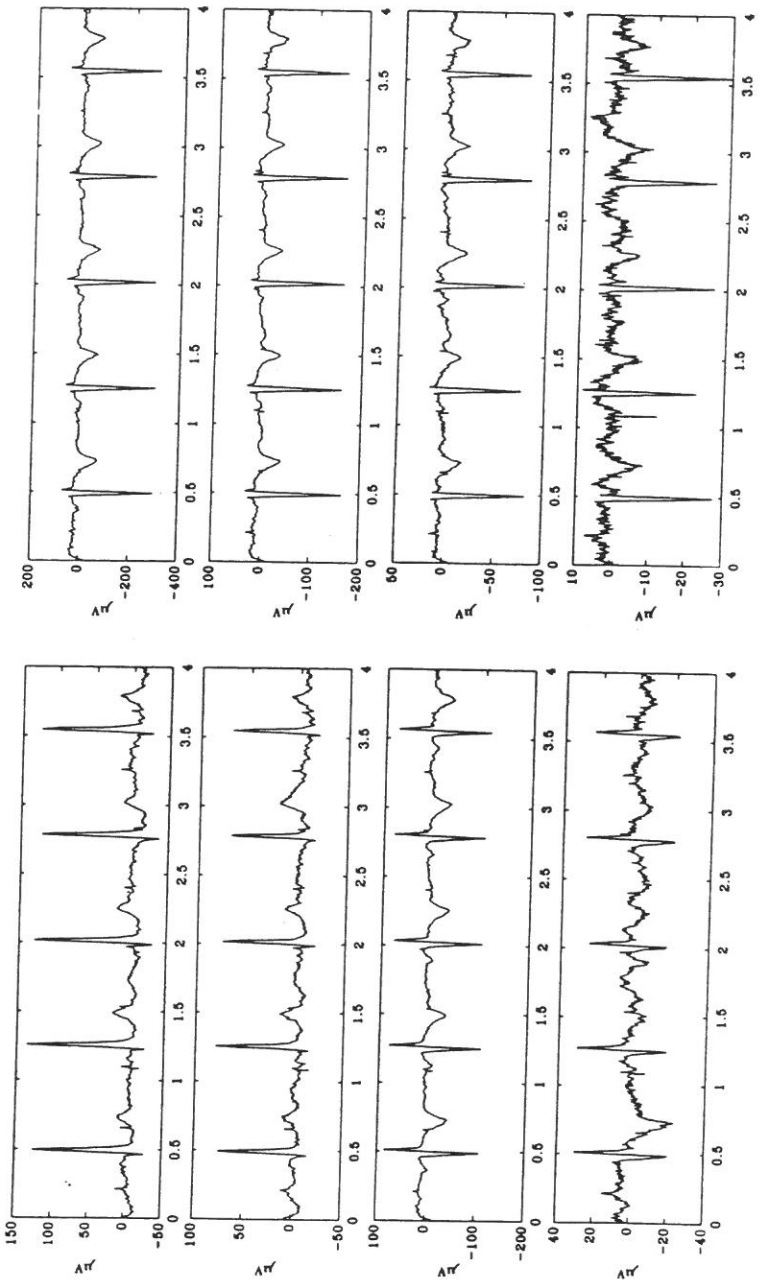

Figure 6.3: *Signals 1 to 8 of the 32-channel data set.*

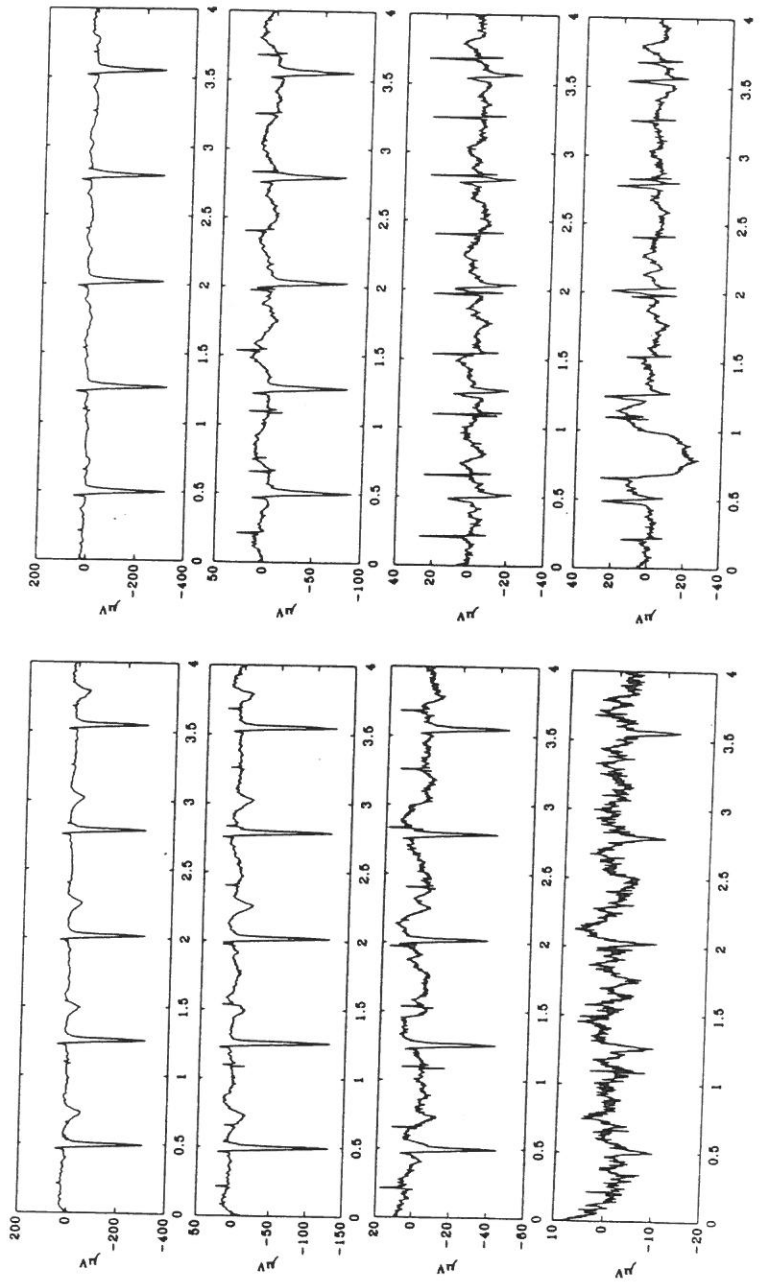

Figure 6.3: *Signals 9 to 16 of the 32-channel data set.*

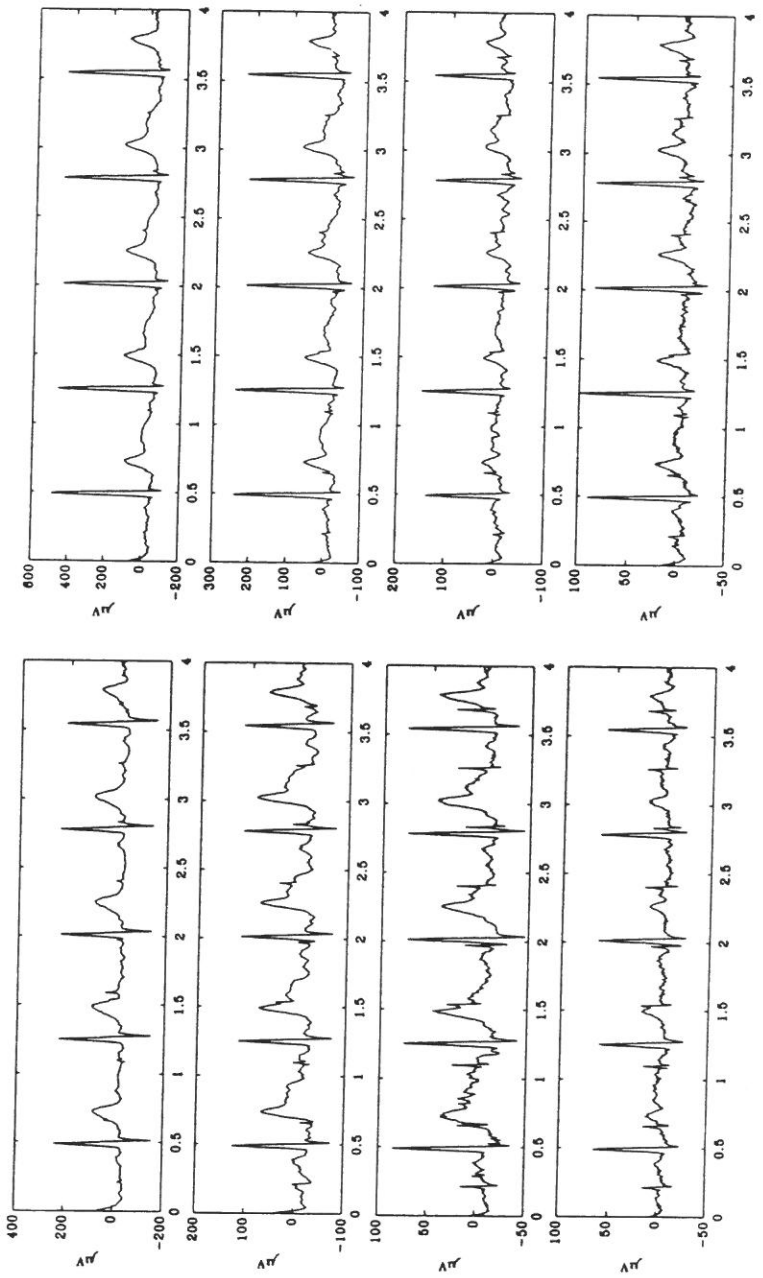

Figure 6.3: *Signals 17 to 24 of the 32-channel data set.*

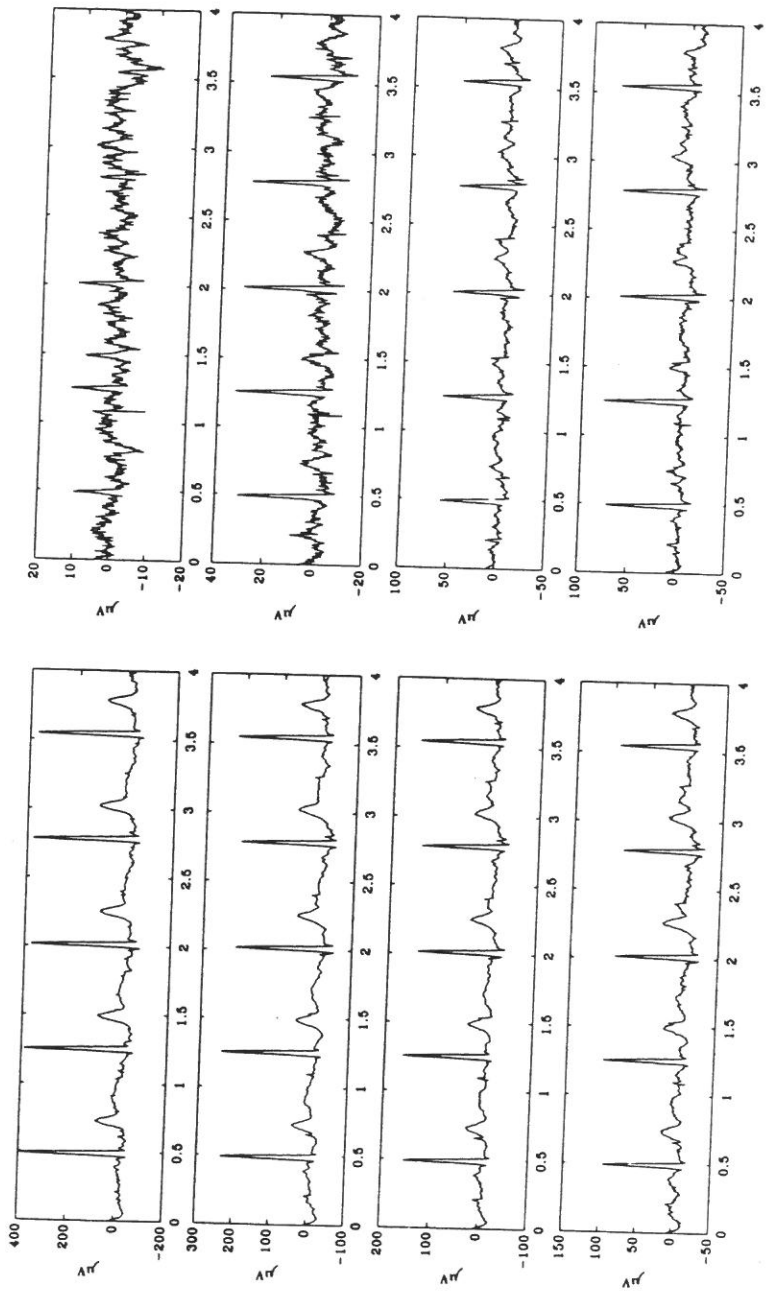

Figure 6.3: *Signals 25 to 32 of the 32-channel data set.*

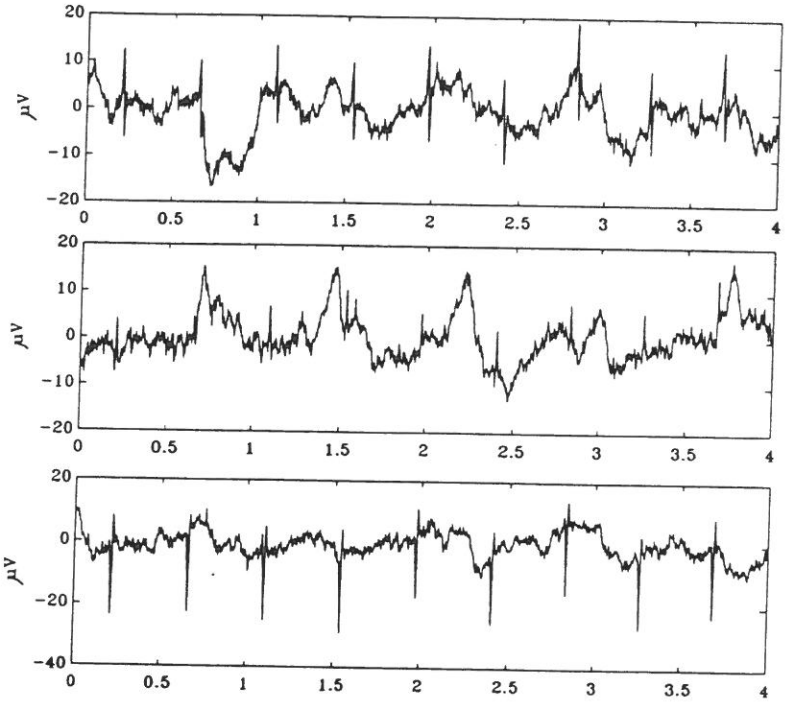

Figure 6.4: *Three MECG-free fetal signals obtained with the second signal separation method, applied to a set of 32 recorded signals.*

We will now apply this QSVD-based signal separation method to the data set with 8 recorded signals (see Figure 6.6), 5 signals recorded from the abdomen and 3 signals from the thorax. The signals are sampled at a rate of 250 Hz and we consider a time interval of 6 seconds, such that the dimension of the data matrix is 8×1500. We selected five intervals containing an isolated maternal QRS-complex (these intervals are indicated on Figure 6.6) and constructed the matrix Z by concatenating these intervals.

The QSVD of the matrix pair (M, Z) finds two directions in the 8-dimensional measurement space, such that the maternal ECG is eliminated in the projection onto these directions. The two resulting signals are shown in Figure 6.5.

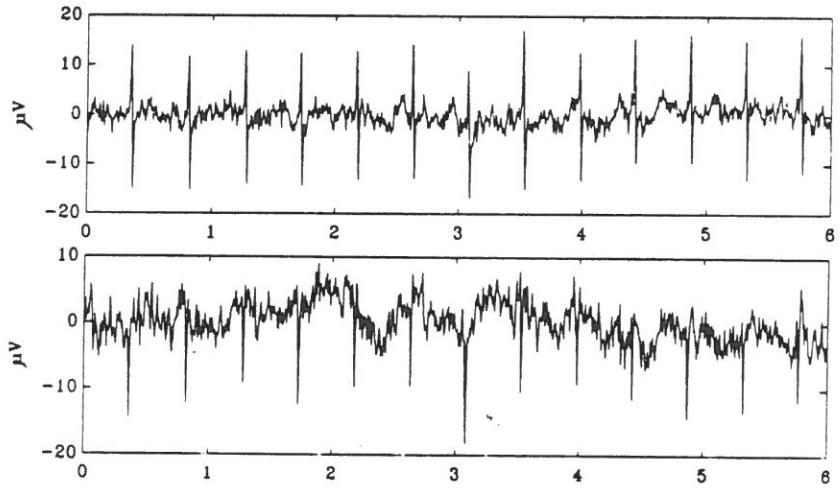

Figure 6.5: *Two MECG-free fetal signals, obtained with the second signal separation method, applied to a set of 8 recorded signals.*

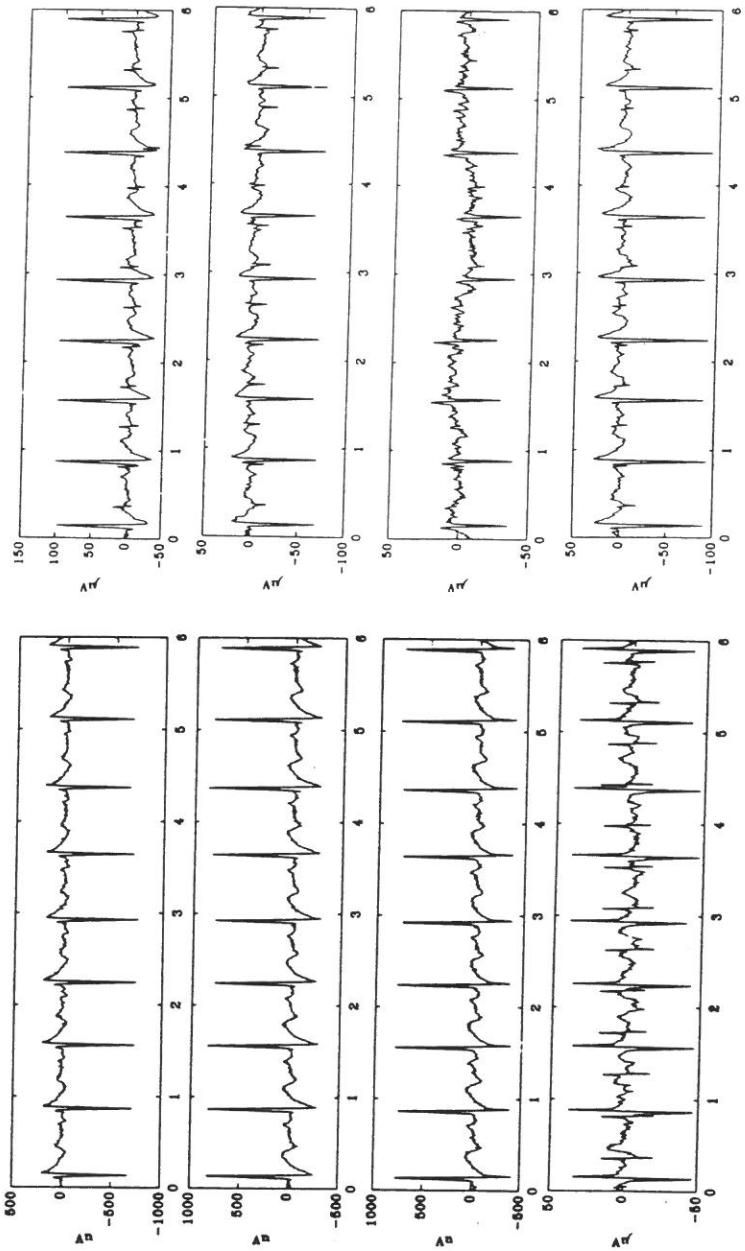

Figure 6.6: *Eight channel data set recorded on patient B.*

6.3.2 FECG-extraction with the on-line QSVD-method

In cardiology, the "orientation" of the adult heart is characterized by the so called **electrical axis** of the heart. The orientation of this electrical axis differs from patient to patient and depends on the patient's age and body build, but is very stable and time-invariant during the course of the recording experiments on one patient. This is a possible explanation for our observation that the subspace of the p-dimensional measurement space, associated to the maternal heart, is time-invariant.

Therefore we can apply the on-line version of the four-step method for the computation of the X-matrix in the QSVD of M and Z, where Z is a matrix, constructed from intervals, containing only parts of the maternal cardiac cycle and selected from the recorded signals. The OSVD of Z is computed as an initialization, while the second OSVD is computed on-line.

This on-line algorithm for QSVD-based signal separation is then applied to the data set with 8 recorded signals (see Figure 6.6), but this time over a period of 44 seconds (= 11000 samples if the sampling rate is 250 Hz). Only one plane rotation is executed in the diagonalization step of each cycle and the forgetting factor α was chosen to be $\alpha = 0.9986$. Figure 6.7 shows four intervals of an obtained MECG-free fetal ECG signal : one interval in the beginning of the algorithm (the first 4 seconds), then an interval after 16 seconds, an interval after 26 seconds and finally an interval after 40 seconds of processing the 8 signals.

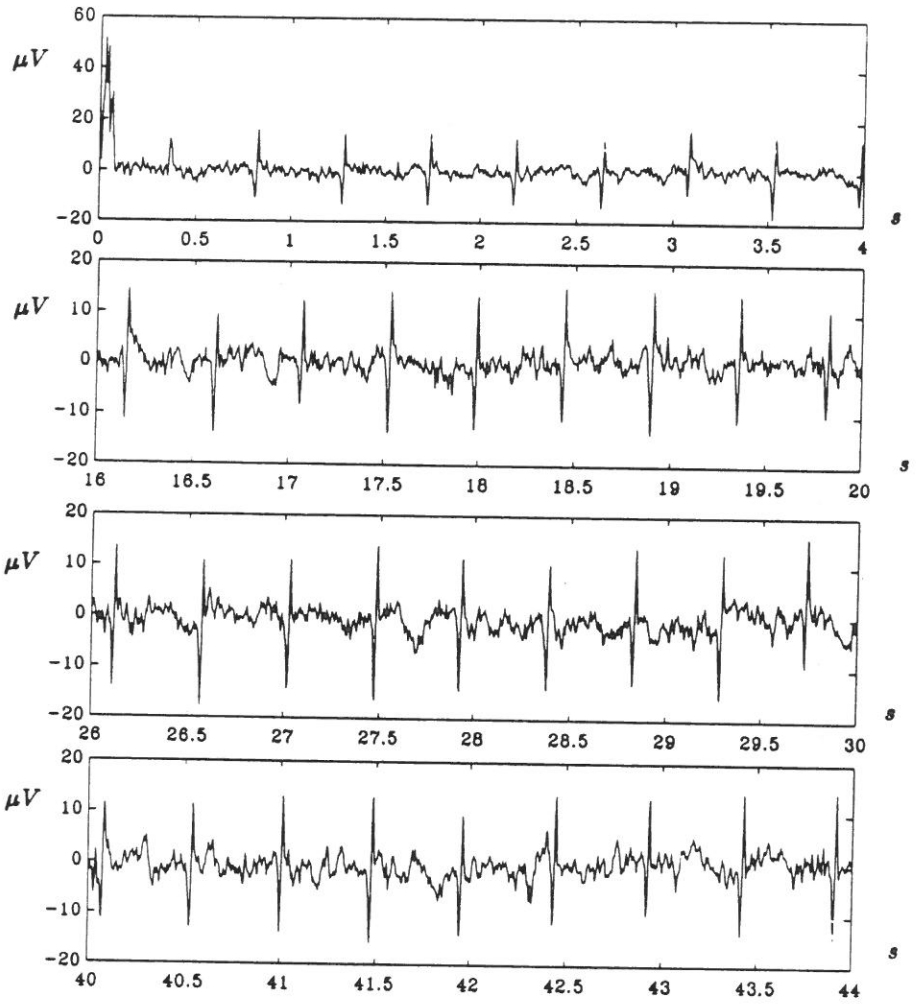

Figure 6.7: *On-line QSVD-based extraction of the fetal ECG, applied to an eight-channel data set. Four intervals, each of 4 seconds, are shown.*

6.4 Conclusion

This Chapter presented another method for SVD-based signal separation, by computing the Quotient SVD of two data matrices. The method requires that there are intervals in the measured signals, in which the disturbing source is dominating or appears solely. If the signal space, corresponding to the disturbing source is furthermore time-invariant, the QSVD can be computed as two consecutive OSVD's, where the first one is then an initialization. For the second OSVD the on-line algorithm presented in Chapter 4 can be applied.

In Chapter 7 this signal separation technique is compared to the OSVD-based method presented in Chapter 5. When applied to the elimination of the MECG in abdominal FECG-detection, the method is quite successful. However, for use in a clinical environment by medical personnel, this method is too complex and not very elegant. Indeed, the initialization step with the visual selection of the isolated maternal complexes is too complicated for use in clinical practice.

Chapter 7

Comparison of the SVD-based signal separation methods

7.1 Introduction

In this dissertation two SVD-based methods for signal separation are developed, discussed and applied to the problem of extracting a fetal electrocardiogram from signals, recorded on the skin of the mother, and therefore containing the much stronger maternal ECG. Both methods try to find in some way or another the coefficients in the linear combinations of the recorded signals (with the disturbance), in order to get some signals that are free from the disturbing influence.

The presented signal separation methods differ in the way they obtain those coefficients :

1. Method 1 obtains the coefficients from some left singular vectors in the Ordinary SVD of the extended data matrix (Chapter 5).
2. Method 2 obtains the coefficients from some columns of the X-matrix in the Quotient SVD of the matrix pair formed by the data matrix and a matrix, constructed from the recorded signals, but only containing some intervals in which the disturbing phenomenon dominates (Chapter 6).

In the next section, both methods will be compared with respect to some chosen criteria, such as restrictions for applicability, suitability for automation, orthogonality of the transfer and the number of recorded signals. Then some pro's and contra's of both methods are mentioned, when applied to the problem of eliminating the MECG from cutaneously recorded potential signals, in order to detect the fetal ECG.

In the last section we will describe two other signal separation methods and apply them to some of our data sets. First, a two-step OSVD-based procedure is developed based on the principles of a method by van Oosterom ([60], [61]). Although the method usually finds some MECG-free fetal signal(s), it has some important drawbacks. Then also the famous adaptive filtering technique by Widrow ([95]) is presented and discussed.

7.2 Comparison of the methods with general criteria.

Restrictions for applicability : the first method requires a signal transfer from sources to measurement points, that is as orthogonal as possible. This can be realized if the signal sources are spatially separated, by putting observation points close to each source. In the FECG application e.g. electrodes are put on the maternal abdomen (close to the fetal heart) as well as on the thorax. If this spatial separation of the observation points is not feasible, then signal separation with this method becomes more difficult.

The second method requires the occurrence of intervals in the recorded signals, in which only the disturbing signal appears or is dominant. For the FECG-application it is required that the fetal ECG is already visible in the recorded signals, because then an interval in which the maternal ECG dominates (in between two fetal QRS-peaks) can be selected.

Suitability for automation : the first method is the most elegant one and can easily be automated (see Appendix A). The second method on the other hand requires a fairly complicated initialization : the visual inspection to select the intervals and the first OSVD-step hamper an efficient automation of the procedure. Moreover, the on-line scheme for the second method can only be applied if the signal space of the disturbing source is time-invariant. In that case the first OSVD must not be updated during the experiment. If applied for FECG-extraction in a clinical environment, the second method would maybe discourage untrained medical personnel to use these techniques, because of their complexity.

Orthogonality of the transfer : this is an explicit condition for the success with the first method. By picking up the disturbing source independently in some extra signals, the transfer is made nearly orthogonal and the disturbing source is observed much stronger, relative to the source(s) of interest. In that case the signal separation will be more successful. The other method does not require an orthogonal transfer for having a successful signal separation. But the more orthogonal the transfer, the higher will be the contribution of wanted

signal in the projection onto a direction, orthogonal to the unwanted subspace.

The number p of recorded signals : suppose one is restricted to a fixed number p of measurement devices (electrodes, antenna's, microphones, sensors, etc.). In the case of the second method, all p of these observers can be located close to the source of interest, such that the influence of the disturbing source is minimized. The first method however requires some of the p sensors (at least r_u , the dimension of the undesired subspace) to be placed close to the disturbing source. The success of this method is indeed based on the fact that the influence of the disturbing source must be as big as possible, in order to have a better separation. Therefore, the number of observers, that can be located close to the source of interest is only $p - r_u$ at the most.

7.3 Pro's and contra's of the methods for FECG-extraction

Throughout this dissertation the extraction of a fetal ECG from recordings, mainly disturbed by the maternal ECG, is treated as the main application for the two presented signal separation methods. We will therefore in this section mention the pro's and contra's of both methods, specifically with respect to this problem of FECG-extraction.

Method 1 : the OSVD of the extended data matrix

PRO's :

1. Since the method finds the coefficients in a linear combination of the recorded signals, it is a filtering technique in the space-domain which leaves the FECG-waveform unaffected, in contrast with filtering in the frequency-domain. In the latter case some frequency components of the useful signal will also be filtered out, which affects the waveform of the resulting fetal ECG.

2. The resultant fetal signals are orthogonal and form a set of principal fetal signals. Since the coefficients in the linear combinations of the recorded signals are found as the columns of an orthonormal matrix, the obtained signals form a "signal basis" for the fetal subspace. Each fetal contribution can then be obtained as the right combination of the obtained orthogonal fetal signals, therefore called principal fetal signals.

3. It is clear that in the fetal subspace more than one set of orthogonal fetal signals can be obtained as "signal basis". The set of principal fetal signals, obtained with this method, is optimal with respect to extremal oriented energy, which means that the first principal fetal signal corresponds with maximal oriented energy, the second principal signal with another extremal value of oriented energy, etc. Therefore this set of principal fetal signals is unambiguously determined, and independent of the orientation of the electrical axis of the fetal heart.

4. Since the set of principal fetal signals forms a "signal basis" for the fetal subspace, it is possible to reconstruct the fetal contributions in each recorded signal as a combination of those principal signals. This is very important for interpretability by the cardiologist. Indeed, the obtained principal signals are "virtual" signals, which are not physically measurable between an electrode pair. By reconstructing the fetal ECG contributions in each recorded signal, it is much easier to interpret these signals, since they refer to exactly known electrode pairs (see Figure 5.10).

5. The method is very elegant to apply in a clinical environment. The only practical problem in using the technique would be the appropriate choice of electrode positions, since this is a critical point. However, tests with a prototype system must lead to a uniform electrode placement strategy, simplifying this practical problem.

6. The method is not limited to a certain class of signal waveforms. No requirements about periodicity, time-invariance, pulse-like waveforms, etc. have to be considered.

7. The method is extremely suitable for a PC-based real-time implementation (see Appendix A), due to the development of an on-line adaptive algorithm for its computational strategy.

8. With this method elimination of 50 Hz net interference is possible in a very simple and elegant way. As demonstrated in Chapter 5, 50 Hz net interference can be removed from the recordings by the addition of two extra signals : one signal directly recorded from the power network and the other a delayed version of this first signal.

CONTRA's

1. At the moment it is still very difficult to determine a general electrode placement strategy, since for each patient the most ideal electrode positions have to be looked for. When using bipolar electrode signals (no reference electrode), which is required for better S/N ratio's and spatial separation of the recorded signals, this problem has a lot of degrees of freedom. The realization of a real-time signal separation unit will however eliminate this problem, since an immediate evaluation of each chosen electrode pair can be performed.

2. If one has only a limited number of electrodes or if one wants to apply a minimum of electrodes for practical reasons, the method requires already at least three signals to be recorded far from the fetal heart (on the thorax, on the arms, on the legs, etc.) such that only a few electrodes are left for application on the maternal abdomen. Even then it is possible to obtain a MECG-free fetal heart signal, only the placement of the abdominal electrodes becomes still more critical, since they have to pick up a fairly strong fetal signal in that case.

Method 3 : the QSVD of two matrices

PRO's :

1. Also this method finds the coefficients in a linear combination of the recorded signals, such that a filtering in the space-domain is performed, which leaves the FECG-waveform unaffected.

2. The method is successful in finding one or more MECG-free fetal signals without special requirements for electrode positioning. Even recordings with a reference electrode can be used. This permits to have a standard electrode positioning "grid", which is very easy to apply in clinical practice.

3. Although the initialization step requires some extensive programming work in order to make it very user-friendly, this method can be implemented on a PC-based system for real-time FECG-extraction, due to the development of an on-line version of the computational strategy.

4. All of the electrodes can be applied on the maternal abdomen, such that the probability to pick up a fetal contribution is higher, when the number of electrode signals is limited. The addition of some extra thoracic signals, that pick up the maternal ECG independently is not required for obtaining a MECG-free fetal signal. However, if some thoracic signals are added, the S/N ratio of the obtained fetal signals is improved.

CONTRA's

1. Where the electrode placement for this method does not put any practical difficulties, the method itself is not elegant for use in a clinical environment. The visual selection of the maternal QRS-intervals by the physician or by the medical personnel is a complicated and time-consuming initialization step.

2. The method requires that the fetal ECG is visible in the recorded signals, in order to select some intervals, in which the maternal ECG dominates. This is exactly in between two fetal QRS-complexes.

In order to evaluate the performance of both methods, we will apply them to the same data set of 8 recorded signals (see Figure 6.6). This set contains five signals recorded from the abdomen of patient B and three signals recorded from the thorax. The first OSVD-based method results in the 8 signals, shown in Figure 7.1. No complete separation of the signals is obtained, since signal 4 and signal 6 still contain contributions from both the MECG and the FECG. This is because the electrode positioning was not good enough for a complete success of this first method. Only one MECG-free fetal signal is obtained (signal 5). This signal is however not optimal with respect to signal-to-noise ratio since in other signals some fetal contributions occur.

If we apply the QSVD-based signal separation method to the same data set, the 8 signals of Figure 7.2 are obtained. In this case there is a complete separation of MECG and FECG : signal 1 and 2 contain only fetal contributions, while signals 3, 4, 5, 7 and 8 contain maternal ECG disturbed by noise. Signal 6 clearly shows the modulation of the baseline by maternal breathing.

These results can be interpreted as follows : if a data set is given and recorded with some electrode positions, the probability is higher that MECG and FECG are separated with the second method. However, the first method is easier, more elegant and gives more optimal results if the electrode positions are ideal. The first method should therefore be used in real-time, such that some chosen electrode positions can be evaluated immediately and changed if no separation of MECG and FECG occurs. Another reason might be that the first method finds orthonormal linear combinations of the recorded signals, which puts an extra constraint on finding the optimal directions, while orthogonality of the directions is not required for the second method (the columns of X in the QSVD of a matrix pair are not orthonormal).

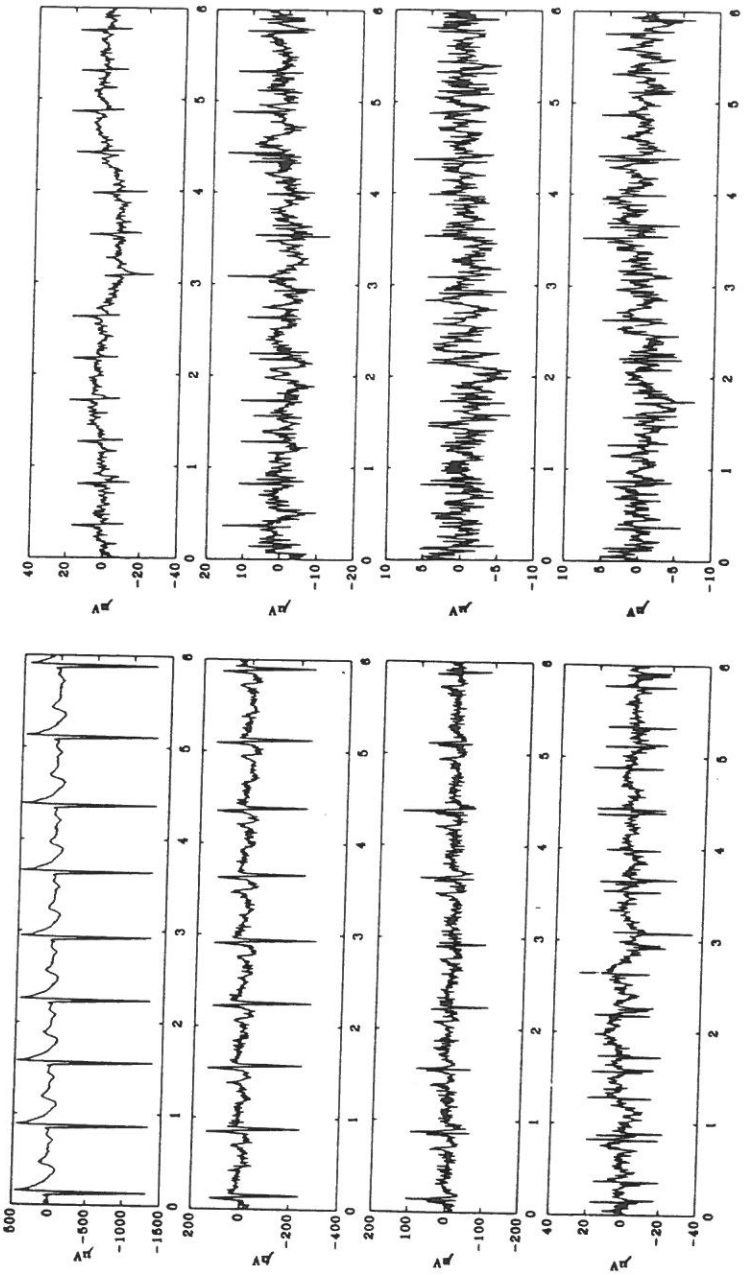

Figure 7.1: *The 8 resultant signals after application of the first SVD-based signal separation method to the 8-channel data set.*

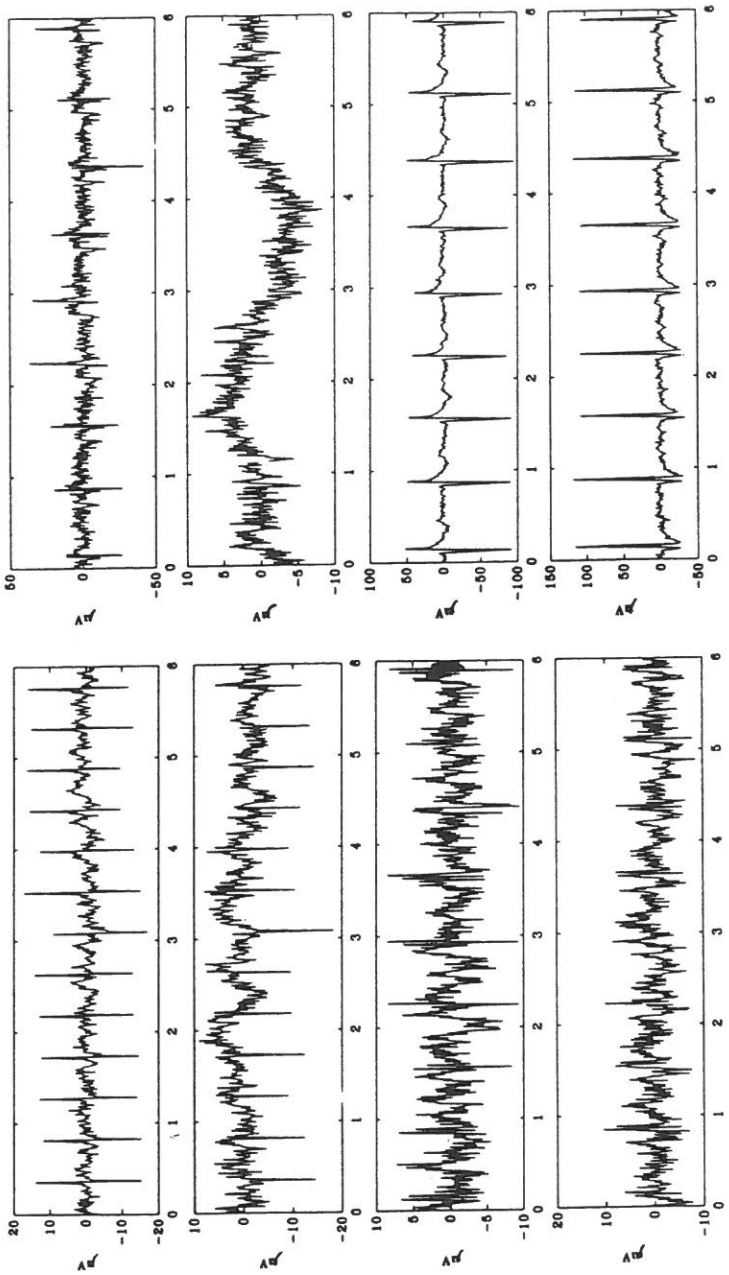

Figure 7.2: *The 8 resultant signals after application of the QSVD-based signal separation method to the 8-channel data set.*

7.4 Comparison with other methods for FECG-extraction

7.4.1 A two-step spatial filter for FECG-extraction

We will briefly present and discuss the method for FECG-detection, as introduced by van Oosterom ([60], [61]), since this is also a SVD-based signal separation method. Furthermore, we will modify this method, such that the second step can be performed with an on-line computational strategy.

By visual inspection of the p signals, recorded on the abdomen of the mother, a time interval, containing a maternal QRS-complex, only disturbed by some noise, is selected. The corresponding data matrix M_m has dimensions $p \times q_m$ and its OSVD is computed as $M_m = U_m \Sigma_m V_m^t$. The rank r_m of M_m can be determined by inspection of the ordinary singular values of M_m on the diagonal of Σ_m. The first r_m columns of U_m form an orthonormal basis for a subspace of the p-dimensional measurement space, the so called **maternal subspace**, since it contains all possible contributions of the maternal ECG. The complementary subspace U_{M0}, formed by the $p - r_m$ last columns of U_m contains no maternal components anymore.

A second time interval is now selected from the p recorded signals, in which only one fetal QRS-complex appears. The corresponding data matrix M_F with dimensions $p \times q_F$ is then projected onto the complementary subspace U_{M0}, to form the matrix $A = U_{M0}^t M_F$, with dimensions $(p - r_m) \times q_F$. The OSVD of A is computed as $A = U_A \Sigma_A^t V_A^t$. The first column $\mathbf{u}_{A1}$ of U_A provides the coefficients of a linear combination of the rows of matrix A with maximum norm. The vector $\mathbf{w}$ obtained as $\mathbf{w} = U_{M0}\, \mathbf{u}_{A1}$ contains the coefficients in a linear combination of the recorded signals, where the MECG is eliminated and an optimal FECG is found in the complement of the maternal subspace.

Although in most cases some MECG-free signal is obtained, the method has some important drawbacks :

1. The visual inspection of the data signals for the selection of the intervals, that contain only a maternal and a fetal QRS-complex respectively, hampers an efficient automation of the procedure. Since the maternal subspace is almost time-invariant throughout most experiments, the first step has to be performed only once to find the complementary subspace U_{m0}.

On the other hand, it is possible that the second step has to be repeated several times, since fetal movements might change the configuration of the set-up. A vector $\mathbf{w}$ obtained in the beginning of an experiment can become completely useless due to fetal movements. This would result in serious practical problems when used in a clinical environment by unexperienced medical personnel.

2. The method is very sensitive to the choice of the selected intervals. Especially the selection of a maternal QRS-interval is quite difficult, because it must appear isolated between two fetal QRS-complexes, occurring more frequently in the recordings. In fact a complete maternal cardiac cycle (the PQRST-wave has a duration of 0.46 s on the average) has to be selected in order to determine the maternal subspace appropriately. Since the fetal QRS-complexes occur very frequently (the fetal heart rhythm is about 140 beats/min i.e. a period of 0.43 s on the average), it is very difficult to obtain a complete maternal cardiac cycle solely.

3. The determination of the dimension of the maternal subspace (rank r_m of M_m) is also very critical. If r_m is underdetermined, it is possible that not all maternal contributions are eliminated. An overdetermination of r_m on the other hand, can reduce the complementary subspace considerably. It can happen that the fetal heart has contributions in the subspace assigned to the maternal heart, such that together with the elimination of MECG, a part of the fetal signal disappears. Therefore, some MECG-free fetal signal may be found in the second step, but this is then only optimal with respect to the restricted complementary subspace, found from the first step. The fetal signal found in this case is not the optimal MECG-free fetal signal that could possibly be obtained from the recordings.

4. The selected intervals are usually very short with respect to the number of recorded signals. This means that the matrix is not overdetermined, such that the assumptions for the additive noise components in each signal are not valid. In such short intervals some components might give a higher singular value (relative to the other singular values) than over a very long interval, resulting in wrong decisions about the rank r_m and giving numerical problems.

We will now slightly modify this method, such that the on-line adaptive algorithm of Chapter 4 can be applied in the second OSVD-step. Suppose therefore that a matrix Z can be constructed by concatenating several intervals, in which the maternal QRS-complex appears solely (in between two fetal QRS-complexes), like we did for our second signal separation method (see Chapter 6). Since the maternal ECG is dominantly present in this matrix Z, the first r_u left singular vectors in the OSVD of Z form an orthonormal basis for the signal space, associated with the maternal heart. The OSVD of Z is partitioned as ($r_u = \text{rank}\,(Z)$)

$$Z = \begin{matrix} r_u & p-r_u \end{matrix} \begin{pmatrix} U_u & U_{uc} \end{pmatrix} \begin{matrix} r_u \\ p-r_u \end{matrix} \begin{pmatrix} \Sigma_u & 0 \\ 0 & \Sigma_{uc} \end{pmatrix} \begin{matrix} r_u & p-r_u \end{matrix} \begin{pmatrix} V_u^t \\ V_{uc}^t \end{pmatrix} \begin{matrix} r_u \\ p-r_u \end{matrix} \begin{matrix} q \end{matrix} \tag{7.1}$$

Projection of the $p \times q$ data matrix M onto the complementary subspace U_{uc}, will eliminate all undesired contributions. This leads to the matrix $M^* = U_{uc}^t M$, with reduced dimensions $(p - r_u) \times q$. This matrix M^* contains contributions from all other source signals. In order to extract now the fetal ECG, a second OSVD computation has to be performed. The OSVD of $M^* = U_m^* \Sigma_m^* V_m^{*t}$ finds the directions of extremal oriented energy in the complementary subspace.

Projection of the reduced data matrix M^* onto these directions, found as the columns of U_m^*, leads to a matrix $S^* = U_m^{*t} M^* = U_m^{*t} U_{uc}^t M$. This matrix S^* contains a number of orthogonal signals, free from maternal ECG. One or more of these signals contain the fetal heart signal. Since the signals obtained in S^* contain contributions from all sources, except from MECG, it are not automatically the columns of U_m^*, corresponding to the largest singular values of M_m^*, that provide the linear combinations to obtain the FECG.

Since the MECG is a nearly time-invariant phenomenon (during the course of a recording session), in the sense that its subspace does not change during the experiments, the first OSVD-step must only be executed once, as an initialization. The second step can then be performed by applying the on-line adaptive algorithm of Chapter 4, this time with $U_0 = U_{uc}$. The other steps of the algorithm are exactly the same as for the first signal separation method.

This leads to the following outline of an on-line version of this two-step SVD-based method for FECG-extraction :

1. Record p signals, containing both MECG and FECG.
2. Select a number of intervals in which the maternal QRS-complex appears isolated and construct a matrix Z by concatenating these intervals.
3. Compute the Ordinary SVD of $Z = U_z \Sigma_z V_z^t$ and initialize $B_0 = 0$ and $U_0 = U_{uc}$ as the last $p - r_u$ columns of U_z
4. Apply the on-line adaptive algorithm from now on

Loop for $i = 1$ to q

$$\mathbf{y}_i = U_{i-1}^t \mathbf{m}_i \tag{7.2}$$
$$C_i = \alpha B_{i-1} + \mathbf{y}_i \mathbf{y}_i^t \tag{7.3}$$
$$B_i = Q_i^t C_i Q_i \tag{7.4}$$
$$U_i = U_{i-1} Q_i \tag{7.5}$$

end loop

Although this method usually finds some MECG-free fetal signal without special requirements for electrode positioning, it still has some very important drawbacks. Tests with the data set of Figure 6.3 e.g. have shown that, together with the elimination of the MECG, some information about the fetal ECG is eliminated. Indeed, the orthogonal projection of the data matrix onto the r_u left singular vectors, that define the so called maternal subspace, still contains fetal contributions. In order to eliminate ALL maternal contributions from the recordings, r_u has to be taken large enough, but then also important information about the fetal ECG is lost. The obtained MECG-free fetal signal will therefore not be optimal at all. With the experiments we did on the data set of Figure 6.3, we found that one or even more MECG-free fetal signals were obtained for different choices of r_u (see Figure 7.3 for $r_u = 3$, 10, 15, 18). Depending on the value for r_u, another fetal signal is found. It is therefore impossible to determine which choice of r_u is optimal and in what sense the obtained signals are optimal.

On the other hand, this technique is very satisfying if only a fetal signal has to be obtained, in order to derive a heart rate from it, or for cases where a fetal trigger is needed.

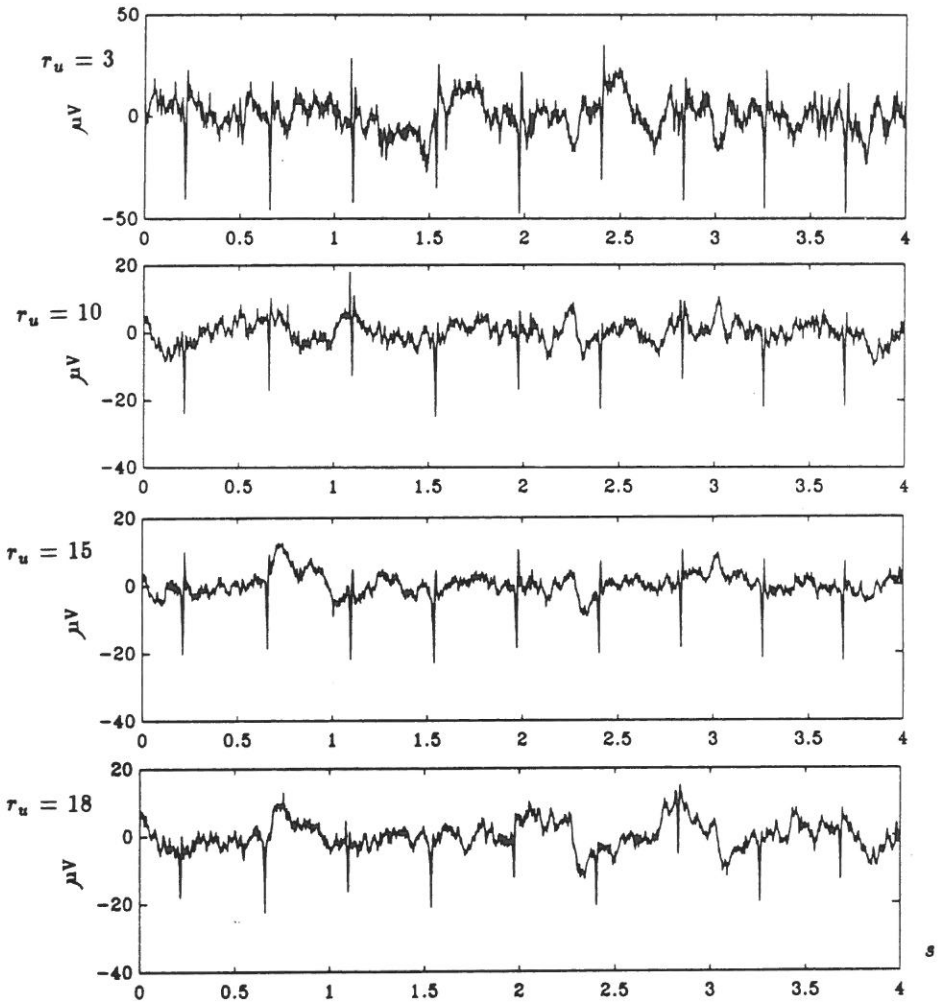

Figure 7.3: *Some of the obtained fetal signals for different values of* r_u.

7.4.2 Adaptive Noise Cancelling for MECG-elimination

In [95] *Widrow* describes a method to cancel the maternal ECG adaptively from an abdominal recording. Therefore he designed an adaptive noise canceller (see Figure 7.4) with one primary input (the abdominal signal containing both MECG and FECG) and four reference inputs (so called chest leads that pick up the MECG individually). The reference signals are filtered to form one reference for the maternal ECG as the filter output. This signal is then subtracted from the abdominal lead signal. The resulting difference signal should be free of MECG and contain only the FECG disturbed by noise.

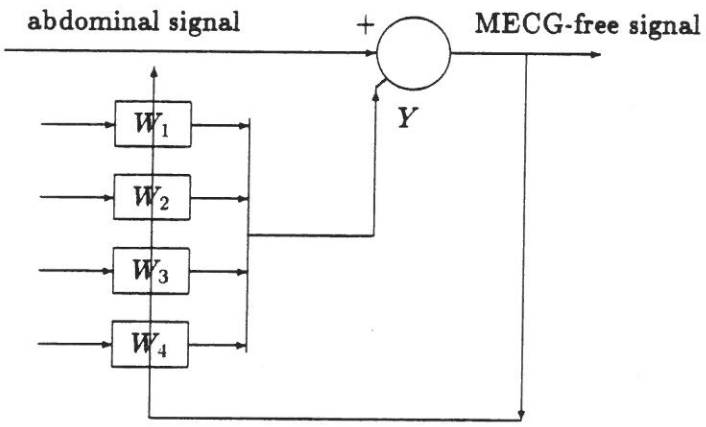

Figure 7.4: *The Adaptive Noise Canceller for MECG-elimination.*

We applied this adaptive noise cancelling technique to the data set recorded from patient A. Since we only recorded three thoracic signals (Figure 5.6), we will use these as three reference inputs, while the abdominal signal of Figure 5.5 is taken as the primary input. We found that the results were very sensitive to the choice of the number IW of filter coefficients and of the convergence factor μ. The best result we obtained was for IW = 175 and $\mu = 5$ % of the input power of the adaptive filter, and is shown in Figure 7.5 The first tracing shows the output Y of the adaptive filter and the second tracing is the difference between the primary input (the abdominal signal) and the filter output.

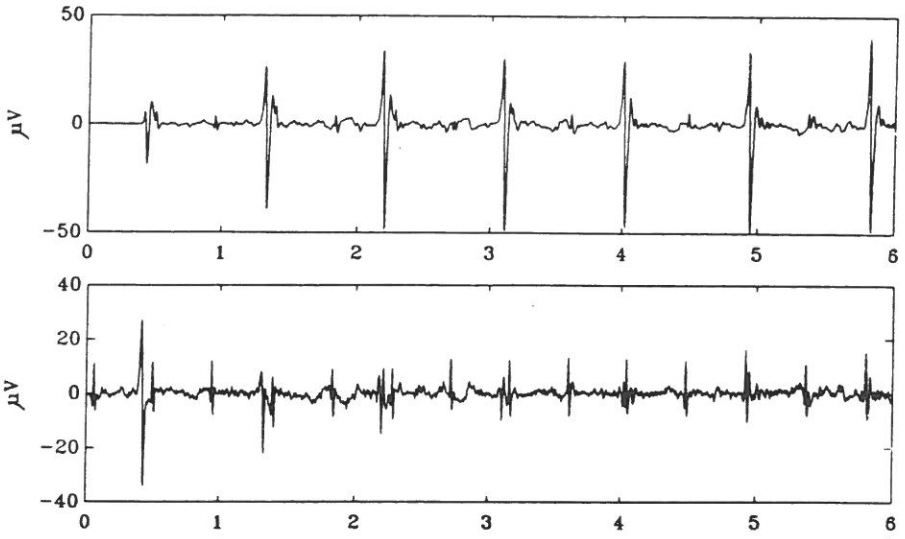

Figure 7.5: *Results obtained with the Adaptive Noise Canceller. The first signal is the filter output, while the second signal should be the MECG-free fetal signal.*

As can be seen from Figure 7.5 this method has a few drawbacks :

- Since even in the thoracic signals some fetal contribution can occur, the filter output can contain parts of the FECG (see the first tracing of Figure 7.5). Some information about the fetal signal will therefore be subtracted from the abdominal signal, together with the estimation of the MECG-component.
- The maternal ECG-contributions are only slowly removed from the abdominal recording. At the end (after about 5 seconds), the signal is almost free from MECG. This might be an indication that the adaptive noise canceller converges not as quickly as our on-line adaptive algorithm.
- The computation of one sample of the resultant signal requires about $12 \times$ IW multiplications and $6 \times$ IW additions, which is an enormous amount if IW is large (in our test IW = 175 !).

We will apply the Adaptive Noise Cancelling also to a longer interval in order to see if the method converges indeed. Consider therefore the three signals of Figure 5.12.b as the three reference signals and the signal of Figure 5.12.a as the primary input. The resultant signals are shown in Figure 7.6. When one compares the second trace with the signal of Figure 5.12.c, obtained with our method, it is clear that the Noice Cancelling does not eliminate all MECG-contributions, and furthermore also removes contributions from the fetal ECG.

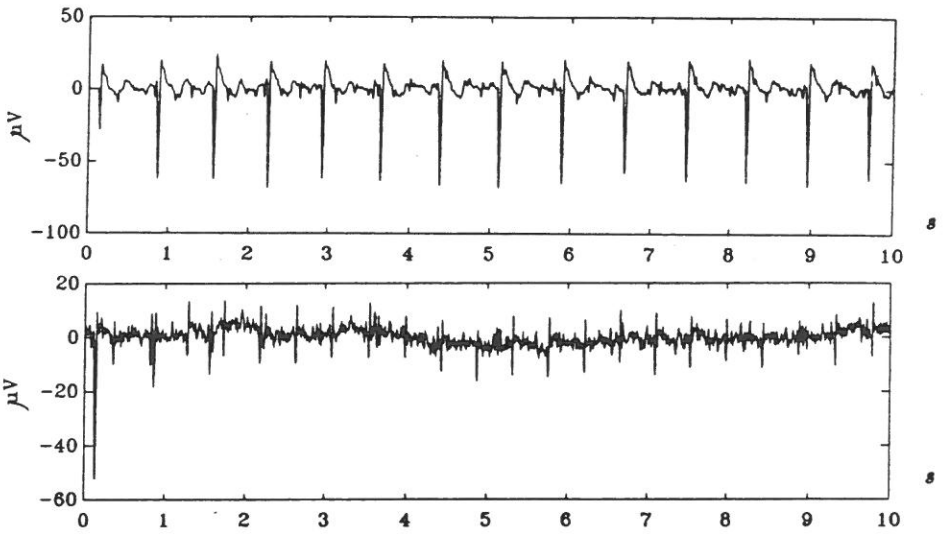

Figure 7.6: *Resultant signals obtained with the Adaptive Noise Canceller for an experiment with four signals (1 primary and 3 reference) over a period of 10 seconds. The first signal is the filter output, while the second signal should be the MECG-free fetal signal.*

7.5 Conclusion

In this Chapter we compared the developed signal separation methods. In a first section, both methods were compared, using some general criteria, such as restrictions for applicability, suitability for automation, orthogonality of the transfer and the number of recorded signals. Where the first method is very suitable for automation and also quite generally applicable, it requires a nearly orthogonal transfer and some extra signals have to be recorded in order to pick up the disturbing source. The second method on the other hand, does not put special constraints upon the transfer and a minimum of recordings is sufficient, but the method is rather complicated for automation. Then some pro's and contra's of both methods are mentioned, when applied to the problem of eliminating the MECG from cutaneously recorded potential signals, in order to detect the fetal ECG. In the last section two other signal separation methods were described, applied for MECG-elimination and compared to our two SVD-based methods.

Chapter 8

Summary of the main results and future work

8.1 Summary of the main results

The work described in this dissertation was headed by a very long title :

> *"Signal Separation Methods based on Singular Value Decomposition and their Application to the Real-Time Extraction of the Fetal Electrocardiogram from Cutaneous Recordings."*

But this title covers everything and allows us to discriminate between four main topics :

1. Signal Separation Methods
2. Singular Value Decomposition
3. The Extraction of the FECG from Cutaneous Recordings
4. On-line processing and real-time implementation

We will therefore describe in this Chapter the main results obtained for each of these four topics and then indicate some perspectives for future research.

1. **Signal Separation Methods :**
   In this dissertation two new signal separation principles were presented. Both of these methods realized the signal separation by finding some weight vectors for obtaining linear combinations of a set of recorded signals.
   Method 1 finds a number of orthonormal weight vectors by computing the OSVD of a data matrix, extended by a number of independent signals that pick up the disturbing source individually (see Chapter 5). By observing the unwanted phenomenon as strongly as possible, it will be eliminated, based on oriented energy considerations (see Chapter 3). The success of the method depends on the orthogonality of the transfer of signals from source to measurement point.

   Method 2 looks for a number of non-orthonormal weight vectors by computing the QSVD of a matrix pair, consisting of the data matrix and a matrix that is constructed from a number of selected intervals, in which the disturbing source is dominant. This method is based upon the concept of oriented signal-to-signal ratio (see Chapter 3) and is a completely new result. Certainly the on-line computation scheme,

that can be applied if the disturbing phenomenon is time-invariant, contains some new ideas. Important in this second method is also that the weight vectors are not orthonormal, which is the case in the first method.

Concerning applicability and suitability for automation the first signal separation method is definitely the most elegant. It only depends quite strongly on the positioning of the measurement points, which is a less severe requirement for method 2. On the other hand, the second method requires that the disturbing signal is time-invariant (meaning that its signal space remains an invariant subspace of the measurement space) and appears dominantly in some time-intervals. In the future it should be examined whether these signal separation methods are also applicable to more difficult problems such as e.g. speech (nonstationary signals, dynamical signal transfer, broadband signals, phase-shift between signals, etc.).

2. **Singular Value Decomposition :**
The most important new result concerning the computation of the SVD is the on-line adaptive scheme for updating the left singular matrix of some given data matrix. The fact that only one plane rotation per cycle suffices for convergence has not been proven analytically, but is demonstrated by an empirical approach. Even if the dimensions increase (by processing more input signals) the example shows that one plane rotation is enough for convergence.

   Another new result here is the approximating method for finding the rotation angle. In contrast with the classical Jacobi-method, that annihilates an off-diagonal element completely, this new strategy will reduce the element substantially. This corresponds to a so called over- or underrelaxation, depending on a change of sign or not. In the final stages, this new method has the same quadratic convergence rate as the Jacobi technique and is important in microcomputing environments, since the computation of a square root is avoided. Also, round-off errors have less impact on the further computations.

   Furthermore, the on-line algorithm is adaptive, since it applies an exponential forgetting factor. This prevents that events from the remote past still have some influence on the present processing, while on the other hand, it permits the very recent events to correct the processing severely.

3. **Extraction of the FECG from Cutaneous Recordings :**
For this biomedical application the two methods are very effective and successful, since they both find in some way or another a signal from the fetal heart, free from contributions of the maternal heart. However, for application in a clinical environment (e.g. implementation of the method in a bedside real-time monitoring system) the first method is the most elegant. Indeed, this technique is extremely simple to use : only ± 8 signals have to be recorded from electrodes on the maternal skin, such that the patient can be very relaxed. The equipment only consists of a set of preamplifiers and a PC with a plug-in board for A/D conversion and for the computational work. From the obtained antepartum MECG-free fetal electrocardiogram the following information and parameters can be derived :

   - the instantaneous fetal heart rate (FHR)
   - arrhythmia (tachycardia, bradycardia)
   - the duration of the QRS-complex
   - the occurrence and the position of the P-wave
   - eventually fetal movements

   In combination with signals, coming from a special transducer that pick up data about fetal breathing movements, the FECG provides information to quantify fetal respiratory sinus arrhythmia ([39]). In combination with information about the arterial blood pressure and with the heart sound signal, the FECG furthermore offers the possibility to determine the fetal systolic time intervals (PEP and VET) as a measure of myocardial contractility.

   Future work with this first signal separation technique, will be pointed towards standard electrode placement strategies and large scale clinical tests. These tests must then really evaluate the methods in a more clinical way and should result in an extended diagnostic knowledge.

   Another important result is the removal of 50 Hz net-interference from biomedical recordings by using the first signal separation method. All that is required is the measurement of an extra signal, directly picked up from the power network.

4. **On-line processing and real-time implementation :**
The fact that for both methods an on-line version is developed, such that the same basic on-line adaptive algorithm can be used in both the cases, is a very important result. This encouraged us to implement this algorithm in software (by programming a PC plug-in board with the TMS-320C25 microprocessor) and in hardware (a digital chip implementation) (see Appendix A). Here further research is directed towards the computations with fixed wordlengths. The smaller the wordlength, the smaller the dynamical range of the problem, but the larger this wordlength, the larger the computational time and the more memory is needed.

8.2 Future research

In this dissertation we presented two new signal separation principles and applied it to the problem of the elimination of the maternal electrocardiogram (MECG) from a set of potential signals, recorded with electrodes on the skin of the mother, in order to detect the fetal electrocardiogram (FECG). The aim of this section is to mention briefly some other domains in which the presented SVD-based signal separation methods might be applied with success.

8.2.1 Beamforming and antenna array applications

The main objective in beamforming is to estimate the signal arriving from a certain desired direction in the presence of noise and interfering signals. In fact, beamforming can be applied to both radiation or reception of energy.

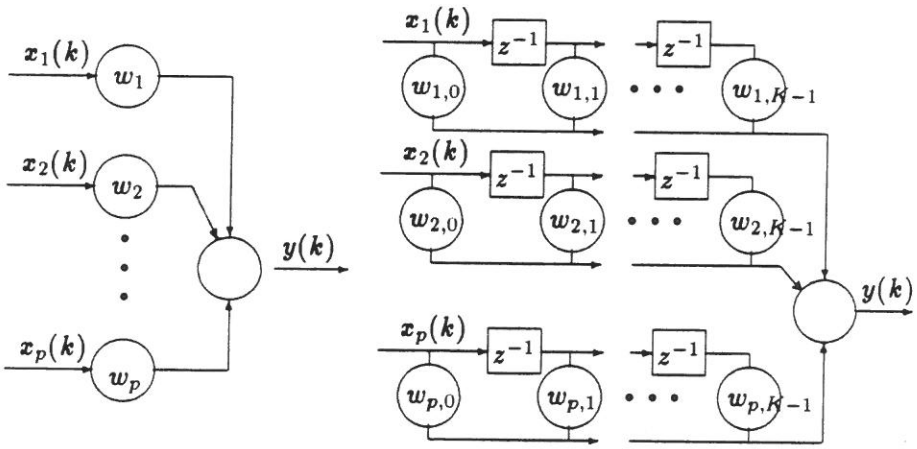

Figure 8.1: *A beamformer for narrowband signals (a) forms a linear combination of the recorded signals, while a beamformer for broadband signals (b) combines delayed versions of the sensor outputs.*

In many practical applications, systems that try to observe spatially propagating signals often encounter the presence of interference signals. Usually, the desired and interfering signals originate from different spatial locations. This can be exploited to separate signal from interference by using a spatial filter at the receiver end. Therefore data have to be collected by an array of sensors, electrodes, microphones, antennas, etc. that are spatially distributed.

A **beamformer** is a processor that linearly combines the spatially sampled time series from each sensor to obtain a scalar output time series. It is important to mention the difference between a beamformer for **narrowband** signals (see the static model of Figure 8.1.a) and a beamformer for **broadband** applications (see the dynamic model of Figure 8.1.b).

According to [91] beamformers can be classified as either data independent or statistically optimum beamformers, depending on how the weights are chosen. The weights in a **data independent** beamformer do not depend on the array data and are designed to present a specified response for all possibly occurring situations. The design of a data independent beamformer can be compared with the design of a J-tap FIR filter : the beamformer is designed to receive a signal from a known direction θ_0. In analogy to bandpass and bandstop FIR filter design, data independent beamformers can be designed to receive any signal arriving from a range of directions or to attenuate any interfering signal arriving from a certain range of directions. The weights in a **statistically optimum** beamformer are chosen, based on the statistics of the array data to "optimize" the array response, according to some chosen criterion. The output must contain minimal contributions due to noise and signals arriving from directions other than the desired signal direction.

The two SVD-based signal separation methods, presented in this work, are statistically optimum beamformers for narrowband signal processing applications. Therefore, the use of our new signal separation principles in antenna applications e.g. (adaptive) antenna arrays, is an interesting topic for future research.

8.2.2 Speech Enhancement

Due to the binaural nature of human hearing, we are able to localize and focus on a particular sound source of interest in so called "cocktail party" situations and noisy environments. From this simple observation we learn that it must be possible to combine multiple microphone signals, such that a speech signal is obtained with better speech-to-noise ratio (SNR), than in any of the recorded signals. This would be an alternative to binaural hearing, in situations where a monaural hearing aid is used (monaural deafness, cochlear implants) [79], [80]. But also in speech recognition, signal enhancement on the basis of multiple microphone processing might be useful. Indeed, most speech recognition systems currently require a SNR of 15 dB or better, while in many practical applications an operating range from 0 to $\pm$ 20 dB is required [81].

Another situation where multiple microphone systems are used to obtain a certain directivity is in situations like discussions in conference rooms, where questions from all over the auditorium can be posed [34]. This directivity is obtained by beamsteering of multidimensional microphone arrays, such that sounds arriving from all directions are attenuated, except for the direction of the speaker.

A specific problem that arises in this kind of applications is the delay of arrival, that exists between the different microphones in the array, due to the relatively slow speed of sound. In speech applications the sampling frequency is of the order of 10 - 20 kHz, such that a distance of 20 cm between two microphones can cause a maximum delay between coherent non-reflected signals of $\pm$ 0.6 ms, i.e. 12 samples if the sampling rate is 20 kHz.

An existing solution for this speech enhancement problem is shown in Figure 8.2 : a two-dimensional Griffiths-Jim beamformer, which is a combination of a phase-aligning beamformer and an adaptive noise canceller [81]. In order to phase-align the speech signals, the direct delay between the two channels is estimated by maximizing the cross-correlation function of the wideband signal. This inherently implies operation in positive (in dB) signal-to-noise ratio conditions, such that the noise does not dominate the cross-correlations.

The adaptive noise canceller in the second stage of the Griffiths-Jim beamformer will then eliminate the correlated noise from the sum of the two phase-aligned speech signals. The reference signal of the adaptive noise canceller is the difference between the two phase-aligned speech signals.

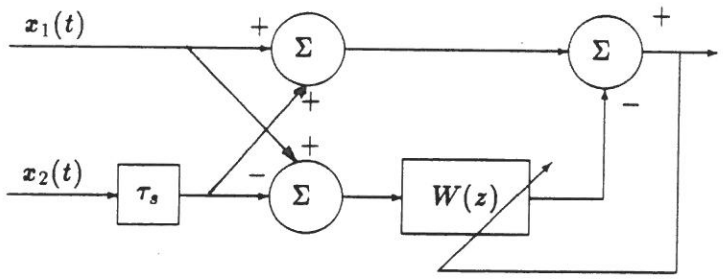

Figure 8.2: *The Griffiths-Jim beamformer.*

To avoid cancellation of speech, because of the possible presence of some speech components in the difference signal, it is best to update the adaptive filter coefficients in the absence of speech. This splits the beamformer's work into two parts : when speech is present, the phase-alignment is done (this has to be done adaptively for the case of a moving sound source), while in the absence of speech the adaptive noise canceller coefficients are updated.

We strongly believe that our two new SVD-based signal separation methods can be very useful in this speech enhancement problem. A first interesting topic is the use of the OSVD-method for phase-alignment in the first stage of the Griffiths-Jim beamformer. Suppose that the OSVD provides information to detect the delay between two or more microphone signals, then our on-line adaptive algorithm can make this delay detection adaptive. Therefore, we expect that the speaking person may move, relatively to the microphone array : this technique will adapt its coefficients according to the loudest direction.

In Chapter 6 it was explained that the QSVD-method required some intervals where the disturbing signal was dominant, or appeared solely. Speech is a typical example of a signal processing application where an on-off situation occurs : when a person is speaking, his voice can be disturbed by noise, but in absence of speech, noise is the dominant signal component. Many of the actually used adaptive beamformers work with this principle, since the

coefficients can then be adapted only when speech is present or absent. The application of our second signal separation method for speech enhancement is therefore a second interesting topic for future research.

However, there are some specific problems for this speech application. First, the transfer of the disturbing source is dynamical and not static as was the case in the MECG-FECG application. One can therefore not use the method that selects some intervals in which noise is dominant and then compute the OSVD as an initialization of the on-line QSVD-algorithm as described in Chapter 6. Another on-line algorithm for QSVD of a matrix pair (A, B) has to be designed, in which the QSVD is updated each time matrix A as well as matrix B are extended with an extra column [54]. Furthermore, speech is a broadband application, such that the principles, designed for narrowband applications, have to be extended in that sense. This will also be the subject of future research.

8.2.3 The Electro-Encephalogram (EEG)

In mapping brain activity, recent approaches use a spatio-temporal source model. In this model the spatio-temporal data, obtained from electrodes on the human scalp, are explained as being produced by sources, each having a fixed position and orientation and some pattern of activity over time [50]. According to the international 10-20 system 19 electrodes ($p = 19$) must be used and positioned on the scalp (see Figure 8.3). This results in a 19-dimensional measurement space. With principal component analysis one can obtain a minimal multidimensional subspace of that measurement space that can adequately describe the data [1].

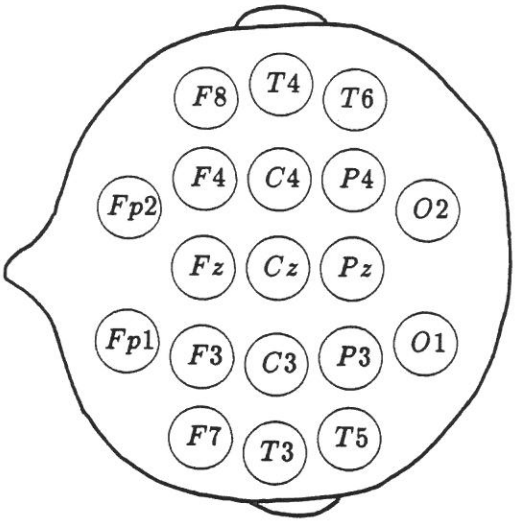

Figure 8.3: *Electrode positioning on the scalp according to the international 10-20 system.*

The use of the first SVD-based signal separation principle for this application is very promising :

1. Computing the OSVD of the data matrix and projection onto the subspace spanned by the left singular vectors, associated with the largest singular values, gives the principal signals that describe the same measured data. Experiments have shown that by this method the signal set can be reduced to a number of $\pm 6 - 8$ principal signals.

2. The columns of the U-matrix in the OSVD of the data matrix contain information about the relative contribution of the principal signals in each of the 19 recorded signals. This enables to visualize which parts of the brains are activated most and how the activity moves through the brains from one side to another.

There will however be some very specific problems in this EEG application. First, the signals are non-stationary and do not have some typical waveform, like e.g. the ECG. It is therefore already very difficult to analyse an EEG visually. Furthermore, the sources are alternatingly active, such that the strongest signal contributions come sometimes from completely different source locations during the experiment. At the moment not enough is known about the source model of the brains, because it is even possible that it has to be modelled by moving sources.

These problems are encountered when the brains are "free-running", this means that the patient is thinking, looking, smelling, etc. On the other hand, experiments with **evoked potentials** might give better results. In this case, the patient has to do some specific action (some reaction test, activate a flashlight, push button, etc.) such that he/she is very concentrated and most of the signal energy in the EEG is due to the brain activity needed to "control" this action. Also, in special cases like epilepsis, where sudden discharges of electrical activity in some places of the brain occur, these SVD-based signal separation techniques are very promising.

Appendix A

Feasibility study of a real-time implementation of the on-line algorithm

A.1 Introduction

In Chapter 4 of this dissertation an on-line adaptive algorithm for use in SVD-based signal separation is presented. The simplicity of its structure and the elegance of its concept make this algorithm extremely suitable for implementation into a real-time environment.

In this Chapter we will discuss two possible implementations of this algorithm : the first one is a software implementation into a system, based on a Personal Computer extended with a DSP-board, and the second one is the implementation into hardware by the design of an Application Specific Integrated Circuit (ASIC).

A.2 PC-based unit for real-time signal separation

A.2.1 Feasibility study

In view of a real-time PC-based unit for signal separation a feasibility study has been performed in the frame of a master's thesis [53]. This study resulted in the realization of a prototype board, with the TMS-32010 microprocessor. Software for the algorithm was written in TMS-assembler.

The design parameters for that study were the following :

- $p = 8$ analog input signals
- $p = 8$ analog output signals
- sampling frequency $f_S = 250$ Hz
- 12 bit A/D conversion
- fixed point arithmetic with simple (16 bits) and double (32 bits) precision

The main features of the TMS-32010 microprocessor can be summarized as follows :

- 200 ns instruction cycle
- 144 words of 16 bit on-chip data RAM
- no ROM
- external memory expansion to a total of 4 K words of 16 bits
- 32 bit ALU / accumulator
- 16 × 16 bit multiply in 200 ns

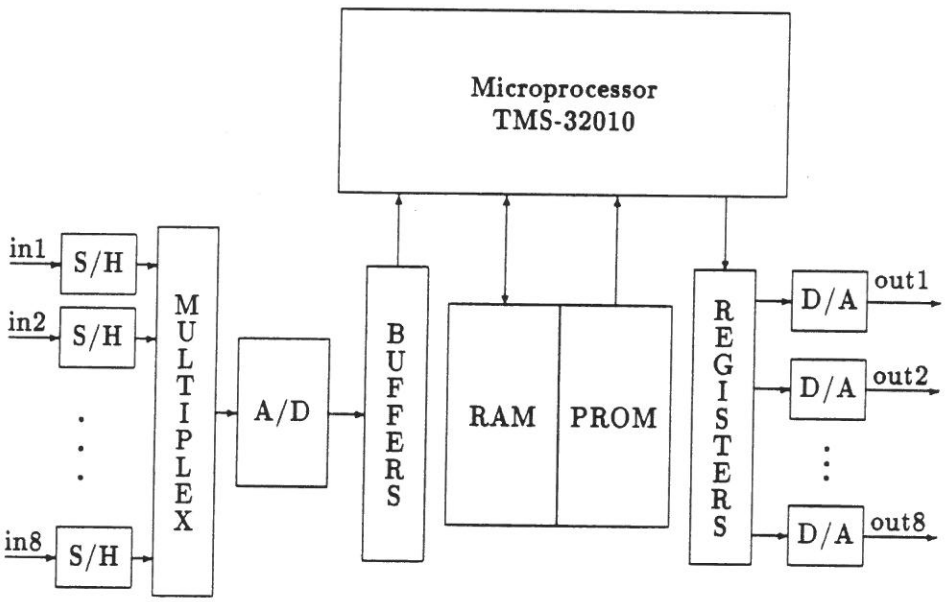

Figure A.1: *The general layout of the prototype board with TMS-32010.*

The general layout of the prototype board is shown in Figure A.1. The input section contains 8 Sample & Hold modules, a multiplexer and an A/D convertor. The output section consists of 8 D/A convertors and data buffers, controlled by decoders. The external data memory was 2 K words of 16 bits and for the program code an external PROM with a capacity of 1 K words of 16 bits was used.

The TMS-32010 had to perform the computational work for the algorithm as well as the control of data transfer and timing. Therefore the microprocessor was programmed in a loop, in which the following tasks were performed in the given order :

1. Control of the input section : p analog input signals were sampled, converted to digital values with the A/D convertor and put in the on-chip RAM of the TMS.

2. The first step of the algorithm : projection of the input p-vector onto the current U-matrix, that is stored in the external RAM.

3. The second step of the algorithm : the rank-one perturbation of the symmetric covariance matrix, residing in the internal RAM of the TMS.

4. Control of the output section : the output p-vector is sent to the output registers and converted to analog values.

5. The third and fourth step of the algorithm : the computation of one Jacobi rotation, the application of this rotation to the covariance matrix and the updating of the U-matrix.

6. Waiting for the following input vector, according to the applied sampling frequency.

Since the design was made for a sampling frequency of 250 Hz, each cycle of the loop had to be executed in 4 ms. In Figure A.2 a timing diagram shows the relative timings for each of the six tasks. On this figure one can remark that the processor is in waiting state for more than half of the available time of 4 ms. Therefore one can conclude that the same design would also permit a sampling frequency of 500 Hz.

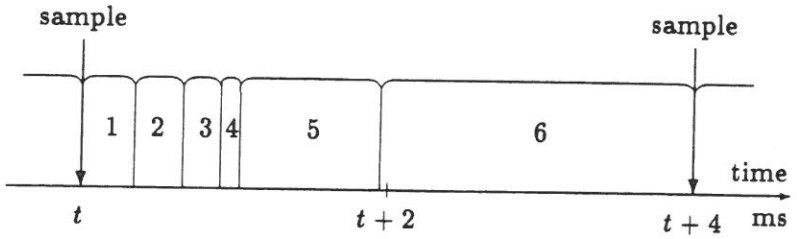

Figure A.2: *Diagram with relative timing of the tasks that the TMS-processor has to perform each 4 ms.*

The results of this study were very successful. However, the prototype itself still had some drawbacks : the fixed point arithmetic made it necessary to use scaling factors in order to prevent overflow and caused a loss of orthonormality of the U-matrix, the amplification of the input signals to rescale them after A/D conversion was not perfect, the computation of a square root was quite time-consuming, etc. Therefore a PC-based system with a DSP plug-in board was designed. In the following section, this system will be described.

A.2.2 A PC-based system

Starting from the successful results of the feasibility study and of the prototype TMS-32010-based board, a PC-based system with DSP plug-in board was developed. The general layout of that system is outlined in Figure A.3 and can be divided into three main parts

1. The Analog Front End performing amplification, isolation, filtering and sampling of the p analog input signals.
2. The DSP plug-in board on which the A/D conversion is performed and upon which the algorithm is implemented in software.
3. The PC with the user-interface, storage and monitoring facilities.

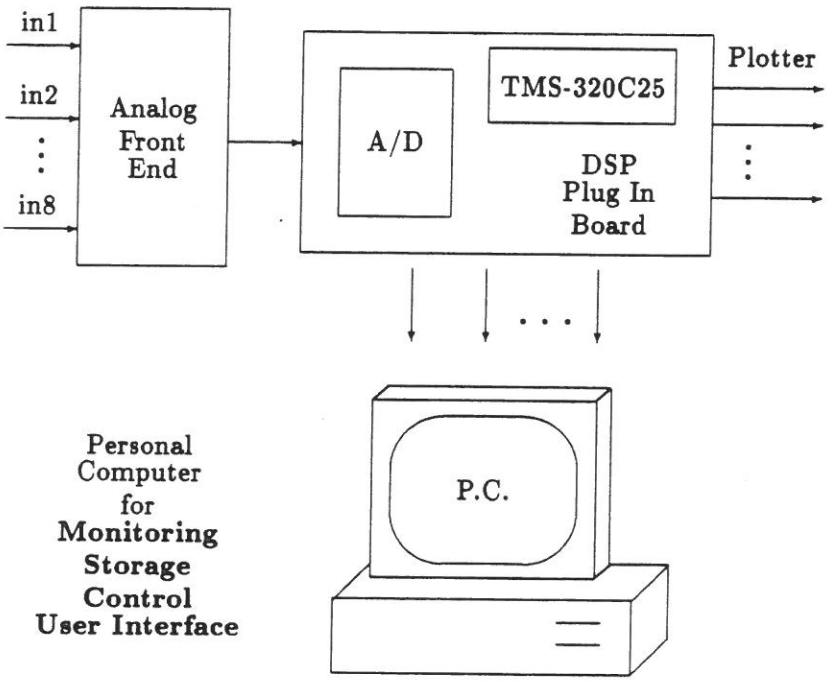

Figure A.3: *General layout of the PC-based system for real-time extraction of the fetal ECG.*

We will now describe each of the three sections in more detail and explain some of the choices for the design parameters.

1. The Analog Front End :

Amplification, isolation and filtering : The analog input signals should be bandfiltered : highpass filtering is needed for elimination of low frequency noise, baseline drift, slow abdominal signals, etc., while lowpass filtering is required to bandlimit the signals in order to prevent aliasing for the given sampling frequency. Isolation is required for patient's safety.

The design parameters will be as follows:

- Isolation : inductive coupling is preferred because optical coupling introduces extra noise and a separate power supply of the front-end is considered unreliable.
- Highpass Filtering : a first order filter with cut-off frequency at 0.1 Hz is implemented, since higher order filters have a non-linear phase, introducing unequal delays between different frequency components.
- Lowpass Filtering : a fifth order active Bessel filter (linear phase) is implemented with cut-off frequency at 80 Hz.
- Amplification should be programmable from the PC-interface if possible.

Sampling : The sampling frequency for this design is chosen to be $f_S = 500$ Hz, such that the Nyquist-condition is not violated. An important requirement for this multichannel signal processing application is that all input channels should be sampled simultaneously. Indeed, sequential sampling of the input signals would introduce phase shifts, such that the time relations between the input signals are disturbed. Since the solution of the signal separation problem is found as one or more linear combinations of the input signals, it is very important that these combinations are computed for the same sampling instants. Therefore the analog front end contains 8 Sample & Hold modules that are enabled simultaneously and then sequentially multiplexed to the A/D convertor.

2. The DSP plug-in board :

Since most of the software for the algorithm was already written in TMS-assembler, a TMS-based plug-in board was preferred. The Burr-Brown DSP carrier (PCI-20202C-1) with TMS-320C25 microprocessor and with two extra modules for high-speed analog input (PCI-20019M-1A) and with a counter/timer generator (PCI-20007M-1) was therefore chosen.

The main features of the TMS-320C25 microprocessor can be summarized as follows :

- 100 ns instruction cycle
- 4 K $\times$ 16 bit words of on-chip masked ROM
- 8 auxiliary registers
- 8-deep hardware stack
- 544 words of 16 bit on-chip data RAM
- 128 K words of memory space (64 K words program / 64 K words data)

For this design floating point arithmetic will be used, since then the problems with overflow and scaling do not appear. The microprocessor has some additional instructions to speed up the execution and has a very fast instruction cycle, such that floating point operations can be performed within the required timing restrictions.

3. The Personal Computer :

The Personal Computer should be AT-compatible with a clock frequency of at least 8 MHz. The PC should display one recorded signal, containing both MECG and FECG, and one MECG-free fetal signal, in moving bar display mode. At least three signals should be stored on hard disk. The user interface will be written in the high level programming language C.

At the moment of writing this dissertation, the PC-based system for real-time FECG-extraction as described here was still under development. This realization is a cooperation in the frame of the European Community Project "New Methods in Perinatal Surveillance" between the K.U. Leuven (ESAT-laboratory Department of Electrical Engineering and the laboratory of Gastrointestinal Motility of the Department of Medical Research), the K.U. Nijmegen (Department of Obstetrics & Gynaecology and the laboratory of Medical Physics and Biofysics) and the V.U. Amsterdam (Laboratory of Medical Physics). It is the aim to build three prototype systems that can be used in universitary hospitals in Europe for large scale clinical tests.

A.3 A digital chip implementation of the on-line adaptive algorithm

Based on the successful results of the feasibility study [53], described in the previous section, the idea originated to design an Application Specific Integrated Circuit to implement the on-line adaptive algorithm in hardware. It is the aim to make the use of the on-line algorithm possible for SVD-based signal processing applications with much higher sampling frequencies (in the range of 10 - 20 KHz) then for the FECG-extraction (500 Hz). These applications can be found in speech processing, telecommunications, modal analysis, image processing, etc.

Already two master's theses in cooperation with the division VSDM of the Interuniversitary Micro Electronics Center (IMEC vzw) were made on this topic [26], [92]. It is not our aim to go in detail on this digital chip implementation, but we will very briefly summarize the main results here.

In order to avoid the computation of a square root or of divisions in the algorithm, the CORDIC algorithm [93] was used in this design. Therefore the rotation angle in the diagonalization step of the on-line algorithm was computed with some CORDIC iterations, requiring only shifts and additions. Fixed word lengths of 12 bits for single and 24 bits for double precision were used.

The software of Cathedral II for digital chip design was used in these studies. Simulations in SILAGE showed that for one cycle in the algorithmic loop about 4500 clock cycles were required if 10 input signals were processed, while $\pm$ 3000 clock cycles were needed if only 6 input signals are considered. In the clock frequency of the ASIC is 10 MHz, then this real-time implementation would permit a sampling frequency of 2.2 KHz and 3.3 KHz respectively. This is still not fast enough to deal with sampling frequencies of $\pm$ 10 - 20 KHz. However, in the new version of Cathedral III faster modules will allow to obtain higher speeds.

Although the digital chip design is not part of this doctoral thesis, it is mentioned here for the sake of completeness.

Appendix B

Pascal routines on VAX / VMS

```
{     DIRECTORY DISK$SISTA:[CALLAERTS.ONLINE]        FILE    :  SVD_ONLIN.PAS   }

program SVD_OnLin (input,output);

{-------------------------------------------------------------------------------
     This program uses the on-line adaptive algorithm to compute the left
     singular matrix in the Ordinary Singular Value Decomposition (OSVD)
     of a given matrix.

     USED SUBROUTINES :

      SVD_Init (CovMatrix, SingBasis, DimIn, DimOut, Interval, Alfa);
        FILE :  'SVD_INIT.PAS'
        This subroutine initializes the symmetric covariance matrix (CovMatrix),
        the singular basis (SingBasis), the number of recorded signals (DimIn),
        the number of resulting signals (DimOut), the number of samples to be
        read in and processed (Interval) and the forgetting factor (Alfa).

      ReadSampleIn (DimIn, SampleIn);
        FILE :  'SVD_IO.PAS'
        This subroutine reads one column of the data matrix from the input file
        Data. This row contains DimIn elements and is put in a vector SampleIn.

     MatrixVectorProduct (SampleIn, SingBasis, DimIn, DimOut, SampleOut);
        FILE :  'PREPROS.PAS'
        This subroutine computes the product of the matrix SingBasis (with
        dimensions DimOut x DimIn) and SampleIn (dimension DimIn) to form
        the vector SampleOut (dimension DimOut).

     WriteSampleOut (DimOut, SampleOut);
        FILE :  'SVD_IO.PAS'
        This subroutine writes the vector SampleOut (dimension DimOut) into
        the file Results.

     Accumulation (SampleOut, DimOut, Alfa, CovMatrix, Piv1, Piv2);
        FILE :  'PREPROS.PAS'
        This subroutine updates the symmetric matrix CovMatrix by accumulating
        the outer product of SampleOut with itself. The previous values of the
        elements in CovMatrix are multiplied with the forgetting factor Alfa.
        The routine also finds the indices of the off-diagonal element of
        CovMatrix with maximum absolute value.

     ComputeRotation (CovMatrix, Piv1, Piv2, Sine, Cosine, Change);
        FILE :  'ROTATION.PAS'
        This subroutine computes the sine and cosine of the angle of the plane
        rotation, that reduces the absolute value of the off-diagonal element
        of CovMatrix on the position (Piv1,Piv2).
        The boolean value Change is TRUE if the diagonal element of CovMatrix
        on position (Piv2,Piv2) is larger than the diagonal element on position
        (Piv1,Piv1).
```

```
ApplyRotation (Sine, Cosine, DimOut, Piv1, Piv2, Change, CovMatrix);
  FILE :  'ROTATION.PAS'
  This procedure performs a plane rotation on CovMatrix. This plane
  rotation reduces the off-diagonal element of CovMatrix on position
  (Piv1,Piv2). If Change is TRUE, some elements are changed, such
  that after the rotation the diagonal element of CovMatrix on position
  (Piv1,Piv1) is larger than the diagonal element on position (Piv1,Piv1)

UpdateSingBasis (Sine, Cosine, DimIn, Piv1, Piv2, Change, SingBasis);
  FILE :  'ROTATION.PAS'
  This procedure applies the same plane rotation to the matrix SingBasis.
  If Change is TRUE, the rows Piv1 and Piv2 of SingBasis are changed.

WritePosterior (DimIn, DimOut, SingBasis, CovMatrix);
  FILE :  'SVD_IO.PAS'
  This procedure writes the matrices SingBasis and CovMatrix into file
  Post.
```

VARIABLES :

NDM	Maximum number of input signals
MAXDIM	Maximum number of samples
Data	Input file that contains a value for DimIn, Interval and the data matrix.
Results	Output file
Apriori	Input file that contains initial values for DimOut, SingBasis and CovMatrix. This initialization is needed if one starts from other initial conditions than usually (SingBasis is identity matrix and CovMatrix is zero matrix).
SingBasis	Orthonormal matrix with dimensions DimOut x DimIn. This matrix approaches the left singular basis of the data matrix.
CovMatrix	Symmetric covariance matrix of the resulting signals (with dimensions DimOut x DimOut).
SampleIn	Input vector (dimension DimIn) that contains one column of the data matrix.
SampleOut	Output vector (dimension DimOut) that contains one column of the output matrix.
Change	Boolean variable that controls the ordening of the diagonal elements of CovMatrix.
Sine, Cosine	Sine and Cosine of the rotation angle, computed with a new approximating method.
Alfa	Exponential forgetting factor in order to forget events from the remote past.
DimIn, DimOut	Dimensions of input and output vectors.
Interval	Number of samples to be processed.
Piv1, Piv2	Coordinates of the off-diagonal element of CovMatrix with the largest absolute value.
Count	Loop counter.

```
const
  NDM    = 50;
  MAXDIM = 25000;

type
  Matrix    =  array [1..NDM,1..NDM]    of REAL;
  Ivector   =  array [1..NDM]           of INTEGER;
  Rvector   =  array [1..NDM]           of REAL;
  Name      =  varying [50]             of CHAR;

var
  Data, Results, Apriori                : TEXT;
  SingBasis, CovMatrix                  : Matrix;
  SampleIn, SampleOut                   : Rvector;
  Change                                : BOOLEAN;
  Sine, Cosine, Alfa                    : REAL;
  DimIn, DimOut, Interval, Piv1, Piv2   : INTEGER;
  Count                                 : 1..MAXDIM;

  %INCLUDE 'SVD_IO.PAS'
  %INCLUDE 'SVD_INIT.PAS'
  %INCLUDE 'PREPROS.PAS'
  %INCLUDE 'ROTATION.PAS'

begin

  SVD_Init (CovMatrix, SingBasis, DimIn, DimOut, Interval, Alfa);

  for Count := 1 to Interval do
  begin

     ReadSampleIn (DimIn, SampleIn);

     MatrixVectorProduct (SampleIn, SingBasis, DimIn, DimOut, SampleOut);

     WriteSampleOut (DimOut, SampleOut);

     Accumulation (SampleOut, DimOut, Alfa, CovMatrix, Piv1, Piv2);

     ComputeRotation (CovMatrix, Piv1, Piv2, Sine, Cosine, Change);

     ApplyRotation (Sine, Cosine, DimOut, Piv1, Piv2, Change, CovMatrix);

     UpdateSingBasis (Sine, Cosine, DimIn, Piv1, Piv2, Change, SingBasis);

  end;

  WritePosterior (DimIn, DimOut, SingBasis, CovMatrix);

  Close (Data);  Close (Results);

end.
```

```
{     DIRECTORY DISK$SISTA:[CALLAERTS.ONLINE]       FILE   :  SVD_IO.PAS    }

procedure ReadSampleIn (N : INTEGER; var X : Rvector);

{-------------------------------------------------------------------------------

     This procedure reads a real vector X of dimension N from file Data.

-------------------------------------------------------------------------------}

var
  I     : 1..NDM;

begin

  for I := 1 to N  do      read (Data,X[I]);
  readln (Data);

end;

{-------------------------------------------------------------------------------

procedure WriteSampleOut (M : INTEGER; Y : Rvector);

{-------------------------------------------------------------------------------

     This procedure writes a vector Y of dimension M into file Results.

-------------------------------------------------------------------------------}

var
  I,L,K : 1..NDM;

begin

   L := M;
   K := 0;
   while L >= 6 do
      begin
        for I := 1 to 6  do     write (Results,Y[K+I]:11:4,' ');
        writeln (Results);
        L := L - 6;
        K := K + 6;
      end;
   if L > 0
      then
        begin
          for I := 1 to L  do     write (Results,Y[K+I]:11:4,' ');
          writeln (Results);
        end;

end;
```

```
{-------------------------------------------------------------------------}

procedure WritePosterior (N,M : INTEGER; A,B : Matrix);

{-------------------------------------------------------------------------
     This procedure writes matrices A and B, resp. of dimension M x N and
     M * M, into file Post.
-------------------------------------------------------------------------}

var
   Post         : TEXT;
   I,J,K,L      : 1..NDM;

begin

   open (Post,'post.out',history := new);
   if status (Post) <> 0 then
      writeln ('Error during opening of postfile');
   rewrite(Post);
   writeln(Post,M);

   for I := 1 to M do
     begin
        L := N;
        K := 1;
        while L >= 6 do
           begin
             for J := (K-1)*6+1 to K*6  do    write (Post,A[I,J]:11:8,' ');
             writeln (Post);
             L := L - 6;
             K := K + 1;
           end;
        if L > 0
           then
             begin
               for J := (K-1)*6+1 to N  do    write (Post,A[I,J]:11:8,' ');
               writeln (Post);
             end;
     end;

   for I := 1 to M do
     begin
        L := M;
        K := 1;
        while L >= 6 do
           begin
             for J := (K-1)*6+1 to K*6  do    write (Post,B[I,J]:11:4,' ');
             writeln (Post);
             L := L - 6;
             K := K + 1;
           end;
        if L > 0
           then
             begin
               for J := (K-1)*6+1 to M  do    write (Post,B[I,J]:11:4,' ');
               writeln (Post);
             end;
     end;

   close (Post);

end;
```

```
{-------------------------------------------------------------------------}
procedure ReadMatrix (M,N : INTEGER; var MAT : Matrix);
{-------------------------------------------------------------------------
    This procedure reads a matrix MAT with dimension M x N from file Apriori
-------------------------------------------------------------------------}
var
  I,J     : 1..NDM;
begin
  for I := 1 to M do
        for J := 1 to N do
            read(Apriori,MAT[I,J]);
end;
```

```
{     DIRECTORY DISK$SISTA:[CALLAERTS.ONLINE]        FILE    :  SVD_INIT.PAS  }

procedure SVD_Init  (var SYM,U    : Matrix;
                     var N,M,NS   : INTEGER;
                     var Factor   : REAL);

{-------------------------------------------------------------------------------

        This procedure initializes the variables of the program SVD_ONLIN.

        In order of occurence, the following actions are performed :
         1.  Opening of the input  file  Data
         2.  Opening of the output file  Results
         3.  The variables N (the number of input signals) and
             NS (the number of samples) are read from the input file Data
         4.  The procedure asks the user to input a value for the exponential
             forgetting factor
         5.  The procedure asks the user if it has to start from initial
             conditions, or if it must continue the computation with
             previous results.
                --> initial conditions :  the matrix U is set equal to the
                    identity matrix, while the symmetric matrix SYM is put
                    zero. The variable M is put equal to N.
                --> previous results   :  first the procedure asks the user
                    for the name of a file that contains those previous results.
                    Then it reads from that file values for M, U and SYM.
                    The matrix U has dimensions M x N, and SYM has dimensions
                    M x M.

        USED PROCEDURE :
          ReadMatrix (P,Q,A)
            FILE :  'SVD_IO.PAS'
            This procedure reads a matrix A with dimensions P x Q from the
            file Apriori.

-------------------------------------------------------------------------------}

var
  FN1,FN2,FN3,B : Name;
  I,J           : 1..NDM;
  NUMBER        : INTEGER;


begin

   B := '[CALLAERTS.ONLINE]';
   write (' --> Enter the name of the  input file  :   ');
   readln(FN1);
   FN1 := B + FN1;
   open (Data,FN1,history := old);
   if status (Data) <> 0 then    writeln ('Error during opening inputfile');
   reset (Data);

   write (' --> Enter the name of the output file  :   ');
   readln(FN2);
   FN2 := B + FN2;
   open (Results,FN2,history := new);
   if status (Results) <> 0 then   writeln ('Error during opening outputfile');
   rewrite (Results);
```

```
    readln(Data,N);
    readln(Data,NS);

    repeat
       write (' --> Enter the forgetting factor (0 <= Factor <= 1) : ');
       readln (Factor);
    until (Factor <= 1) and (Factor > 0);
    writeln;

    repeat
       writeln;
       write ('      1.  START on-line computation from initial conditions');
       writeln;
       write ('      2.  CONTINUE on-line computation with previous results');
       writeln;
       write ('      -->  Enter choice :  ');
       readln (NUMBER);
    until (NUMBER = 1) or (NUMBER = 2);
    writeln;

    if NUMBER = 1
       then
         begin
           M := N;
           for I := 1 to N do
             begin
               for J := 1 to N do
                   begin
                     SYM[I,J] := 0.0;
                     U[I,J] := 0.0;
                   end;
               U[I,I] := 1;
             end;
         end
       else
         begin
           write (' --> Enter the name of the apriori file :   ');
           readln(FN3);
           FN3 := B + FN3;
           open (Apriori,FN3,history := old);
           if status (Apriori) <> 0 then
              writeln ('Error during opening inputfile');
           reset (Apriori);
           readln (Apriori,M);
           ReadMatrix (M,N,U);
           ReadMatrix (M,M,SYM);
         end;

end;
```

```
{    DIRECTORY DISK$SISTA:[CALLAERTS.ONLINE]          FILE  :   PREPROS.PAS   }

procedure MatrixVectorProduct  (X      : Rvector;
                                MAT    : Matrix;
                                N,M    : INTEGER;
                                var Y  : Rvector);

{-------------------------------------------------------------------------------
     This procedure computes the product between an M x N matrix MAT and a
     real vector X of N elements.
     The result is a real vector Y with dimension M.

     Inputs  :    MAT  a real matrix with dimension M x N
                  N    dimension of the input vector X
                  M    dimension of the output vector Y
                  X    a real vector

     Outputs :    Y    a real vector formed by  MAT * X
-------------------------------------------------------------------------------}

var
  I,J : 1..NDM;

begin

  for I := 1 to M do

    begin

      Y[I] := 0;
      for J := 1 to N do
          Y[I] := Y[I] + MAT[I,J]*X[J];

    end

end;

{-------------------------------------------------------------------------------

procedure Accumulation (Y        : Rvector;
                        M        : INTEGER;
                        Factor   : REAL;
                        var SYM  : Matrix;
                        var P,Q  : INTEGER);

{-------------------------------------------------------------------------------
     This procedure adds the outer product of a vector Y with itself to a real
     symmetric matrix SYM with dimension M x M.
     The elements of SYM are multiplied by some forgetting factor <= 1.
     Only the upper triangle is computed because of the symmetry.
     The procedure also finds the off-diagonal element with maximum absolute
     value and its coordinates (P,Q).

     Inputs :   Y       a real vector
                M       dimension of the vector and of the symmetric matrix
                Factor  the forgetting factor
     Outputs :  SYM     the new symmetric matrix of dimension M x M
                (P,Q)   the coordinates of the maximum off-diagonal element.
-------------------------------------------------------------------------------
```

```
var
  I,J    : 1..NDM;
  Max    : REAL;

begin

  Max := 0.0;
  for I:= 1 to M do
      for J := I to M do

          begin

            SYM[I,J] := SYM[I,J]*Factor + Y[I]*Y[J];
            if (J > I) and (abs(SYM[I,J]) > Max) then
                begin
                  Max := abs(SYM[I,J]);
                  P   := I;
                  Q   := J;
                end
          end
end;

{-------------------------------------------------------------------------------}

procedure Normalize    (MAT       : Matrix;
                        N,M       : INTEGER;
                        var NMAT  : Matrix);

{-------------------------------------------------------------------------------
     This procedure normalizes the rows of matrix MAT.

     Inputs :   MAT     the M x N matrix that has to be normalized
                N,M     dimension of the matrix
     Output :   NMAT    the matrix after normalization
-------------------------------------------------------------------------------}

var
  I,J : 1..NDM;
  NOR : REAL;

begin

  for I := 1 to M do

    begin

      NOR := 0.0;
      for J := 1 to N do
          NOR := NOR + sqr(MAT[I,J]);
      NOR := sqrt(NOR);
      for J := 1 to N do
          NMAT[I,J] := MAT[I,J]/NOR;

    end

end;
```

```
{   DIRECTORY DISK$SISTA:[CALLAERTS.ONLINE]              FILE  :  ROTATION.PAS

procedure ComputeRotation (SYM      : Matrix;
                           P,Q      : INTEGER;
                           var S,C  : REAL;
                           var CH   : BOOLEAN);

{-------------------------------------------------------------------------------
    This procedure computes the sine and cosine of the rotation angle for the
    off-diagonal element of the symmetric matrix SYM on the position (P,Q).
    The method is a combination of the overrelaxation by Pope and Tompkins,
    and a new underrelaxation approach for large rotation angles.

     Inputs :  SYM      a real symmetric matrix
               (P,Q)    the coordinates of the off-diagonal element whose
                        absolute value has to be reduced.
     Outputs : S,C      sine and cosine of the rotation angle
               CH       a boolean parameter that is TRUE if an ordering on the
                        diagonal is needed.
-------------------------------------------------------------------------------}

var
  K,X,CA,SA,W    : REAL;

begin

  {  Computation of the parameter K.
     If   |K| <  2  then the underrelaxation method is used for the computation
                    of C and S.
     If   |K| >= 2  then the overrelaxation method by Pope and Tompkins is used
                    for the computation of C and S.     }

       K := (SYM[P,P]-SYM[Q,Q])/SYM[P,Q];

       if abs(K) < 2
          then
            begin

               X   :=  sqr(K);
               W   :=  1.0/sqrt(2.0);
               CA  :=  (64.0 - X)/(64.0 + X);
               SA  :=  (1.0 + CA)*abs(K)/8.0;
               C   :=  (SA + CA)*W;
               S   :=  (SA - CA)*W;
               if  (K < 0) or ((K = 0)  and (SYM[P,Q] > 0))   then S := -S;

            end

          else
            begin

               X   :=  4.0*sqr(K);
               C   :=  (X - 1.0)/(X + 1.0);
               S   :=  -(1.0 + C)/(2*K);

            end;

end;

{-------------------------------------------------------------------------------}
```

```
procedure ApplyRotation (S,C      : REAL;
                         M,P,Q    : INTEGER;
                         CH       : BOOLEAN;
                         var SYM : Matrix);

{-------------------------------------------------------------------------------
     This procedure applies a plane rotation to a symmetric matrix SYM.
     A plane rotation is a left and right multiplication of the matrix SYM
     by an orthonormal matrix, equal to the identity matrix, exept for
     the elements on the crossing of rows P and Q with columns P and Q.
     These elements are determined by S and C, which are the sine and cosine
     of the plane rotation angle.

     Inputs :  S,C     sine and cosine of the plane rotation angle
               M       dimension of the symmetric matrix SYM
               (P,Q)   coordinates of the off-diagonal element of SYM with
                       largest absolute value.
               CH      a boolean parameter that is TRUE if an ordering on
                       the diagonal of SYM is needed.

     Output :  SYM     the symmetric matrix rotated in 2 dimensions
                       ( in the P-Q plane )
-------------------------------------------------------------------------------}

var
  X,Y    : REAL;
  I      : 1..NDM;

begin

  if P > 1 then
     for I := 1 to P-1 do
           begin

             X := SYM[I,P]*C - SYM[I,Q]*S;
             Y := SYM[I,P]*S + SYM[I,Q]*C;
             if CH then  begin
                           SYM[I,P] := Y;
                           SYM[I,Q] := X;
                         end
                   else  begin
                           SYM[I,P] := X;
                           SYM[I,Q] := Y;
                         end;
           end;

 if Q-P > 1 then
    for I := P+1 to Q-1 do
           begin

             X := SYM[P,I]*C - SYM[I,Q]*S;
             Y := SYM[P,I]*S + SYM[I,Q]*C;
             if CH then  begin
                           SYM[P,I] := Y;
                           SYM[I,Q] := X;
                         end
                   else  begin
                           SYM[P,I] := X;
                           SYM[I,Q] := Y;
                         end;
           end;
```

```
   if Q < M then

      for I := Q+1 to M do

            begin

              X := SYM[P,I]*C - SYM[Q,I]*S;
              Y := SYM[P,I]*S + SYM[Q,I]*C;
              if CH then  begin
                            SYM[P,I] := Y;
                            SYM[Q,I] := X;
                          end
                    else  begin
                            SYM[P,I] := X;
                            SYM[Q,I] := Y;
                          end;
            end;

  X := (SYM[P,P] - SYM[Q,Q])*S + 2.0*C*SYM[P,Q];
  if CH then  begin
                Y        := abs(SYM[P,P] - X);
                SYM[P,P] := abs(SYM[Q,Q] + X);
                SYM[Q,Q] := Y;
              end
       else  begin
                SYM[P,P] := abs(SYM[P,P] - X);
                SYM[Q,Q] := abs(SYM[Q,Q] + X);
              end;
  SYM[P,Q] := -SYM[P,Q] + X*C;

end;

{-------------------------------------------------------------------------------}


procedure UpdateSingBasis (S,C     : REAL;
                           N,P,Q   : INTEGER;
                           CH      : BOOLEAN;
                           var U   : Matrix);


{-------------------------------------------------------------------------------
     This procedure applies a plane rotation to an orthogonal matrix U.
     This corresponds to the multiplication of the matrix U with an orthonormal
     matrix, equal to the identity matrix, exept for the elements on the
     crossing of rows P and Q with columns P and Q.
     These elements are determined by S and C, which are the sine and cosine
     of the plane rotation angle.
     The effect of this multiplication is that only the rows P and Q of
     U-matrix are changed.

     Inputs :  S,C   sine and cosine of the Jacobi rotation angle
               N     number of columns of the orthonormal matrix
               P,Q   the indices of the only 2 rows to change
               CH    a boolean parameter that is TRUE if the rows P and Q
                     have to be changed.
     Output :  U     the orthonormal matrix rotated in 2 dimensions
                     ( in the P-Q plane )
-------------------------------------------------------------------------------}
```

```
var
  I      : 1..NDM;
  X,Y    : REAL;

begin

  for I := 1 to N do

    begin

      X := U[P,I]*C - U[Q,I]*S;
      Y := U[P,I]*S + U[Q,I]*C;
      if CH then  begin
                    U[P,I] := Y;
                    U[Q,I] := X;
                  end
            else  begin
                    U[P,I] := X;
                    U[Q,I] := Y;
                  end;
    end

end;
```

```
{     DIRECTORY DISK$SISTA:[CALLAERTS.ONLINE]        FILE    :  GSVD_ONLIN.PAS    }

program GSVD_OnLin (input,output);

{-------------------------------------------------------------------------------
     This program uses the on-line adaptive algorithm to compute the X-matrix
     in the Ordinary Singular Value Decomposition (QSVD) of a given matrix pair.

     USED SUBROUTINES :

      GSVD_Init (CovMatrix, XMatrix, DimIn, DimOut, Interval, Alfa);
        FILE :  'GSVD_INIT.PAS'
        This subroutine initializes the symmetric covariance matrix (CovMatrix),
        the X-matrix (XMatrix), the number of recorded signals (DimIn),
        the number of resulting signals (DimOut), the number of samples to be
        read in and processed (Interval) and the forgetting factor (Alfa).

      ReadSampleIn (DimIn, SampleIn);
        FILE :  'SVD_IO.PAS'
        This subroutine reads one column of the data matrix from the input file
        Data. This row contains DimIn elements and is put in a vector SampleIn.

      Normalize (XMatrix, DimIn, DimOut, XNMatrix);
        FILE :  'PREPROS.PAS'
        This subroutine normalizes the rows of a matrix XMatrix with dimensions
        DimOut x DimIn and puts the result in matrix XNMatrix.

      MatrixVectorProduct (SampleIn, XNMatrix, DimIn, DimOut, SampleOut);
        FILE :  'PREPROS.PAS'
        This subroutine computes the product of the matrix XNMatrix (with
        dimensions DimOut x DimIn) and SampleIn (dimension DimIn) to form
        the vector SampleOut (dimension DimOut).

      WriteSampleOut (DimOut, SampleOut);
        FILE :  'SVD_IO.PAS'
        This subroutine writes the vector SampleOut (dimension DimOut) into
        the file Results.

      Accumulation (SampleOut, DimOut, Alfa, CovMatrix, Piv1, Piv2);
        FILE :  'PREPROS.PAS'
        This subroutine updates the symmetric matrix CovMatrix by accumulating
        the outer product of SampleOut with itself. The previous values of the
        elements in CovMatrix are multiplied with the forgetting factor Alfa.
        The routine also finds the indices of the off-diagonal element of
        CovMatrix with maximum absolute value.

      ComputeRotation (CovMatrix, Piv1, Piv2, Sine, Cosine, Change);
        FILE :  'ROTATION.PAS'
        This subroutine computes the sine and cosine of the angle of the plane
        rotation, that reduces the absolute value of the off-diagonal element
        of CovMatrix on the position (Piv1,Piv2).
        The boolean value Change is TRUE if the diagonal element of CovMatrix
        on position (Piv2,Piv2) is larger than the diagonal element on position
        (Piv1,Piv1).
```

```
ApplyRotation (Sine, Cosine, DimOut, Piv1, Piv2, Change, CovMatrix);
  FILE :  'ROTATION.PAS'
  This procedure performs a plane rotation on CovMatrix. This plane
  rotation reduces the off-diagonal element of CovMatrix on position
  (Piv1,Piv2). If Change is TRUE, some elements are changed, such
  that after the rotation the diagonal element of CovMatrix on position
  (Piv1,Piv1) is larger than the diagonal element on position (Piv1,Piv1)

UpdateSingBasis (Sine, Cosine, DimIn, Piv1, Piv2, Change, XMatrix);
  FILE :  'ROTATION.PAS'
  This procedure applies the same plane rotation to the matrix XMatrix.
  If Change is TRUE, the rows Piv1 and Piv2 of XMatrix are changed.

WritePosterior (DimIn, DimOut, XMatrix, CovMatrix);
  FILE :  'SVD_IO.PAS'
  This procedure writes the matrices SingBasis and CovMatrix into file
  Post.
```

VARIABLES :

NDM	Maximum number of input signals
MAXDIM	Maximum number of samples
Data	Input file that contains a value for DimIn, Interval and the data matrix.
Results	Output file
Apriori	Input file that contains the initial values for DimOut, XMatrix and CovMatrix. These matrices are the result of a previous SVD computation, which is the initialization of the on-line version of the QSVD-algorithm.
XMatrix	Matrix with dimensions DimOut x DimIn. This matrix approaches the X-matrix in the QSVD of the given matrix pair.
CovMatrix	Symmetric covariance matrix of the resulting signals (with dimensions DimOut x DimOut).
SampleIn	Input vector (dimension DimIn) that contains one column of the data matrix.
SampleOut	Output vector (dimension DimOut) that contains one column of the output matrix.
Change	Boolean variable that controls the ordening of the diagonal elements of CovMatrix.
Sine, Cosine	Sine and Cosine of the rotation angle, computed with a new approximating method.
Alfa	Exponential forgetting factor in order to forget events from the remote past.
DimIn, DimOut	Dimensions of input and output vectors.
Interval	Number of samples to be processed.
Piv1, Piv2	Coordinates of the off-diagonal element of CovMatrix with the largest absolute value.
Count	Loop counter.

```
const
  NDM    = 50;
  MAXDIM = 25000;

type
  Matrix    =  array [1..NDM,1..NDM]    of REAL;
  Rvector   =  array [1..NDM]           of REAL;
  Name      =  varying [50]             of CHAR;

var
  Data, Results, Apriori                : TEXT;
  XMatrix, CovMatrix, XNMatrix          : Matrix;
  SampleIn, SampleOut                   : Rvector;
  Change                                : BOOLEAN;
  Sine, Cosine, Alfa                    : REAL;
  DimIn, DimOut, Interval, Piv1, Piv2   : INTEGER;
  Count                                 : 1..MAXDIM;

  %INCLUDE 'SVD_IO.PAS'
  %INCLUDE 'GSVD_INIT.PAS'
  %INCLUDE 'PREPROS.PAS'
  %INCLUDE 'ROTATION.PAS'

begin

  GSVD_Init (CovMatrix, XMatrix, DimIn, DimOut, Interval, Alfa);

  for Count := 1 to Interval do
  begin

     ReadSampleIn (DimIn, SampleIn);

     Normalize (XMatrix, DimIn, DimOut, XNMatrix);

     MatrixVectorProduct (SampleIn, XNMatrix, DimIn, DimOut, SampleOut);

     WriteSampleOut (DimOut, SampleOut);

     MatrixVectorProduct (SampleIn, XMatrix, DimIn, DimOut, SampleOut);

     Accumulation (SampleOut, DimOut, Alfa, CovMatrix, Piv1, Piv2);

     ComputeRotation (CovMatrix, Piv1, Piv2, Sine, Cosine, Change);

     ApplyRotation (Sine, Cosine, DimOut, Piv1, Piv2, Change, CovMatrix);

     UpdateSingBasis (Sine, Cosine, DimIn, Piv1, Piv2, Change, XMatrix);

  end;

  WritePosterior (DimIn, DimOut, XMatrix, CovMatrix);

  Close (Data);  Close (Results);  Close (Apriori);

end.
```

```
{    DIRECTORY DISK$SISTA:[CALLAERTS.ONLINE]        FILE   :  GSVD_INIT.PAS    }

procedure GSVD_Init (var SYM,X     : Matrix;
                     var N,M,NS    : INTEGER;
                     var Factor    : REAL);

{-------------------------------------------------------------------------------

        This procedure initializes the variables of the program GSVD_ONLIN.

        In order of occurence, the following actions are performed :
         1.  Opening of the input  file  Data
         2.  Opening of the output file  Results
         3.  Opening of the input  file  Apriori
         4.  The variables N (the number of input signals) and
             NS (the number of samples) are read from the input file Data
         5.  The procedure asks the user to input a value for the exponential
             forgetting factor
         6.  The procedure reads from the file Apriori values for M and for
             the matrix X.
         7.  The procedure asks the user if it has to start from initial
             conditions or from previously obtained results :
                --> initial conditions : the matrix SYM is set zero
                --> previous results   : the matrix SYM is read from Apriori.

       USED PROCEDURE :
         ReadMatrix (P,Q,A)
           FILE :  'SVD_IO.PAS'
           This procedure reads a matrix A with dimensions P x Q from the
           file Apriori.

-------------------------------------------------------------------------------}
var
  FN1,FN2,FN3,B : Name;
  I,J           : 1..NDM;
  NUMBER        : INTEGER;

begin

   B := '[CALLAERTS.ONLINE]';
   write (' ---> Enter the name of the  input file  : ');
   readln(FN1);
   FN1 := B + FN1;
   open (Data,FN1,history := old);
   if status (Data) <> 0 then   writeln ('Error during opening inputfile');
   reset (Data);

   write (' ---> Enter the name of the output file  : ');
   readln(FN2);
   FN2 := B + FN2;
   open (Results,FN2,history := new);
   if status (Results) <> 0 then  writeln ('Error during opening outputfile');
   rewrite (Results);
```

```
    write (' ---> Enter the name of the apriori file : ');
    readln(FN3);
    FN3 := B + FN3;
    open (Apriori,FN3,history := old);
    if status (Apriori) <> 0 then   writeln ('Error during opening inputfile');
    reset (Apriori);

    readln(Data,N);
    readln(Data,NS);

    repeat
       write (' ---> Enter the forgetting factor (0 <= Factor <= 1) : ');
       readln (Factor);
    until (Factor <= 1) and (Factor > 0);
    writeln;

    readln (Apriori,M);
    ReadMatrix (M,N,X);

    repeat
       writeln;
       write ('      1.  START on-line computation from initial conditions');
       writeln;
       write ('      2.  CONTINUE on-line computation with previous results');
       writeln;
       write ('      -->  Enter choice :   ');
       readln (NUMBER);
    until (NUMBER = 1) or (NUMBER = 2);
    writeln;

    if NUMBER = 1
       then
         for I := 1 to N do
               for J := 1 to N do
                     SYM[I,J] := 0.0
       else
         ReadMatrix (M,M,SYM);

end;
```

Bibliography

[1] ACHIM, A., RICHER, F., SAINT-HILAIRE, J.M., "Methods for Separating Temporally Overlapping Sources of Neuroelectric Data", *Brain Topography*, vol. **1**, no. 1, 1988.

[2] ALSTE, J.A. van, SCHILDER, T.S., "Removal of Base-Line Wander and Power-Line Interference from the ECG by an Efficient FIR Filter with a Reduced Number of Taps", *IEEE Trans. Biomed. Eng.*, vol. BME-**32**, no. 12, pp. 1052-1060, 1985.

[3] AUTONNE, L., *Bull. Soc. Math. France*, vol. **30**, pp. 121-133, 1902.

[4] BEMMEL, J.H. van, "Detection of weak electrocardiograms by autocorrelation and crosscorrelation of envelopes", *IEEE Trans. Biomed. Eng.*, vol. BME-**15**, pp. 17-23, Jan. 1968.

[5] BENNETT, W.R., "Spectra of quantized signals", Bell Syst. Tech. J., vol. **27**, pp. 446-472, July 1948.

[6] BERGVELD, P., MEIJER, J.H., "A new technique for the suppression of the MECG", *IEEE Trans. Biomed. Eng.*, vol. BME-**28**, pp. 348-354, Apr. 1981.

[7] BERGVELD, P., KOLLING, A.J., PEUSCHER, J.H.J., "Real-time fetal ECG recording", *IEEE Trans. Biomed. Eng.*, vol. BME-**33**, pp. 505-509, May 1986.

[8] BUNCH, J.R., NIELSEN, C.P., SORENSEN, D.C., "Rank-One Modification of the Symmetric Eigenproblem", *Numer. Math.*, vol. **31**, pp. 31-48, 1978.

[9] BUNCH, J.R., NIELSEN, C.P., "Updating the Singular Value Decomposition", *Numer. Math.*, vol. **31**, pp. 111-129, 1978.

[10] CALLAERTS, D., DE BONDT, F., "Real-time scheiding van het elektrocardiogram van moeder en foetus", Master's thesis, Dept. of Elec. Eng., K.U. Leuven (B), July 1984.

[11] CALLAERTS, D., "Het ontwerp van on-line technieken voor signaalverwerking die gebruik maken van singuliere waardenontbinding - deel 1", Jaarverslag van het eerste mandaat van de specialisatiebeurs I.W.O.N.L., Sept. 1985.

[12] CALLAERTS, D., VANDERSCHOOT, J., VANDEWALLE, J., SANSEN, W., VANTRAPPEN, G., JANSSENS, J., "An adaptive on-line method for the extraction of the complete fetal electrocardiogram from cutaneous multilead recordings", *Journal of Perinatal Medicine*, vol. **14**, no. 6, pp. 421-433, 1986.

[13] CALLAERTS, D., "Het ontwerp van on-line technieken voor signaalverwerking die gebruik maken van singuliere waardenontbinding - deel 2", Jaarverslag van het tweede mandaat van de specialisatiebeurs I.W.O.N.L., Sept. 1986.

[14] CALLAERTS, D., VANDERSCHOOT, J., VANDEWALLE, J., SANSEN, W., "An on-line adaptive algorithm for signal processing using SVD", in *Signal Processing III*, Amsterdam (NL) : Elsevier Science Publ. (North Holland), EURASIP 86, The Hague, pp. 953-956, Sept. 1986.

[15] CALLAERTS, D., VANDEWALLE, J., SANSEN, W., " On-line separation of vector signals using a new adaptive SVD-algorithm ", *Proc. of Benelux Meeting on Systems and Control*, Houthalen (B), p. 187, Jan 1987.

[16] CALLAERTS, D., VANDERSCHOOT, J., VANDEWALLE, J., SANSEN, W., VANTRAPPEN, G., JANSSENS, J., " Fetal Electrocardiogram Measuring Method and Equipment (FEMME)", *Journal of Perinatal Medicine*, vol. **15**, Suppl. 1, World Symposium on Computers in the Care of Mother, Fetus and Newborn, Vienna, pp. 33, March 1987.

[17] CALLAERTS, D., VANDEWALLE, J., SANSEN, W., MOONEN, M., " On-line Algorithm for Signal Separation based on SVD", in *SVD and Signal Processing : Algorithms, Applications and Architectures*, Deprettere, E., Editor, North-Holland, pp. 269-276, Sept. 1987.

[18] CALLAERTS, D., SANSEN, W., VANDEWALLE, J., "Description of a real-time system to extract the Fetal Electrocardiogram", Submitted to *Clinical Physics and Physiological Measurements*, Proc. of Workshop on Current Status and Future of Fetal Electro- and Phonocardiography, Ischia (I), Sept. 1988.

[19] CALLAERTS, D., DE MOOR, B., VANDEWALLE, J., SANSEN, W., "Comparison of SVD-methods to extract the Fetal Electrocardiogram from cutaneous electrode recordings", Submitted to Medical & Biological Eng. & Comp., Jan. 1989.

[20] CALLAERTS, D., VANDEWALLE, J., "The use of SVD-based techniques for signal separation", *Proc. of the Tenth Symp. on Inform. Theory in the Benelux*, Houthalen (B), pp. 109-115, May 1989.

[21] CALLAERTS, D., VANDEWALLE, J., SANSEN, W., "Comparison of signal separation methods based on SVD and GSVD", *Proc. of 12ieme Coll. sur le Traitement du Signal et des Images GRETSI*, Juan-les-Pins (Fr), pp. 177-180, June 1989.

[22] CALLAERTS, D., VANDEWALLE, J., "Adaptive Singular Value Decomposition and its use for Adaptive Signal Separation", *Proc. of the Int. Symp. on Math. Theory of Networks and Systems, MTNS-89*, Amsterdam, June 1989.

[23] CHUNG, E.K, "Electrocardiography : practical applications with vectorial principles", Harper & Row Publ. Inc., Hagerstown (Maryland, USA), 1980.

[24] CREMER, M., "Uber die direkte Ableitung der Aktionsströme des menschlichen Herzens vom Osophagus un über das Elektrokardiogramm des Fötus", *Münch. Med. Wschr.*, vol. **53**, p. 811, 1906.

[25] DAMEN, A.A., VAN DER KAM, J., "The use of the Singular Value Decomposition in Electrocardiography", *Med. Biol. Eng. Comput.*, vol. **20**, pp. 473-482, July 1982.

[26] DE BOECK, M., DE WACHTER, D., "Studie van het on-line algoritme voor de extractie van het foetaal elektrocardiogram met het oog op chipimplementatie", Master's thesis, Dept. of Elec. Eng., K.U. Leuven, Belgium, 1987.

[27] DE MOOR, B., VANDEWALLE, J., STAAR, J., "Oriented Energy and Oriented Signal-to-Signal Ratio Concepts in the Analysis of Vector Sequences and Time Series", in *SVD and Signal Processing : Algorithms, Applications and Architectures*, Deprettere, E., Editor, North-Holland, pp. 209-232, Sept. 1987.

[28] DE MOOR, B., "Mathematical Concepts and Techniques for Modelling of Static and Dynamic Systems", *PhD. thesis*, Dept. of Elec. Eng., Katholieke Universiteit Leuven, Belgium, June 1988.

[29] DE MOOR, B., GOLUB, G.H., "Generalized Singular Value Decompositions : A proposal for a standardized nomenclature", Internal Report, Dept. of Computer Science, Stanford Univ., 1989.

[30] ECKHART, C., YOUNG, G., "A principal axis transformation for non-Hermitian matrices", *Bull. Amer. Math. Soc.*, vol. **45**, pp. 118-121, 1939.

[31] EYK, A. van, "Abdominale Foetale ECG opname", Techn. Univ. Twente, Enschede (NL), Rep. 1224.0093, 1976.

[32] FEINBERG, B., KREBS, H.B., "Intrapartum Fetal Heart Rate Patterns", *Fetal Monitoring : Physiology and Techniques of Antenatal and Intrapartum Assessment*, Ed. J.A.D. Spencer, Castle House Publ. Ltd., Tunbridge Wells, 1989.

[33] FERRARA, E.R., WIDROW, B., "Fetal electrocardiogram enhancement by time sequenced adaptive filtering", *IEEE Trans. Biomed. Eng.*, vol. BME-**29**, pp. 458-460, June 1982.

[34] FLANAGAN, J.L., JOHNSTON, J.D., ZAHN, R., ELKO, G.W., "Computer-steered microphone arrays for sound transduction in large rooms", *J. Acoust. Soc. Am.*, vol. **78**, pp.1508-1518, Nov. 1985.

[35] FORSYTHE, G.E., HENRICI, P., "The Cyclic Jacobi Method for Computing the Principal Values of a Complex Matrix", *Trans. Amer. Math. Soc.*, vol. **94**, pp. 1-23, 1960.

[36] GOLUB, G.H., KAHAN, W., "Calculating the Singular Values and pseudo-inverse of a Matrix", *SIAM Numer. Anal.*, vol. **2**, no. 2, pp. 205-224, 1965.

[37] GOLUB, G.H., REINSCH, C., "Singular Value Decomposition and Least Squares Solutions", *Numer. Math.*, vol. **14**, pp. 403-430, 1970.

[38] GOLUB, G.H., VAN LOAN, C.F., "Matrix Computations", North Oxford Academy, 1983.

[39] GOOVAERTS, H.G., "Instrumentation for the Quantitative Assessment of Fetal Respiratory Sinus Arrhytmia", *PhD. thesis*, Lab. of Medical Physics, Vrije Universiteit Amsterdam (NL), Sept. 1989.

[40] HANSEN, P.C., NIELSEN, H.B., "Singular Value Decomposition of images", *Proc. of 3-th Scand. Conf. on Image Analysis*, pp. 301-307, Copenhagen, 1983.

[41] HON, E.H., "Instrumentation of Fetal Heart Rate and Fetal Electrocaridiography II : A Vaginal Electrode", *Am. J. Obstet. Gynecol.*, vol. **86**, p. 772, 1963.

[42] HON, E.H., PETRIE, R.H., "Clinical Value of Fetal Heart Rate Monitoring", *Clinical Obstet. and Gynecol.*, vol. **18**, no. 4, pp. 1-23, 1975.

[43] HUHTA, J.C., WEBSTER, J.G., "60-Hz Interference in Electrocardiography", *IEEE Trans. on Biomed. Eng.*, vol. BME-**20**, no. 2, 1973.

[44] HUNTER, C.A., LANSFORD, K.G., KNOEBEL, S.B., BRAUNLIN, R.J., "A Technique for Recording Fetal ECG During Labour and Delivery", *Obstet. Gynecol.*, vol. **16**, p. 567, 1960.

[45] JACOBI, C.G.J., "Uber ein Leichtes Verfahren Die in der Theorie der Sacularstorungen Vorkommendern Gleichungen Numerisch Aufzulosen", *Crelle's J.*, vol. **30**, pp. 51-94, 1846.

[46] KLEMA, V.C., LAUB, A.J., "The singular value decompostion : its computation and some applications", *IEEE Trans. Automatic Control*, vol. AC-**25**, no. 2, pp. 164-167, 1980.

[47] LAWSON, C.L., HANSON, R.J., "Solving least squares problems", Englewood Cliffs : Prentice Hall Series, 1974.

[48] LOAN, C.F. van, "Generalizing the Singular Value Decomposition", *SIAM, J. Num. Anal.*, vol. **13**, no. 1, pp. 76-83, 1976.

[49] LONGINI, R.L., REICHERT, T.A., YU, J.M. et al., "Near-orthogonal basis functions : A real time fetal ECG technique", *IEEE Trans. Biomed. Eng.*, vol. BME-**24**, pp. 39-43, Jan. 1977.

[50] MAIER, J., DAGNELI, G., SPEKREIJSE, H., DIJK, B.W. van, "Principal components analysis for source localization of VEPs in man", *Vision Res.*, vol. **27**, pp. 165-177, 1987.

[51] MAX, J., "Méthodes et techniques de traitement du signal et applications aux mesures physiques", *Masson*, Paris, 1977.

[52] MONZINGO, R., MILLER, T., "Introduction to Adaptive Arrays", *Wiley and Sons*, New York, 1980.

[53] MOONEN, M., SWEVERS, J., "Signaalverwerkingseenheid voor de extractie van het foetaal elektrocardiogram 1", Master's thesis, Dept. of Elec. Eng., K.U. Leuven, Belgium, 1986.

[54] MOONEN, M., VAN DOOREN, P., VANDEWALLE, J., "Parallel updating algorithms : Part 1. The Ordinary Singular Value Decomposition", Submitted for publication, Internal Report, ESAT, Dept. Elec. Eng., K.U. Leuven (B).

[55] MORGENSTERN, J., CZERNY, H., SCHMIDT, H., SCHULZ, J., WERNICKE, K., "Fetal Systolic Time Intervals (STI) as a Measure of Myocardial Contractility", *Fetal and Neonatal Physiological Measurements*, Ed. P. Rolfe, Pitman Medical, London (UK), 1980.

[56] NAGEL, J., SCHALDACH, M., "Processing the Abdominal Fetal ECG using a new method", *Fetal and Neonatal Physiological Measurements*, Ed. P. Rolfe, Pitman Medical, London (UK), 1980.

[57] OLDENBURG, J.T., MACKLIN, M., "Changes in the conduction of the fetal electrocardiogram to the maternal abdominal surface during gestation", *Am. J. Obstet. Gynecol.*, vol. **129**, pp. 425-433, 1977.

[58] OOSTENDORP, T.F., "The potential distribution generated by the fetal heart at the maternal abdomen", *Journal of Perinatal Medicine*, vol. **14**, no. 6, pp. 435-444, 1986.

[59] OOSTENDORP, T., "Modelling the Fetal ECG", *PhD. thesis*, K.U. Nijmegen, Netherlands, Jan. 1989.

[60] OOSTEROM, A. van, ALSTERS, J., "Removing the maternal component in the fetal ECG using singular value decomposition", in *Electrocardiography '83*, I. Ruttkay-Nedecky and P. MacFarlane, Eds., Amsterdam, The Netherlands : Excerpta Medicine, pp. 171-176, 1984.

[61] OOSTEROM, A. van, "Spatial Filtering of the Fetal Electrocardiogram", *Journal of Perinatal Medicine*, vol. **14**, no. 6, pp. 411-419, 1986.

[62] OSBORNE, E.E., "On Least Squares Solutions of Linear Equations", *Journal ACM*, vol. **8**, pp. 628-636, (1961).

[63] PAIGE, C.C., SAUNDERS, M., "Towards a Generalized Singular Value Decompostion", *SIAM J. Num. Anal.*, vol. **18**, pp. 398-405, 1981.

[64] PAIGE, C.C., "Computing the Generalized Singular Value Decomposition", *SIAM J. Sci. Statist. Comput.*, vol. **7**, pp. 1126-1146, 1986.

[65] PARLETT, B.N., "The Symmetric Eigenvalue Problem", *Prentice Hall*, Englewood Cliffs, N.J., 1980.

[66] PHELAN, J.P., "Tests of Fetal Well-Being Using the Fetal Heart Rate", *Fetal Monitoring : Physiology and Techniques of Antenatal and Intrapartum Assessment*, Ed. J.A.D. Spencer, Castle House Publ. Ltd., Tunbridge Wells, 1989.

[67] PLONSEY, R., "Bioelectric Phenomena", *Mc Graw-Hill*, New York, 1969.

[68] POPE, D.A., TOMPKINS, C., "Maximizing Functions of Rotations - Experiments Concerning Speed of Diagonalization of Symmetric Matrices using Jacobi's Method", *J. Assoc. Comp. Mach.*, vol. **4**, pp. 459-466, 1957.

[69] REICHERT, T.A., LONGINI, R.L., CROWLEY, J.S., YU, J.M., "A noninvasive extraction of the fetal electrocardiogram", *Comput. Biomed. Res.*, vol. **10**, pp. 1-7, 1977.

[70] ROCHE, J.B., HON, E.H., "The fetal electrocardiogram V : comparison of lead systems", *Am. J. Obstet. Gynecol.*, vol. **92**, pp. 1149-1159, 1965.

[71] SCHIFRIN, B.S., CLEMENT, D., "Routine Antepartum Fetal Heart Rate Monitoring", *Fetal Monitoring : Physiology and Techniques of Antenatal and Intrapartum Assessment*, Ed. J.A.D. Spencer, Castle House Publ. Ltd., Tunbridge Wells, 1989.

[72] SCHULER, G., "The Additive Fetal Electrocardiogram", *Dig. 6th Int. Conf. on Med. Electr. and Biol. Eng.*, Tokyo, Japan, 1965.

[73] SHARMAN, K.C., "Adaptive Algorithms for Estimating the Complete Covariance Eigenstructure", *Proc. ICASSP-86*, Tokyo (J), pp. 1401-1404, 1986.

[74] STAAR, J., VANDEWALLE, J., "Singular Value Decomposition : A reliable tool in the algorithmic analysis of systems", *Journal A*, vol. **23**, pp. 69-74, 1982.

[75] STAAR, J., "Concepts for reliable modelling of linear systems with applications to on-line identification of multivariable state space descriptions", *PhD. thesis*, Dept. of Elec. Eng., Katholieke Universiteit Leuven, Belgium, 1982.

[76] STEWART, G.W., "A Method for Computing the Generalized Singular Value Decomposition", *Matrix Pencils*, ed. B. Kagstrom and A. Ruhe, Springer Verlag, New York, pp. 207-220, 1983.

[77] SUREAU, C., TROCELLIER, R., "Etude de quelques problèmes techniques en électrocardiographie foetale", *Med. Elec. Biol. Eng.*, vol. **1**, pp. 181-188, 1961.

[78] TALMON, J.L., "Pattern Recognition of the ECG, a structured analysis", *PhD. thesis*, Krips repro Meppel, V.U. Amsterdam (NL), 1983.

[79] VAN COMPERNOLLE, D., "Hearing Aids using Binaural Processing Principles", *Int. Symp. on Digital Processing Hearing Aids*, Wolfheze (NL), Aug. 1988.

[80] VAN COMPERNOLLE, D., "Adaptive Filter Structures for Enhancing Cocktail Party Speech from Multiple Microphone Recordings", *Proc. of 12ieme Coll. sur le Traitement du Signal et des Images GRETSI*, Juan-les-Pins (Fr), pp. 513-516, June 1989.

[81] VAN COMPERNOLLE, D., "Spectral Estimation Using a Log-error Criterion with Applications to Speech Recognition in Noisy Environments", *Int. Conf. Acoust. Speech & Signal Processing*, pp. 258-261, 1989.

[82] VANDERSCHOOT, J., VANDEWALLE, J., SANSEN, W., VANTRAPPEN, G., JANSSENS, J., "An application of SVD to the extraction of weak bioelectrical signals", *Revue HF - XII*, pp. 253-258, 1983.

[83] VANDERSCHOOT, J., VANDEWALLE, J., JANSSENS, J., SANSEN, W., VANTRAPPEN, G., "Extraction of weak bioelectrical signals by means of Singular Value Decomposition", in *Analysis and Optimization of Systems*, Lecture Notes in Control and Information Sciences 63, Bensoussan, A., Lions, J.L., Eds, Springer Verlag, Berlin, pp. 434-448, 1984.

[84] VANDERSCHOOT, J., VANTRAPPEN, G., JANSSENS, J., VANDEWALLE, J., SANSEN, W., "A reliable method for fetal ECG extraction from abdominal recordings", in *Medical Informatics Europe 84*, Lecture Notes in Medical Informatics 24, Roger, F.H. et al, Eds., Springer Verlag, Berlin, pp. 249-254, 1984.

[85] VANDERSCHOOT, J., VANTRAPPEN, G., JANSSENS, J., SANSEN, W., VANDEWALLE, J., CALLAERTS, D., "The use of Singular Value Decomposition in Multilead Abdominal FECG", *Europ. J. Obst. Gynec.*, reprod., Biol. 20, 1985.

[86] VANDERSCHOOT, J., CALLAERTS, D., SANSEN, W., VANDEWALLE, J., VANTRAPPEN, G., JANSSENS, J., "Two Methods for Optimal MECG Elimination and FECG Detection from Skin Electrode Signals ", *IEEE Trans. Biomed. Eng.*, vol. BME-34, No. 3, pp. 233-243, 1987.

[87] VANDEWALLE, J., DE MOOR, B., "A variety of applications of Singular Value Decomposition in Identification and Signal Processing", in *SVD and Signal Processing: Algorithms, Applications and Architectures*, Deprettere, E., Editor, North-Holland, Sept. 1987.

[88] VANDEWALLE, J., VANDERSCHOOT, J., DE MOOR, B., "Source separation by adaptive singular value decomposition", *Proc. IEEE ISCAS Conf.*, Kyoto, June 1985, pp. 1351-1354, 1985.

[89] VANDEWALLE, J., VANDERSCHOOT, J., DE MOOR, B., "Filtering of vector signals based on the singular value decomposition", *7th European Conf. on Circuit Theory and Design*, Prague, Sept. 1985, pp. 458-461.

[90] VANDEWALLE, J., CALLAERTS, D., (1988) "Singular Value Decomposition : a powerful concept and tool in signal processing", *Proc. of Conf. on Mathematics in Signal Processing*, Warwick (UK), Dec. 1988.

[91] VEEN, B.D. van, BUCKLEY, K.M., "Beamforming : A Versatile Approach to Spatial Filtering", *IEEE, Trans. on ASSP*, vol. **5**, no. 2, pp. 4-24, 1988.

[92] VERTONGEN, M., WEIJERS, J., "Digitaal chipontwerp voor on-line scheiding van het elektrocardiogram van moeder en foetus met behulp van singuliere waardenontbinding", Master's thesis, Dept. of Elec. Eng., K.U. Leuven, Belgium, 1989.

[93] VOLDER, J.E., "The CORDIC Trigonometic Computing Technique", *IRE Trans. on Electronic Comp.*, pp. 330-334, Sept. 1959.

[94] WHEELER, T., MURRILLS, A., SHELLEY, T., "Measurement of the fetal heart rate during pregnancy by a new electrocardiographic technique", *Brit. J. Obstet. Gynecol.*, vol. **85**, pp. 12-17, 1978.

[95] WIDROW, B., GLOVER, J.R., McCOOL, J.M., KANNITZ, J., WILLIAMS, C.H.S., HEARN, R.M., ZEIDLER, J.R., DONG, E., GOODLIN, R.C., "Adaptive noise cancelling : principles and applications", Proc. IEEE, vol. **63**, pp. 1692-1716, Dec. 1975.

[96] WILKINSON, J.H., "The Algebraic Eigenvalue Problem", *Clarendon Press*, Oxford, 1965.

NEDERLANDSE SAMENVATTING

Signaalscheidingsmethodes, gebaseerd op de Singuliere Waarden Ontbinding, en hun toepassing op reële-tijd extractie van het cutaan opgemeten foetale electrocardiogram.

In dit proefschrift worden twee signaalscheidingsmethodes, gebaseerd op de Singuliere Waarden Ontbinding (SWO) van één of meer matrices, voorgesteld en besproken. Om de werking van de methodes te illustreren werden ze toegepast op reële data, meer specifiek voor de scheiding van het foetale electrocardiogram (FECG) en dat van de moeder (MECG). Hierbij wordt uitgegaan van een reeks potentiaalsignalen, simultaan opgemeten met behulp van electrodes op de huid van de moeder.

Hoofdstuk 1 : Inleiding en overzicht van het proefschrift.

In vele ingenieursdisciplines kunnen problemen, processen of systemen beschreven worden met behulp van één of meerdere signalen, die een bepaalde informatie bevatten over het proces of systeem dat geobserveerd wordt. Vaak komt het echter voor dat men een specifiek fenomeen (en daarom énkel de signalen die door dit fenomeen gegenereerd of uitgezonden worden) apart wil observeren, maar dat de omgeving dit niet toelaat, doordat er vele storende invloeden zijn van allerlei aard. Daardoor meet of ontvangt men vaak een signaal dat de superpositie is van meerdere oorspronkelijke signalen, waarvan er sommige gewenst zijn, daar ze nuttige informatie bevatten, terwijl andere ongewenst zijn, vermits ze de observatie van de gewenste signalen op één of andere manier verstoren.

Indien we veronderstellen dat de signalen afkomstig zijn van "signaalbronnen" die ruimtelijk verspreid zijn in een medium, en indien dit medium tevens lineair, statisch en isotroop is, kan elk geobserveerd signaal $m_i(t)$ beschouwd worden als de superpositie van een beperkt aantal gewenste en ongewenste signalen $s_j(t)$, gestoord door additieve ruis $n_i(t)$

$$m_i(t) = \sum_{j=1}^{r} t_{ij}\, s_j(t) + n_i(t) \qquad (i = 1, \ldots, p)$$

Vermits men echter één specifiek fenomeen wenst te bestuderen, moeten signaalscheidingsmethodes toegepast worden. Deze bestaan meestal uit de eliminatie van de meest storende signalen en de extractie van de gewenste signalen. Indien de signaalspectra van verschillende bronnen elkaar overlappen, kunnen de klassieke analoge of digitale filtertechnieken echter geen oplossing bieden, zodat andere methodes moeten ontwikkeld worden.

De methodes voor signaalscheiding die in dit werk worden voorgesteld, vinden een gepaste lineaire combinatie van een aantal simultaan opgemeten observaties (op hun beurt elk een lineaire combinatie van originele bronsignalen). Het zal tevens blijken dat hierbij de keuze van de observatiepunten een rol kan spelen.

<u>Hoofdstuk 2 :</u> De cutane detectie van het foetale electrocardiogram.

De detectie van het foetale electrocardiogram (FECG), uitgaande van potentiaalsignalen, gemeten met behulp van electrodes op de huid van de moeder, wordt vooral bemoeilijkt door de aanwezigheid van de veel sterkere signalen afkomstig van het moederhart. Ook 50 Hz interferentie, veroorzaakt door het net, kan de metingen verstoren. Deze biomedische signaalscheidingstoepassing is ideaal om de werking van de ontwikkelde methodes te kunnen verklaren en illustreren. Vandaar dat in dit hoofdstuk de problematiek rond deze toepassing wat meer wordt toegelicht. Tevens wordt aangegeven wat de klinische waarde is van een antepartum foetaal electrocardiogram. De bestaande methodes voor de detectie van het FECG worden opgesplitst in twee grote groepen : enerzijds de methodes, die met behulp van minder of meer ingewikkelde technieken het signaal van het moederhart rechtstreeks en met een gepaste schaalfactor aftrekken van een abdominaal signaal, en anderzijds de methodes, die met behulp van een gepaste lineaire combinatie of gewogen som van een aantal electrodesignalen het MECG willen elimineren.

In een volgende paragraaf wordt het FECG-probleem beschreven met een wiskundig model, als een soort invers probleem. Dit model bevat een bepaalde onzekerheid, veroorzaakt door het verschil tussen verschillende personen, alsook verschillen die bij eenzelfde patiënt optreden tijdens de zwangerschap.

Zo kan de ganse configuratie van bronnen veranderen door foetale bewegingen en kunnen de geleidingsmechanismen in de loop van de zwangerschap beïnvloed worden door de veranderende eigenschappen van het vruchtwater en door foetale groei. Tenslotte wordt een theoretische oplossing uitgewerkt voor het signaalscheidingsprobleem, steunend op een geometrische interpretatie van het signaalmodel. Deze oplossing geeft ook aan aan welke voorwaarden de coëfficiënten in de gewogen som van opgemeten signalen moeten voldoen.

<u>Hoofdstuk 3 :</u> Formulering van wiskundige begrippen met behulp van Singuliere Waarden Ontbinding.

Dit hoofdstuk vormt de wiskundige fundering van het proefschrift. Met behulp van de Singuliere Waarden Ontbinding (SWO) worden een aantal wiskundige begrippen gedefinieerd en omschreven en er kunnen karakteristieke waarden voor berekend worden.

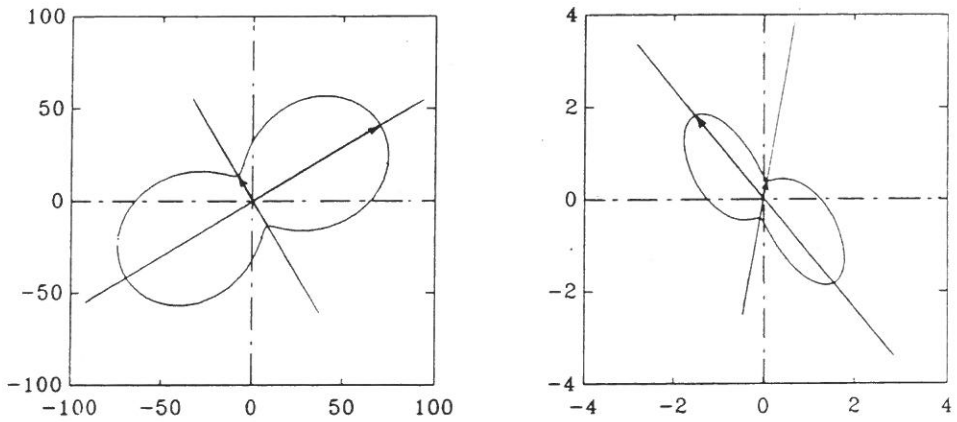

Figuur 1: *Links de geöriënteerde energie van een signaalset in alle richtingen. Rechts de geöriënteerde signaal-signaalverhouding van twee signaalsets in alle richtingen.*

Enkele van de belangrijkste concepten voor meerkanaalssignaalverwerking, die in dit hoofdstuk gedefinieerd worden zijn de begrippen meetruimte en signaalruimte, de geöriënteerde energie van een reeks signalen en de geöriënteerde signaal-signaal verhouding van twee reeksen signalen in dezelfde meetruimte (zie Figuur 1). Er wordt een onderscheid gemaakt tussen de Gewone SWO (GSWO) van een matrix en de Quotiënt SWO (QSWO) van een matrixpaar. Beide matrixontbindingen, gekend uit de lineaire algebra, worden gedefinieerd en hun belangrijkste eigenschappen worden weergegeven. Er wordt ook een verband aangetoond tussen het begrip geöriënteerde energie van een signaalset en de GSWO van de overeenkomstige datamatrix. Analoog daarmee is er ook een verband tussen het begrip geöriënteerde signaal-signaal verhouding van twee reeksen signalen en de QSWO van de overeenkomstige datamatrices. Daardoor kunnen GSWO en QSWO aangewend worden om specifieke waarden en extrema voor de gedefinieerde wiskundige begrippen te berekenen. Dit laatste maakt het mogelijk om enkele signaalscheidingsprincipes uit te werken op basis van de gedefinieerde wiskundige begrippen, terwijl GSWO en QSWO een handige, robuste en numeriek stabiele methode vormen om de berekeningen uit te voeren.

<u>Hoofdstuk 4 :</u> Een nieuw on-line algoritme voor SWO-gebaseerde signaalscheiding.

De Singuliere Waarden Ontbinding (SWO) is een wiskundige techniek uit de lineaire algebra, die een matrix ontbindt als een produkt van drie andere matrices met zeer specifieke kenmerken. Deze ontbinding is verwant met de meestal beter gekende Eigenwaarden Ontbinding. Er bestaan een aantal zeer betrouwbare routines voor de berekening van de GSWO en de QSWO, maar ze gebruiken allen een off-line strategie, d.w.z. dat alle gegevens beschikbaar moeten zijn alvorens de berekening kan beginnnen. Maar in reële-tijd toepassingen voor signaalverwerking, waar de gegevens sequentieel ter beschikking komen, geeft deze off-line strategie problemen met betrekking tot de hoeveelheid rekenwerk en de adaptiviteit van de methode.

In vele toepassingen volstaat het ook om enkel de links singuliere matrix van de SWO te berekenen, in plaats van de drie matrices van de volledige ontbinding. Daarom werd een algoritmisch schema ontwikkeld om adaptief en on-line de links singuliere matrix van een gegeven matrix te berekenen, waarbij de datamatrix kolom per kolom beschikbaar wordt. Telkens nieuwe informatie wordt toegevoegd door een nieuwe kolom van de matrix, wordt de huidige kennis over de linkssinguliere matrix aangepast.

Vermits de basis van het algoritme het aanpassen van de covariantiestruktuur van de datamatrix betreft, wordt de vlakke rotatie gebruikt om de symmetrische matrix te diagonaliseren. Hoewel de Jacobimethode optimaal is wat betreft de bepaling van de rotatiehoek, in de betekenins van een maximale stap in de richting van diagonalizatie, wordt een nieuwe methode voorgesteld die een licht suboptimale rotatiehoek berekent, zonder echter een worteltrekking te moeten uitvoeren. Terwijl de Jacobi-methode een niet-diagonaalelement van de symmetrische matrix volledig nul maakt, zal deze nieuwe methode de absolute waarde van het element behoorlijk reduceren. Dit komt overeen met een zogenaamde over- of onderrelaxatie en heeft meer voordelen bij gebruik van microcomputers of -processoren, daar afrondingsfouten in de Jacobi-methode ervoor zouden kunnen zorgen dat een element in feite niet exact nul wordt gemaakt. De nieuwe methode heeft in de laatste stappen van het iteratieve diagonalizatieproces dezelfde kwadratische convergentiesnelheid als de originele Jacobi-methode.

Omdat het zeer moeilijk is om een analytisch bewijs te geven voor de convergentie van het adaptieve on-line algoritme, wordt voor een meer empirische benadering gekozen. Deze benadering toont met enkele simulaties aan dat het algoritme vrij snel convergeert naar een bijna-diagonaalmatrix, zelfs indien er slechts één rotatie (over een rotatiehoek, gevonden met de nieuwe benaderende methode) per algoritmische cyclus wordt toegepast. Op deze manier wordt het rekenwerk voor één cyclus van het algoritme gereduceerd tot een grootte-orde $O\ (4p^2 + 13p)$ optellingen en vermenigvuldigingen. In de volgende hoofdstukken worden de twee signaalscheidingsmethodes voorgesteld en zodanig aangepast dat het adaptieve on-line algoritme in beide technieken kan gebruikt worden.

Hoofdstuk 5 : Signaalscheiding d.m.v. Singuliere Waarden Ontbinding van een uitgebreide data matrix.

In dit hoofdstuk wordt de eerste signaalscheidingsmethode, gebaseerd op het begrip geöriënteerde energie van een signaalset, voorgesteld. De coëfficiënten in de lineaire combinatie van de opgemeten signalen worden gevonden door de links singuliere matrix in de GSWO van de "uitgebreide" datamatrix te berekenen. Dit betekent dat de datamatrix niet enkel werd opgebouwd uit signalen die zowel gewenste als ongewenste signaalbijdragen bevatten, maar uitgebreid werd met een aantal onafhankelijke signalen, die de storende bron afzonderlijk oppikken. In een eerste punt wordt de oplossing van het probleem voorgesteld en bewezen onder ideale omstandigheden (een loodrechte lineaire overdracht van de signalen van signaalbron naar meetpunt). Verder wordt de invloed van niet-loodrechte signaaloverdracht bestudeerd en dit resulteert in enkele opmerkingen in verband met de plaatsing van de meetpunten.

In een volgende paragraaf wordt deze methode toegepast op de eliminatie van het electrocardiogram van de moeder (MECG) en de detectie van het foetale ECG (FECG). Hiervoor moeten zowel signalen op de buik van de moeder worden opgemeten, als signalen in de buurt van het moederhart, die het MECG afzonderlijk oppikken. Door deze ruimtelijke spreiding van de electrodes, wordt een bijna-loodrechte overdracht van de signalen bereikt. Tevens wordt aangegeven op welke manier men de foetale bijdragen in elk van de opgemeten signalen afzonderlijk kan bekomen. Door opeenvolgende hartcycli van de resulterende foetale signalen uit te middelen, verkrijgt men informatie over de golfvorm van het FECG (de duur van het QRS-complex, de P-golf, enz.). Verder wordt het on-line adaptieve algoritme, dat in het vorige hoofdstuk werd ontwikkeld voor de berekening van de linkssinguliere matrix in de GSWO van de uitgebreide datamatrix, gebruikt om het ECG van moeder en foetus op een adaptieve wijze te scheiden (zie Figuur 2).

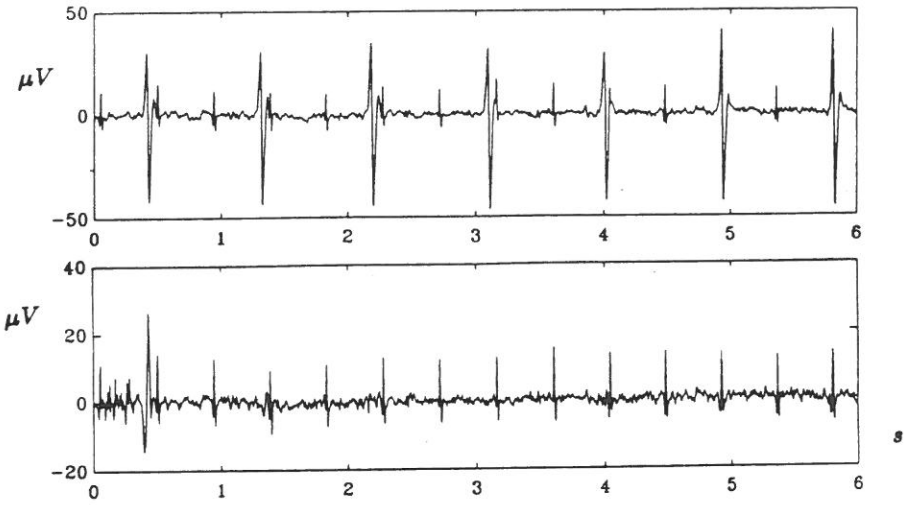

Figuur 2: *Eén signaal zoals het werd opgenomen tussen twee electrodes op de buik van de moeder, zodat het zowel MECG als FECG bevat, en één signaal als resultaat van onze adaptieve scheidingsmethode.*

In een laatste paragraaf wordt bewezen dat dezelfde signaalscheidingsmethode kan aangewend worden om 50 Hz interferentie van het elektriciteitsnet uit biomedische metingen te verwijderen. Hiervoor moet de datamatrix uitgebreid worden met een signaal dat rechtstreeks van het net wordt opgepikt, en hetzelfde signaal maar dan in kwadratuur met zichzelf.

Hoofdstuk 6 : Signaalscheiding d.m.v. de Quotient Singuliere Waarden Ontbinding van twee matrices.

De tweede signaalscheidingsmethode, die in dit hoofdstuk wordt voorgesteld, is gebaseerd op het begrip geöriënteerde signaal-signaal verhouding van twee signaalsets, dat in Hoofdstuk 3 werd gedefinieerd. De coëfficiënten in de lineaire combinatie van de opgemeten signalen, nodig om de signaalbijdragen te scheiden, worden gevonden door de QSWO te berekenen van een matrixpaar. Dit paar bestaat uit de datamatrix, die de monsters bevat van de originele opgemeten signalen, en een matrix, die wordt samengesteld uit één of meerdere geselecteerde intervallen, waarin het ongewenste signaal domineert of afzonderlijk voorkomt. Met een tweedimensionaal voorbeeld wordt aangetoond dat de methode inderdaad succesvol is en dat de orthogonaliteit van de signaaloverdracht (van bron naar meetpunt) een invloed heeft op het resultaat.

Een belangrijke observatie is het feit dat de QSWO van een matrixpaar kan berekend worden als twee opeenvolgende GSWO's. Dit wordt in een theorema bewezen en leidt tot een on-line adaptief schema voor de berekening van de X-matrix in de QSWO. Indien het ongewenste fenomeen tijdsinvariant is, kan de berekening van de eerste GSWO inderdaad als initializatie gebruikt worden voor de tweede stap, die wordt toegepast op de gehele datamatrix en die het gewenste signaal probeert te detecteren. De methode werd zodanig ontworpen dat deze tweede stap adaptief kan uitgevoerd worden met het on-line adaptieve algoritme, zodat het gewenste fenomeen tijdsvariant mag zijn. Het verschil met de vorige methode is echter dat de coëfficiënten in de verschillende lineaire combinaties van de opgemeten signalen, niet orthogonaal moeten zijn.

In een volgende paragraaf wordt deze tweede methode weer toegepast voor de detectie van het FECG, uitgaande van potentiaalmetingen op de huid van de moeder. Het volstaat om enkel signalen op de buik van de moeder op te meten en hieruit enkele intervals te selecteren, waarin het MECG dominant aanwezig is, i.e. tussen twee foetale QRS-complexen in (zie Figuur 3). Zowel de datamatrix, als de matrix die werd samengesteld uit de geselekteerde intervals, definiëren een puntenwolk in de p-dimensionale meetruimte.

De QSWO zoekt díe richtingen in de meetruimte, waarin de verhouding van de geöriënteerde energie van de ene wolk (de datamatrix) tot de geöriënteerde energie van de andere wolk extreem is. Enkele van deze richtingen bevatten een foetaal signaal, vrij van bijdragen van het ECG van de moeder.

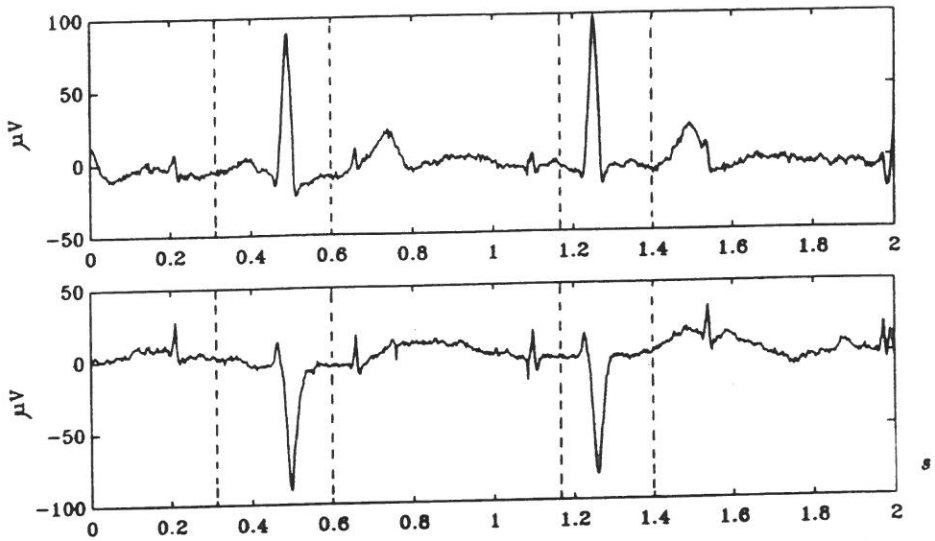

Figuur 3: *Twee abdominaal opgemeten signalen met aanduiding van intervals, waarin het MECG domineert.*

Er wordt ook aangetoond dat het toevoegen van een aantal extra signalen, die enkel informatie van het moederhart oppikken, een positieve invloed heeft op de signaal-ruis verhouding van het resulterende signaal. Inderdaad, door de ruimtelijke spreiding van de electrodes, wordt de signaaloverdracht van signaalbronnen (moederhart en foetaal hart) naar meetpunt (electrode) bijna-loodrecht. Verder werd het on-line adaptieve algoritme gebruikt om MECG en FECG op een adaptieve wijze te scheiden. Hoewel de methode met succes een bruikbaar MECG-vrij foetaal hartsignaal kan detecteren, is ze niet soepel en te complex om in een klinische omgeving te gebruiken. Dit is te wijten aan de visuele selectie van de intervallen en aan de ingewikkelde initializatiestap.

Hoofdstuk 7 : Vergelijking van de SWO-gebaseerde signaalscheidingsmethodes.

In dit hoofdstuk worden de twee voorgestelde signaalscheidingsmethodes met elkaar vergeleken. Beide methodes trachten op een bepaalde manier de coëfficiënten te vinden in de lineaire combinatie van de opgemeten signalen, zodat de verschillende signaalbijdragen van elkaar gescheiden kunnen worden. In eerste instantie worden de methodes op een algemene manier met elkaar vergeleken op basis van enkele criteria : beperkingen voor toepassing, mogelijkheid tot automatisatie, eisen in verband met orthogonaliteit van de signaaloverdracht en het minimum aantal op te meten signalen.

Vervolgens worden enkele voor- en nadelen van beide methodes opgesomd, indien ze gebruikt wordt voor de detectie van het foetale ECG. De belangrijkste conclusie hier is dat beide methodes bevredigende tot zeer goede resultaten geven, maar dat de eerste methode qua elegantie en mogelijkheid tot gebruik in een klinische omgeving het meest geschikt is. De vergelijking van de methodes kan ook als volgt bekeken worden : gegeven een reeks opgemeten signalen, die een duidelijk zichtbaar FECG bevatten, dan in er meer kans om (na visuele selectie van de nodige intervallen en na een eerste initializerende GSWO) met de tweede methode een MECG-vrij foetaal signaal te vinden, dan met methode 1, omwille van de eisen i.v.m. de electrodeposities. Maar indien men een toestel moet ontwerpen dat een signaalscheidingsmethode implementeert, zodat het FECG in reële tijd kan gedetecteerd worden en de electrodeposities interactief aangepast kunnen worden, dan is de eerste methode veruit de meest interessante.

In een tweede deel van dit hoofdstuk worden de twee methodes vergeleken met twee andere bestaande methodes voor de eliminatie van het MECG en de detectie van het FECG. Eerst wordt een twee-staps techniek voor FECG-extractie voorgesteld (ook gebaseerd op de Singuliere Waarden Ontbinding). We pasten deze techniek aan zodat ons on-line algoritme erop kan toegepast worden. Ondanks het feit dat in de meeste gevallen een bruikbaar foetaal signaal wordt gevonden, vrij van MECG, heeft deze methode toch een aantal belangrijke nadelen. Vervolgens wordt ook de bekende adaptieve filtering techniek van Widrow voorgesteld en toegepast op enkele van onze datasets.

Hoofdstuk 8 : Overzicht van de belangrijkste resultaten en perspektieven voor de toekomst.

Dit hoofdstuk geeft een kort overzicht over de ontwikkelde methodes, hun nut en enkele van de belangrijkste behaalde resultaten in dit proefschrift. Zoals de titel aangeeft kan het werk opgesplitst worden in vier hoofdonderwerpen :

1. Methodes voor Signaalscheiding
2. Singuliere Waarden Ontbinding (SWO)
3. Detectie van het Foetale Electrocardiogram
4. On-line verwerking en reële-tijd implementatie

De twee methodes voor signaalscheiding die in dit werk worden voorgesteld, zoeken elk op een of andere manier de gewichtsvectoren voor het bepalen van de lineaire combinaties van een aantal opgemeten signalen. De eerste methode vindt orthonormale gewichtsvectoren door de Gewone SWO te berekenen van de datamatrix, uitgebreid met een aantal onafhankelijke signalen die de storende bron afzonderlijk oppikken. Door het ongewenste fenomeen zo sterk mogelijk te observeren, kan het geëlimineerd worden op basis van beschouwingen i.v.m. geöriënteerde energie. De tweede methode vindt een aantal niet-orthonormale gewichtsvectoren door de Quotient SWO van een matrixpaar te berekenen en is een volledig nieuw resultaat. In de toekomst dient nagegaan te worden of deze signaalscheidingsmethodes eveneens toepasbaar zijn op meer ingewikkelde problemen zoals bijvoorbeeld spraaksignalen (niet stationair, dynamische signaaloverdracht, breedbandige signalen, fazeverschil tussen signalen, etc.).

Het belangrijkste nieuwe resultaat bij de berekening van de GSWO is de ontwikkeling van een on-line adaptief schema dat de linkssinguliere matrix van een gegeven matrix aanpast telkens er een kolom wordt toegevoegd. Het feit dat slechts één enkele rotatie moet uitgevoerd worden per cyclus van het algoritme is niet analytisch bewezen maar wel op een empirische wijze. Verder werd een nieuw methode uitgewerkt om de rotatiehoek te berekenen, die in tegenstelling tot de klassieke Jacobi-methode geen worteltrekking vereist, wat erg belangrijk is in microcomputer omgevingen.

De twee signaalscheidingsmethodes werden toegepast voor de detectie van het foetale electrocardiogram (FECG), uitgaande van potentiaalmetingen afkomstig van electrodes op de moederhuid. Beide methodes zijn zeer succesvol en effectief, daar ze een foetaal hartsignaal bekomen, vrij van bijdragen van het moederhart. In de toekomst moet worden uitgekeken naar standaard electrodeplaatsing strategieën. Klinische testen op grote schaal moeten de methodes in praktijk kunnen evalueren. Belangrijk is tevens dat de eerste methode kan aangewend worden om 50 Hz interferentie vanwege het net te elimineren uit biomedische metingen.

Het feit dat voor beide signaalscheidingsmethodes een on-line versie werd ontwikkeld, zodat het on-line adaptieve algoritme in de drie gevallen kan gebruikt worden, is een zeer belangrijk resultaat. Daarom werd dit algoritme geïmplementeerd, zowel in software (door een PC-insteekbord met TMS-320C25 microprocessor te programmeren) als in hardware (door het ontwerp van een digitale IC). In beide toepassingen is het onderzoek naar eindige woordlengteberekeningen in de toekomst belangrijk.

Verder werden enkele perspektieven voor toekomstig onderzoek met deze signaalscheidingstechnieken voorgesteld op het gebied van straalvorming en antenne toepassingen, spraakverbetering met behulp van meerdere microfoons in ruissterke omgevingen, zoals bij cockpitgesprekken, mobiele telefoon, enz. en tenslotte op het gebied van principiële komponenten analyse van het electro-encefalogram (EEG).

Appendix A : Haalbaarheidsstudie van een reële-tijds implementatie van het on-line algoritme.

In Hoofdstuk 4 werd het on-line adaptieve algoritme ontwikkeld en uitgewerkt voor de berekening van de linkssinguliere matrix in de GSWO van een matrix. Dit algoritme kan in beide signaalscheidingsmethodes gebruikt worden om op adaptieve wijze het ongewenste signaal te elimineren. Maar ook in andere signaalverwerkingstoepassingen gebaseerd op de principiële componenten reductie of rangbepaling, kan dit on-line adaptieve algoritme het rekenwerk aanzienlijk verminderen, zodat reële-tijd implementaties mogelijk worden.

In dit hoofdstuk worden twee implementaties van dit algoritme besproken. De eerste is een software-implementatie in een systeem, bestaande uit een Personal Computer, uitgebreid met een insteekbord voor DSP. Een prototype van zulk systeem wordt momenteel gerealizeerd in het kader van een Europees project "New Methods in Perinatal Surveillance" in samenwerking met de K.U. Nijmegen en de V.U. Amsterdam. De tweede is de implementatie van het algoritme in hardware door het ontwerp van een digitale geïntegreerde schakeling. Deze realizatie gebeurt momenteel met behulp van de Cathedral II & III software van de VSDM-divisie van het Interuniversitair Micro-Electronica Centrum (IMEC v.z.w.).

Appendix A : Pascal routines voor VAX / VMS.

Deze Appendix bevat de twee programma's SVD ONLIN en GSVD ONLIN voor de on-line berekening van de GSWO en QSWO.